Chem Soc Rev

Stereoelectronic power of oxygen in control of chemical reactivity: the anomeric effect is not alone

Stereoelectronic power of oxygen in control of chemical reactivity: the anomeric effect is not alone

Igor V. Alabugin,[a]* Leah Kuhn,[a] Michael G. Medvedev[c], Nikolai V. Krivoshchapov[c,d], Vera A. Vil'[c], Ivan A. Yaremenko,[c] Patricia Mehaffy,[a] Meysam Yarie,[b] Alexander O. Terent'ev[c], Mohammad Ali Zolfigol[b]

[a]Department of Chemistry and Biochemistry, Florida State University, Tallahassee, Fl 32306, USA.

[b]Department of Organic Chemistry, Faculty of Chemistry, Bu-Ali Sina University, Hamedan 65167, Iran.

[c]N. D. Zelinsky Institute of Organic Chemistry, Russian Academy of Sciences, 47 Leninsky prosp., 119991 Moscow, Russian Federation

[d]Lomonosov Moscow State University, Leninskie Gory 1 (3), Moscow, 119991, Russian Federation

Corresponding author: alabugin@chem.fsu.edu (I. V. Alabugin).

Abstract

Although carbon is the central element of organic chemistry, oxygen is the central element of stereoelectronic control in organic chemistry. Generally, a molecule with a C-O bond has both a strong donor (a lone pair) and a strong acceptor (e.g., a σ*C-O orbital), a combination that provides opportunities to influence chemical transformations at the opposite ends of the electron demand spectrum. Oxygen is a stereoelectronic chameleon that adapts to the varying situations in radical, cationic, anionic, and metal-mediated transformations.

Arguably, the most historically important stereoelectronic effect is the anomeric effect (AE), i.e., the axial preference of acceptor groups at the anomeric position of sugars. Although AE is generally attributed to hyperconjugative interactions of σ-acceptors with a lone pair at oxygen (negative hyperconjugation), recent literature reports suggested alternative explanations. In this context, it is timely to evaluate the fundamental connections between AE and a broad variety of O-functional groups. Such connections illustrate the general role of hyperconjugation with oxygen lone pairs in reactivity. Lessons from the AE can be used as the conceptual framework for organizing disjointed observations into a logical body of knowledge. In contrast, neglect of hyperconjugation can be deeply misleading as it removes the

stereoelectronic cornerstone on which, as we show in this review, the chemistry of organic oxygen functionalities is largely based.

As negative hyperconjugation releases the "underutilized" stereoelectronic power of unshared electrons (the lone pairs) for the stabilization of a developing positive charge, the role of orbital interactions increases when the electronic demand is high and molecules distort from their equilibrium geometries. From this perspective, hyperconjugative anomeric interactions play a unique role in guiding reaction design.

In this manuscript, we discuss the reactivity of organic O-functionalities, outline variations in the possible hyperconjugative patterns, and showcase the vast implications of AE for the structure and reactivity. On our journey through a variety of O-containing organic functional groups, from textbook to exotic, we will illustrate how this knowledge can predict chemical reactivity and unlock new useful synthetic transformations.

Organic chemistry of oxygen-containing functional groups through the prism of AI:

Oxygen is one of the key elements of the chemical universe with many important biological functions including respiration, photosynthesis, and biosynthesis. Furthermore, in combination with carbon, oxygen is also an essential architectural component for the construction of organic molecules. Like a sprinkle of spice, incorporation of oxygen adds many useful properties including polarity, H-bond formation, hydrophilicity, Lewis basicity etc. that help to convert plain hydrocarbon molecules into medicinally active molecular entities. Not surprisingly, the O-containing functional groups, from ethers and alcohols to ketones and carboxylic acid derivatives, define much of undergraduate chemistry.

The role of oxygen in organic synthesis is equally profound. The reactivity patterns of O-functionalities are diverse with much of this diversity traceable to the chameleonic properties of this element, as oxygen combines high electronegativity with Lewis basicity. This combination is essential for creating controlled charge separation in nucleophilic and electrophilic synthons that define strategic thinking in synthetic route planning. Furthermore, presence of the lone pairs also gives oxygen the stereoelectronic power to direct chemical reactions. This power is especially clearly manifested when an electron-deficient intermediate or transition state are formed in the direct proximity. From this point of view, the role of oxygen in chemical reactions is similar to a conductor directing a musical performance.

Considering the diversity of O-functionalities, it is useful to identify the general themes that can be used as a foundation for the rational control of reactivity. Here, we examine the common features of organic oxygen chemistry revealed through the stereoelectronic prism of the anomeric effect (Figure 1). Historically, this phenomenon was introduced to explain unusual conformational preferences in carbohydrates where the presence of an endocyclic oxygen in a glycoside leads to an "abnormal" axial conformational preference which becomes more pronounced for stronger acceptor substituents at the "anomeric" carbon increases.[1, 2] The magnitude of anomeric stabilization can be evaluated by comparing the energy difference between the respective axial and equatorial conformers in cyclohexane and tetrahydropyran (THP, Figure 1 center). The effect can be evaluated more accurately if one considers that the C-O bonds in tetrahydropyran are shorter than C-C bonds in cyclohexane.[3, 4] The analogous conformational preference, i.e. the *generalized anomeric effect*, is observed in acyclic systems where two heteroatoms are connected to the same central carbon ($X-CR_2-Y$) or, even more generally, to the same atom A (X-A-Y)).[5, 6]
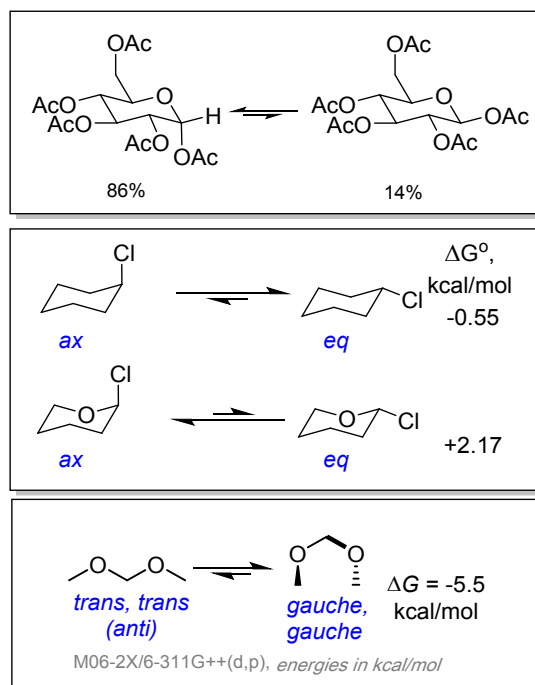
Figure 1. Manifestations of anomeric effect. Axial preference for acceptor groups at the anomeric positions of sugars (top) and cyclic O-heterocycles (center); conformational preferences of acyclic acetails associated with the generalized anomeric effect (bottom).

The origin of anomeric effect is generally attributed to a stabilizing hyperconjugative interaction between the antibonding C-X orbital and the vicinal oxygen lone pair (LP). This interaction is strengthened in the axial 2-X THP conformer where the C-X bond is aligned with the p-type lone pair of the endocyclic oxygen. The hyperconjugative model was first proposed to explain the axial C-Cl bond lengthening observed in the X-ray geometries of chlorinated dioxanes, which could not be intuitively explained by the electrostatic model.[7, 8] This model is supported by computational evaluations of such interactions[9-13,] provided by the Natural Bond Orbitals (NBO) approach.[14]

Although the hyperconjugative model is now a textbook explanation of anomeric effect, several literature reports argue for the primary importance of electrostatic factors. For example, Wiberg and Rable acknowledge the complexity of anomeric effect but advocate for the greater importance of bond polarization and electrostatics[15] whereas Mo and coworkers uses Block Localized Wavefunction (BLW) analysis "to disprove the hyperconjugation explanation for the anomeric effect".[16, 17] Even though the authors state that "this disproval does not mean the rejection of the existence of hyperconjugative interactions within molecules", several other reports also conclude that hyperconjugation is less important than electrostatics. For example, Ferro-Costas, Mosquera and coworkers state that "QTAIM

properties dissent from the view of the hyperconjugative model, but agree with an interpretation based upon electron–electron repulsions".[18-24]

In the preceding companion paper, [25] we have analyzed the inherent complexity of this situation to show that such controversies are unavoidable when several factors contribute to the overall molecular energy in a similar way and when each of these factors corresponds to a relatively small perturbation of a very large total electronic energy. However, we also illustrated that it is the hyperconjugative interaction that defines the key reactivity trends. In the present manuscript, we will show the general picture of reactivity for the organic oxygen functional groups crumbles once hyperconjugation is removed from its conceptual foundation.
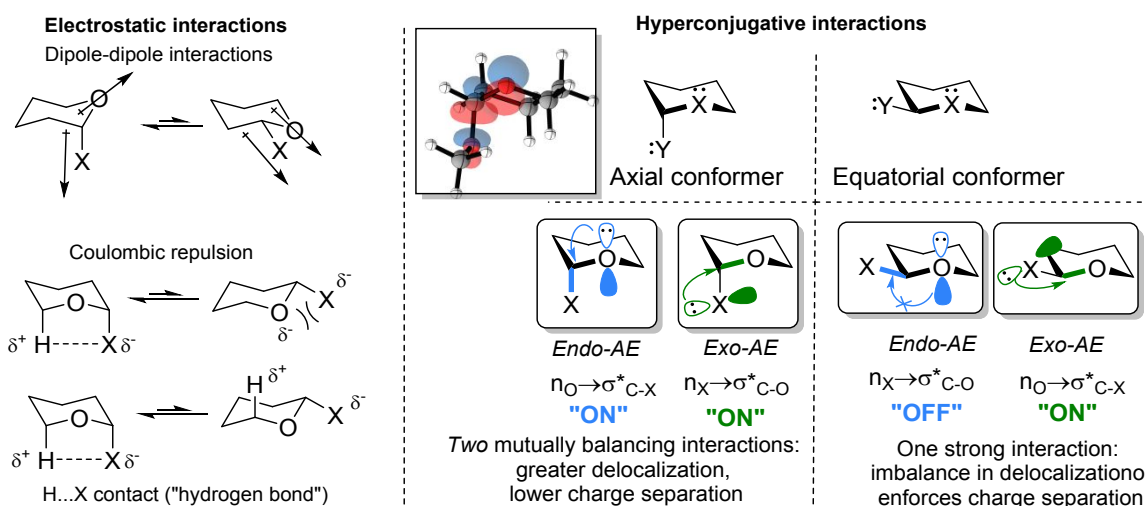
Figure 2. Literature explanations for the origin of the anomeric effect

In this manuscript, we will show that *all* O-containing functional groups that serve as the textbook backbone of organic chemistry benefit from delocalizing interactions that are analogous to the hyperconjugative contribution to anomeric effect.   As such interactions generally involve hyperconjugation from a lone pair at oxygen to σ-acceptors, we used the term "anomeric" broadly to denote this stereoelectronic interaction rather than the old definition of a carbohydrate conformational preference. In doing so, we refer our reader to the analysis of Filloux[26] who, when discussing how language influences our understanding of scientific phenomena, distinguished "anomeric effect" from "anomeric interactions". The "anomeric effect" is a cumulative phenomenon effect based on the interplay of orbitals, electrostatics, and steric factors in acetals whereas "anomeric interactions" are stereoelectronic orbital interactions originating from negative hyperconjugation (i.e., the donation from oxygen lone pairs to the antibonding C-X orbitals).

Separating "anomeric effect" from "anomeric interactions" explains how "anomeric" is used in a more general sense that transcends the historic definition of a conformational effect in the chemistry of carbohydrates.[26] Such expansion is useful because hyperconjugative "anomeric interactions" are found in many organic functionalities, both familiar and exotic. The acceptor C-X bonds are not limited to X=N,O,Hal - C-H bonds in certain molecules, i.e., the C-H bonds at sp²-hybridized carbons, can be stronger acceptors than the C-O bonds in the classic anomeric systems. Furthermore, donation from the oxygen lone pairs can affect chemistry of even relatively weak C-X acceptors when the C-X bonds are stretched and broken. As illustrated in Figure 3, the consequences of $n_O \rightarrow \sigma^*C\text{-}X$ hyperconjugation in organic chemistry are ubiquous and come in a rich variety of patterns and effects on stability, reactivity, molecular shapes, and supramolecular behaviour.
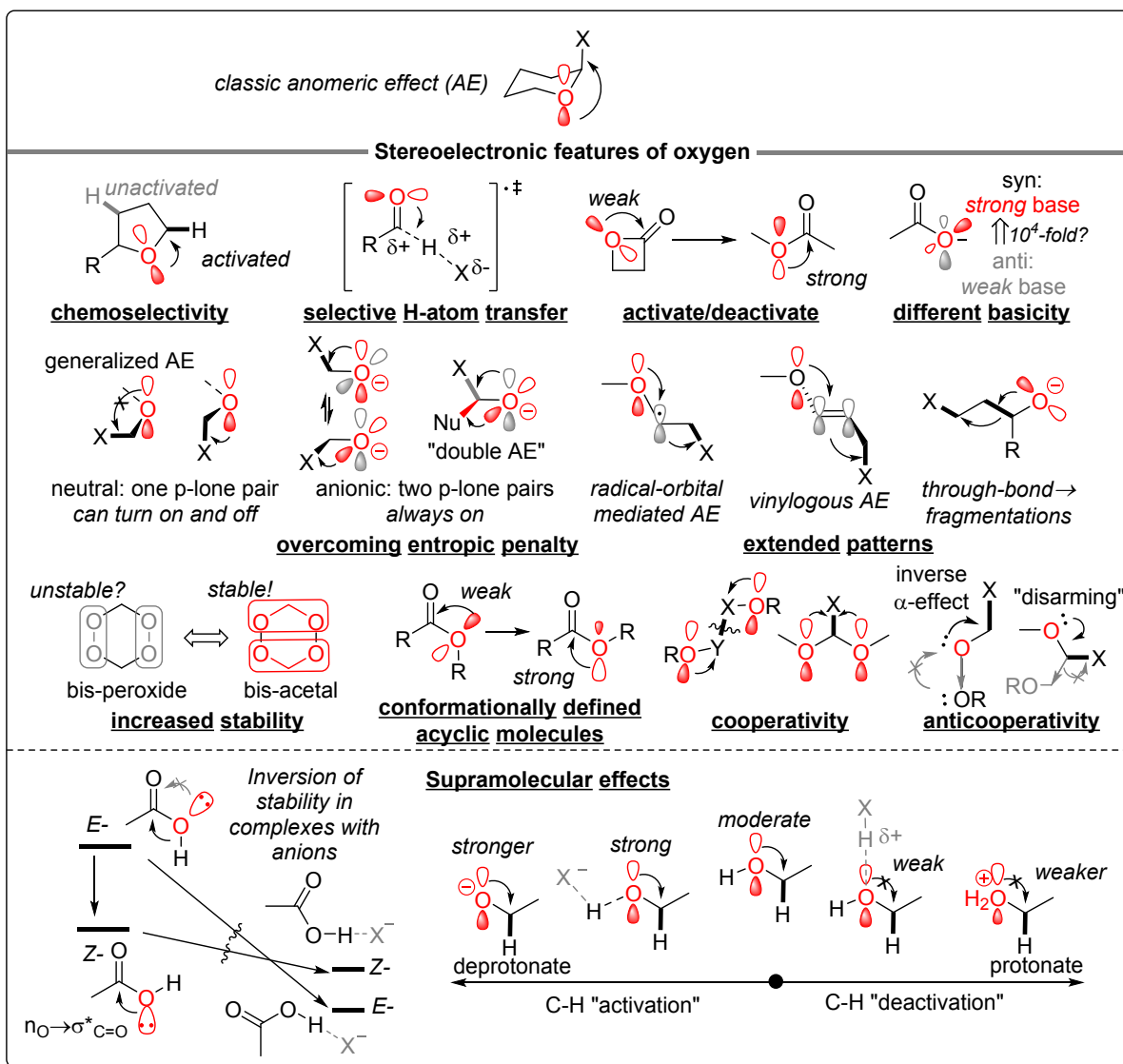
Figure 3. Selected stereoelectronic features of oxygen and their impact on organic chemistry beyond the classic anomeric effect

Even though we will uncover and describe a number of consequences of negative hyperconjugation, our goal is not to provide an exhaustive overview of all documented literature examples of anomeric effect. Rather, we hope that it can be a primer for organic chemists who want to understand how the stereoelectronic power of the lone pairs of oxygen can control reactivity and how to use this power to design new reactions.

In the following sections, we connect anomeric hyperconjugation with the important and useful reactivity patterns. Our narrative will be based on the progression from functional groups with a single oxygen atom, where anomeric interactions are weak in the ground state, to systems with multiple oxygen atoms, where a network of two or more strong anomeric interactions is present in the reactants. In these more complex systems, the alternative delocalizing interactions can either co-exist or compete. In chemical reactions, anomeric effects can either get sacrificed or be amplified, providing either a layer of stereoelectronic protection or a boost in reactivity.

In order to stay focused on the stereoelectronic attributes of oxygen, we will not include nitrogen functionalities in our present discussion. Nitrogen has its own interesting stereoelectronic features, including the inverse anomeric effect, but these features are outside of the scope of this review and will not be discussed here.
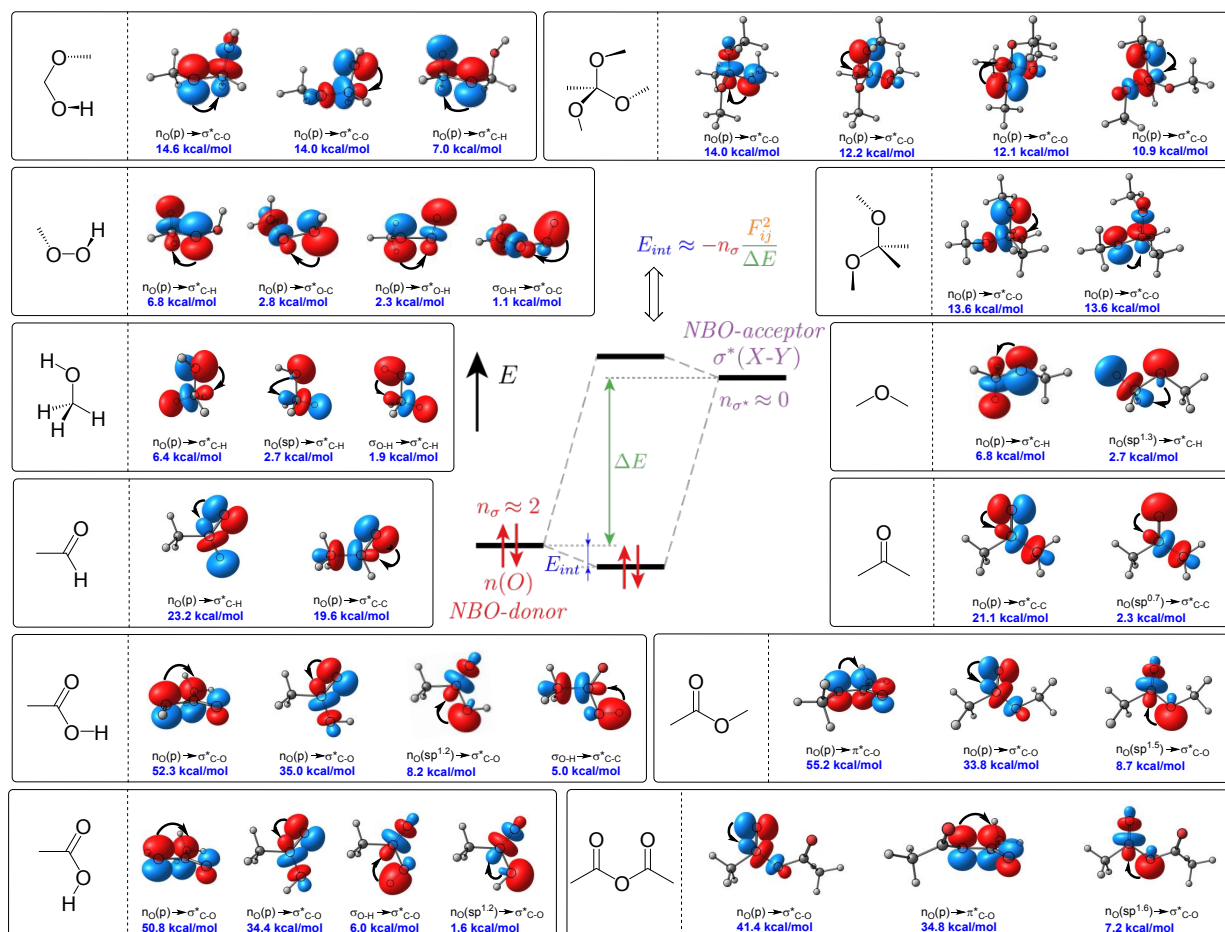
Figure 4. A selection of donor-acceptor anomeric interactions in organic O-functionalities. E_{int} values are computed for the Natural Bond Orbital method (NBO) using the second-order perturbation approximation for the PBE0-D3BJ/aug-cc-pVTZ/CPCM(H2O) level of theory. The orbital interaction diagram at the center of the scheme shows the equation used to calculate the interaction energy—E_{int}—and its contributors: F_{ij} is the Fock matrix element between natural bond orbitals i and j, ε_σ and $\varepsilon_{\sigma*}$ are the energies of the σ and σ* NBO's, and n_σ is the population of the donor orbital.[27]

As one can see, it is nearly unavoidable to have at least one bond aligned with the p-type oxygen lone pair. In the following sections, we will show that this bond is often the locus of chemical reactivity. Complexity of anomeric interactions increases with an increasing number of oxygen atoms. The constructive interplay of several effects can lead to interesting reactivity consequences. In order to lay the foundation for the more complex cases, we will start with the simplest members of this functional group family – alcohols and ethers.

Functional groups with one oxygen

In the classic anomeric systems (e.g., acetals), the oxygen lone pairs interact with relatively strong σ-acceptors, i.e., the C-X bonds to electronegative heteroatoms. Consequences of such strong anomeric interactions are quite obvious and have been well-recognized.[1, 28, 29] However, even in the absence of additional heteroatoms, a single oxygen atom of an ether or an alcohol can influence structure and reactivity in significant ways. For example, the effect of the oxygen lone pairs on the elongation of the coplanar C-D bonds is evident in the crystal structure of $CD_3OD…ND_3$ complex (Figure 5).
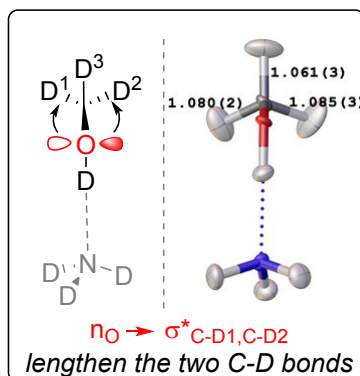
Figure 5. C-D bond lengthening due to $n_O \rightarrow \sigma^*_{C-H}$ interactions in a crystal of $CD_3OD…ND_3$ complex (powder neutron diffraction at 4.2K, CSD ID: HUWREX01).[30]

In the following sections, we will illustrate how anomeric assistance by oxygen can be used to break the usually unreactive C-C and C-H bonds. These strong non-polar bonds are weak σ-acceptors in the ground state where the effects of negative hyperconjugation are small. However, such effects can be dramatically amplified in the transition states as a consequence of a greater acceptor power of the breaking bonds. Although such effects are not always discussed in the context of anomeric effects, we will show that this connection can serve as the common theme for organizing the diverse reactivity of O-containing functionalities.

Such anomeric assistance can be observed in both homolytic and heterolytic α-C-X bond cleaving processes. As one would expect, the extent of such assistance correlates with increased electron demand due to the higher electron deficiency of the breaking bonds. Such increase is especially pronounced in heterolytic processes (e.g., a hydride shift) leading to the formation of an oxacarbenium ion, but they are also noticeable in homolytic processes that form radical species stabilized by a 2c,3e-bond. This is summarized in Figure 6 which describes a thought experiment where the two bond scissions, heterolytic and homolytic, at an anomeric center are compared to a hypothetical situation where the anomeric effect is not active and the cost for the heterolytic and homolytic C-X bond scission is identical. It shows how a

potential energy surface for the hypothetical idealized reaction would be changed once the anomeric effect is introduced and converted into either a dative π-bond with an empty p-orbital at the cationic center or into a 2c,3e-bond with a radical center. The differences between the top (idealized) and bottom (real) energy curves would reflect the extent of anomeric stabilization in the real system – the stabilization is expected to be higher for the more electron-deficient cationic systems.
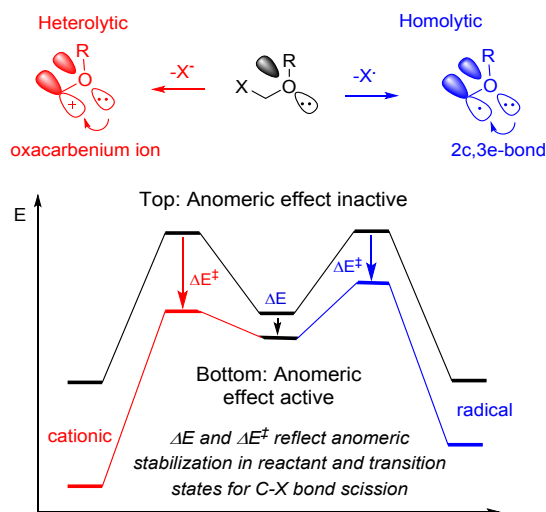
Figure 6. Formation of oxacarbenium ions and radicals stabilized by 2c,3e-interaction with the oxygen lone pairs via C-X bond heterolysis and homolysis is assisted by kinetic anomeric effect. The top energy surface corresponds to a strictly hypothetical idealized reaction where the anomeric effect is inactive and the thermodynamic costs for the heterolytic and homolytic C-X bond scission are identical.

Alcohols and ethers: the role of anomeric effect/lone pair assistance in C-H activation

A quick illustration of anomeric hyperconjugation with the participation of C-H bonds is provided in Figure 7. The $n_O \rightarrow \sigma^*_{C-H/C-C}$ interactions are moderate in magnitude (~6-7 kcal/mol at the PBE0-D3BJ/aug-cc-pVTZ level) but weaker than negative hyperconjugative interactions in the functional groups discussed later (with the exception of peroxides). The relative weakness of anomeric hyperconjugation in the ground state does not preclude it from playing a significant role in the chemical reactivity of alcohols and ethers. If these interactions are amplified as the C-H and C-C bonds are broken, negative hyperconjugation can provide selective transition state stabilization in C-H and C-C activating reactions.

$n_O(p) \rightarrow \sigma^*_{C-H}$: **moderate** $n_O(sp) \rightarrow \sigma^*_{C-H}$: **weak** $\sigma_{O-H} \rightarrow \sigma^*_{C-H}$: **weak**

$n_O(p) \rightarrow \sigma^*_{C-H}$
6.4 kcal/mol

$n_O(sp) \rightarrow \sigma^*_{C-H}$
2.7 kcal/mol

$\sigma_{O-H} \rightarrow \sigma^*_{C-H}$
1.9 kcal/mol

$n_O(p) \rightarrow \sigma^*_{C-H}$: **moderate** $n_O(sp^{1.3}) \rightarrow \sigma^*_{C-H}$: **weak**

$n_O(p) \rightarrow \sigma^*_{C-H}$
6.8 kcal/mol

$n_O(sp^{1.3}) \rightarrow \sigma^*_{C-H}$
2.7 kcal/mol

PBE0-D3BJ/aug-cc-pVTZ/CPCM(H$_2$O)
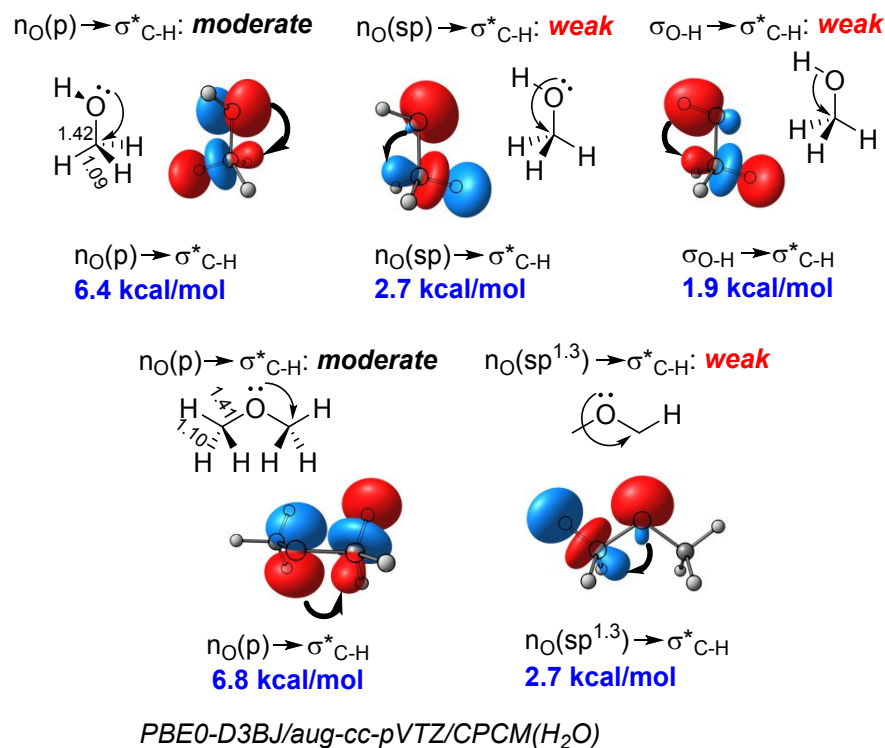
Figure 7. Stereoelectronic portraits of methanol and dimethyl ether

A variety of reactive intermediates can take advantage of anomeric assistance, especially if such intermediates are electron deficient. The stabilizing effect of oxygen is fully pronounced for the formation of carbocation species (~20 kcal/mol stabilization relative to a primary cation, Figure 8). If transition states (TS) for the formation of such cations are late, i.e., product-like, a large part of this stabilization is already present in the TS. Such TS stabilization lowers the activation barriers for α-hydride abstraction, explaining the relatively fast rate of such processes and their utility in C-H activation (*vide infra*).

Hydride Affinity

$H^- + H_2\overset{+}{C}-OH \xleftarrow{\Delta H = 252.4} H_3C-OH$ **Alcohol**

$H^- + H_2\overset{+}{C}-CH_3 \xleftarrow{\Delta H = 270.5} H_3C-CH_3$ **Alkane**
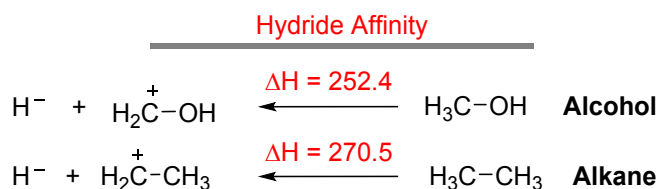
Figure 8. Lower hydride affinity in carbocations related to alcohols reflects the large stabilization of the cationic center by oxygen lone pairs (enthalpies calculated using the enthalpies of formation in the gas phase)[31]

The C-H BDEs in ethers indicate that the α-C-H bonds are weaker than sp^3 C-H bonds in hydrocarbons.[32] Comparison of calculated C-H BDEs in methane, ethane, methanol, and dimethyl ether suggests that both

the OH and OMe groups decrease the BDE by ~9 kcal/mol relative to H and ~5 kcal/mol relative to a Me group. A similar trend explains the 5 kcal/mol difference between the α- and β-CH BDEs in tetrahydrofuran.[33] This C-H weakening effect can be amplified by other factors. For example, the C-H BDEs in 1,4-dioxane is likely to reflect the captodative nature of this radical originating from the stereoelectronic chameleonism[34] of oxygen (α-oxygen is a p-donor, β-oxygen is a σ-acceptor, Figure 9). In this scenario, which has been referred to as "radical homoanomeric effect" by Giese and coworkers, the lone pair and the σ*C-O acceptor interact through the relay radical orbital.[35]

All values are in kcal/mol; most are experimental, except for two calculated marked with *
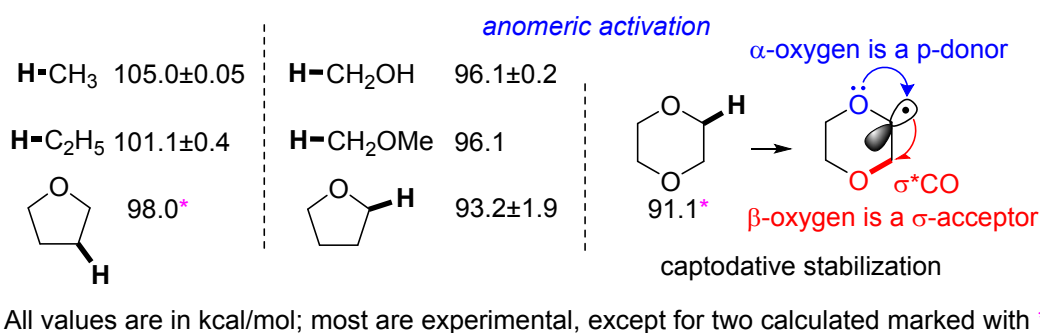
Figure 9. C-H bond dissociation enthalpies illustrating the lower strength of α-C-H bonds in ethers and methanol. Computed values (marked with asterisks) were estimated from isodesmic and isogyric reactions at CBS-Q/6–311+G(d,p) level of theory.[36]

White and coworkers reported selective C-H oxidations by H_2O_2 with a bulky, electrophilic Fe(II) catalyst and acetic acid as an additive.[37] Anomeric activation enables the selective oxidation of five- and six-membered cyclic ethers into lactone products (Figure 10). Interestingly, a bis-overoxidized product is formed from a seven-membered cyclic ether. In the latter case, the lactone formation is not observed and adipic acid is isolated instead in 87% yield. This interesting behavior is likely to be associated with variations in the anomeric assistance at the intermediate stages of C-H activation. The anomeric assistance is strong in the non-oxidized ether reactants but weakens dramatically, once the ether is converted into a lactone, where the $n_O \rightarrow \sigma$*$_{CH}$ interactions with the remaining CH_2 group are dramatically weakened since the lone pairs of the -O- unit are depleted by donation to the σ*CO and π*CO orbitals of the carbonyl. The sharp drop in anomeric activation is important because it partially protects the lactone products from over-oxidation. Apparently, this defense is weakened in more flexible seven-membered rings but the exact details of this interesting mechanistic scenario are still unknown.
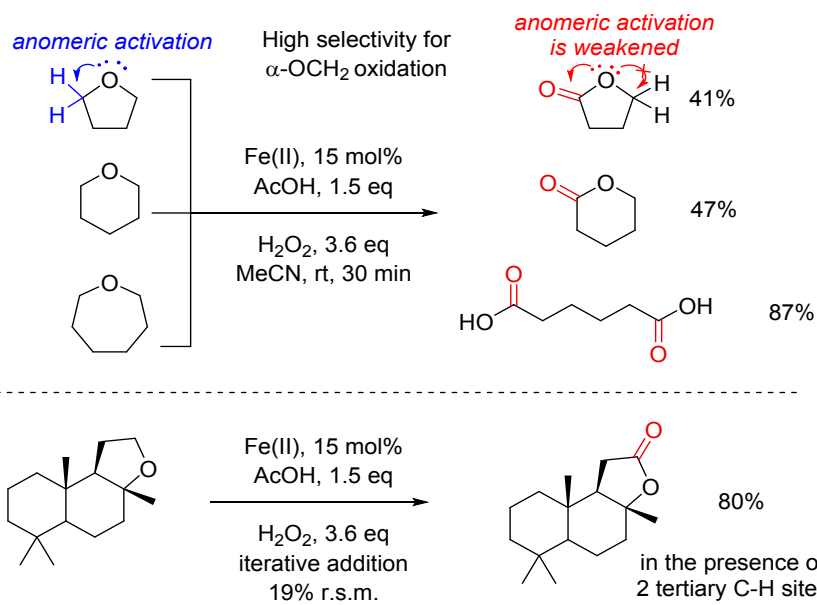
Figure 10. Top: The ring-size effects on the anomeric activation of aliphatic secondary C–H bonds in site-selective methylene oxidation. Bottom: highly selective oxidations of (−)-ambroxide

Anomeric assistance significantly increases the rate of homolytic C–H bond cleavage in cyclic ethers.[38] For example, Malatesta and Ingold reported that the tetrahydrofuran (THF) oxygen makes adjacent hydrogens ~2860 times as reactive as the hydrogens in cyclopentane towards t-butoxy radicals at -60 °C (Figure 11).[39]
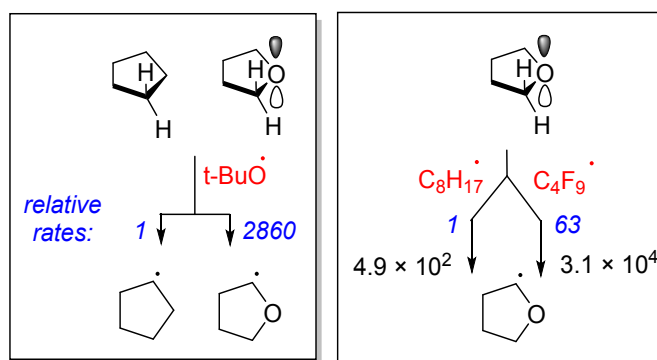
Figure 11. The activating effect of an α-oxygen on the rates of H-atom abstraction by t-BuO radical (left) and increased anomeric activation for reactions with electrophilic radicals (right)

Such effects become stronger when the breaking C-H bond interacts with a better acceptor, i.e., a more electrophilic radical. For example, Shtarev et al.[40] have shown that reactions of the n-perfluorobutyl radical with THF and diethyl ether at 22 °C (3.1×10^4 and 2.2×10^4 M^{-1} s^{-1}, respectively, in 1,3-bis-trifluoromethyl)benzene (BTB)) are much faster than the reactions of the n-octyl radical with the same H-

donors (4.9×10^2 and 1.2×10^2 M^{-1} s^{-1}, respectively).   This work illustrates that the rate constants for H-atom abstraction by the n-C$_4$F$_9$ radical takes greater advantage of the transition state polar effects. Increased donation from the α-oxygen atom to the breaking bond can stabilize the H-atom transfer TS, serving as one of such effects.

The anomeric activation also facilitates the formation of α-tetrahydrofuranyl radical from tetrahydrofuran in reactions with electrophilic radical species.[41-48] Intriguingly, the α-alkoxy radicals formed from ethers via H-abstraction by an electrophilic radical can be intercepted by Co[49] and Ni[50] catalysts to initiate synthetically promising cross-coupling reactions. A particular elegant example of C(sp^3)–H cross-coupling that took advantage of the unique properties of the α-oxy C(sp^3) C-H bonds was developed by Doyle and coworkers who used aryl chlorides as both the cross-coupling partners and the source of electrophilic chlorine radicals. Aryl chloride activation with the Ni catalyst under photoredox-mediated conditions generates a Ni(III) aryl chloride intermediate with a photochemically labile Ni-Cl bond (Figure 12).   The final cross-coupled product is formed via reductive elimination from the anomerically activated Ni(III) species.
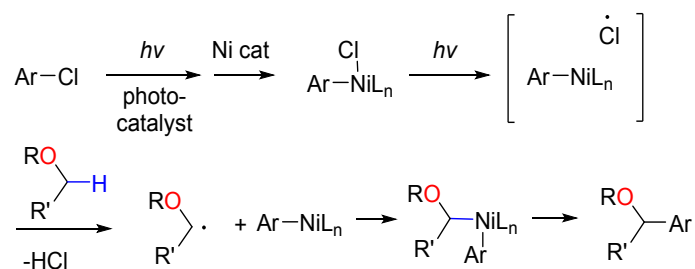
Figure 12.   Direct C(sp^3)–H cross coupling between ethers and aryl chlorides mediated by catalytic generation of chlorine radicals

As expected from the principle of microscopic reversibility, anomeric effect controls not only the radical generation but also the reaction of anomeric radicals with D(H)-donor. The radicals from ^{4}C$_1$-restricted carbohydrates transformed into α-products via α-attack, while β-products were obtained from ^{1}C$_4$-restricted substrates via β-attack.[51] In both cases, the radical center and the incipient C...D bond are aligned with the oxygen p-lone pair. The α- and β-stereoselectivity in S$_N$1-type anomeric allylation is also controlled by the kinetic anomeric effect by using similar conformationally restricted substrates (Figure 13).[52]
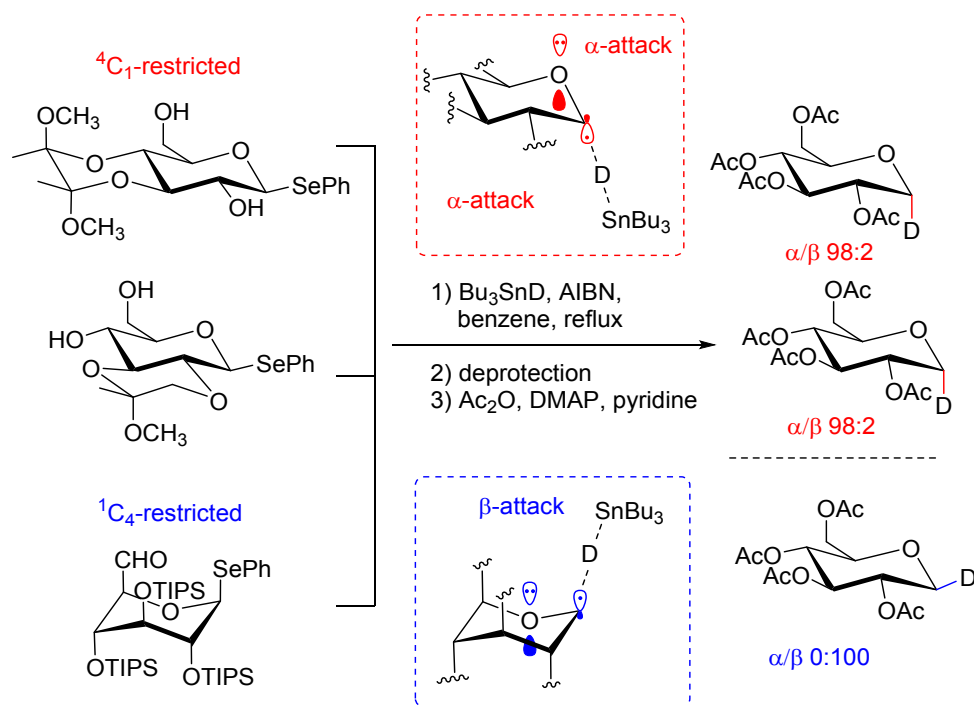
Figure 13. Control of selectivity in intermolecular H-atom abstraction using kinetic anomeric effect

The donor properties of α- C-H bonds in ethers are further illustrated by their reactivity to such highly electrophilic reagents as singlet O_2.[53] Although this species generally does not react with C–H bonds in saturated hydrocarbons, $^1O_2$ was recently reported to induce direct oxidative hydroperoxidation of α-C–H bonds of ethers with excellent site selectivity and good yields (Figure 14). The chemical reaction rate of THF with singlet O_2 (3.8×10^3 $M^{-1}s^{-1}$) is comparable with that for an inactivated olefin, e.g., 2-methyl propene (4.4×10^3 $M^{-1}s^{-1}$). This reaction rate corresponds well to a singlet O_2 lifetime of ~ 21 μs and to the measured quantum yield for the reaction of singlet O_2 with THF solvent (0.93).
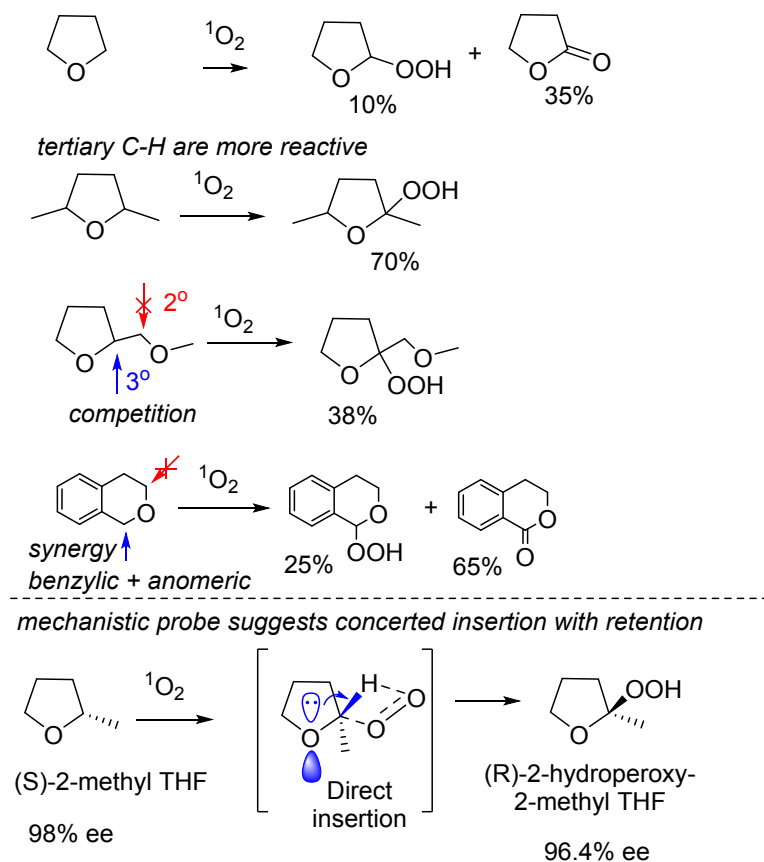
Figure 14. Reaction of singlet O_2 with α- C–H bond of ethers

Although stereoelectronic aspects of the hydroperoxidation of the α- C–H bond by singlet O_2, e.g., the reactivity towards axial and equatorial C-H bonds, remain unknown, chiral (*S*)-2-methyl THF (98% ee) yields (*R*)-2-hydroperoxyl-2-methyl THF in >96% ee. Hence, this reaction occurs via a single-step direct insertion process with retention of configuration. Furthermore, the process is sensitive to the C-H bond strength: the tertiary α-C-H bonds are more reactive than the C-H bonds in the OCH_2 and OCH_3 groups. This trend is in an agreement with the high electrophilicity of singlet oxygen, suggesting the electronic assistance provided by the anomeric effect has to be essential. The combination of benzylic and anomeric interactions leads to a synergistic activation. In the absence of a tertiary α-C-H bond, it is also possible to oxidize the OCH_2 groups. However, the α-C-H bonds in the resulting alkoxy hydroperoxides are more reactive than the α-C-H bonds in the starting materials, so over-oxidation to lactones is a problem.

The importance of anomeric effects in oxidation of C-H bonds with electrophilic reagents is well-illustrated in reactions of alkyl esters with methyl(trifluoromethyl)dioxirane (TFDO) reported by Asensio et al.[54] Because both O lone pairs at the internal ester oxygen are deactivated by interactions with the carbonyl group (vide infra), this oxygen cannot provide anomeric assistance to electrophilic C-H activation at the

adjacent positions (Figure 15). Furthermore, when the anomeric effect does not operate, oxygen acts as a deactivating substituent due to a combination of inductive effect, rehybridization, and hyperconjugation.[55]
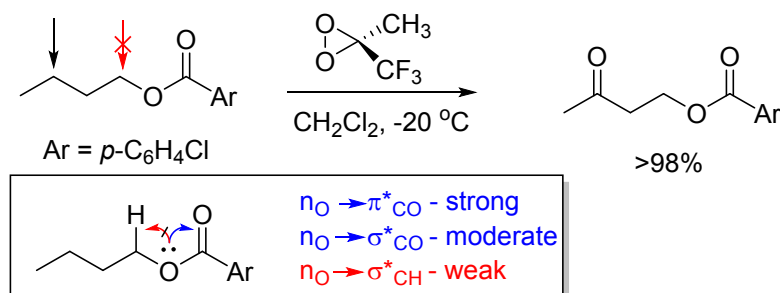
Figure 15. The α-C-H activating effect of α-oxygen substituent disappears once oxygen lone pairs are engaged in stronger conjugative and hyperconjugative interactions

Lee and coworkers illustrated the importance of anomeric activation on the insertion of alkylidene carbenes into C-H bonds (Figure 16).[56] Selectivity of this process reveals the stereoelectronic nature of the activating effect. Only the axial C-H_a bond aligned with the p-type lone pair of endocyclic oxygen was activated whereas the axial C-H_b bond remained untouched.
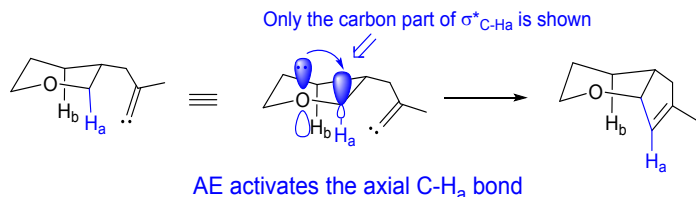
Figure 16. An axial C-H bond is activated stereoelectronically by the adjacent oxygen atom. The analogous equatorial C-H bonds are deactivated via a rehybridization effect. Only the carbon part of the targeted σ*C-H orbital is shown for clarity.

Rh-catalyzed insertion of acceptor-substituted carbenoid prefers the position next to the oxygen atom,[57] rather than the benzylic position. Davies et al. reported remarkable chemoselectivity achieved through modification of the oxygen substituent.[58] C-H insertion at the pentenyl silyl ether proceeded in 94% yield and high diastereoselectivity (>94% de). In contrast, C-H activation products in the analogous reaction with 2-pentenyl acetate were formed in a lower yield and, in agreement with the lack of anomeric activation, were derived from C-H activation at the alternate allylic site (Figure 17).
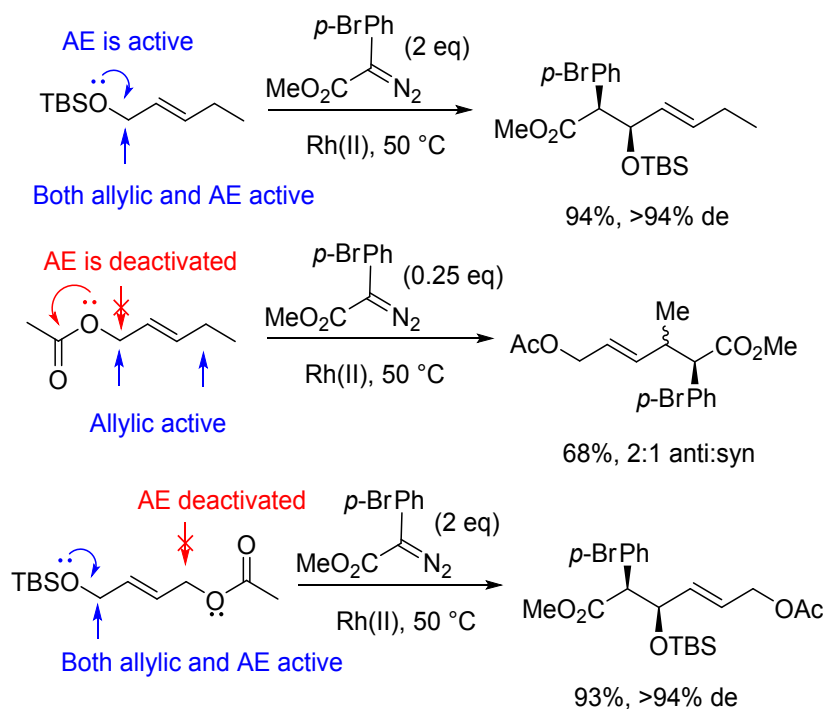
Figure 17. Lack of anomeric activation at an allylic site overrides allylic C-H activation. Therefore competition between allylic and anomeric C-H activation can be controlled by deactivation of anomeric effect in esters.

The activating influence of oxygen can be transmitted through the aromatic systems. Liang et al.[59] observed that Rh-catalyzed intermolecular C-H aminations by sulfonimidamides as the nitrene precursors is more efficient in substrates with *p*- or *o*-OR donor substituents than in ethyl benzene (Figure 18). Reactivity dropped even more in the presence of an electron-withdrawing *p*-nitro group. For 2,3-dihydrobenzofuran substrate, the nitrenoid insertion was only observed at the the benzylic position. Lack of reactivity at the α-position relative to the oxygen atom was attributed to "delocalization of the oxygen atom's nonbonding electrons into the aromatic ring decreasing the ability of this lone pair of electrons to activate the vicinal C-H bond."[60] Alternately, this result can be attributed to the synergy of benzylic activation with the "vinylogous" anomeric effect as the lone pair of oxygen can transmit its activating effect through the π-system. The combination of the benzylic activation and "vinylogous" anomeric effect accounts for the lack of C-H activation at the O-CH$_2$-group where only the single anomeric effect operates.
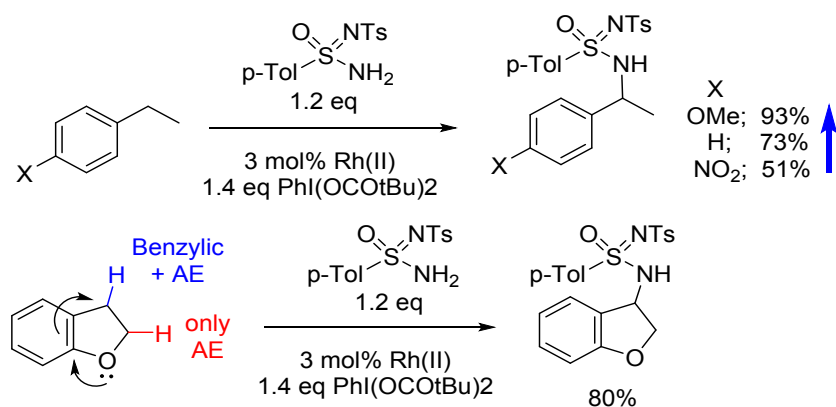
Figure 18. Activating effect of oxygen substitution in electrophilic C-H aminations can be transmitted through an aromatic system

The next logical step in increasing the electron demand while activating C-H bonds is to progress from H-atom transfer to hydride transfer. The hydride departure would create a cationic center, the perfect electron-deficient environment for taking the full advantage of donor properties of an adjacent oxygen atom. Because a hydride shift in a neutral system would separate charges, this is a generally unfavorable process but anomeric activation can overcome this penalty. Thus, hydride transfers with the formation of anomeric cations are quite facile and useful in a variety of ways.[61, 62]

When a carbocation already exists, hydride shifts are much easier as the charge separation penalty does not apply. For example, a cyclic ether intermediate in an unusual functionalization of olefins reported by Kataoka and co-workers readily undergoes a transannular 1,5-hydride shift to a carbocation center.[63] The resulting oxacarbenium intermediate undergoes hydrolysis during the workup to afford the final hydroxyketone product (Figure 19).
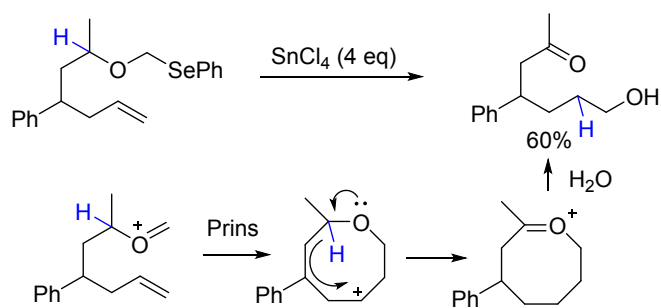
Figure 19. Anomeric assistance to transannular hydride shift

Of course, the story of anomeric assistance to hydride shifts goes back to pinacol and semi-pinacol rearrangements where oxygen anomeric assistance to heterolytic bond scission is essential for these

processes. Calculated TS structures for the 1,2-H-shift have the oxygen p-type lone pair aligned with the breaking bond (Figure 20).[64]
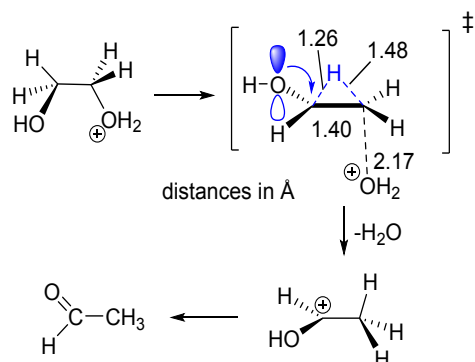
Figure 20. Anomeric assistance to pinacol rearrangement in ethylene glycol

Maulide and coworkers used an intramolecular Prins cyclization to create a cyclic ether intermediate with a carbocation center.[65] The cyclization step is suggested to proceed through an endo-trig ring closure at an oxacarbenium ion. One can also suggest an exo-tet cyclization of an anomerically activated protonated hemiacetal (Figure 21).[66] When this cascade is started with a chiral alcohol, this sequence can be used for a directed enantio- and diastereoselective formal aldehyde alkylation.
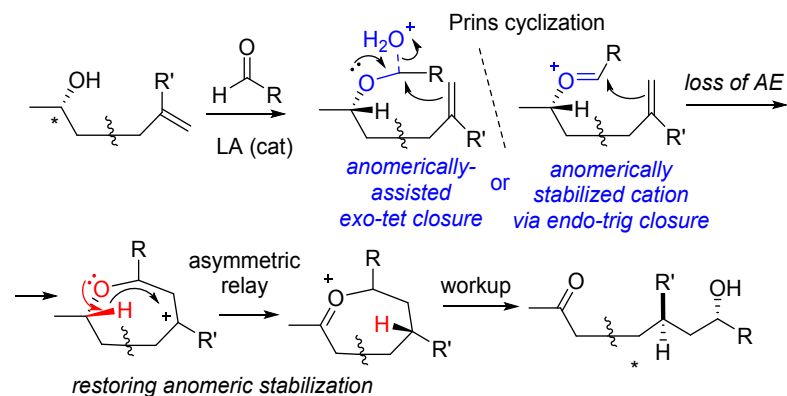
Figure 21. Anomeric assistance to the formation of cationic precursor for an anomerically-assisted hydride shift: note that a single oxygen atom controls reactions at two different carbons via anomeric interactions.

A diastereoselective hydride transfer was developed by Gagosz, Chiba and coworkers using methyl ethers or acetals as hydride donors and tertiary alcohols or alkenes as carbocation precursors under acid-catalyzed reaction conditions.[67] The selectivity was suggested to originate from the pseudo-equatorial preference for substituents in a 6-membered chair-like transition state. Note that the "exo-anomeric" interaction successfully competes with the combined effect of benzylic stabilization and additional alkyl groups in competition for the cationic center (Figure 22).
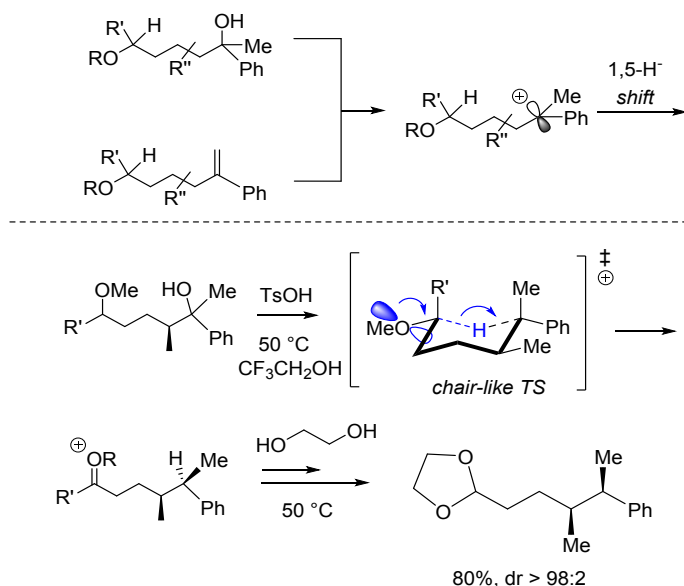
Figure 22. Exo-anomeric assistance to 1,5-hydride shift

A number of interesting transformations where the role of such an acceptor is played by a cationic alkyne π-complex were described by groups of Sames and Gagosz.[68, 69] Cationic catalyst alleviates the charge separation penalty. In these examples (Figure 23), even a single anomeric donor in combination with a cationic acceptor can lead to a productive intramolecular hydride shift in an ether. The anomeric interactions ensure high regioselectivity of Lewis acid catalyzed hydride transfer from THF to the activated alkyne.[61]
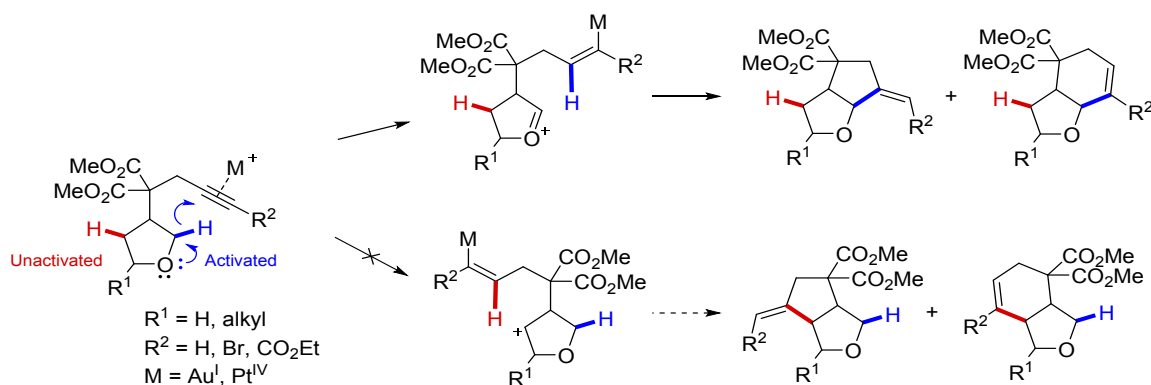
Figure 23. Anomeric assistance accounts for the chemoselectivity of Lewis acid catalyzed hydride transfer that initiates a cyclization cascade.[68, 69]

Anomeric anions and anomeric nucleophiles

Despite being destabilized by the antibonding interaction of the oxygen lone pairs and the anionic center, anomeric anions have interesting properties.[70, 71] The equatorial α-Li derivative is ~5 kcal/mol more stable than the axial Li-derivative (Figure 24).[72] An interesting feature of the axial conformer is that instead of having a classic C-Li bond, this species prefers a geometry where the Li-cation coordinates with both the C-anion and the O-lone pair.

Axial   Equatorial

Energy in kcal/mol, M06-2X/def2QZVP
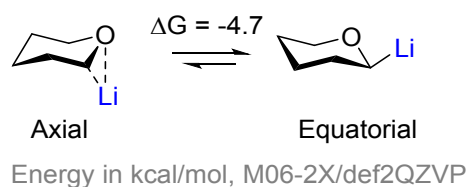
Figure 24. Calculated axial/equatorial difference for the anomeric R-Li THP derivative[72]

Because the acidity of the C-H bonds in ethers is quite low (pK$_a$ of dimethyl ether in DMSO is 49),[73] the formation of anomeric anions in the absence of a carbanion-stabilizing group attached to the anomeric carbon mostly relies on reductive metalation. In particular, 2-lithiotetrahydropyrans can be readily obtained by lithiation of 2-(thiophenyl)tetrahydropyrans.[74-76] Independent of the stereochemistry of the reactant, the initially formed kinetic product corresponds to the axial anion. This interesting observation was attributed to the intermediate formation of an anomeric radical in a process believed to be initiated by electron transfer to the σ*C-S orbital with subsequent C-S fragmentation via the loss of the thiolate anion (Figure 25). This non-planar radical rapidly equilibrates between the quasi-equatorial and quasi-axial epimers and exists largely in the axial configuration where the radical center can be stabilized better by the overlap with the oxygen p-type lone pair. Upon one electron reduction, the kinetically formed product is the axial carbanion, which is metastable towards isomerization into the equatorial anion but protected by the relatively slow rate of the inversion process.

The carbanion formation slows down the axial/equatorial equilibration because carbanions (as well as their Li-analogs) are generally more configurationally stable than radicals. Furthermore, the anomeric anions are more configurationally stable than alkyl anions due to hybridization effects. As a consequence of Bent's rule, carbon puts more p-character to its bond to oxygen, a more electronegative element.[77] This leaves more s-character in the lone pair and increases pyramidalization in anomeric carbanions. Such pyramidalized anions better resist planarization and epimerization.
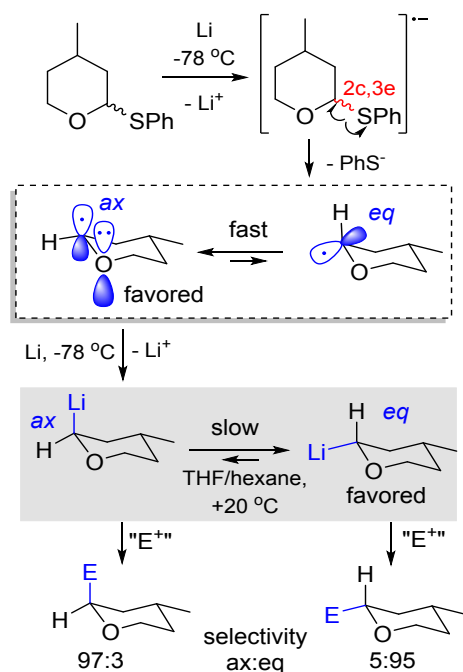
Figure 25. Kinetic and thermodynamic control in the anomeric anion formation allows stereoselective reactions with electrophiles (the reported numbers correspond to reaction with acetone)

Upon warming, the axial kinetic products can be efficiently epimerized to the more stable equatorial 2-lithiotetrahydropyrans. These preferences are consistent with the σ^*_{C-H} orbitals being better hyperconjugative acceptors than σ^*_{C-Li} orbitals. In addition, organolithium compounds generally exist as aggregates in solution, so the steric effects favoring the equatorial conformers are likely to be significant. From that point of view, it is remarkable that the metastable kinetic axial products persist long enough to be effectively trapped.

Recently, Herzon disclosed an elegant application of these ideas to the synthesis of di- and tri-glycosides.[78] Understanding kinetic and thermodynamic behavior of anomeric anions provides efficient access to both α- and β-anomers of 2-deoxy and 2,6-dideoxyglycoside products from simple carbohydrate donors without directing groups and glycosyl promotors (Figure 26). One can either trap the initially formed axial anion or let the anomeric effect to assist in transforming such anion into the more stable equatorial conformer that can be trapped at a later point.

Additionally, MP2/6-311+G(d,p) computations found that even remote ring substituents in sugars and their deoxy-analogs can have a significant impact on the relative stability of the axial and equatorial anomeric anions which are consistent with the effect of O-chelation and through-bond hyperconjugative interactions (i.e., the double hyperconjugation[79]). These effects can compete with the direct anomeric interactions and mask their consequences.

LiDBB: lithium di-tert-butylbiphenylide
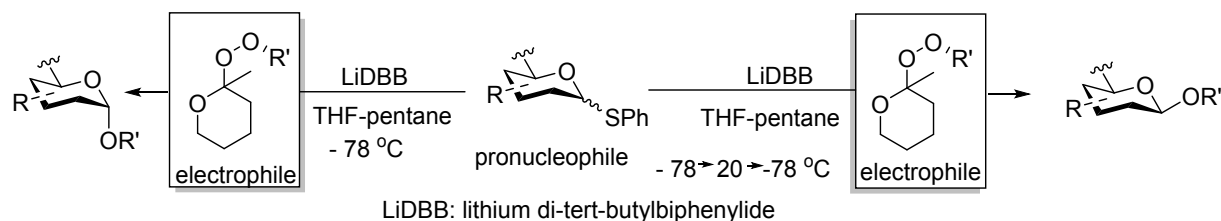
Figure 26. Application of selection formation of anomeric anions to glycoside synthesis.

Other α-C-X bonds in ethers are also anomerically activated.

A lot of attention has been devoted recently to anomeric stannanes – due to low electronegativity, Sn is an intrinsically good nucleophile. However, at the same time, the C-Sn bond is a good hyperconjugative acceptor that can take advantage of the α-oxygen lone pairs. This seeming paradox is well understood to originate from the relatively low σ^* energies characteristic for the weak bonds.[80, 81]

Falck and coworkers found that α-alkoxystannanes undergo Stille-type cross-coupling with acyl chlorides with the formation of α-hetero-substituted ketones when cocatalyzed by Pd and Cu(I) salts.[82] Although α-benzoyloxy or acetyloxy groups were used more often, the MOM ethers also react well. Coupling of chiral α-alkoxystannanes proceeds with retention of configuration (Figure 27).

MOM = -CH$_2$OCH$_3$
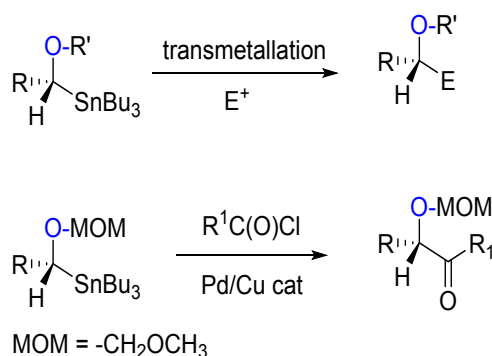
Figure 27. The utility of α-alkoxystannanes as nucleophilic reagents

Bode and coworkers used reliable reactivity of α-alkoxy stannanes for the development of Stannyl Amine Protocol (SnAP) reagents for the synthesis of N-heterocycles.[83] These bifunctional reagents use an aldehyde as a functional group for cross-coupling and as the source of one of the carbon atoms in the ring. The initial intermolecular coupling of the two starting materials takes place via imine formation whereas the second, intramolecular cyclization step is likely to benefit from the anomeric activation of the C-Sn bond (Figure 28). Note that the anomeric C-Sn bond is the only one of four C-Sn bonds of the tetralkyl tin

moiety that undergoes activation in the presence of Cu catalyst. The activating α-heteroatom (O or N) can be either endocyclic or exocyclic.[84]
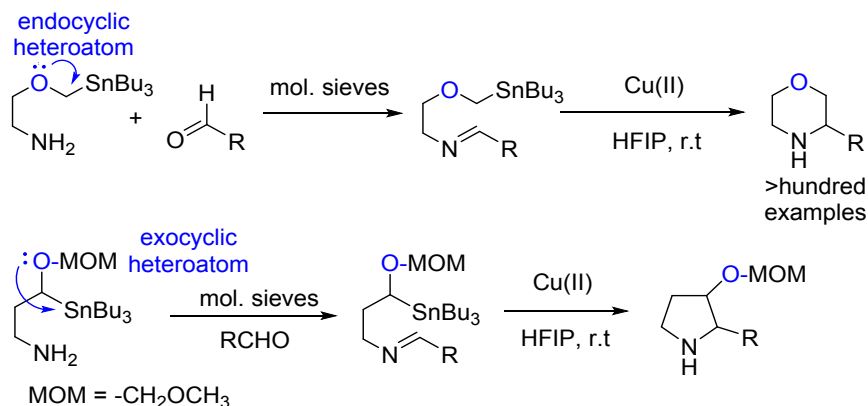
Figure 28. The utility of anomeric stannanes as Stannyl Amine Protocol (SnAP) reagents

Although the present mechanistic conjecture is that the organostannane is converted to a carbon radical upon oxidation by copper, as an enantiomerically enriched SnAP-reagent gave a racemic product expected from a radical pathway, the significant enantioselectivity observed for the ring closure of a racemic reagent in the presence of chiral ligands, suggests that the copper center is likely to be intimately involved in the cyclization step.[85] Hence, the full mechanistic picture may be quite complex and one cannot completely rule out a Sn to Cu transmetalation followed by nucleophilic addition to the imine. Such transmetallations are known and have been reported to occur with stereoretention.[82, 86] Many of the SnAP reagents are commercially available and have been used for the synthesis of heterocyclic systems of different sizes including a variety of bi- and spiro-cycles.

As discussed earlier, augmenting the inherent weakness of carbon-tin bonds by anomeric activation opens an attractive approach to stabilized C-centered radicals. Walczak and coworkers merged Cu(I) catalysis with blue light irradiation to develop highly stereoselective C(sp^3)–S cross-coupling reactions.[87] Careful mechanistic studies and computational analysis evaluated possible photochemical and/or Cu-catalyzed scenarios. Both the inner-sphere pathway where the Cu-C bond is preserved and the outer-sphere pathway where an anomeric radical is formed transiently are assisted by anomeric delocalization and lead selectively to the formation of α-thioglycosides (Figure 29).

PMP = p-methoxyphenyl
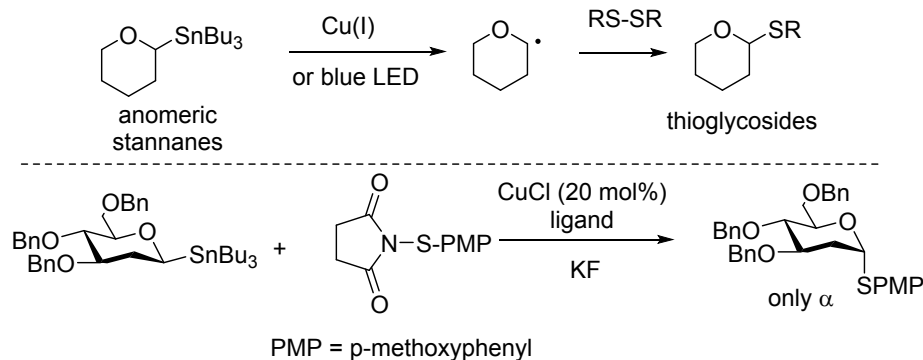
Figure 29. Use of anomeric stannanes in highly stereoselective C(sp^3)–S cross-coupling reactions

Other anomeric nucleophiles find synthetic applications as well. For example, Molander has used potassium 1-(alkoxy)alkyltrifluoroborates as partners in palladium-catalyzed cross-coupling reactions with a variety of aryl and heteroaryl chlorides in high yields. These reactions proceed with complete retention of configuration and allow one to use enantioenriched nucleophilic species with virtually no loss of enantiomeric purity regardless of the cross-coupling partner.[88]

Very recently, Zhu and Walczak[72] calculated conformational preferences of tetrahydropyran rings substituted with a transition metal at the anomeric carbon. In many cases, late transition metals were found to adopt the axial position at C2 of tetrahydropyrane or synclinal geometry in acyclic systems (Figure 30). Authors explained the observed preferences by hyperconjugative interactions between the endocyclic heteroatom and the σ* acceptor orbitals of the C–M bond ("the metalloanomeric effect"). The anomeric preferences of late transition metals correlate with the oxidation state of the metal and reveal potentially useful factors in the design of new metal-catalyzed reactions.

Figure 30. Conformational analysis of the axial/equatorial differences in substituted tetrahydropyrans at M06-2X/def2QZVP//M06-2X/def2TZVP level. $\Delta E(O)$ refers to the difference of electronic energies between equatorial and axial isomers in a substituted tetrahydropyran in a chair form (Gibbs free energies at 298 K reported in parentheses). $\Delta E(CH_2)$ refers to the difference of electronic energies between equatorial and axial isomers in a substituted cyclohexane in a chair form (Gibbs free energies at 298 K reported in parentheses). AE refers to the difference of electronic energies and Gibbs energies at 298 K (in parentheses). Background coding: orange/blue = equatorial/axial isomer preferred. Phen = 1,10-phenantroline, Me = methyl. (Figure adopted from ref. 72 with permission from American Chemical Society, copyright 2020)

Figure legend:

$\Delta E(O) = E_{eq}(O) - E_{ax}(O)$ Eq. (1)
$AE = \Delta E(O) - \Delta E(CH_2)$ Eq. (2)

Element / R group / $E_{eq}(O) - E_{ax}(O)$ / AE

1	2	10	11	12	13	14	15	16	17
Li Li -4.80 (-4.69) -5.90 (-5.60)	**Be** BeCl -0.96 (-1.23) -1.46 (-1.73)				**B** B(OMe)$_2$ -0.46 (-1.24) -0.73 (-0.30)	**C** CMe$_3$ -6.00 (-6.91) -1.34 (-0.39)	**N** NMe$_2$ 1.01 (0.66) 0.86 (0.51)	**O** OMe 1.33 (1.35) 1.38 (1.80)	**F** F 2.47 (2.29) 2.59 (2.51)
Na Na -3.80 (-3.34) -5.46 (-4.71)	**Mg** MgCl -6.13 (-5.85) -7.53 (-7.45)				**Al** Al(OMe)$_2$ -4.55 (-4.17) -5.82 (-5.22)	**Si** SiMe$_3$ -3.16 (-5.25) -1.19 (-1.85)	**P** PMe$_2$ -1.06 (-1.38) 1.42 (2.97)	**S** SMe 1.04 (0.48) 1.65 (0.89)	**Cl** Cl 3.29 (2.91) 3.52 (3.30)
K K -3.40 (-3.56) -5.17 (-3.81)	**Ca** CaCl -6.04 (-5.62) -0.71 (-2.97)	**Ni** NiClPhen 0.41 (0.64) 2.83 (3.25)	**Cu** Cu 3.13 (2.29) 1.75 (0.77)	**Zn** ZnCl 0.92 (1.78) -0.25 (0.95)	**Ga** GaMe$_2$ 0.07 (-1.07) -1.32 (-4.12)	**Ge** GeMe$_3$ -2.26 (-4.44) -0.94 (-1.91)	**As** AsMe$_2$ -0.81 (1.26) 0.15 (2.22)	**Se** SeMe 1.60 (1.66) 2.23 (2.11)	**Br** Br 4.16 (3.79) 4.33 (4.14)
Rb Rb -3.05 (-3.05) -2.61 (-1.77)	**Sr** SrCl -5.34 (-5.90) -3.58 (-5.50)	**Pd** PdClPhen 3.02 (3.25) 4.86 (5.73)	**Ag** Ag 4.01 (4.23) 2.43 (1.94)	**Cd** CdCl 1.61 (1.21) 0.31 (-0.10)	**In** InMe$_2$ 0.13 (0.12) -1.65 (0.17)	**Sn** SnMe$_3$ -1.04 (-4.34) -0.85 (-2.83)	**Sb** SbMe$_2$ -0.96 (-3.58) -0.32 (-2.87)	**Te** TeMe 1.59 (1.56) 2.07 (1.95)	**I** I 4.54 (4.06) 4.70 (4.46)
Cs Cs -3.10 (-3.66) -4.91 (-5.10)	**Ba** BaCl -4.53 (-5.70) -0.72 (-2.98)	**Pt** PtClPhen 2.50 (2.20) 4.18 (4.84)	**Au** Au 4.73 (4.23) 3.88 (3.17)	**Hg** HgCl 1.88 (1.53) 0.94 (1.01)	**Tl** TlMe$_2$ -0.87 (1.18) -0.70 (-0.74)	**Pb** PbMe$_3$ 0.46 (-1.09) 0.12 (-1.12)	**Bi** BiMe$_2$ -0.91 (0.15) -0.54 (2.23)	**Po** PoMe 1.86 (-3.30) 2.23 (-3.07)	**At** At 4.81 (4.38) 4.92 (4.72)

Alcohols:

Intrinsically, the donor abilities of the lone pairs of ethers and alcohols are similar. This similarity sometimes leads to problems with chemoselectivity if both the ether and the alcohol functionalities are present in the same molecule. From this point of view, the most useful property of anomeric $n_O \rightarrow \sigma^*_{C-H}$ delocalization in alcohols is that it is variable and tunable.

Oxidation of alcohols to ketones is a common problem associated with C-H activation in methylene groups. It arises because the alcohol products have weaker, anomerically-activated, C-H bonds than the reactant hydrocarbons. In order to prevent the over-oxidation of alcohols, their anomeric activation

should be weakened or, ideally, fully suppressed. Such control can be based on either a chemical transformation or a supramolecular coordination.

This utility of chemical transformation in control of anomeric interactions is well illustrated by the work of Wender et al. on oxyfunctionalization of bryostatin analogue.[89] Although their reaction with dimethyl dioxirane (DMDO) is remarkably selective for only one position (C-9) among the several available ether functionalities, the selectivity suffers if a secondary alcohol was present at C26, since the latter underwent competitive oxidation to a ketone. An elegant solution to this problem comes from converting the C-26 alcohol to an acetate derivative where the anomeric C-H activation is largely suppressed. This stereoelectronically cognizant modification completely inhibited C-26 oxidation and led to highly selective C-9 hydroxylation (Figure 31).
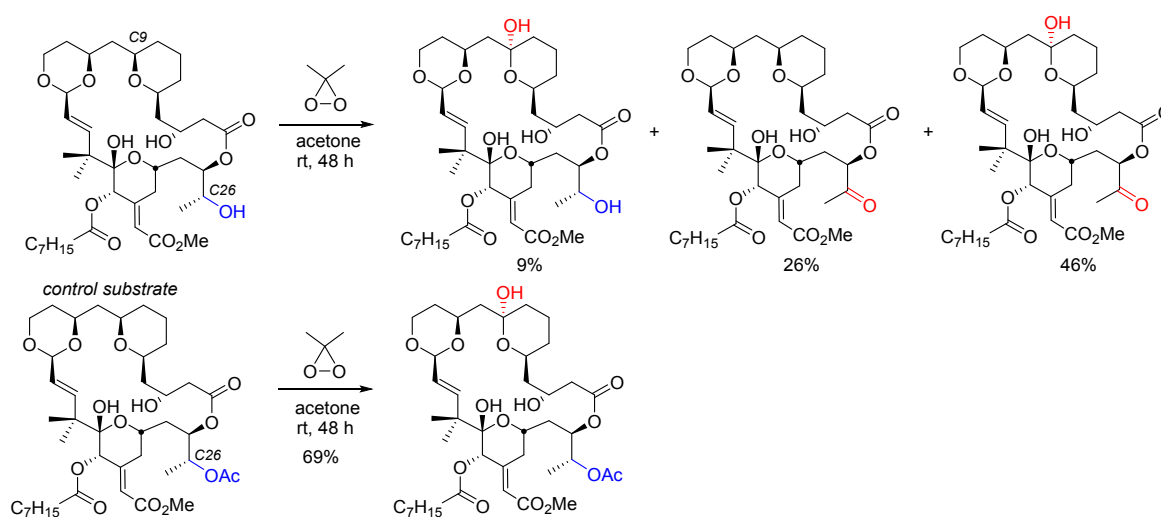
Figure 31. Preventing the undesired C-H activation by converting alcohols into esters in order to deactivate anomeric $n_O \rightarrow \sigma^*_{C-H}$ interaction

An elegant supramolecular solution to moderating anomeric activation is provided by using fluorinated alcohols, such as 2,2,2-trifluoroethanol (TFE) and 1,1,1,3,3,3-hexafluoro-2-propanol (HFIP), as solvents.[90] Both TFE and HFIP engage in hydrogen bonding with the initially formed alcohol product, thus preventing over-oxidation by deactivation of the α-C–H bond. This concept is commonly referred to as "polarity reversal" but it can also be described as a decrease of anomeric assistance by lowering the donor ability of the oxygen (Figure 32). It is surprising how efficient this relatively subtle perturbation is reported to be.
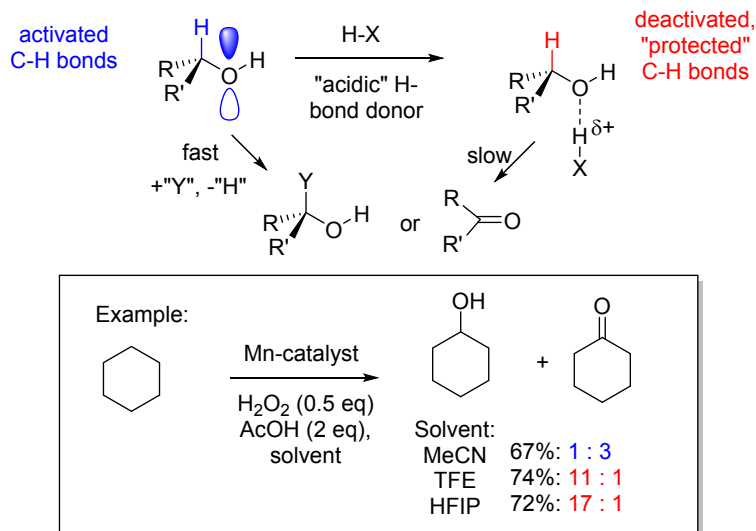
Figure 32. Top: The "polarity reversal" concept as an example of weakened anomeric assistance. Bottom: an example of selective oxidation of methylenic C–H bonds in a hydrocarbon by using solvent effects

An elegant further expansion of this concept is to use alcohols, ethers, amines, and amides, i.e., the functionalities generally vulnerable towards oxidation but made relatively robust by this effect, as directing groups for predictable C–H oxidations at remote positions. In the absence of hyperconjugative activation the α-C-bonds can be stronger than hydrocarbon C-H bonds due to rehybridization (increased s-character in the C-H bond forming carbon hybrid orbital) as a consequence of Bent's rule (Figure 33).[91]
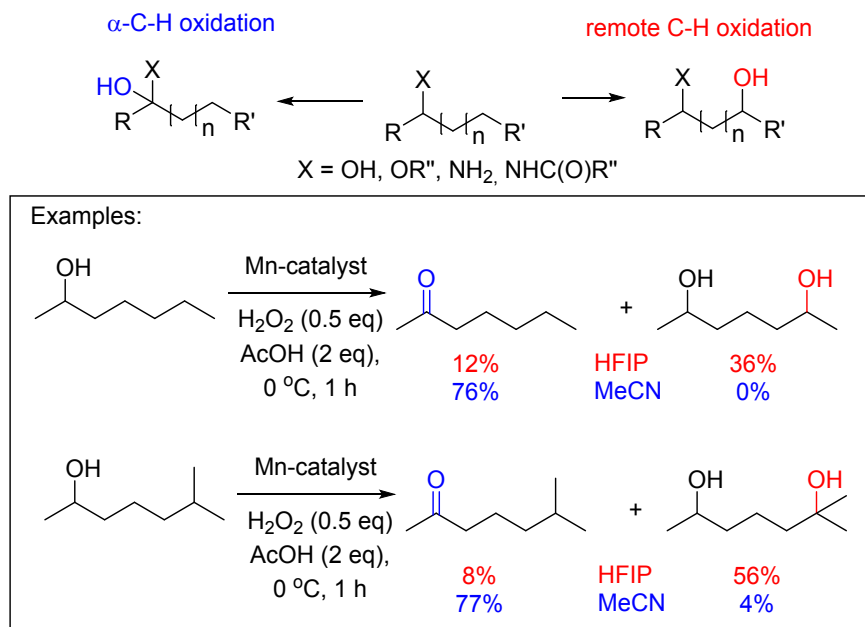
Figure 33. Protection of α-C-H bonds of alcohols from oxidation allows the use of alcohols as directing groups for remote oxidation

In principle, the deactivating effect of O…H-X hydrogen bonding with acidic partners can be applied to all O-containing functionalities. On the other hand, the activating effect of O-H…Y hydrogen bonding is a unique feature of alcohols. From the practical point of view, it should provide a way to selectively activate alcohols in the presence of ethers as only in alcohols the anomeric donation from oxygen can be amplified when the OH group is H-bonded to a basic partner.

These effects account for the significant solvent effects on the rate of radical H-abstraction from alcohols.[92] For example, the importance of oxygen lone pair assistance explains why the 2–5 fold rate enhancements in water vs. 1,3-bis(trifluoromethyl)benzene were observed for α-H-atom abstraction from alcohols but not from ethers with a RCF_2 radical (Figure 34).

Reaction with $RCF_2^{\bullet}$	$10^3 \times k_H / M^{-1}s^{-1}$	
	in BTB	in H_2O
(oxane structure)	31	33
(isopropanol structure)	3	12
(2-propanol diol structure)	16	48
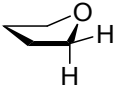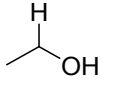
BTB = 1,3-bis(trifluoromethyl)benzene

Figure 34. Effect of water on the rate of H-abstraction in ethers and alcohols.

The protonation state of alcohols can either activate or deactive the α-C-H bond. Computed C-H BDEs for the α-C-H bond in methanol, methoxide, methoxonium cations and their H-bonded complexes reveal significant changes in the C-H bond strengths (14 kcal/mol increase upon protonation and 21 kcal/mol decrease upon deprotonation**Error! Reference source not found.**). [93] These changes illustrate clearly the importance of oxygen lone pairs in reactivity. Deprotonation increases electron density in the oxygen lone pairs and further activates the α-C-H bond by stabilizing the developing radical center through the much stronger hyperconjugative electron delocalization (Figure 35). On the other hand, when the oxygen atom is protonated, the remaining lone pair becomes a weak donor, the stabilizing effect by donation from the oxygen to the radical center is lessened, and the α-C-H bond becomes stronger.
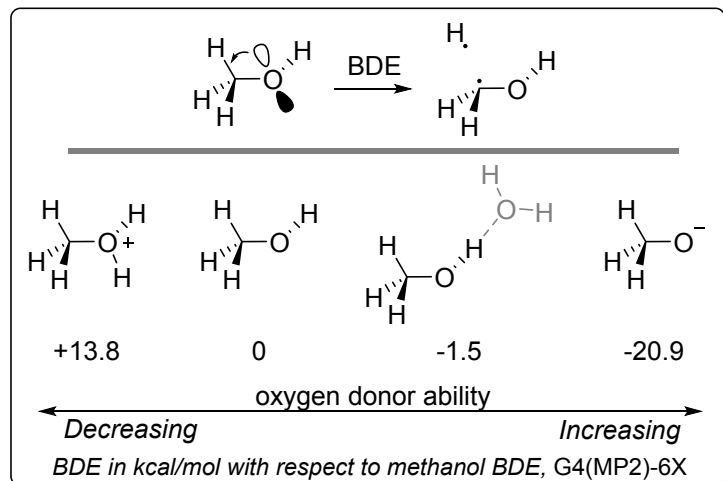
Figure 35. Effect of protonation, deprotonation and X…H-O hydrogen bonding on the BDE of the alcohol α-C-H bonds. Deprotonation and H-bonding increase the donor ability of the oxygen lone pair resulting in a smaller C-H BDE.[93]

Similar C-H weakening effects have been also observed by NMR- and IR-spectroscopic studies of alcohols that illustrate that negative hyperconjugation is already significant in the ground state, well before the α-C-H bonds are stretched or broken.[94, 95]

These observations suggest that perturbations in local pH or electrostatic effects can be used to control stereoelectronics. An interesting example of such selectivity control is provided when H-bonding of an OH group to an anionic moiety activates an adjacent hydrogen in the presence of multiple other α-OR C-H bonds (Figure 36). One can suggest that this activation is the origin of selectivity in H-atom transfer involved in operation of RNR Class 1 enzyme where the OH group at the ribose C3' position is H-bonded to a carboxylate moiety of Glu441. Such H-bonding should increase the donor ability of the O-atom and weaken the C3'-H bond. After H-atom removal, formation of an α-radical acidifies the OH proton and facilitates the OH deprotonation with the formation of a transient ketyl radical anion. In the next step of this anomerically-assisted cascade, these species can undergo a heterolytic β-CO-scission that generates a radical at the β-carbon. The overall sequence of reactions is an example of the so-called "spin-center shift", a process that combines radical and polar elementary steps for generating synthetically useful radicals.[96]
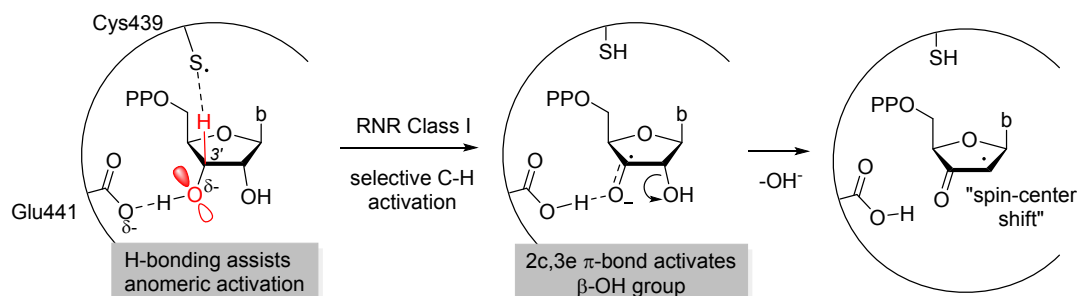
Figure 36. An example of selective C-H bond activation in a polyfunctional substrate by using H-bond in the cavity of catRNR Class 1 enzyme

MacMillan and coworkers used amplification of hyperconjugative $n_O \rightarrow \sigma^*_{C-H}$ interactions in alcohols for selective activation of α-C-H bonds. In particular, α-alkylation of alcohols with methyl acrylate is made possible by a highly selective hydrogen atom transfer in the presence of tetra-n-butylammonium phosphate. This additive was shown to be a suitable base for enhancing the selectivity for α-C-H bonds in alcohols in the presence of bonds with lower or identical BDEs (i.e., allylic, benzylic, α-C=O, and α-ether C-H bonds).[97] Importantly, because H-bonding is transient and reversible, the basic H-bonding partner for the activated substrate can be used in catalytic amounts. Figure 37 provides illustrative examples of remarkable selectivity achieved by using this approach.
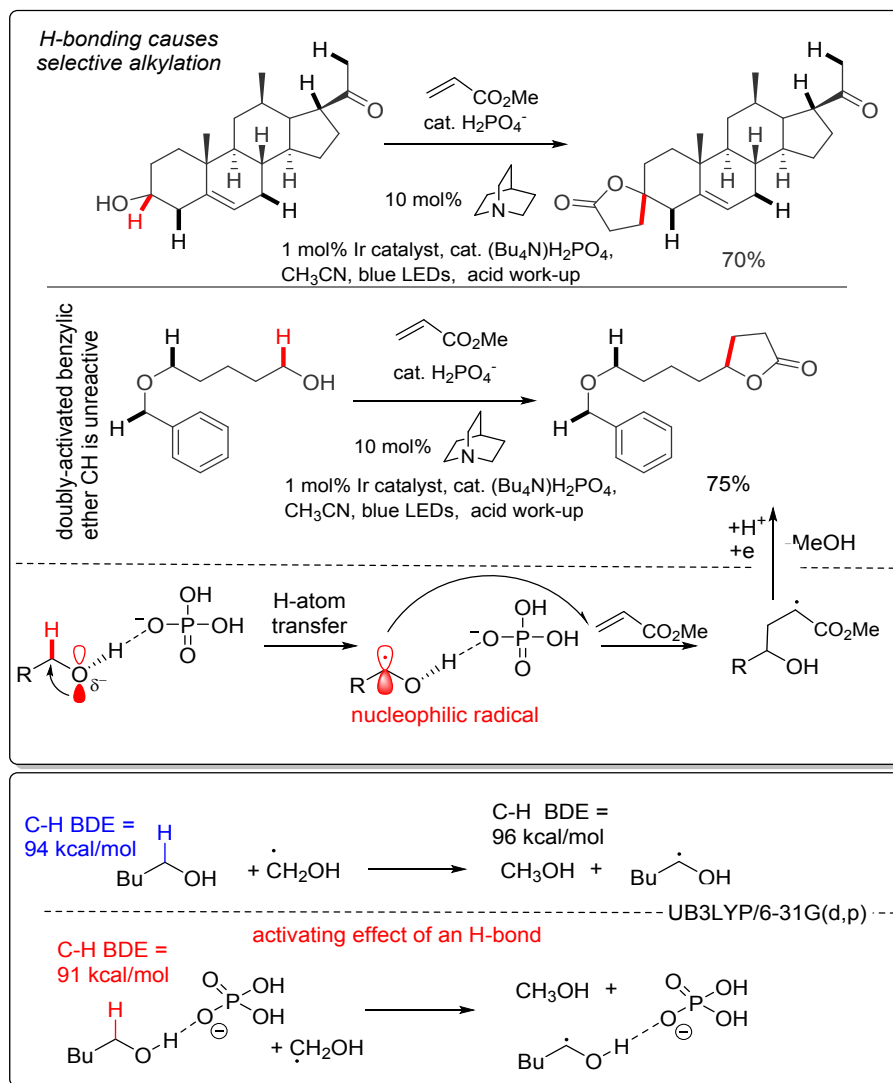
Figure 37. Top: Selective activation of alcohols in the presence of other C-H activating groups by using amplification of anomeric effect. Bottom: calculated effect of phosphate…H-O hydrogen bonding on the BDE of of an α-C-H bond in an alcohol[97]

Activation of α-CH bonds in alcohols also opens interesting synthetic opportunities, such as access to other radicals via spin-center shift. For the spin-center shift to operate, one needs a radical to be positioned between an α-heteroatom X (usually O or N) and a leaving β-O-H group. In this way, the radical serves as a relay between a pair of electrons of X (or an acidic X-H bond that can be deprotonated) and the σ^* C-O orbital that is primed for a heterolytic scission. Such condition is satisfied in the product of a α-OH alkyl radical ortho-addition to an N-containing aromatic heterocycles (X=N,Y=O) (Figure 38). Macmillan and coworkers used this approach to develop a dual catalytic alkylation of heteroarenes, using alcohols as mild alkylating reagents.[98] The advantage of this method is the ability to use inactivated

alcohols as latent alkylating reagents via the successful merger of photoredox and hydrogen atom transfer catalysis.
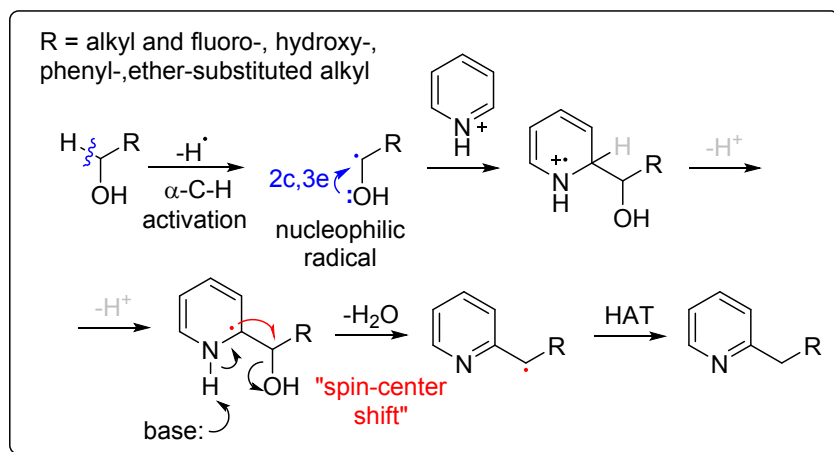
Figure 38. Formal radical alkylation by an alcohol made possible by enhanced anomeric effect

Although an alcohol oxygen is a moderate donor, it can provide enough anomeric assistance to activate the α-C-H bond for formal hydride shift to a strong cationic acceptor. An interesting disproportionation of spiroketals into ketoesters reported by Deslongchamps and coworkers provides an early example of such process (Figure 39).[99] The transformation proceeds quantitatively under reflux of the spiroketal in aqueous hydrochloric acid. The preferred product is consistent with the axial attack on the oxocarbenium ion, which places the newly formed oxygen lone pair antiperiplanar to the forming C-H bond.
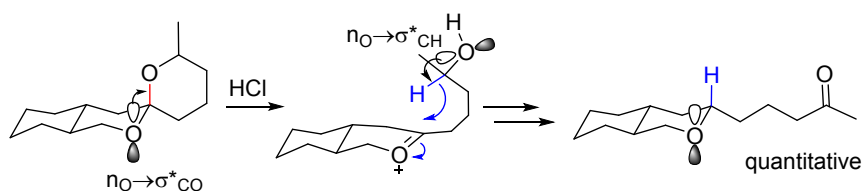
Figure 39. Formal disproportionation of spiroketals into ketoesters via anomerically assisted formal hydride shift

Increased donor ability of oxygen in metal alkoxides contributes to the efficiency of the Meerwein–Pondorf–Verley reduction (and the reverse Oppenauer oxidation).[100] The two lone pairs of the alkoxide oxygen In the Al-isopropoxide/ketone complex can contribute to the anomeric C-H weakening (Figure 40).
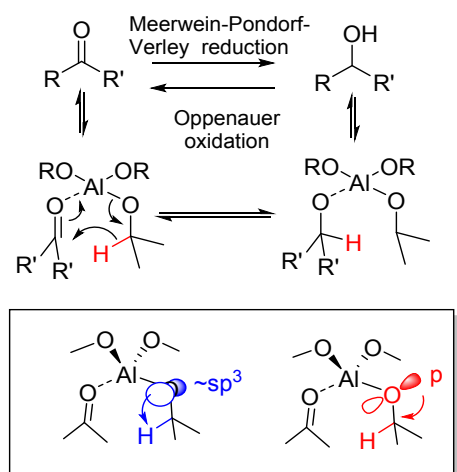
Figure 40. The role of anomeric effect in the Meerwein–Pondorf–Verley reduction of ketones and the Oppenauer oxidation of alcohols

The effect of full deprotonation on the donor ability is dramatic. For example, the much greater radical-stabilizing ability of anionic oxygen leads to increased stabilization of the conjugate base of α-hydroxy radicals, explaining a 5 pK_a unit increase in their OH acidity relative to the acidity of normal alcohols (Figure 41).[101] In return, once the OH bond of benzylic alcohol is deprotonated, the α-C-H BDE decreases by ~30 kcal/mol.
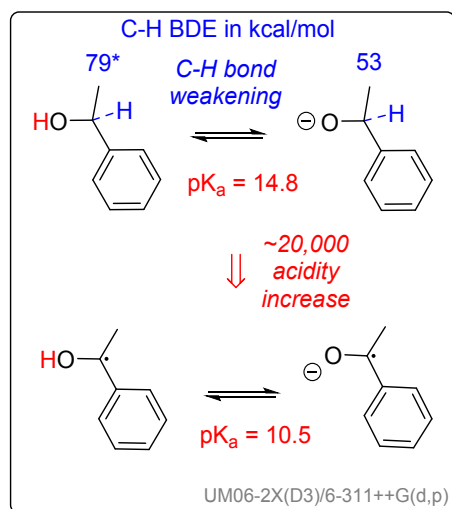
Figure 41. Two consequences of strong 2c,3e-bonds with anionic oxygen: increased O-H acidity in α-radicals and decreased C-H BDE in alkoxide anions. * BDE from [102], pK_a from [101, 103]

The dramatic increase in acidity of OH groups induced by the adjacent radical center can lead to interesting consequences in reactivity. For example, So et al. reported that, in the gas phase, such C(.)-OH groups are comparable in acidity to a carboxyl group - the difference in stability between a carboxylate and alkoxide tautomer can be less than 1 kcal/mol (Figure 42). Herein, alkoxide and carboxylate can be both present at an equilibrium that, without the radical center, would usually favor the carboxylate formation.[104]

G4 energies at 0 K with zero-point energy (E0+ ZPE)
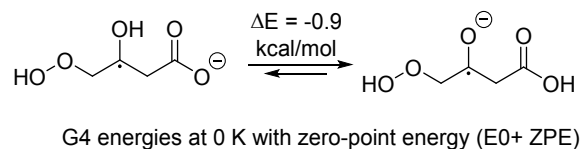
Figure 42. Proton transfer from an OH group to carboxylate is nearly thermoneutral.

To make it even more interesting, the stereoelectronic peculiarities of anionic oxygen extend beyond a simple increase in the donor ability. Similarly to a fluorine substituent, the negatively charged monovalent oxygen is also *stereoelectronically promiscuous.* In contrast to the neutral divalent oxygen which has only one p-type lone pair (along with a sp^n hybrid), an alkoxide anion has two stereochemically important p-type lone pairs on oxygen, both of which can interact with the vicinal σ-acceptors. This has two consequences. First, it removes geometric restrictions on the orientation of the vicinal acceptor orbital and lifts the usual entropic penalty for stereoelectronic alignment. Second, presence of two donors creates the possibility of their interaction with two acceptors giving rise the possibility of *two mutually orthogonal anomeric interactions* (Figure 43). The two effects can play different but complementary roles. A number of interesting features of anionic reactions may stem from this "double anomeric effect".

Increased donor ability of anionic centers

The anatomy of neutral and anionic O-atoms
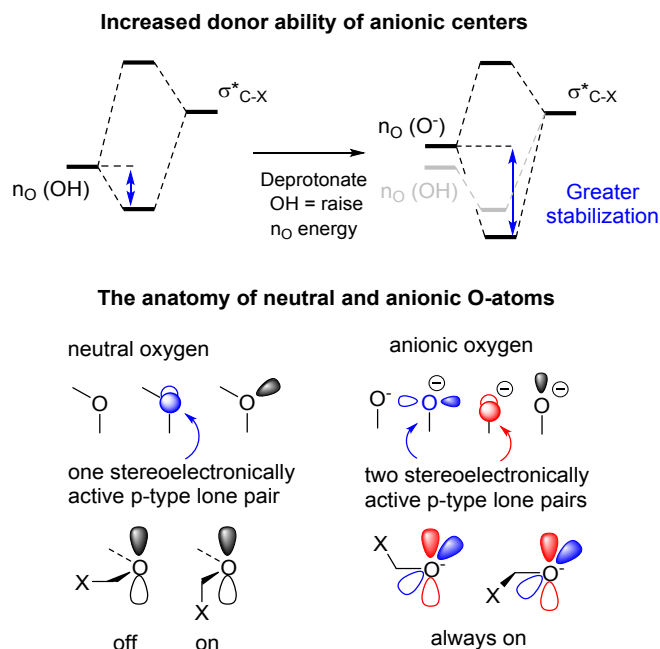
Figure 43. Can the differences between neutral and anionic oxygen lead to double anomeric effect?

In the following sections, we will illustrate how strong anomeric assistance by the negatively charged donors can impose exceptionally large effects on C-C scission in pericyclic reactions.

Breaking C-C bonds as σ-acceptors:

In a landmark paper, Evans and Golob reported that the oxy-Cope rearrangement is dramatically (10^{17}!) accelerated by deprotonation of the OH group at the central C-C bond (Figure 44).[105]

R	rel. rate (b:a)
OMe	10^{12}
H	10^{17}
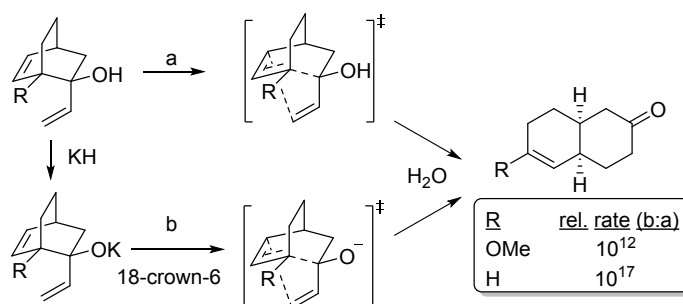
Figure 44. Large rate enhancements of the oxy-Cope rearrangement provided by anionic TS stabilization. The effect is less pronounced when significant electron assistance is already available in the neutral state (e.g., an OR group is present at the other carbon of the breaking C-C bond). However, even in the latter scenario, the accelerating effect is significant as the deprotonation still leads to 10^{12}-fold acceleration (Figure 44). The electronic origin of this effect is in the dramatic increase of the donor ability of the lone pairs at anionic oxygen. The raised lone pair energy may be further complemented by the absence of any

geometric restrictions at such donation in the case of anionic oxygen, where two stereoelectronically active p-type lone pairs can donate efficiently to any vicinal acceptor.

Similar increases are known for the anionic versions of popular pericyclic reactions such as oxy-Claisen, amino-Cope rearrangements, and the retro-Diels-Alder reaction.[106-109] All of these processes share the same electronic origin: anionic oxygen is a superior partner for delocalizing transient radical character when a C-C bond is broken during the bond reorganization process.

Computational analysis by Baumann and Chen revealed that the moderate effect of a neutral 3-OH donor on the parent 1,5-hexadiene system (>3 kcal/mol decrease in the activation barrier and ~100-fold increase in the reaction rate) is dramatically amplified by deprotonation (Figure 45).[110] The 10^{20}-fold acceleration is consistent with the experimentally observed effects illustrated in Figure 44. Baumann and Chen also suggested an interesting conceptual approach to rationalizing such extreme effects on reactivity based on the "increased transition state acidity".[111]
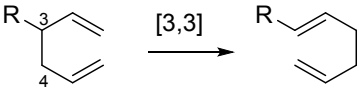
R	C3–C4 Distance, Å	$\Delta G^{\ddagger}$, kcal/mol	k, s^{-1}
H	1.548	36.3	1.6×10^{-14}
OH	1.552	33.8	1.1×10^{-12}
O^{-}	1.604	6.3	1.6×10^{8}

Figure 45. Effect of a neutral and anionic O-donor on the rate of Cope rearrangement in 1,5-hexadiene system

Indeed, the correlation between the difference in the pK_a values of the pair of reactants and the pair of transition states correlates well with the change of the two free energies of activation. This correlation is not surprising considering the effect of increased donor ability of anionic oxygen on its radical stabilizing ability (Figure 41).

Remote C-C activation in ethers and alcohols: The power of anomeric assistance can expand beyond the oxygen's direct neighbors. Furthermore, such behavior is not limited to pericyclic reactions. For example, a remote oxygen atom can accelerate C-C fragmentations in radical cascades. Such effect was studied in detail for the transformation of aromatic enynes into α-Sn-substituted naphthalenes, a process that is terminated by a C-C bond scission (Figure 46). The efficiency of fragmentation can be enhanced by introduction of an oxygen atom next to the breaking bond. A notable electronic feature of this process is

that the breaking bond provides an electronic relay in a stabilizing through-bond (TB) interaction between the lone pair and the radical center.[112-114]
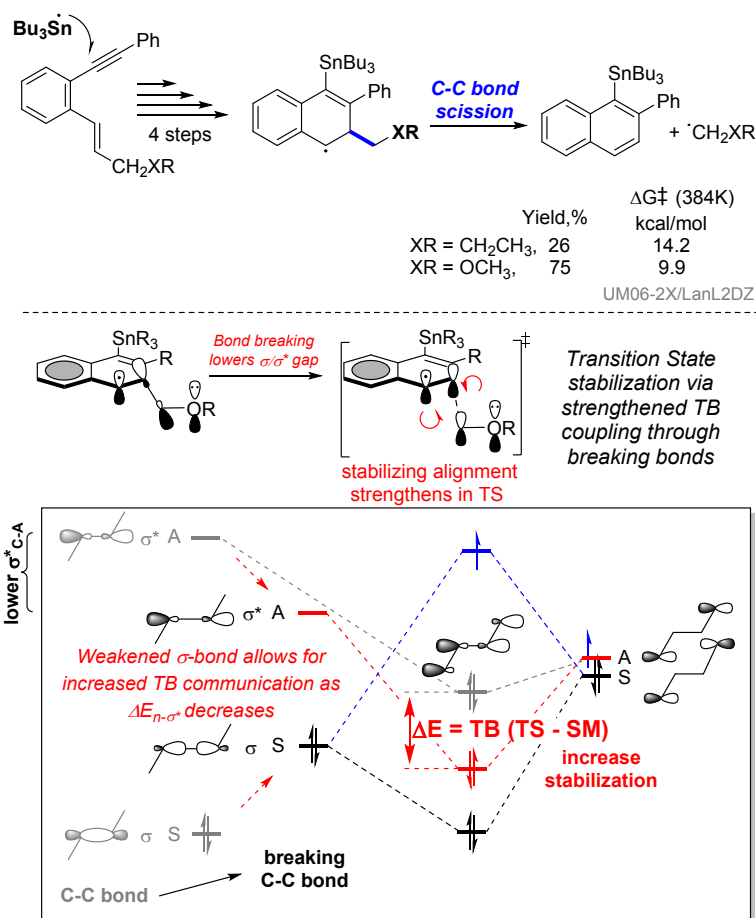
Figure 46. Anomeric interaction between the β-O-atom and the breaking bond increased efficiency of C-C fragmentation. Insert: Electronic coupling between non-bonding orbitals in 1,4-diradicals and β-oxygen substituted radicals strengthens in the TS, facilitating C-C bond fragmentation. Additional stabilization due to TB coupling through a breaking bridging bond is shown as ΔE (red). σ and σ* energies in the starting radical are shown in grey

Stabilizing through-bond (TB) interaction between a benzylic radical and the lone pair at the δ-position was identified as one of the sources of transition state stabilization for the O-containing system. The increase in TB interaction through stretched bonds is documented by NBO orbital interaction energies. In the fragmentation process, the energy of the σ*-antibonding bridge orbital is lowered, decreasing the ΔE_{ij} term for the stabilizing interaction that couples the non-bonding orbitals (i.e., the C-radical and the O-lone pair). Furthermore, the calculated molecular geometry in the CCOH moiety changes to adopt the coplanar arrangement between the radical center and the p-type lone pair on oxygen along the reaction path. Understanding such effects is helpful in the rational design of radical leaving groups.

More recently, Pratt, Studer and coworkers showed that such fragmentations do not have to be assisted by aromatization.[115, 116] The key design feature is in "upgrading" the anomeric effect in alcohols by deprotonation. This approach led to efficient base-promoted radical allylation mediated by C-C fragmentation and loss of α-oxy radical shown in Figure 47. The key C-C scission is also assisted by through-bond coupling of an oxygen's lone pair with the radical center. Computations clearly show how the strength of this interaction depends on the donor strength of the oxygen lone pair. As the oxygen becomes more anionic (alcohol -> H-bonded alcohol -> lithium alkoxide -> oxygen anion), the stabilization is growing larger in both the transition state and the β-oxy radical product (Figure 47b).
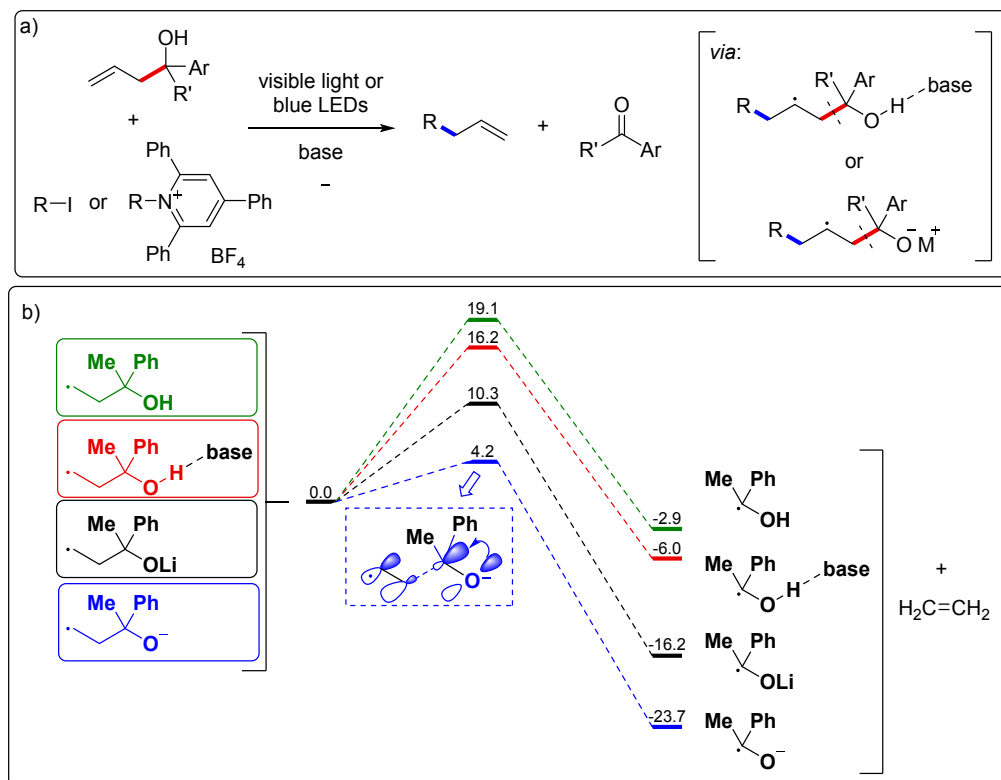
Figure 47. Effect of OH deprotonation on the anomeric interaction between an O-atom and a breaking bond can be used to fine-tune the rate of a radical C-C fragmentation.

Non-radical (heterolytic) fragmentation of this type are used widely in organic synthesis. The general pattern for such reactions involves a 1,4-disubstituted push-pull system where communication of oxygen lone pairs with an acceptor via a bridge σ-bond weakens this bond. Especially fast are the reactions where anionic oxygen serves as the donor component. Such reactions lead to the formation of a C=O moiety along with a new carbon-carbon π-bond that can belong to an alkene, an alkyne or an allene. In particular, alkynes are formed when the intervening relay between oxygen and the remote acceptor involves a

double bond (Figure 48). The "alkynogenic" fragmentations have to break the stronger C(sp3)-C(sp2) bond while the "alkenogenic" and "allenogenic" fragmentations break the weaker C(sp3)-C(sp2) bonds.
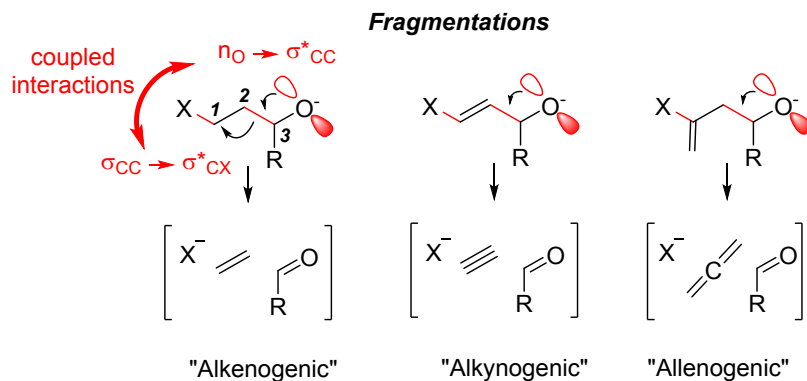
Figure 48. Anomeric coupling between a leaving group X and anionic oxygen through a breaking σ-bond is the key design feature in alkene-, alkyne-, and allene-forming fragmentations.

The pioneering work of Eschenmoser expanded the earlier heterolytic metal-mediated fragmentations of 1,4-dibromocyclohexanes reported by Grob to fragmentations of β-hydroxy ketones (Figure 49).[117, 118] The fragmentations could be induced either by hydroxide or by a Grignard reagent.
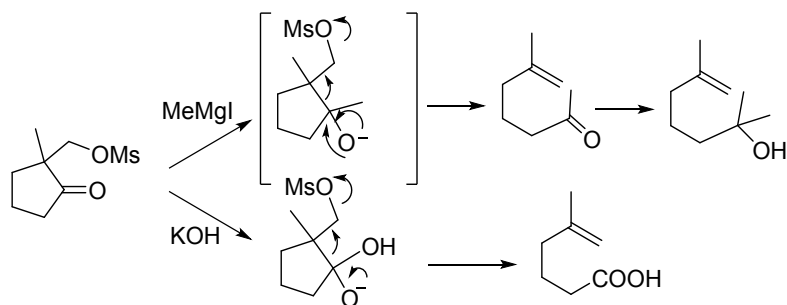
Figure 49. Eschenmoser's fragmentation

The conformational requirements for a concerted fragmentation of this type is that the lone pair on O, the C1-X and C2-C3 σ bonds have to be antiperiplanar for maximum orbital overlap in the transition state. The all anti-periplanar arrangement is met in the staggered conformation. Due to stereoelectronic promiscuity of anionic oxygen, rotation around C2-C3 bond has a relatively small effect as long as the proper alignment with the C1-C2 bond is maintained.

This requirement is illustrated by the classic work of Wharton[119, 120] on the conformational requirements for the concerted Grob fragmentation. The fragmentation of stereoisomeric monotosylates of 1, 10-

dihydroxyldecaline under basic condition proceeded cleanly only when the antiperiplanar arrangement of the C-OTs and C-C at the ring junction was possible (Figure 50).

a= KO*t*Bu, HO*t*Bu, 1h, 40°C
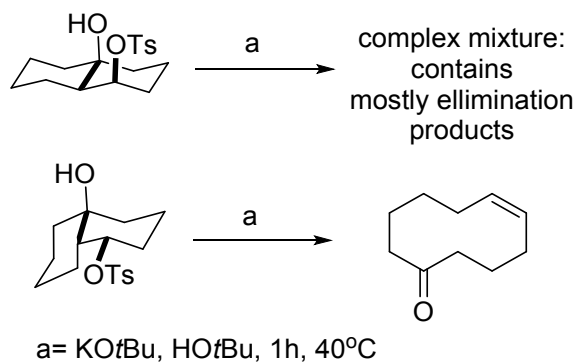
Figure 50. Wharton's example of stereoelectronic control

Use of epoxides as leaving groups has the advantage of retaining a hydroxyl group after rearrangement. Holton et al. used this process to generate the key eight-membered ring on route to taxane ring system (Figure 51).[121]
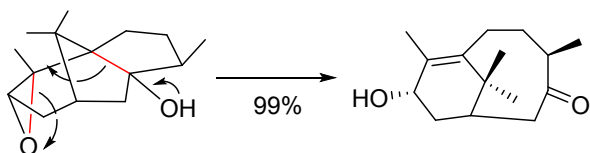
Figure 51. Holton's use of epoxide fragmentation

The power of alkynogenic fragmentations of this type is illustrated by Eschenmoser-Tanabe alkynyl ketone synthesis (Figure 52).[122-124] The fragmentation is driven by the loss of molecular nitrogen from the sulfonyl hydrazone precursor.
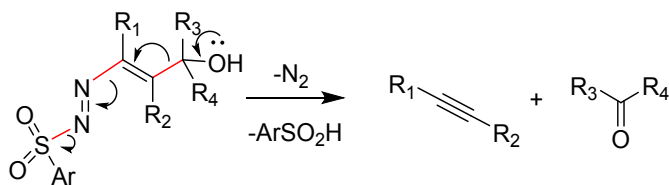
Figure 52. Eschenmoser-Tanabe fragmentation

More recently, Dudley et al. reported that β-triflyl-α, β-unsaturated ketones also undergo efficient C-C fragmentation to give alkynes.[125, 126] Addition of stabilized carbanionic nucleophiles to cyclic vinylogous

acyl triflates (VATs) triggers a ring-opening fragmentation to give acyclic β-keto esters and related products (Figure 53).

X= -CH$_2$, -NR
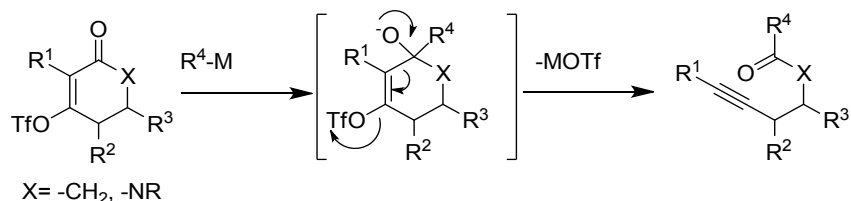
Figure 53. Formation of alkynes via Dudley fragmentation

Williams et al. used isomeric vinyl triflates to open a similar route to allenes. Organolithium and Grignard reagents, including alkyl, aryl, and alkynyl nucleophiles, smoothly added and induced fragmentation. Interestingly, stoichiometric quantities of nucleophile allowed formation of allenic ketones (Figure 54) whereas the excess of reagent gave allenic alcohols.[127] Cramer et al. further expanded the fragmentation of vinyl triflates towards the heteroatom-nucleophiles.[128] This reaction leads to trisubstituted allenes with a terminal carbonyl functionality at the oxidation level of a carboxylic acid.

R^1= Me, Pr, allyl; R^1= Me, Pr, allyl, Bn;
NuH = BnOH, PhOH, PhSH, H$_2$O, NH$_3$, BnNH$_2$,
PhNH$_2$, Bn(Me)NH, TsNH$_2$, morpholine
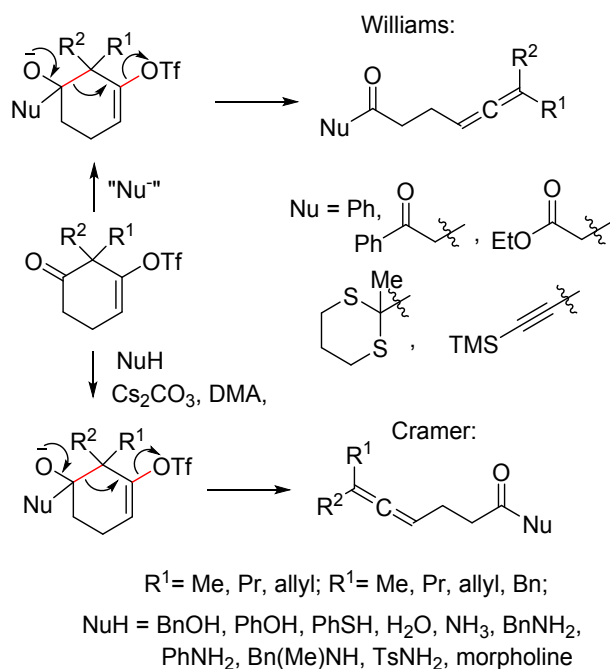
Figure 54. Formation of carbonyl-substituted allenes through a C-C fragmentation

Laconsay et al. used computational analysis to test the length limit for the concerted bond scissions in the so-called divergent fragmentations, i.e., the fragmentations that involve the formation of two (or more)

distinct products from a single substrate.[129] An interesting feature of these fragmentations is that three

bonds are broken and not all of these bonds are parallel. Interestingly, for the system shown in Figure 55,

the computed Path B ("imine" formation) is stepwise and has a post-TS bifurcation to the alternative Path

A (the "enamine" path). In contrast, the Path A is asynchronous but still concerted. It is tempting to

attribute this difference to the transiently developing character at O3. As oxygen anions are

"stereoelectronically promiscuious" due to the presence of several lone pairs (vide infra), they can re-

direct electron density even if the breaking bonds are not aligned.
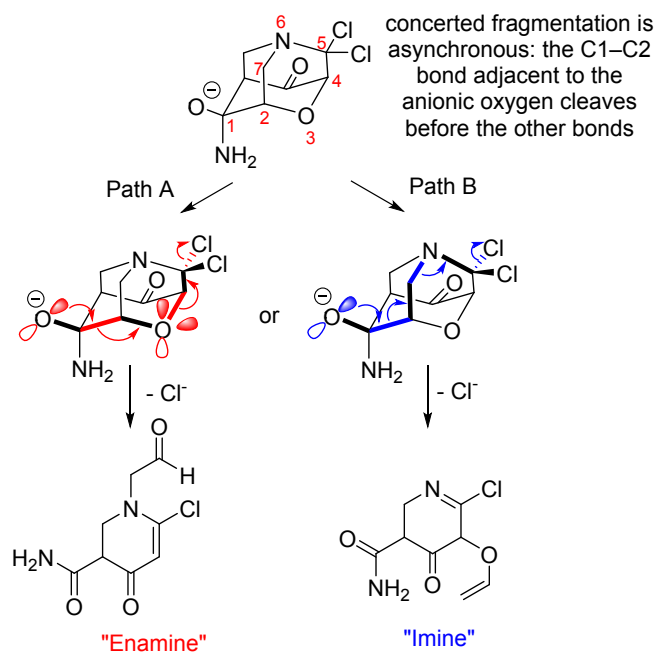
Figure 55. Divergent fragmentations occur when multiple bonds are broken and not all of these bonds are

parallel

In the above reactions, a negatively charged oxygen transmits electron density to a departing group in a

process that ultimately transforms that alkoxide moiety into a carbonyl group. The reacting donor lone

pair in this process is incorporated in the newly formed C=O bond. However, the other lone pairs are

preserved giving rise to new anomeric-like interactions in the ketone and aldehyde products. The effect

of these interactions on reactivity will be discussed in the next section.

Aldehydes and ketones

The main directions of aldehyde reactivity, i.e. oxidative C-H activation (e.g., oxidation to carboxylic acids)

and nucleophilic addition to the carbonyl group, are affected by the anomeric effect. We will start our

discussion with the former to show that oxidative C-H activation of aldehydes can be expanded into many useful reactions orchestrated by the carbonyl oxygen lone pair.

But first let's discuss the stereoelectronic portraits in Figure 56. Importantly, the magnitude of the $n_O \to \sigma^*_{CH}$ interaction in aldehydes is dramatically increased in comparison to that in alcohols and ethers (23-26 vs. 6-7 kcal/mol). This increase comes from two sources: the much shorter C=O bond that brings the interacting orbitals closer and the greater acceptor ability of C-H bonds at the sp^2-hybridized carbons. A similar increase is observed for the $n_O \to \sigma^*_{CC}$ interaction in ketones. Later, we will see that even the classic anomeric $n_O \to \sigma^*_{CO}$ interaction in acetals are weaker than these non-traditional interactions. Since $n_O \to \sigma^*_{CH}$ hyperconjugative interactions moves some of electron density from oxygen, its magnitude increases in non-polar media, e.g., 25.5 kcal/mol (vacuum) vs. 23.2 kcal/mol (water) for acetaldehyde. This computational observation suggests that C-H activation of aldehydes should be sensitive to solvent effects.

$n_O(p) \to \sigma^*_{C-H}$
23.2 kcal/mol

$n_O(p) \to \sigma^*_{C-C}$
19.6 kcal/mol

$n_O(sp^{0.7}) \to \sigma^*_{C-H}$
0.6 kcal/mol

$n_O(sp^{0.7}) \to \sigma^*_{C-C}$
1.6 kcal/mol

$n_O(p) \to \sigma^*_{C-C}$
21.1 kcal/mol

$n_O(sp^{0.7}) \to \sigma^*_{C-C}$
2.3 kcal/mol

PBE0-D3BJ/aug-cc-pVTZ/CPCM(H$_2$O)
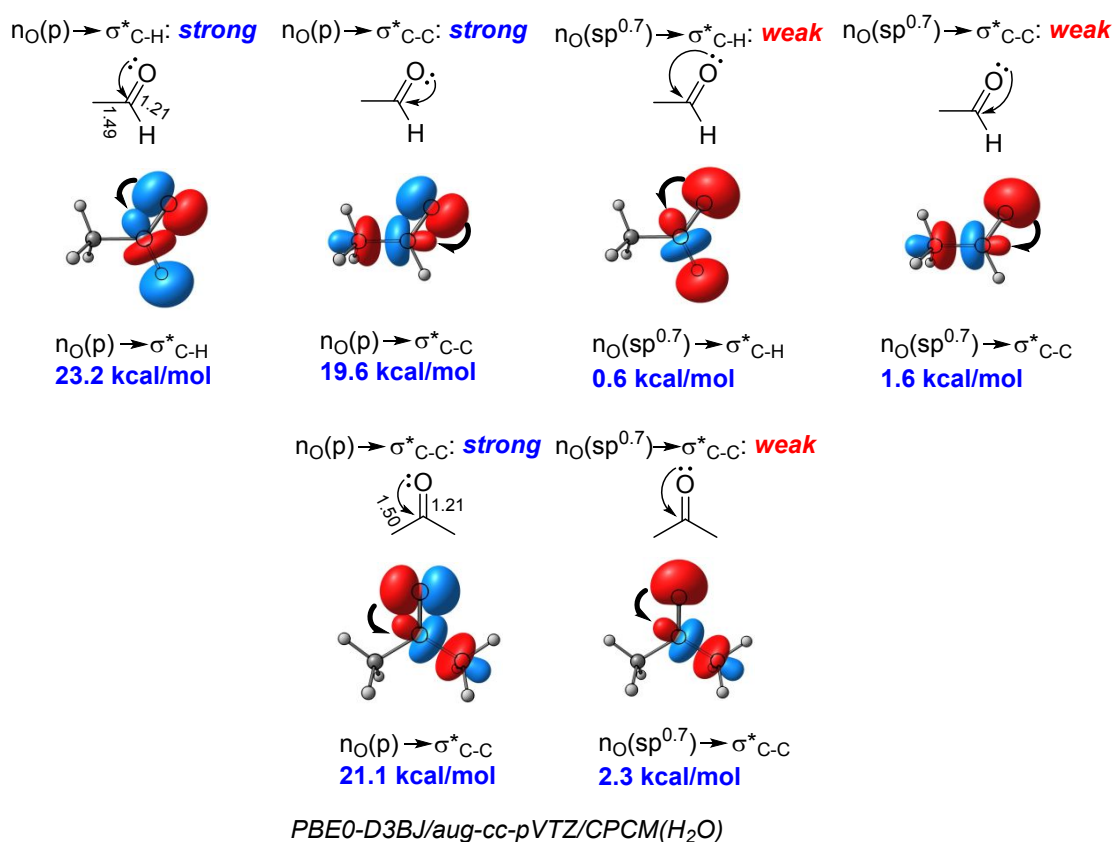
Figure 56. Stereoelectonic portraits of anomeric interactions in an aldehyde and a ketone

In our subsequent discussion, we will illustrate how the anomalously high anomeric activation assists in C-H activation in aldehydes, explaining why, in a seeming paradox, the C(sp²)-H bonds of aldehydes are weaker than C(sp³)-H bonds of alkanes.

C-H activation: Even though the $n_O \rightarrow \sigma^*_{CH}$ interaction in aldehydes cannot be probed via conformational effects due to the lack of rotation around the C=O bond, the importance of this anomeric interaction is immediately apparent in C-H activation in aldehydes. The $n_O \rightarrow \sigma^*_{CH}$ hyperconjugation greatly assists both homolytic and heterolytic C-H bond scissions, as this orbital interaction eventually evolves into a 2c,3e-bond in an acyl radical or in a π-bond in an oxacarbenium ion (Figure 57).[130]
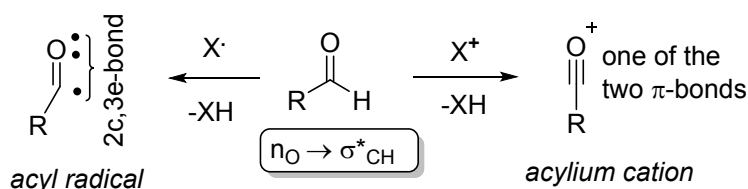
Figure 57. Conversion of anomeric $n_O \rightarrow \sigma^*_{CH}$ interaction into a 2c,3e-bond in an acyl radical and a π-bond in an oxacarbenium ion.

The former effect manifests itself as the source of dramatic weakening of the aldehyde C-H bond dissociation energy (BDE). The ~88 kcal/mol BDE for a C(sp²)-H bond in aldehydes is especially striking in comparison to the ~111 kcal/mol BDE for the less polar C(sp²)-H bond in ethene (Figure 58).[131] As a result, the sp²-C(O)-H bonds in aldehydes are even weaker than typical sp³-C-H bonds in alkanes and, even more strikingly, weaker than the anomerically activated sp³-C-H bond of dimethyl ether (96 kcal/mol).[32]
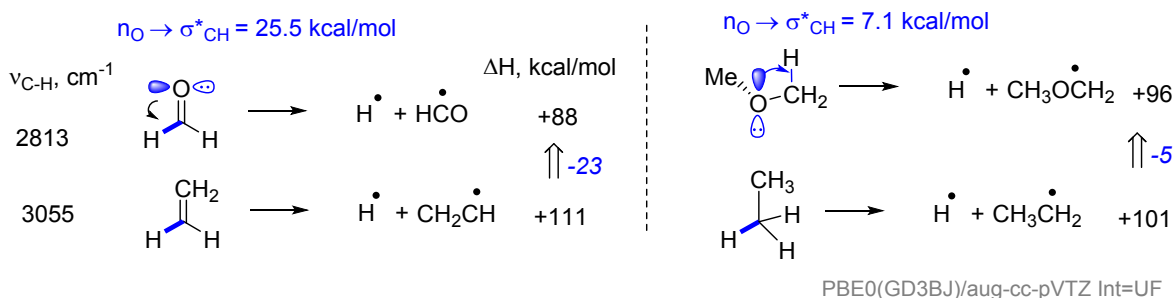
Figure 58. The large $n_O \rightarrow \sigma^*$C-H interactions (NBO energies, in kcal/mol) manifest themselves as decreased C-H bond BDE and red shifted C-H stretching frequencies in aldehydes.

The weakness of the aldehyde C-H bond accounts for the applications of aldehydes as a convenient source of acyl radicals.[132] Furthermore, successful design of such applications depends on taking full advantage of the C-H activation by the carbonyl lone pair.

The importance of such interactions is supported by a number of experimental results. For example, the rate of H-atom abstraction depends strongly on the acceptor property of the "spectator" C-R bond at the carbonyl carbon. As the p-lone pair of the carbonyl oxygen cannot escape interacting simultaneously with the adjacent σ^*_{C-R} and σ^*_{C-H} bonds, increasing the σ^*_{C-R} acceptor ability redirects the oxygen's stereoelectronic power and minimizes the oxygen's assistance in breaking the C-H bond (Figure 59).[133] The >100-fold difference between the HAT rates for R=OEt relative to R=Et illustrates that the classic anomeric $n{\rightarrow}\sigma^*_{CO}$ interaction serves as a protective force for the C-H bond of the formate ester.
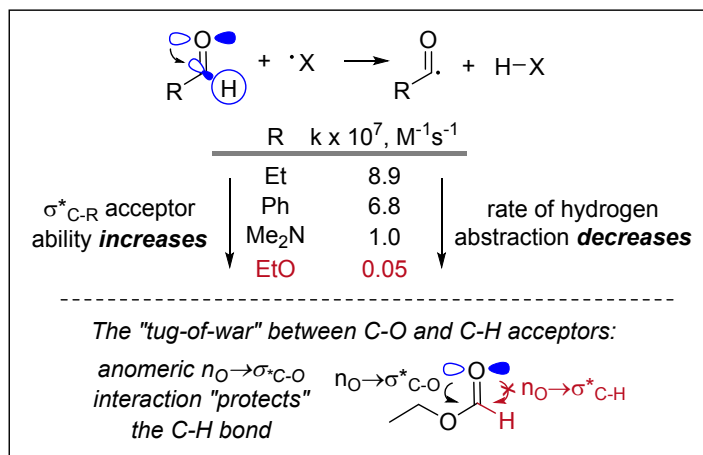
Figure 59. The tug-of-war between two acceptors: increasing the acceptor ability of the "spectator" σ^*_{C-R} orbital decreases the rate of hydrogen abstraction[133]

Additionally, the rate of hydrogen abstraction depends strongly on the TS polarity. As the α-oxygen atom is a stereoelectronic donor, H-atom abstraction from the aldehyde C(O)-H bond proceeds faster when the abstracting radical is electrophilic (Figure 60). The slower reactions of nucleophilic alkyl radicals suggest a less polarized transition state where the anomeric assistance is not fully activated. This understanding helps in the design of practical radical transformations of aldehydes. For example, thermal peroxide-initiated decarbonylation of aldehydes is relatively inefficient because the alkyl radical resulting from acyl radical decarbonylation participates in the H-atom abstraction poorly, rendering this key chain transfer step slow. In contrast, the electrophilic thiyl radical propagates the chain very well.[134] Here, understanding the nature of the anomerically assisted transition state allowed replacing an inefficient propagation sequence by a much more efficient two-step sequence.

A.

anomeric $n_O \longrightarrow \sigma^*_{CH:}$ assistance: increases if X is electrophilic

B.

R = nucleophilic alkyl radical

C. Efficient chain propagation via polarity reversal catalysis:

R'S = electrophilic thiyl radical

$$R^{\bullet} + R'S\text{-}H \xrightarrow{\text{fast}} R\text{-}H + R'S^{\bullet}$$
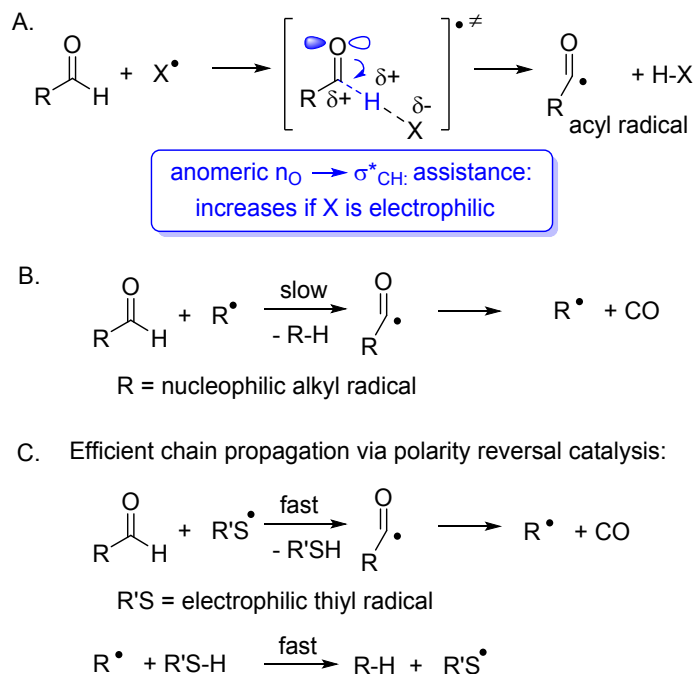
Figure 60. Practical issues in thermal peroxide-initiated decarbonylation of aldehydes. A: Assistance to C-H radical abstraction in aldehydes by $n_O \rightarrow \sigma^*$C-H interactions is greater for electrophilic radicals. B: C-H abstraction from aldehydes by nucleophilic alkyl radicals is slow. C: Replacing an inefficient propagation step by the much faster polarity-matched H-abstractions.

For the same reasons, hydrogen abstraction from aldehydes by electrophilic oxygen-centered radicals proceeds in a clean manner. The great success of photoredox activation of aldehydes in radical cascades implicitly depends on using relatively electrophilic odd-electron species for the chain-propagating C-H activation, usually O- or N-centered radicals or radical-cations.[135, 136]

On the other hand, if oxidation of aldehydes is undesirable, it can be prevented via a stereoelectronic strategy based on *deactivation* of the anomeric effect. For example, fast oxidation of aldehydes to the corresponding benzoic acids complicates production of aldehydes from methylbenzenes by aerobic oxidation. Hydrogen bonding to the oxygen atom of the aldehyde product deactivates the C–H bond toward HAT. A convenient strategy for preventing benzaldehyde over-oxidation to the carboxylic acid and achieving selective benzylic C–H oxidation of methylarenes is to use HFIP as the solvent (Figure 61). By engaging the benzaldehyde oxygen in a protective H-bond with HFIP, Pappo and coworkers succeeded in converting *para* -xylene into *para* -tolualdehyde in almost quantitative yields at complete conversion.[137, 138] In order to take advantage of this subtle effect, one needs to carefully choose the catalyst - as illustrated

by the fact that even strongly acidic conditions in the Amoco purified terephthalic acid (PTA) process do not prevent the full oxidation of both p-xylene methyl groups.

Amoco PTA process: a) Co(II), Mn(II), HBr, HOAc, H_2O
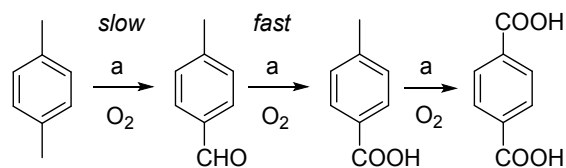
Partial oxidation: b) Co(II), N-hydroxyphthalimide (cat), HFIP, rt

H-bonding weakens anomeric assistance
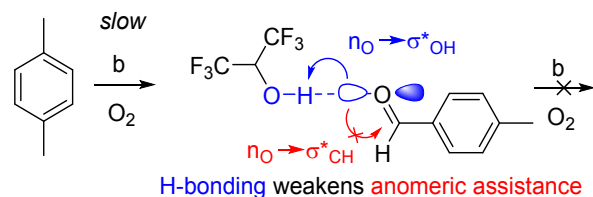
Figure 61. Promoting C-H deactivation in aldehydes by H-bonding in HFIP

Nucleophilic addition: Nucleophilic addition reactions activate additional anomeric effects in carbonyl compounds due to their tetrahedral intermediates (TIs). Such effects will be discussed in subsequent sections where we will show that anomeric stabilization in TIs consists of multiple interactions stabilizing both the TIs and the TSs connecting them. These multiple effects stabilize the adjacent part of the PES and allow interconversion of carbonyl compounds to go fast. This kinetic feature plays an important role in the rapidly developing dynamic covalent chemistry of carbonyls.[139-144]

Although the $n_O \rightarrow \sigma^*_{CH}$ donation clearly weakens the aldehyde C-H bond, this effect is insufficient for unlocking hydride-donating ability of aldehydes. The sp^2 C-H bond is still relatively strong and electron density is moved to the oxygen. However, this situation can be changed by conversion of an aldehyde to a hemi-acetal where the C-H bond is ~sp^3-hybridized and one more oxygen can assist in the hydride shift.

An illustrative example of such activation is provided by the Tishchenko reaction, a classic organic transformation that involves disproportionation of an aldehyde in the presence of an alkoxide (Figure 62). This process is driven by trading a single anomeric effect to a double anomeric effect as discussed earlier. The Al(OR)$_3$-catalyzed version of this reaction was suggested to involve the initial coordination of an aldehyde with aluminum, followed by formation of a hemiacetal intermediate and completed with a hydride transfer that furnishes the ester product. Considering that suprafacial 1,3-shifts are symmetry-forbidden, a formal 1,5-shift in the cyclic intermediate is suggested as a more likely key step of this transformation.
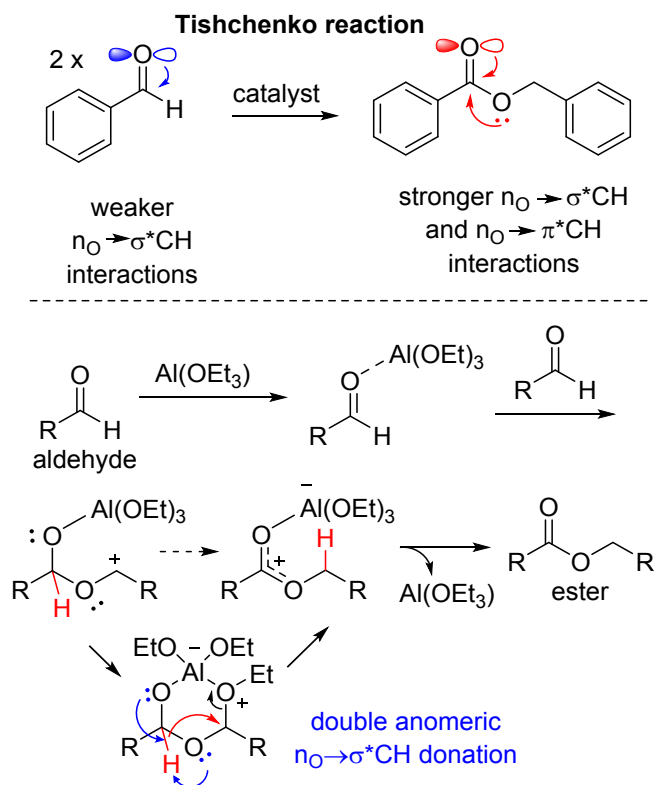
Figure 62. The classic Tishchenko reaction can be promoted by increased anomeric stabilization in the suggested hydride-shift TS and product intermediate.

Thermodynamically, the Tishchenko reaction is driven by "anomeric frustration" of aldehydes. Even though the aldehyde $n_O \rightarrow \sigma^*_{C-H}$ interactions are moderately strong, aldehyde disproportionation is favorable if it can pair the oxygen lone pairs with a better hyperconjugative acceptor. In the Tishchenko reaction, the disproportionation converts two aldehydes into a "two-oxygen" functionality discussed in the following sections, i.e., the ester. Having two oxygens at the same carbon relieves the frustration by providing the oxygen lone pairs with good partners for the very strong stabilizing intramolecular donor-acceptor delocalizing interactions with the carbonyl moiety.

The mixed aldol-Tishchenko reaction involves the reaction of the aldol product with an aldehyde (preferably not enolizable) to yield an ester (Figure 63). The second part of this process, i.e., the formation of β-acyloxy alcohols from β-hydroxy ketones with aldehyde, is known as the "Evans-Tishchenko reduction". The reaction can be promoted by a variety of catalysts, from aluminum alkoxides[145] to SmI$_2$,[146] and chiral versions of this process are known as well.[147-152] Abu-Hasanayn and Streitwieser[153] reported that the isotope effect for the rate-determining hydride transfer is normal and substantial (the experimental k_H/k_D value of 2.0 for the reaction of lithium enolate of isobutyrophenone with two molecules of

benzaldehyde). This value indicates a significant degree of the transition state C-H breaking which is certainly promoted by the combined anomeric assistance of the two α-oxygens.
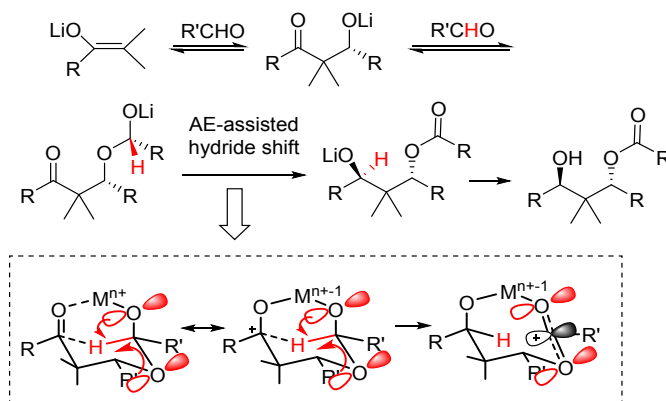
Figure 63. Formation of a diol-monoester in the aldol–Tishchenko reaction between a lithium enolate and two aldehyde molecules

Considering the examples described so far, one has to wonder if the broad importance of anomeric effect in aldehyde chemistry is fully appreciated. For example, can C-H activation in aldehydes by transition metals[154-157] also be assisted by the anomeric effect? This is a reasonable hypothesis as the σ^*C-M orbitals can be quite low in energy and, hence, serve as good hyperconjugative acceptors.[72, 80] Although the possible role of anomeric effect in transition metal catalyzed reactions is essentially unexplored, such tole is likely to be significant. For example, the initial breakthrough in metal-mediated hydroacylation came when cationic Rh species were used to promote 4-pentenal cyclisations.[158, 159] Increased electrophilicity at the metal is a favorable feature for taking advantage of anomeric assistance for α-C-H activation. Furthermore, the anomeric $n_O \rightarrow \sigma^*_{C-M}$ interaction may also stabilize the metal acyl intermediate and prevent the competing decarbonylation process (Figure 64). The importance of such interactions will depend on the metal, its oxidation state, and the presence of other electron-accepting or donating groups in the molecule. The interplay of these factors can provide interesting stereoelectronic puzzles which, once solved, may open convenient approaches for fine-tuning the catalyst reactivity.
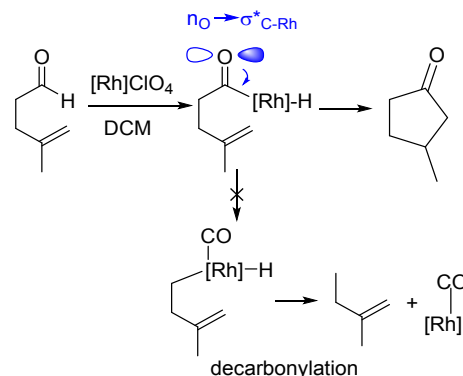
Figure 64. The possible involvement of anomeric $n_O \rightarrow \sigma^*_{C-M}$ interactions in chemistry of metal acyl intermediates

Finally, it is worth mentioning that umpolung of anomeric effect can be accomplished by n-π* photochemical excitation of ketones. This excited state has dual reactivity originating from a) involvement of the singly occupied in-plane p orbital on oxygen and b) from behavior of the electron-rich, "radical-anion like" π-system (Figure 65).[160] As the in-plane oxygen p-orbital becomes electron deficient, its increased interaction with the vicinal C-C or C-H bonds promotes their scission (Norrish type I fragmentation) or a ring expansion with the formation of O-substituted carbenes.[161] These examples illustrate that oxygen, like Dr. Jekyll and Mr. Hyde, has a dual personality and can be either a p-donor (oxygen lone pair) or a p-acceptor (O-centered radical).

Figure 65. Umpolung of anomeric effect by light leads to typical photochemical reactions of ketones

The reactive nature of half-filled non-bonding orbitals on oxygen is further illustrated by chemistry of O-centered radicals where the very strong $\sigma_{C-C} \rightarrow n_O$ positive hyperconjugation paves the way for the C-C fragmentations (i.e., β-scission) with a concomitant C=O moiety formation.[162-171]

Interestingly, changes in the nature of O-species can control the selectivity of β-scission. While the fragmentations of metal alkoxides favor fragmentation of a C-aryl bond, radical fragmentations of similar substrates proceed via C-alkyl bond scission.[172, 173] This difference in selectivity is consistent with the greater acceptor ability of σ^*C-aryl bonds relative to C-alkyl bond in $n_O \rightarrow \sigma^*_{CC}$ interactions that assist in the C-C scission. As the alkoxide O-M bond elongates in the TS, oxygen is likely to gain more alkoxide character and, importantly, as the metal departs to the ipso-position of the aryl ring, it still, through the residual O...M interaction, "anchors" the incipient oxygen lone pair, so the latter is aligned perfectly with the breaking C...aryl bond (Figure 66). Radical fragmentations proceed in the opposite way because oxygen radical is a strong acceptor and the donor ability of sigma C-C bonds follows the opposite trend (C-alkyl>C-aryl). One has to note, however, that nature of the metal can be the decisive factor in this case, as the metal can intercept the developing carbanionic character at the aryl group via a formal M/C-C bond insertion. In this scenario, the anomeric effect is likely to be a supporting effect but its relative contribution to the reaction success is yet unknown.
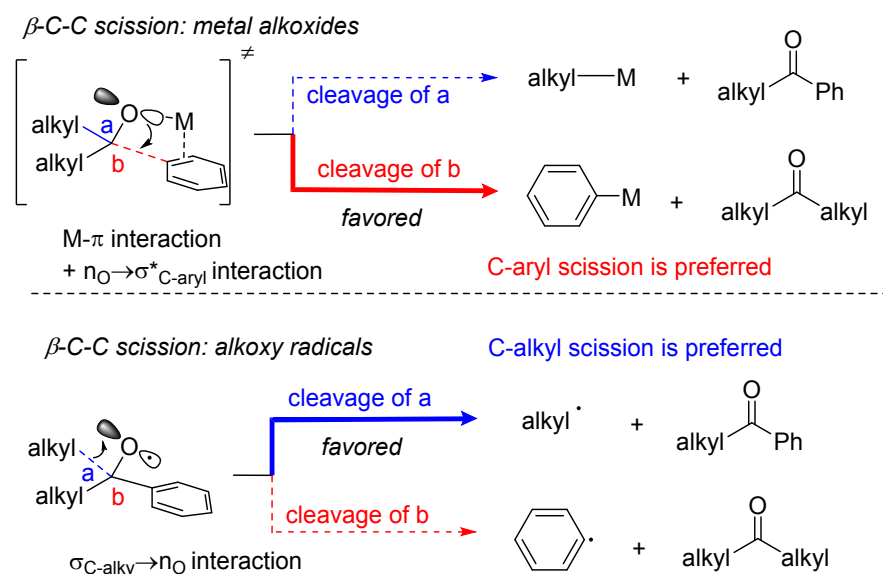
Figure 66. Umpolung of anomeric effect in oxygen radical leads to a different selectivity for β-scission

Functional Groups with Two Oxygens

The chemistry of functional groups with two oxygens is where the studies of anomeric effect originated. This is, of course, not surprising. Presence of two oxygens provides the right combination of a good donor (the lone pairs) and a good acceptor (the σ^*CO orbitals) which when positioned properly (i.e., when both oxygen atoms are attached to the same central atom) can serve as the source of significant

hyperconjugative stabilization. The anomeric effect is a consequence of "stereoelectronic chameleonism" of oxygen (its ability to be either a donor or an acceptor, depending on electronic demand).[34, 174, 175]

An interesting corollary is that stereoelectronic interactions in such systems come as a part of interconnected network, the simplest of which is a pair of $n_O \rightarrow \sigma^*_{CO}$ interactions in acetals. The network becomes more complex in esters where three lone pairs of the two oxygens are involved in delocalizing interactions (vide infra).

The stereoelectronic nature of these effects is also illustrated by the value of correct mutual arrangements – when the two oxygens are too close (peroxides) or too far away (1,4-dioxa functionalities), the importance of anomeric effects generally diminishes as oxygen lone pairs are not stabilized by strong vicinal acceptors. However, we will show below that even for those "non-anomeric functionalities", this stereoelectronic factor can be reactivated, as illustrated particularly well by the recent successful use of anomeric effect as a new tool in peroxide chemistry (vide infra).

Acetals and hemiacetals

A quick glance in the relative magnitude of the pair of anomeric interactions in acetals and hemiacetals is provided by NBO data in Figure 67. The interactions are quite strong – at the order of 14-15 kcal/mol (much stronger than 6-7 kcal/mol $n_O \rightarrow \sigma^*_{C-H}$ donations for ethers and alcohols in Figure 7). For hemiacetal, the σ^*C-OMe group is a slightly better acceptor that the σ^*C-OH but this trend is likely to be strongly affected by the nature of H-bonding and by the media pH. In the absence of cyclic constraints, these functionalities adopt a conformation where p-type lone pairs align very well with the σ^*C-O acceptors.

$n_O \rightarrow \sigma^*_{C-O}$: *strong* $n_O \rightarrow \sigma^*_{C-O}$: *strong*

$n_O(p) \rightarrow \sigma^*_{C-O}$
14.0 kcal/mol

$n_O(p) \rightarrow \sigma^*_{C-O}$
14.6 kcal/mol

$n_O(p) \rightarrow \sigma^*_{C-O}$: *strong* $n_O(p) \rightarrow \sigma^*_{C-O}$: *strong*

$n_O(p) \rightarrow \sigma^*_{C-O}$
13.6 kcal/mol

$n_O(p) \rightarrow \sigma^*_{C-O}$
13.6 kcal/mol
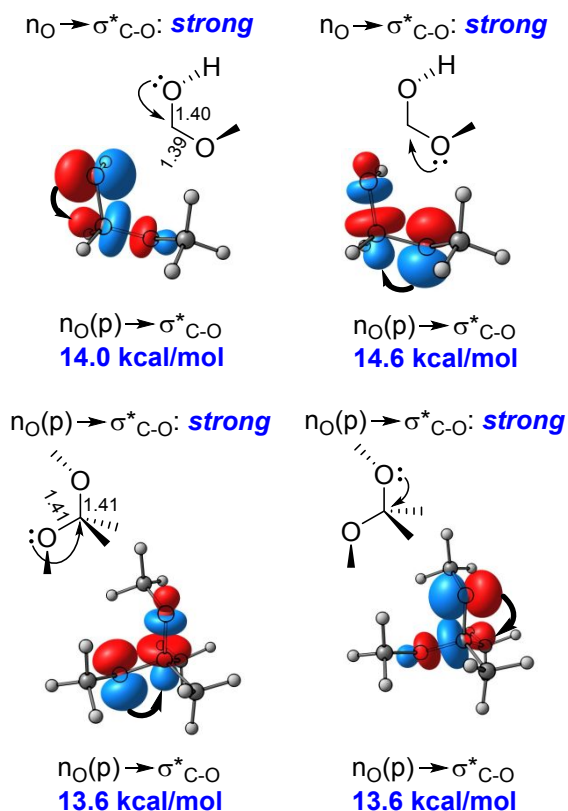
PBE0-D3BJ/aug-cc-pVTZ/CPCM(H_2O)

Figure 67. Stereoelectronic portrait of acetal and hemiacetal. Note that anomeric interactions come in pairs to delocalize electron density in the opposite directions, avoiding the unfavorable charge separation

These hyperconjugative interactions are reflected in the dramatic difference in conformational properties of acyclic acetals and their all carbon analogs. In contrast to the extended zigzag conformation of pentane, 1,1-dimethoxymethane (aka "2,3-dioxapentane") prefers a twisted gauche,gauche geometry ($\Delta G \sim$ 5-6 kcal/mol, Figure 68). The stereoelectronic contribution to this preference involves aligning the p-type lone pair of oxygen with the σ^*_{C-O} acceptor.

Of course, the $n_O \rightarrow \sigma^*_{C-O}$ interactions also contribute to the ~1 kcal/mol greater stability of axial 2-OMe tetrahydropyran relative to the equatorial conformer. Note that the difference is smaller than the difference between anti,anti- and gauche,gauche-conformations of 1,1-dimethoxymethane because the equatorial conformer of 2-OMe-THP does not lose *all* of anomeric stabilization because the exo-anomeric effect is active in both axial and equatorial conformers.
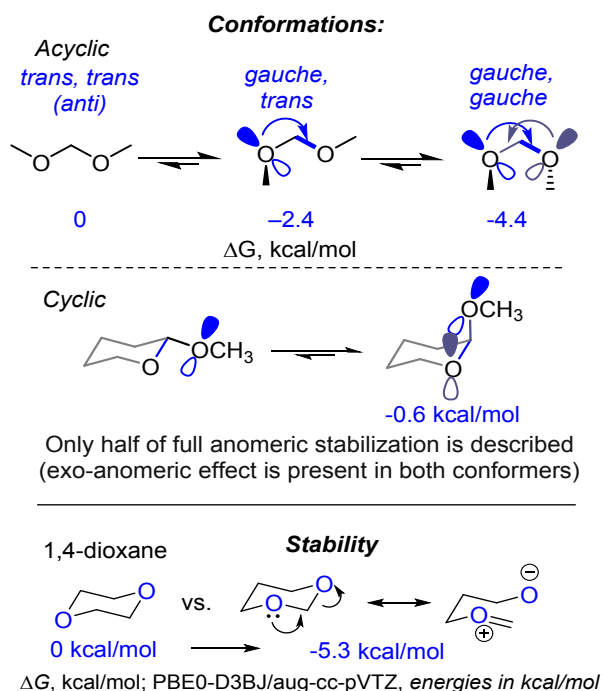
Figure 68. Top: Conformational preferences in acyclic and cyclic acetals are associated with the generalized anomeric effect. Bottom: Stabilization of acetals illustrated by comparison of 1,3- and 1,4-dioxane

The stabilizing power of anomeric delocalization is also illustrated by the fact that 1,4-dioxane is ~5 kcal/mol less stable than 1,3-dioxane. This difference clearly indicates the presence of a stabilizing effect, specific to the acetal subunit of 1,3-dioxane. Although the endocyclic C-O bonds are not aligned well with the p-type oxygen lone pairs, the effect is still apparently large enough to contribute to the observed trend in stability.

The anomeric effect is ubiquitous in the chemistry of acetals where many processes are controlled by the stereoelectronics of $n_O \rightarrow \sigma^*_{CX}$ interactions. For example, the protection of alcohols by converting them to methoxymethyl ether (MOM) in reaction with chloromethyl methyl ether (MOM-Cl) relies on the anomeric effect. As a conductor directing a musical performance, the lone pair of oxygen provides anomeric assistance to *both* the C-Cl bond breaking and the C-O bond making (Figure 69). The kinetic consequences of anomeric assistance are dramatic: ethanolysis of chloromethyl methyl ether proceeds ~ 10^{13} times faster than ethanolysis of propyl chloride.[176] The acceleration is even greater (~10^{14} times faster) in comparison to methyl chloride. Although the anomeric assistance develops to a greater extent along the S_N1 path, the S_N2 reaction with ethoxide ion was also evaluated to be much faster (by a factor of about 10^5) for MOM-Cl than for methyl chloride.[177]
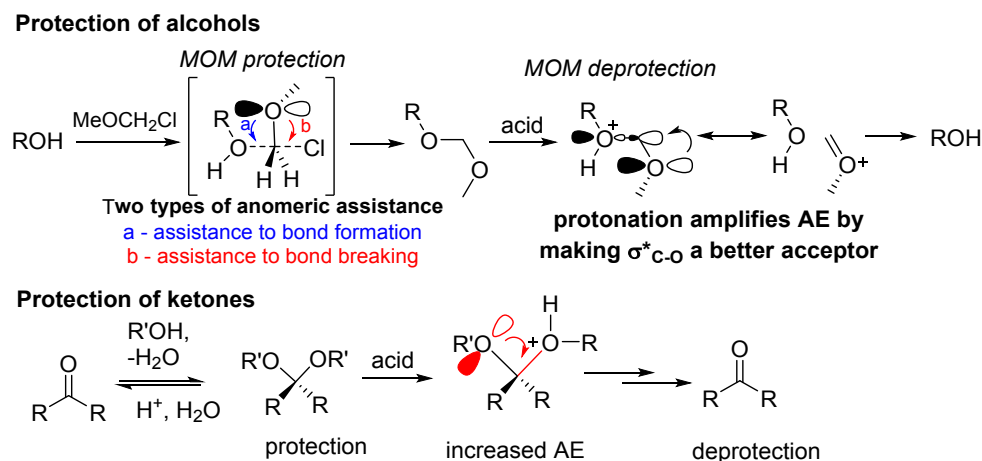
Figure 69. Top: Protection of MOM-alcohols and MOM-deprotection are assisted by anomeric effect. Bottom: Protection of ketones as acetals and subsequent deprotection also benefit from anomeric effect

Not surprisingly, the acid-catalyzed hydrolysis of the MOM-protected alcohols is also aided by the anomeric effect. Protonation of the leaving group weakens the breaking C-O bond by amplifying the anomeric $n_O \rightarrow \sigma^*_{CO}$ interaction. This effect explains why the MOM-protection is so readily removed under acidic conditions. The same reaction (reversible formation of acetals) serves for protection/deprotection of aldehydes and ketones.

Dussault and coworkers creatively used a similar approach for selective formation of alkyl hydroperoxides.[178] The standard methods for nucleophilic introduction of the OOH group require prolonged reaction with concentrated solutions of hydrogen peroxide under strongly basic conditions. However, once hydrogen peroxide is "half-ketalized" to form 2-hydroperoxy-2-methoxypropane, the latter can take advantage of the anomeric effect and reacts with alkyl halides under mild conditions (Figure 70). The desired alkyl hydroperoxides are formed cleanly upon deprotection under slightly acidic conditions. In this example, anomeric effect controls regioselectivity of OOH group transfer by directing which of the two C-O bonds in the protected alkyl hydroperoxide will be broken. Not surprisingly, the anomeric assistance leads to clean reactions and high selectivity.
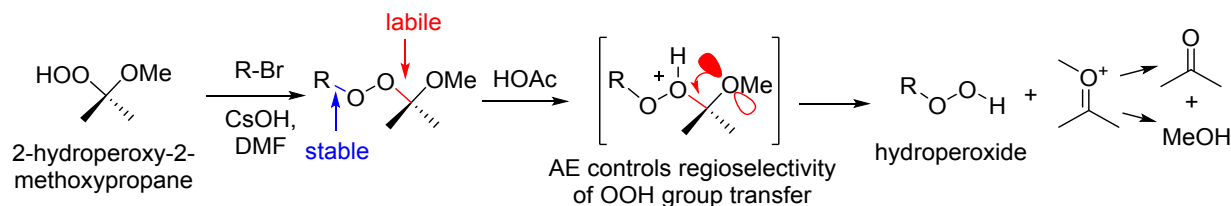
Figure 70. Convenient synthesis of alkyl hydroperoxides by selective OOH group transfer from 2-hydroperoxy-2-methoxypropane, the "half-ketalized" hydrogen peroxide

An alternative approach to making the $n_O \rightarrow \sigma^*_{C-O}$ interactions stronger involves increasing the donor ability of oxygen. Dussault and coworkers used this idea to elegantly control the regioselectivity of nucleophilic attack at an O-O bond in developing practical ways to transfer an electrophilic alkoxyl ("RO+") from organic peroxides to organometallics.[179] This process would offer an alternative to traditional nucleophilic methods for etherification. Whereas reactions of dialkyl peroxides are largely limited to transfer of methoxide or primary alkoxides, monoperoxyacetals display significantly expanded reactivity, transferring primary, secondary, or tertiary alkoxy electrophiles toward destabilized carbanions through highly regioselective attack on the non-acetal oxygen of the peroxide. The tetrahydropyranyl monoperoxyacetals are quite stable but react readily with sp³ and sp² organolithium and organomagnesium reagents to furnish ethers.
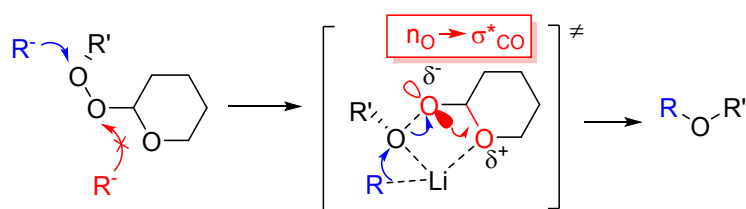
Figure 71. The possible amplification of anomeric effect leads to efficient transfer of an electrophilic alkoxyl ("RO+") moiety from organic peroxides to organometallics

The structural and mechanistic data suggest that cleavage to alkoxy radicals is unlikely in the above process. The calculated TS geometries involve an S_N2-like arrangement of the carbanion, the lithiated oxygen, and the departing oxygen but with a side-on of the Lewis acidic Li cation with the attacked oxygen and the acetal oxygen of the THP moiety. As oxygen is generally less sterically encumbered than carbon, similar yields are obtained for transfer of primary, secondary, and tertiary alkoxides. The acetal group significantly lowers the barrier for reaction with the organometallic partner. Control experiments suggest that the bidentate coordination between the Lewis-acidic Li-cation and the two oxygens is not sufficient to explain the results, as evidenced by the poor reactivity observed with methoxyethyl peroxide. An intriguing hypothesis for the enhanced yield includes amplification of the anomeric effect in the THP moiety in the transition state and the reaction product (Figure 71). The nucleophilic O-O bond cleavage creates a transient anionic center that can take advantage of the $n_O \rightarrow \sigma^*_{CO}$ anomeric interaction with the

endocyclic C-O bond of the tetrahydropyrane ring, especially since the acceptor ability of this C-O bond is synergistically increased by Li…O coordination.

Terent'ev and coworkers developed an elegant approach to synthesis of wide range of 1,2,4,5-tetraoxanes[180, 181] and 1,2,4,5,7,8-hexaoxanes[182, 183] via reaction between acetals and hydroperoxides (Figure 72). The use of the acetal function allows synthesis of tris-peroxides from C_6–C_{12} cycloalkanones. We will discuss later that such cyclic bis- and tris-peroxides are more accurately described as bis- and tris-acetals significantly stabilized by anomeric effect (vide infra).[184, 185]
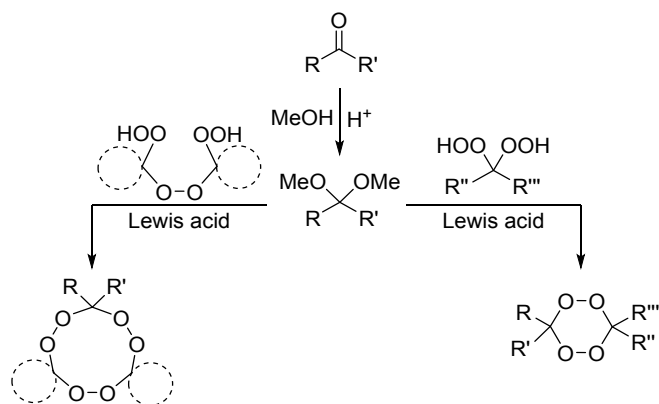
Figure 72. Synthesis of cyclic peroxides from acetals and hydroperoxides.

The Petasis-Ferrier rearrangement (PFR) is a valuable process that utilizes the dual (O- vs. C-) reactivity of enolates for controlled formation of C-C bonds via an anomerically-controlled isomerization.[186-189] The acid-catalyzed ring opening forms an enol concomitantly with an anomerically stabilized cationic center. The latter serves as an electrophile that can, in the last step of the PFR cascade, recapture the enol at the C-terminus. In the key step on route to the cationic intermediate, the C-O scission is assisted by anomeric stabilization by a lone pair of an adjacent heteroatom (Figure 73). The Au-catalyzed versions of PFR utilize alkynes as carbonyl equivalents.[190-196]
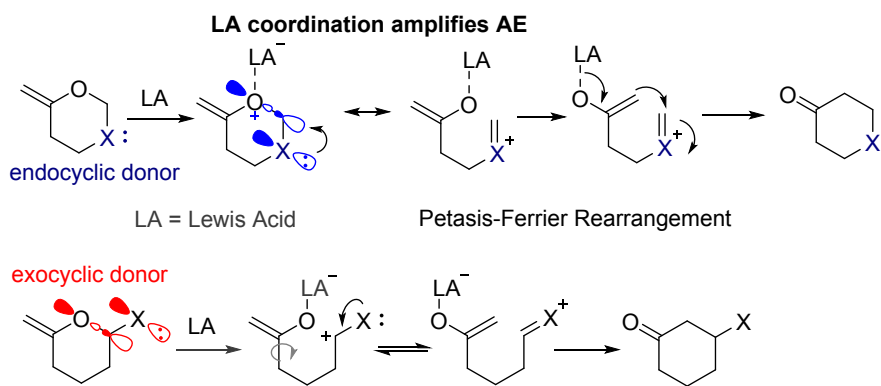
Figure 73. Two possible anomeric stabilization patterns for the Petasis-Ferrier rearrangement.

Double assistance from the two acetal oxygens leads to an efficient 1,5-hydride shift that transforms a quite stable (tertiary+benzylic) cation into a dioxacarbenium ion under mild conditions.[67] Reaction diastereoselectivity is consistent with the chair-like TS for the shift. The transiently formed dioxacarbenium ion is trapped by reaction with a nucleophile followed by the acetal ring opening (Figure 74).
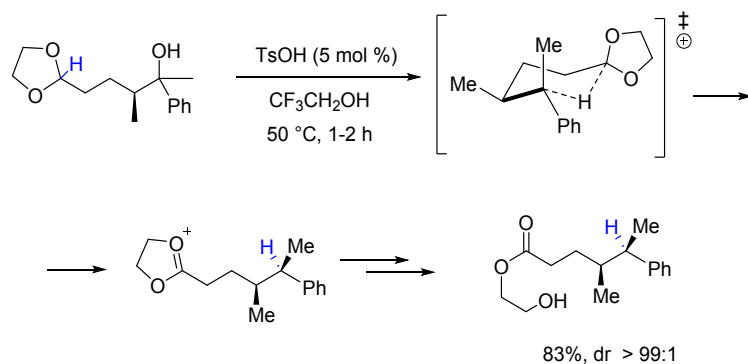
Figure 74. Anomeric assistance in an acetal leads to efficient 1,5-hydride shift to a tertiary benzylic cation

Stereoelectronically defined cyclic acetals such as carbohydrates were instrumental in the discovery of anomeric effect. Not surprisingly, anomeric effect manifests itself broadly in carbohydrate reactivity.[197] We will not discuss this topic in detail here as a superb analysis by Kirby is available in the literature.[2] Hence, we will provide only a few illustrative examples.

We will start by suggesting that the importance of anomeric effect in acetals transcends organic chemistry to define many aspects of biology, economy, and, even, human history. A large part of natural organic molecules are oligo- and polymeric carbohydrates which predominantly exist in cyclic acetal forms. For example, cellulose, the most abundant polymer in nature (representing about 1.5×10^{12} tons of the total annual biomass production), is composed of the β-anomer of D-glucose[198] whereas starch corresponds to

different polymeric forms (amylose and amylopectin) composed of α-anomeric D-glucose units (Figure 75). The C-O bond linking the monomer glucose units is axial in the α-anomer (starch) and equatorial in the β-anomer (cellulose). Intuitively, one would think that AE should be important for the difference in properties of these α- and β-anomers of glucose. For example, if hydrolysis of cellulose were not fully assisted by kinetic anomeric effect, one could argue from a simplified point of view that the trees grow tall and wooden houses can survive hurricanes because of deactivation of the anomeric effect. In contrast, the role of starch in food sources (from rice, wheat, and potatoes to beer brewing) would be enabled by anomeric activation. Every time when we enjoy a bowl of Irish stew with a glass of beer, we would be grateful for the stereoelectronic power of oxygen.
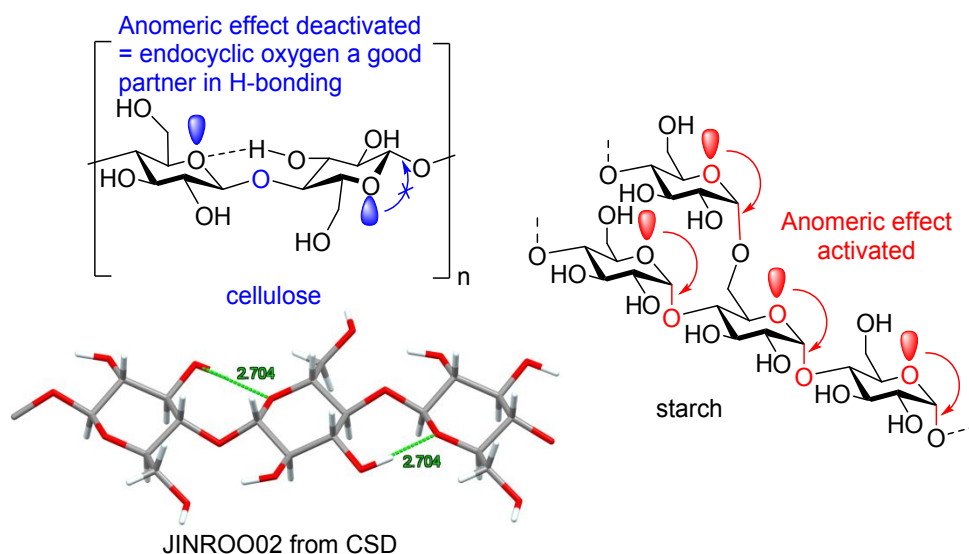
Figure 75. Difference in anomeric effect account for the contrasting properties of cellulose (left) and starch (right, amylopectin - the branched component of starch). A crystallographically determined geometry for a cellulose unit from the Cambridge Structural Database is given to illustrate the importance of intramolecular H-bonding with the endocyclic oxygen.

In reality, the anomeric effect's influence on the relative reactivity of conformationally flexible anomeric systems is not straightforward.[199] We will show examples below where a less stable equatorial anomer can react faster that the axial anomer and that the anomeric effect can be activated in the TS for the solvolysis by a conformational change of a non-anomerically stabilized reactant. Hence, indirect effect of AE on the shape, molecular packing, and H-bonding ability of the endocyclic oxygen atom, as well as the availability of suitable hydrolyzing enzymes, may be more important for the observed differences in the reactivity of starch and cellulose.

In particular, Kirby reiterated that methyl α-glycosides, with axial leaving groups, are hydrolyzed more slowly than the equatorial anomers.[2] In the case of aryl glycosides, the α-isomers are hydrolyzed faster than the β-anomers[200], but the effect is relatively small, and complicated by the initial proton transfer equilibrium needed to activate the leaving group. Remarkably, it is the β-series where the acid hydrolysis is enhanced by the introduction of electron-withdrawing substituents while substitution in the phenyl group in phenyl α-D-glycosides have a very small effect on the reaction rates.[201]

Because complex carbohydrates often possess additional polar substituents that combine (or compete) with the anomeric effect to yield new cooperative stereoelectronic patterns, it is helpful to start with the simpler systems. Formation of the oxacarbenium ion via the axial leaving group departure from an α-glycoside proceeds through a more stabilized TS than the analogous departure in the equatorial β-conformer. Due to the principle of microscopic reversibility, the reverse process (i.e., the addition of nucleophiles to the oxacarbenium ion) proceeds through the same transition state and preferentially provides the axial product (i.e., the 1,2-cis glycoside in Figure 76).[202-204]
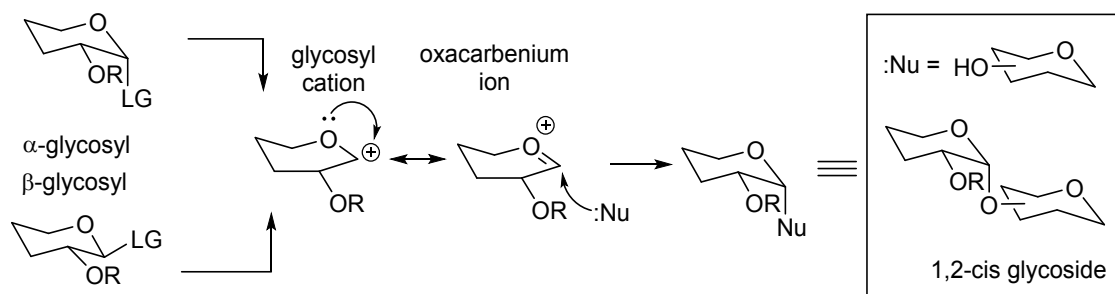
Figure 76. Conversion of α- and β-glycosides into glycosyl cations and their reactions with nucleophiles. Note that this mechanism is oversimplified: currently glycosylation is regarded as proceeding at the S_N1/S_N2 interface.[205]

Interestingly, the greater stabilization of the axial TS does not mean that the ionization of an α-glycoside proceeds faster. In many cases, the β-anomeric systems with an equatorial leaving group undergo much faster solvolysis.[206] This behavior stems from the differences in the anomeric stabilization of reactants and the ionization transition states. For the α- glycoside, such stabilization is present in *both* the reactant and the TS. For the β-glycoside, however, such stabilization only becomes significant in the electron-deficient product-looking transition state (Figure 77).
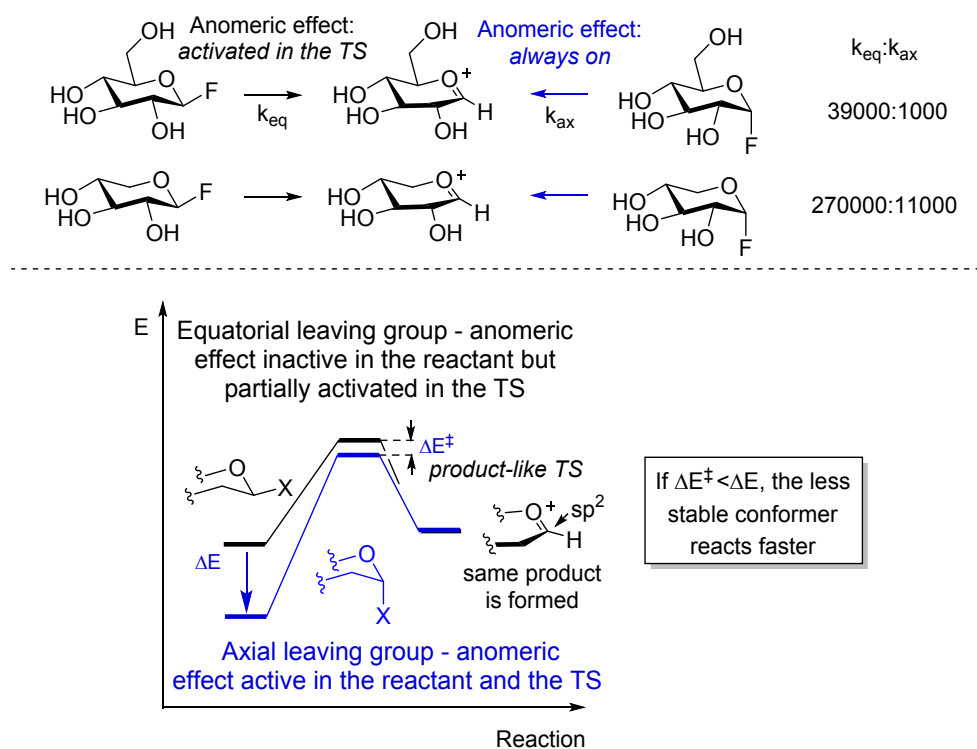
Figure 77. If the two conformers do not interconvert, the combination of inactive AE in the reactant and substantial TS stabilization leads to the faster solvolysis of equatorial vs axial leaving groups.

Several intriguing reports provided evidence for "anomeric memory" in mass-spectrometry, i.e preservation of the memory of the stereochemistry of the glycosidic bond in the monosaccharide fragments.[207, 208] However, the most recent study based on a combination of cryogenic vibrational spectroscopy and ion mobility-mass spectrometry suggests that the ions do not retain a memory of their anomeric configuration.[209] At least for ionization of protected galactosides derived from the different anomers, the IR signatures indicate that, if the anomeric C-O bond breaks, the investigated fragments exhibit an identical structure.

A more detailed mechanistic picture of anomeric ionization involves species with varying degrees of charge separation. For example, the anomeric triflates formed transiently in reactions of glycosyl donors form the spectrum of the contact and solvent separated ion pairs. Although the equilibrium concentration of such ionic species is low, their formation is fast due to the strong anomeric assistance. The calculated Gibbs free energy penalty for breaking the axial C-O bond in 2,3,4,6-tetra-O-methyl-α-D-glucopyranosyl triflate is only 10.4 kcal/mol. Ionization of the equatorial leaving group is more difficult (13.5 kcal/mol, M06-2X/6-311++G(d,p))[210] but still accessible under the ambient conditions. The solvent separated ion pair was evaluated to be about 15 kcal/mol higher than the axial triflate (Figure 78).
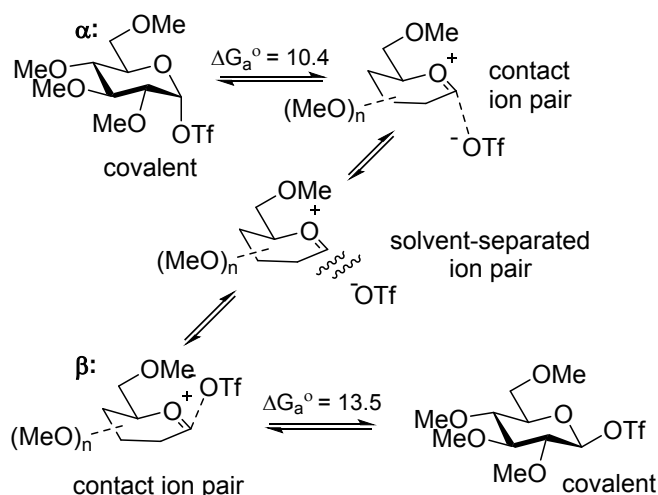
Figure 78. The spectrum of intermediates and activation energies (in kcal/mol) for solvolysis of the two anomeric triflates.

Furthermore, conformational analyses of these ion pairs indicated that the oxacarbenium ions can adopt a number of conformations of similar stability and that this stability depends on the relative location of the counter anion. The relatively small difference for the above cations suggests that structural distortions can allow flexible molecules to reach alternative stereoelectronic arrangements of similar magnitude.
 In order to understand such effects, Kirby and coworkers designed several families of bicyclic acetals with increasingly strict structural constrains. Interestingly, tetrahydropyranyl acetals derived from trans-oxadecalin shows only a modest acceleration for the axial conformer and only under the acid-catalyzed conditions (the corrected rate factor of 13),[211] perhaps because the free end of the chair can still twist to position a lone pair of electrons antiperiplanar to the leaving group. Additional constraints in a stiffer tricyclic structure make the expected effects larger (the factor of 60 under acidic conditions) (Figure 79).[212]
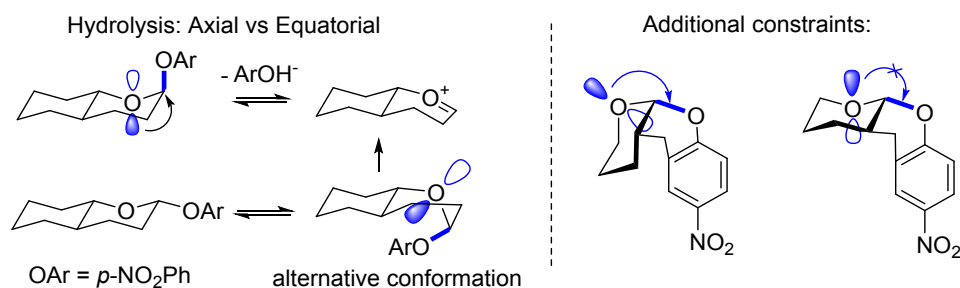
Figure 79. Left: Structural distortions allow reaching a stereoelectronically favorable conformation**.** Right: Greater rigidity makes structural distortions more difficult

To overcome the formation of alternative geometries where the anomeric effect is partially activated, the rigid 9-oxabicyclo[3.3.1]nonane was eventually chosen for evaluating the full role of stereoelectronic assistance to the ionization process. This rigid bicyclic system enforces a nearly orthogonal arrangement of the cation p-orbital and the oxygen p-lone pair in the putative oxacarbenium ion (Figure 80). In this geometry, the lone pairs of the ring oxygen cannot assist the exocyclic C-OR cleavage and this acetal is hydrolyzed ca. 10^{13} times slower than its axial tetrahydropyranyl analog. This difference in reactivity corresponds to ~19 kcal/mol contribution for the stereoelectronic barrier to the cleavage of an equatorial tetrahydropyranyl acetal (a model β-glucoside) in its ground-state chair conformation.[213]

Rigid acetals

oxygen and cation
p-orbitals are nearly
orthogonal
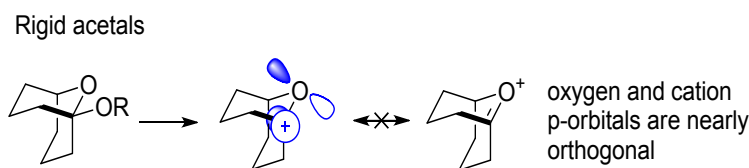
Figure 80. The inefficiency of anomeric n_O/σ^*_{CO} interaction in a bicyclic acetal is translated to the poor resonance stabilization in an anti-Bredt oxacarbenium ion

These studies provided important insights into the nature of stereoelectronic control of reactivity. Although anomeric assistance is very hard to switch off completely, it is variable and tunable. Changes in reaction conditions and substrate structure impose additional effects on reactivity and selectivity. In particular, such factors as ion pair formation, substituent effects, involvement of the boat conformation, and participation of neighboring groups further enrich this complex picture.[205, 214]

Such effects have been studied extensively in enzyme-catalyzed reactions of sugars where the active sites show remarkable flexibility in catalyzing all possible types of stereoselective hydrolysis.[215] Nature mastered the active site designs that allow the hydrolysis to proceed with the high degree of control and to follow either the inversion or the retention for both α- and β-glycosidases. Depending on the enzyme type, the transformations include one- or two-step mechanisms where the external (water) and internal nucleophiles (the catalytic carboxylic group residues) can participate in chemistry at the anomeric center either together or sequentially.[216]

Hydrolysis of a glycoside with net inversion of anomeric configuration is generally achieved via a one-step, single-displacement mechanism involving oxocarbenium ion-like transition states. The reaction typically occurs with the assistance from two carboxylic acids, that are typically located at a relatively large distance of 6-11 Å. On the other hand, hydrolysis with net retention of configuration generally requires a two-step, double-displacement mechanism where one of the enzyme carboxylates serves as a temporary tether for

the glycosyl intermediate. This process proceeds via two transition states with oxacarbenium character. In this case, the more intimate involvement of the assisting carboxylic acid/carboxylate pair requires closer proximity between the respective amino acid residues (~ 5.5 Å). Independent of the mechanism and the adopted conformation for each particular scenario, the relatively flexible transition states are likely to enjoy significant anomeric interaction supplemented, when needed, with non-covalent interactions within the catalytic cavity. For α-glycosides, the anomeric stabilization present in the starting material would increase in the TS due to protonation of the axial leaving group and the C-O bond stretching associated with the leaving group departure. For β-glycosides, the anomeric stabilization would be smaller initially but increase as planarization of the TS geometry would provide a better overlap between the endocylic lone pair and the breaking C-O bond (Figure 81).
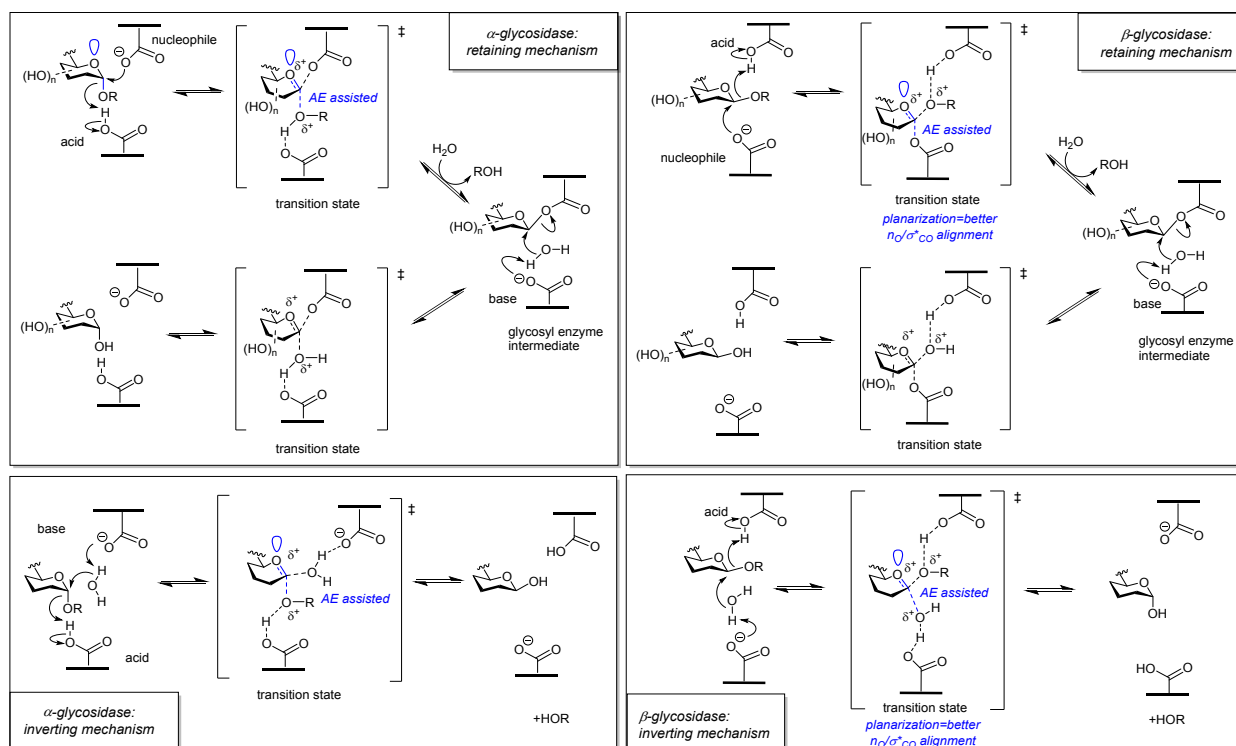
Figure 81. The flexibility of anomeric stabilization allows selective enzyme-catalyzed transformations at the anomeric center.

Radical reactions: The activating effects of anomeric delocalization on radical reactions is generally smaller in comparison to the cationic processes. Even then, the observed C-H bond dissociation energies (BDEs) at the anomeric positions of in ketals can come as a surprise. In fact, the C-H BDEs in 1,1-dimethoxymethane and diethyl ether are essentially identical (~93 kcal/mol). Although both ketals and ethers are activated relative to alkanes (i.e., their BDEs are ~5 kcal/mol lower than a typical secondary C-

H bond, Figure 82),[131, 217] their similarity to each other is counterintuitive as it is clear that *two* lone pairs (in acetals) should stabilize the radical center better than *one* lone pair (in ethers). So, why is the formation of a more stabilized radical paradoxically come with a greater thermodynamic penalty?

The answer to this seeming paradox comes logically from analysis of the full set of stereoelectronic effects in this system. One can consider acetals to be *deactivated by* the anomeric effect because, in order for the lone pairs of oxygen to stabilize the α-radical center formed after C-H bond scission, a strong $n_O \rightarrow \sigma^*_{CO}$ interaction has to be *sacrificed* for the reactant to adopt the right conformation where the p-type lone pairs are aligned with the weaker C-H acceptors. This is reflected in the ~5 kcal/mol penalty[185] for this conformational change. As the result, reactant stabilization compensates for the product stabilization.
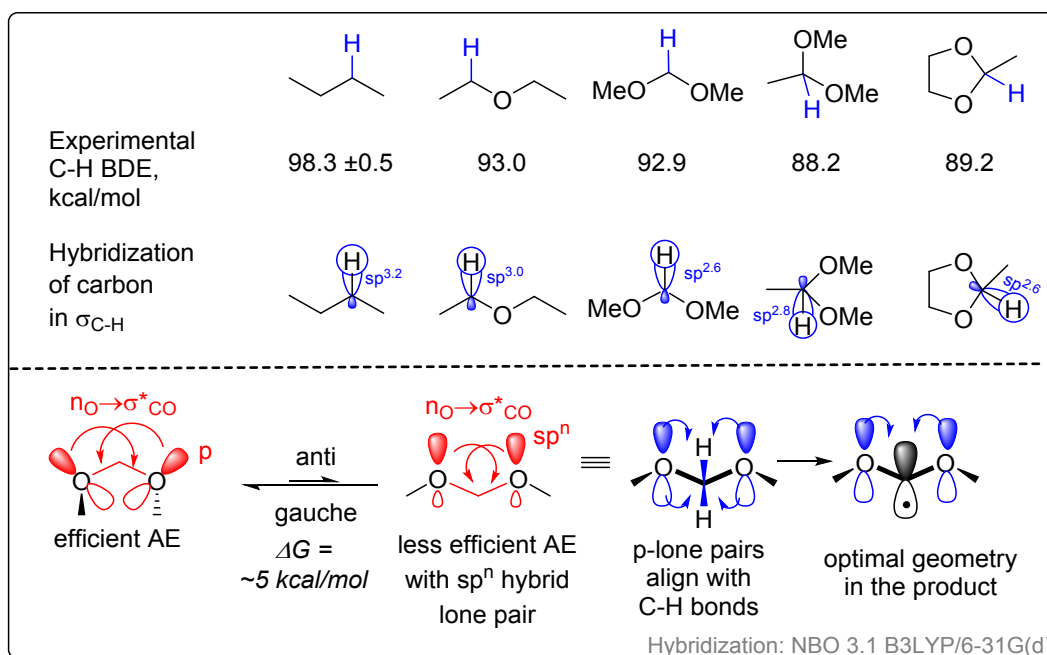
Figure 82. Anomeric lowering of the C–H Bond Dissociation Energy (BDE) of acetals is compensated by the sacrifice of the strong reactant stabilizing $n_O \rightarrow \sigma^*_{CO}$ interactions. Experimental BDEs are taken from [218] for 2-Me-1,3-dioxolane, and from [217] for the other molecules.

Interestingly, confining the anomeric center into a nearly flat (albeit syn) geometry in 1,3-dioxolane makes the acetal C-H bond slightly stronger (~1 kcal/mol, Figure 82) than the C-H bond in MeCH(OMe)$_2$. This deactivation may arise from hybridization effects associated with increase in s-character in the C-H bond of acetals which render the C-H bond stronger. This is a consequence of rehybridization (i.e., the p-character increase) in the strained C-C bonds of the five-membered ring.[77]

The enhanced reactivity of the acetal C-H bond can be used to capture electron-deficient radicals. An interesting consequence of such control is suggested for the conformationally-controlled fragmentation of Esperamicin A_1. Esperamicin A_1 is a natural enediyne antibiotic which DNA-damaging biological activity is based on its transformation into p-benzyne diradicals via Bergman cyclization (Figure 83A).[219] Due to its high reactivity, the possible mechanism for the auto-protection from this toxin by the enediyne-producing microorganisms is of much interest.[220] It was suggested that the "conformationally-gated" Bergman cyclization could serve as such a mechanism based on the observation that Esperamicins are exported out of the producing cell in a full, unfragmented form but fragment into the aromatized and carbohydrate parts upon their activation and subsequent Bergman cyclization.

To test this model, Baroudi et al. prepared the model enediynes with the carbohydrate-mimicking acetal and found them undergo fragmentation into an aromatic core after their Bergman cyclization product is intercepted by transfer of the weak C-H bond from the anomeric position (Figure 83B,C).[221] Formation of an anomerically stabilized radical extends the cascade and renders this endergonic cycloaromatization irreversible.[222] Because trapping of *p*-benzynes in such reactions requires the carbohydrate moiety to reach a suitable orientation for the intramolecular H-abstraction step, this step is "conformationally gated" and provides a potential way to couple dissociation from the enediyne/protein complexes with the conversion of prodrugs into an activated form. From this perspective, *the anomerically controlled C-H abstraction provides a possible mechanism for preventing premature activation of this DNA-damaging natural product inside the microorganism where it is produced.*

It is possible that the relatively large steric bulk of enediyne substituents places them equatorially and the C-H bond axially at the anomeric center, thus assisting in the H-atom transfer. Interestingly, an unexpected O→C transposition found in these radical cascades (Figure 83C) was developed further into an metal-free conversion of phenols into substituted benzamides and benzoic esters.[223]
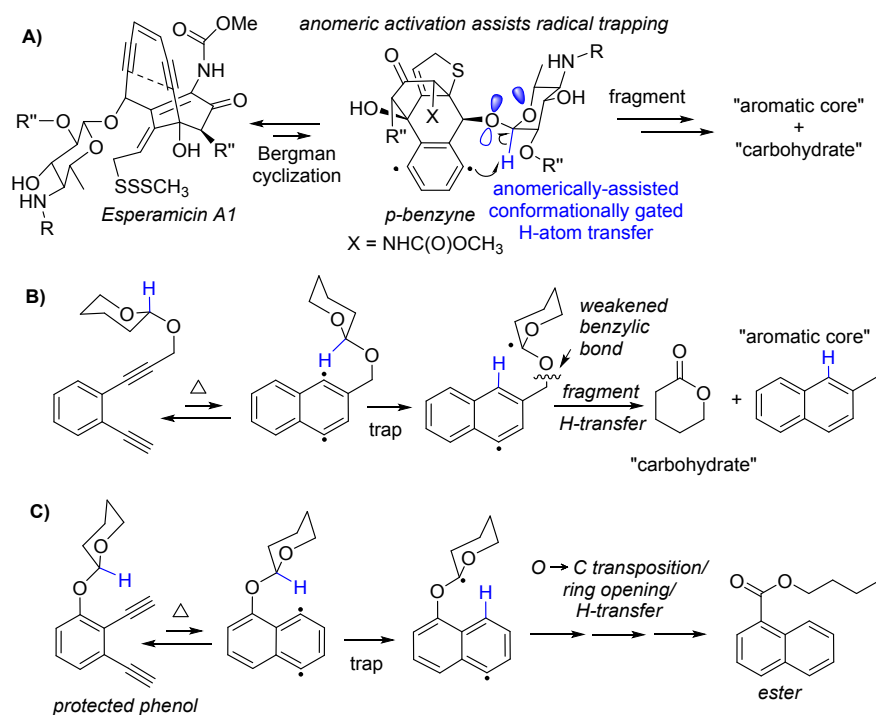
Figure 83. A) The fragmentation of Esperamicin A1, B) The fragmentation of esperamicin mimics initiated by intramolecular H-abstraction from an anomeric position, C) O→C radical transposition triggered by the anomeric radical formation.

The stereoelectronic component of radical H-atom transfers in acetals was illustrated by Hayday and Kelvey, who found that the cis isomer of 2-methoxy-4-methyl tetrahydropyran undergoes hydrogen atom abstraction by triplet benzophenone at ambient temperature 8 times faster that its trans isomer.[224] Considering that the preferred orientations for exo methoxy groups aligns their stereoelectronically active lone pair with the ring C-O bond (due to the exo-anomeric effect), this example is complicated by the conformational change required for the exo-OMe group to assist in C-H activation. In this context, it is interesting to analyze H-atom abstraction in more conformationally well-defined substrates, 1,3-dioxanes (Figure 84).[225] As expected, the equatorial isomer with two lone pairs always aligned with the target axial C-H is more reactive in both cases. The difference in reactivity, however, is moderate suggesting that even the less reactive isomer may still be significantly activated, possibly by the C-H overlap with the equatorial lone pair. In addition, the earlier, reactant-like TSs for these quite exergonic reactions may be less sensitive to the anomeric TS-stabilizing influence than less exergonic reactions where only one oxygen atom assists in the α-radical formation.

Hayday and Kelvey:

Relative rates in reaction with Ph₂CO triplet

8   1

endo+exo anomeric activation

more stable   favorable for H-abstraction

Beckwith and Easton:

Relative rates in reaction with t-BuO radical:

11   1

double-endo anomeric activation
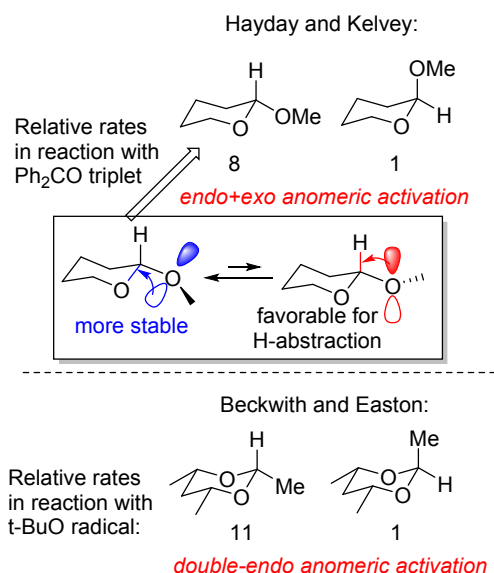
Figure 84. Comparison of stereoelectronic features in C-H activation in two doubly-activated anomeric systems

Selective radical activation of the anomeric C-H in 1,3-dioxolane was used by Doyle and coworkers to develop a redox-neutral formylation of aryl chlorides.[226] An elegant feature of this approach is that activation of aryl chlorides leads to the formation of the Ar-Ni(L)$_n$-Cl species that undergoes a homolytic Ni-Cl bond scission to produce a chlorine radical upon photochemical excitation (Figure 85). The electrophilic radical is ideal for C-H activation at the anomeric position of 1,3-dioxolane. An interesting feature of this process is that this radical is intercepted via a "rebound" to the Ni^{II} species, forming an intermediate that is likely to be stabilized by $n_O \rightarrow \sigma^*_{C-Ni}$ hyperconjugation, setting the stage for the final reductive elimination step of this cross-coupling cascade. The ~9:1 CH vs. CH$_2$ selectivity for C-H activation is higher than the 5:1 selectivity predicted from the relative C-H BDEs and stoichiometry suggesting that polar effects contribute to the favorable kinetics of the C-H abstraction. Even higher selectivity was observed when aryl bromides were used for this transformation as one would expect from the Hammond-Leffler postulate (the later transition state for bromine abstraction is more affected by the alkyl radical product stability).
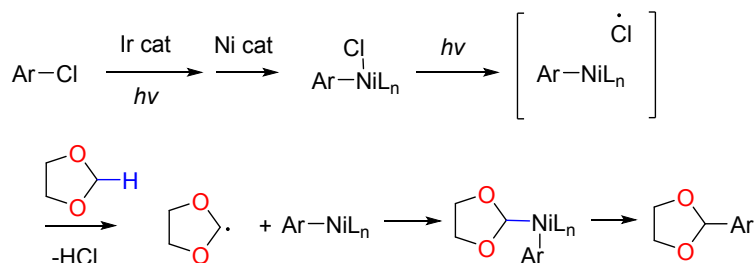
Figure 85. Coupling transition metal catalysis with photochemical Ni-Cl bond scission for C-H activation in a cyclic acetal as a part of a cross-coupling cascade

Rhodium-catalyzed carbene insertion into the anomeric C-H bond in carbohydrates reported by Lecourt et al. also shows a preference for the axial anomeric C-H bonds (Figure 86). Although the *exo*cyclic oxygen activates both the axial and the equatorial anomeric C-H bonds, the synergy between exo- and endo-anomeric activation is only possible for the hydrogen in the axial position. This added anomeric interaction significantly increases the reaction yield (from 35 to 85%) and controls the regioselectivity of the reaction. The carbene showed no insertion into the equally accessible C3-H bond. Introduction of a competing doubly-activated 3-O-benzyl group resulted in a 5:2 ratio of 1,7-C-H insertion into the benzyl position and the equatorial anomeric C-H. However, when the second anomeric interaction is "switched on" for the axial C-H bond, the ratio of the products goes to 1:1.[227] This example suggests that the additional lone pair stabilizes the C-H insertion transition state as much as conjugation with a phenyl substituent.
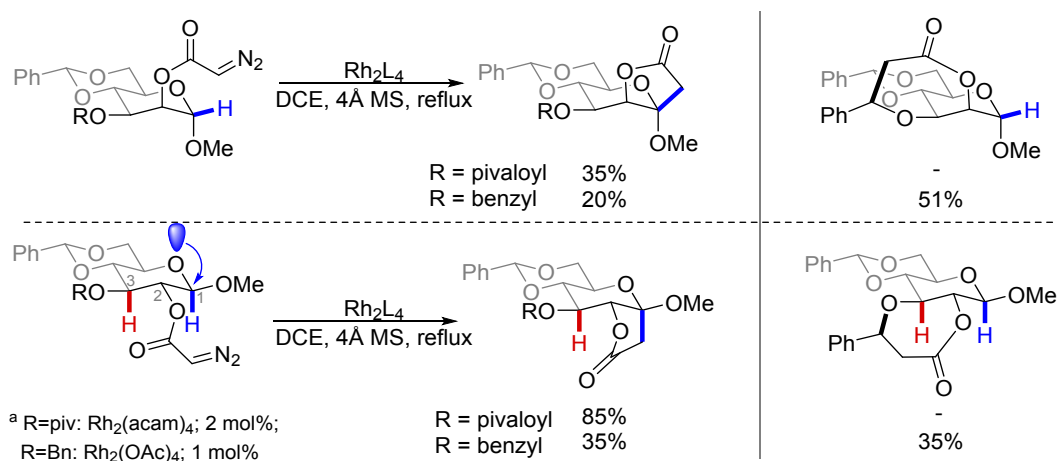
Figure 86. Influence of the anomeric effect on metal carbene insertion into C-H bonds

Gem-diols, hemiacetals, tetrahedral intermediates in additions to ketones and aldehydes:

The stabilizing role of hyperconjugation is evident when comparing equilibriums between keto- and hydrate forms of ketones and aldehydes. Comparison of acetone and formaldehyde clearly illustrates that the only reason why ketones exist in the carbonyl form instead of hydrate is C-H/π*CO interaction (Figure 87). If this donation is taken away (as in formaldehyde or hexafluroacetone), the anomerically stabilized gem-diols are more stable than their respective carbonyl counterparts. For similar reasons, the cyclic

oxocarbons C_nO_n, such as cyclohexanehexaone were only prepared as their hydrated gem-diol derivatives, e.g. dodecahydroxycyclohexane.[228]
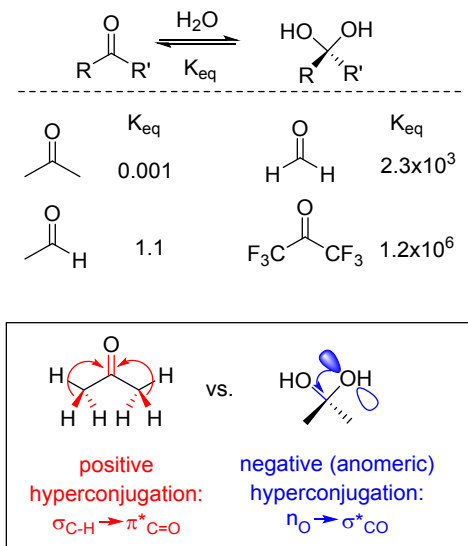
Figure 87. The tug-of-war between positive hyperconjugation in ketones and negative hyperconjugation in gem-diols explains the greater stability of gem-diols produced from aldehydes and acceptor-substituted ketones

This data is consistent with the general thermodynamic landscape of the reaction of ketones with water. For example, addition of water to acetone is ~6 kcal/mol endergonic at M06-2X/6-311++G(d,p) level of theory. However, the ΔE for the same process is strongly negative (~-9 kcal/mol). This difference suggests that the reason why formation of "anomeric" diols from ketones is unfavorable is entropic, similar to other addition reactions where two molecules are converted into one. If one considers only the intrinsic electronic effects, the gem-diols are clearly favored as a consequence of the anomeric effect. This simple comparison also illustrates why formation of cyclic hemiketals (e.g., sugars) is much more common – in the case of intramolecular addition, the entropic penalty is lower (i.e., acyclic-to-cyclic conversion is less entropically costly than conversion of two molecules into one).
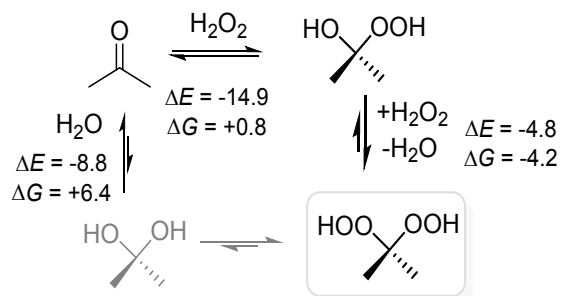
M06-2X/6-311++G(d,p), *Energies in kcal/mol*

Figure 88. General thermodynamic landscape for the reaction of acetone with H_2O_2 and water.[229]

Interestingly, addition of hydrogen peroxide to a carbonyl is more favorable than addition of water. In particular, the reaction of acetone with H_2O_2 is close to being thermoneutral at the same level of theory. Furthermore, substitution of the remaining OH group to an OOH moiety in the reaction with H_2O_2 is >4 kcal/mol exergonic, rendering double "peroxidative condensation" of acetone with H_2O_2 thermodynamically favorable (Figure 88). We will show in section on organic peroxides that this difference between gem-diols and gem-dihydroperoxides is an example of "stereoelectronic frustration" due to the lack of anomeric stabilization in H_2O_2 and the relief of this frustration when anomeric effect is activated in organic peroxides.[229]

It is also interesting to compare the thermodynamic landscapes for the reactions of carbonyls with alcohols and alkoxides (Figure 89). Whereas the reaction with methanol is similar to the reaction with water (exothermic but endergonic), reactions with "free" methoxide and its lithium salt are much more favorable. The reaction with free methoxide is only uphill by ~1 kcal/mol in the gas phase (and ~11 kcal/mol downhill when solvation is included). The more favorable thermodynamics here is consistent with the greater stabilizing effect of the $n_{O^-} \rightarrow \sigma^*_{CO}$ interaction in the anionic addition product relative to the $n_{OH} \rightarrow \sigma^*_{CO}$ interaction in the neutral hemiketal. Interestingly, the Li-alkoxide addition is even more favorable since it takes advantage from the increase in $n_{OLi} \rightarrow \sigma^*_{CO}$ over $n_{OH} \rightarrow \sigma^*_{CO}$ stabilization and with the Li...O chelation in the product.

				Gas phase $\Delta G, \Delta H$	MeOH $\Delta G, \Delta H$

kcal/mol, M06-2X(D3)/6-31++G(d,p) Integral=UltraFine

Gas phase $\Delta G, \Delta H$ / MeOH $\Delta G, \Delta H$:

2.6, -9.7   2.7, -6.1
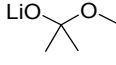
-11.4, -24.4   -5.1, -17.0
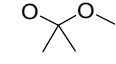
-10.5, -22.1   -0.6, -11.1

0.5, -11.9   -1.4, -10.5

Figure 89. Thermodynamics of parent carbonyls reacting with methanol and methoxide. Blue values are computed with SMD=MeOH and using the MeOH concentration of 24.75 mol/L.[230]

As expected from the lower stability of aldehydes and in agreement with their more favorable equilibrium constants for hydration reactions (Figure 87), the calculated methanol addition free energy is more favorable for ethanal than for acetone (~4 kcal/mol in the gas phase, Figure 89).[231]

The equilibrium between hemiacetals and aldehydes can be shifted if hemiacetals are stabilized by an additional factor. For example, Drahoňovský and Lehn have shown that reversible formation of hemiacetals can be accomplished via either protonation or metal cation coordination (Figure 90). The resulting dynamic hemiacetal systems can selectively adjust to the most suitable partner, e.g., forming a macrocycle to accommodate Pb(II) and an acyclic dimer to bind Zn(II). Similar transformations are possible via transacetalation of formaldehyde acetals (formal metathesis), which provide well-behaved dynamic libraries of cyclophane formals.[232]
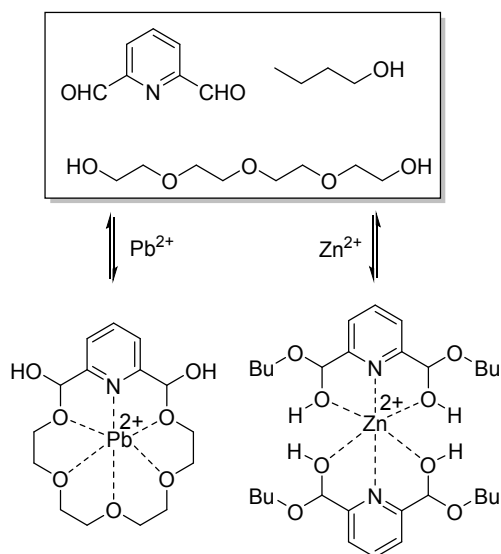
Figure 90. Metal cation selection by dynamically formed hemiacetals: a) Formation of the macrocycle derived from tetraethyleneglycol promoted by Pb(II). b) Formation of the hemiacetal complex derived from 1-butanol promoted by Zn(II).

Interestingly, conversion of hemiacetals to vinyl ethers is thermodynamically unfavorable, partially due to the loss of anomeric effect. From the thermodynamic point of view, it is better to prepare vinyl ethers by addition of O-centered nucleophiles to alkynes, in a process that starts with a high energy functionality and does not sacrifice anomeric stabilization (Figure 91).[196]

$\Delta H = +20.9$
$\Delta G = +9.0$
$-H_2O$

Energies in kcal/mol,
at the M06-2X/6-31+G(d,p)
level of theory
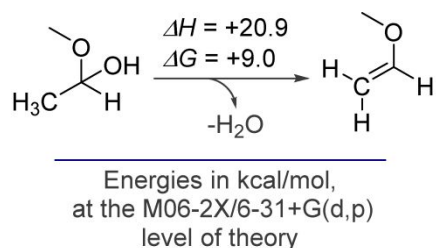
Figure 91. Loss of anomeric stabilization renders formation of vinyl ethers from hemiacetals thermodynamically unfavorable

Carboxylic acid derivatives:

The similarities between these functional groups are obvious. Due to the presence of a carbonyl group, these functionalities have a strong C=O π-acceptor - the usual target of nucleophilic attack and a good partner in intramolecular donor-acceptor interactions. But even for the subset of carboxylic derivatives with a RC(O)-O-/ fragment, a number of interesting differences exist as illustrated by variations in strain in the three O-containing five-membered cyclic systems in Figure 92. In particular, the cyclic ester (lactone) is *more* strained than the respective acyclic ester while succinic anhydride is *less* strained than an acyclic anhydride. To make it even more puzzling, the respective cyclic *peroxy*anhydride is not only more strained than the peroxy acetic acid but the peroxyanhydride strain is twice larger than the lactone strain.

Esters

cyclic =
more strained

ΔH = -3.9 kcal/mol

Anhydrides

cyclic =
less strained

ΔH = 2.0 kcal/mol

Peroxy Anhydrides

cyclic =
more strained

ΔH = -8.3 kcal/mol
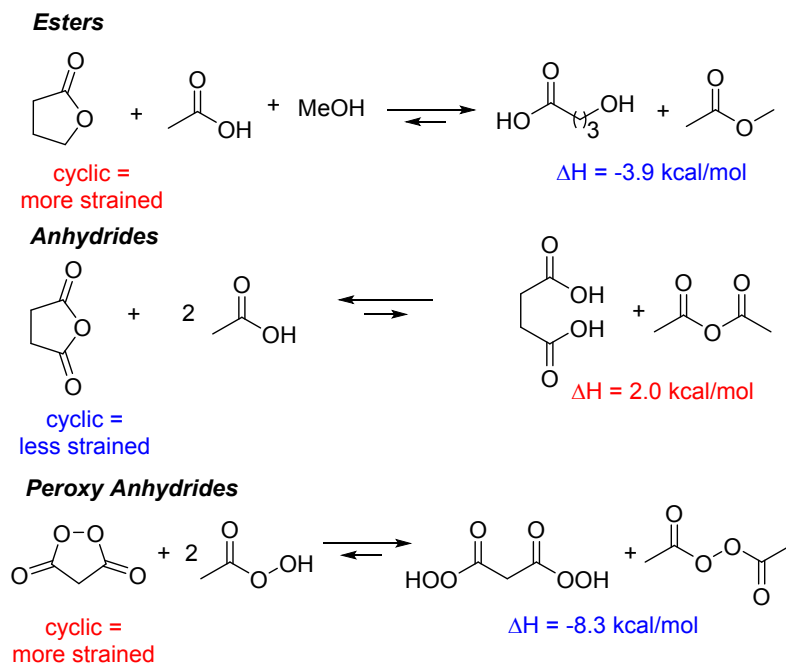
PBE0-D3BJ/aug-cc-pVTZ/CPCM(H$_2$O)

Figure 92. Comparison of strain in three RC(O)-O-/ carboxylic acid derivatives

Differences between acyclic RC(O)-O-/ carboxylic acid derivatives are illustrated by their conformational profiles. For example, the conformational preference for esters is very narrow and favors Z-isomers (vide infra). This strong preference is valuable in molecular design - a comprehensive review of conformations from Cambridge Structural Database suggests that the O=C–O-C torsion angle of acyclic esters rarely deviates considerably from 0° despite being commonly counted as a rotatable bond,[233] Figure 93. Carboxylic acids also show the Z-preference but the distribution of the O=C–O-C dihedrals is broader than for esters, indicating that small deviations from planarity are not uncommon (not what one would expect based on smaller size of H compared to the R group of esters!). Furthermore, the E-conformer of acids is also well-documented, albeit considerably less represented than the Z-isomer. On the other hand, the distribution of OCOC dihedral angles in crystal structural of acyclic anhydrides is relatively broad with considerable contribution of strongly non-planar geometries.
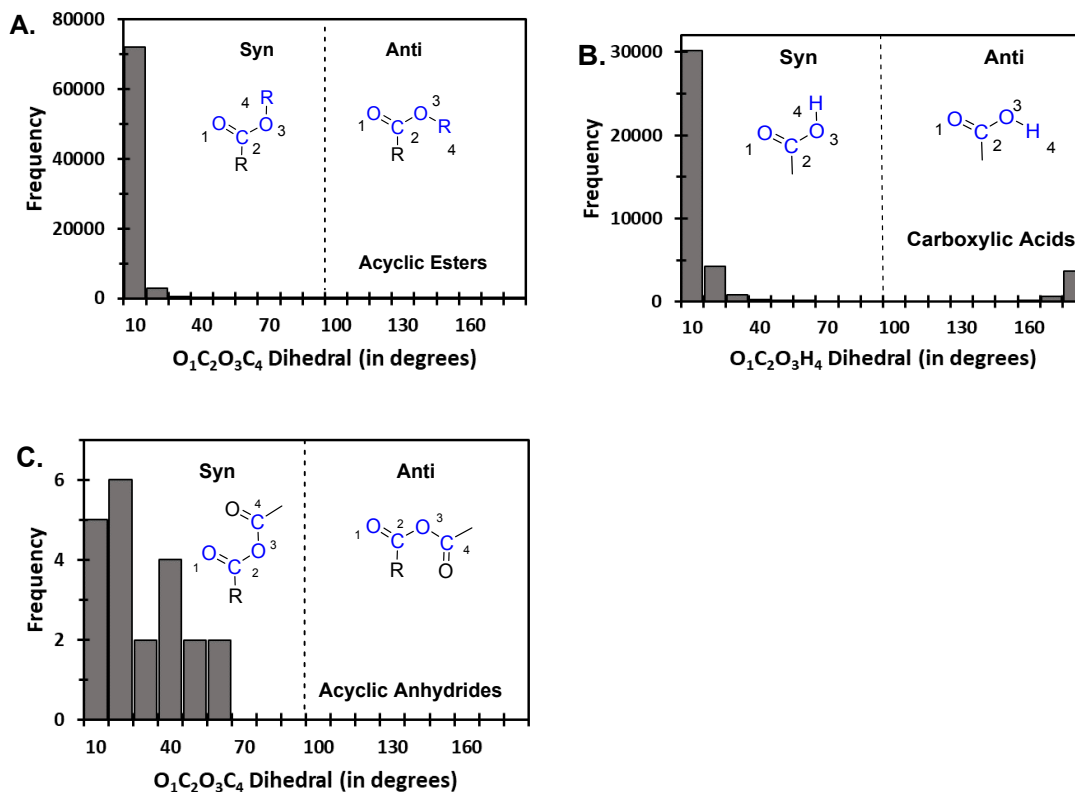
Figure 93. Distribution of the O=C–O-C torsion angle for selected carboxylic acid derivatives in Cambridge Structural Database. A: Acyclic esters. B: Carboxylic acids. C: Acyclic anhydrides.

In the next sections, we will show how such differences arise naturally and can be explained logically from the interplay of electronic factors with the key contributions from the anomeric effect.

Esters

In the chemistry of acetals, the anomeric effect is based on the interaction between an oxygen lone pair and a single C-O bond. In esters, there are *two* bonds between the carbonyl oxygen and the central carbon. Although this is a trivial observation, it also means that, in the carbonyl group of an ester, there are *two* acceptors that can engage *both* lone pairs of an adjacent oxygen from the OR group into separate donor-acceptor interactions. Although both of these interactions are conceptually related to the anomeric effect (as they involve the donation from a lone pair to an antibonding orbital), the stronger of them (i.e., the $n_O \rightarrow \pi^*_{CO}$ interaction, Figure 94 - left) is known, of course, as the ester resonance. This textbook interaction involves the best acceptor (the carbonyl π^*) and the best donor (the p-type lone pair of oxygen). Its effect on stabilizing esters and moderating their electrophilic properties is well-known. This interaction also contributes to the 10-15 kcal/mol rotational barrier around the ester C-O bond.

To carbonyl:
$n_O(p) \rightarrow \pi^*_{C-O}$: **strong**

From carbonyl:
$n_O(p) \rightarrow \sigma^*_{C-OR}$: **strong**

To carbonyl:
$n_O(sp^{1.5}) \rightarrow \sigma^*_{C-O}$: **moderate**

$n_O(p) \rightarrow \pi^*_{C-O}$
55.2 kcal/mol

$n_O(p) \rightarrow \sigma^*_{C-O}$
33.8 kcal/mol

$n_O(sp^{1.5}) \rightarrow \sigma^*_{C-O}$
8.7 kcal/mol

$n_O(p) \rightarrow \pi^*_{C-O}$: **strong**

$n_O(p) \rightarrow \sigma^*_{C-OR}$: **strong**

$n_O(sp^{1.4}) \rightarrow \sigma^*_{C-O}$: **weak**

$n_O(p) \rightarrow \pi^*_{C-O}$
52.5 kcal/mol

$n_O(p) \rightarrow \sigma^*_{C-O}$
33.7 kcal/mol

$n_O(sp^{1.4}) \rightarrow \sigma^*_{C-O}$
1.5 kcal/mol

PBE0-D3BJ/aug-cc-pVTZ/CPCM(H₂O)
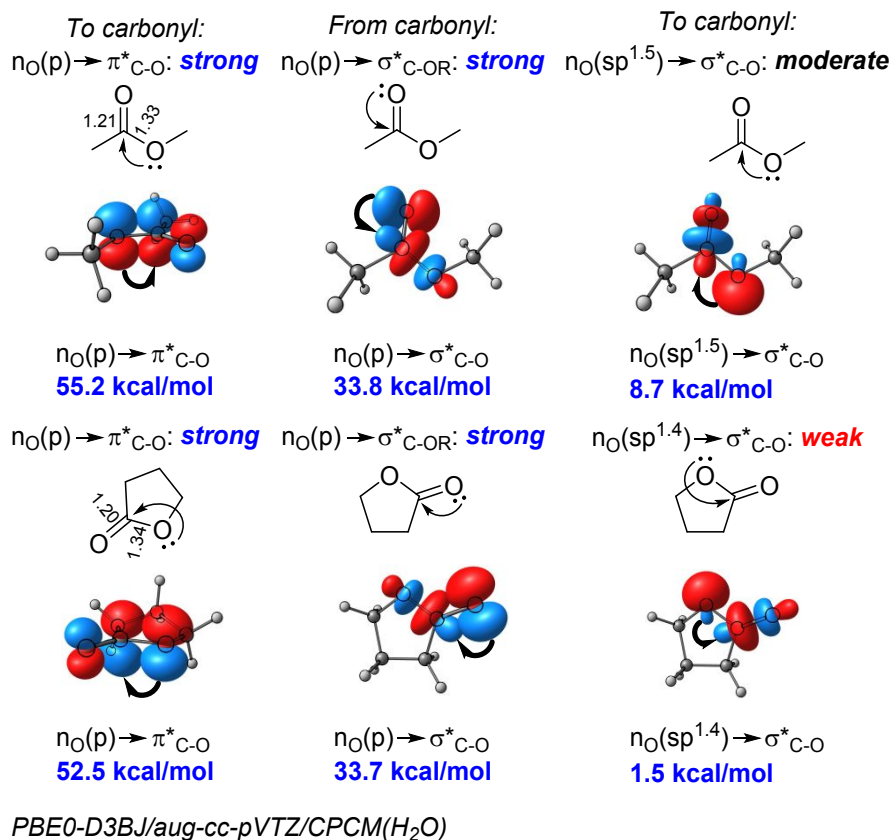
Figure 94. The stereoelectronic portraits of an acyclic ester and a lactone. The sp^n lone pair at the carbonyl oxygen is of lower stereoelectronic importance and not shown here

The 2nd largest delocalizing interaction in esters is the classic anomeric $n_O \rightarrow \sigma^*_{C-OR}$ interaction where the carbonyl oxygen serves as a *donor* (Figure 94 - center). Note that this effect is much larger in magnitude than the analogous $n_O \rightarrow \sigma^*_{C-O}$ interaction in acetals. This increase is a simple geometric consequence of a very short C=O bond length that brings the interacting donor and acceptor orbitals much closer than the C-O bonds in acetals. Although this hyperconjugative interaction cannot be determined from a conformational change, it has a large effect on ester chemistry (vide infra) by facilitating heterolytic C-O scissions. It also has an effect at the ground state structure of esters as it partially compensates for the shift of electron density associated with the $n_O \rightarrow \pi^*_{CO}$ "ester resonance". Since the anomeric $n_O \rightarrow \sigma^*_{C-OR}$ interaction transfers electron density *from* the carbonyl, it alleviates charge separation in the O=C-O moiety which is why this interaction grows in importance as polarity of the media increases. Note that difference in the NBO estimates of $n_O \rightarrow \pi^*_{CO}$ and $n_O \rightarrow \sigma^*_{C-OR}$ interactions decreases by ~1/4th between water and vacuum (~21 vs 16 kcal/mol).

The third interaction is the weaker of the two donations to the carbonyl group, i.e. the $n{\to}\sigma^*_{C=O}$ donations from the σ-type sp^n lone pair of oxygen to the carbonyl's σ^*_{CO} orbital (Figure 94 - right). Although it is not usually mentioned in an undergraduate class, this hyperconjugative interaction contributes to the greater stability of Z-isomers of esters and related functionalities, known as "Z-effect".[234] It has other consequences for reactivity that we will outline below. The differences in stability of the two conformers are significant: ~8 kcal/mol for methyl acetate.[235, 236]
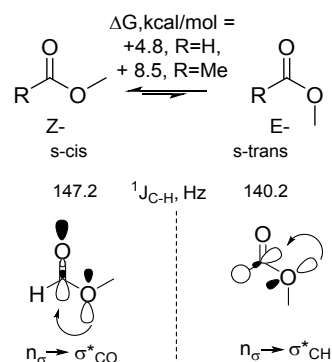
Figure 95. Conformational effects on stability and direct C-H coupling constants in formic esters.

The stereoelectronic nature of this stabilization is consistent with the conformational dependence of the $^1J_{C-H}$ values in the NMR in alkyl formates. In these esters, the $^1J_{C-H}$ is ~7 Hz larger in the more abundant s-cis (Z) rotamer than in the minor s-trans (E) rotamer where the $n_O{\to}\sigma^*_{CH}$ interaction is activated to weaken the C-H bond (Figure 95).[237]

The cis preference becomes even stronger when the OR group is changed from methoxy to the bulky tert-butoxy group (Figure 96). Interestingly, the earlier NMR work suggested that cis preference is weaker for the bulky group due to the potential interaction between the substituent and the carbonyl oxygen.[238] However, more recent microwave spectroscopy data with support from computations revealed a greater cis preference for tert-butyl formate in comparison to methyl formate.[239]

R	ΔE
Me	7.6
tBu	11.0

Energies in kcal/mol, MP2/6-311++G(d,p)
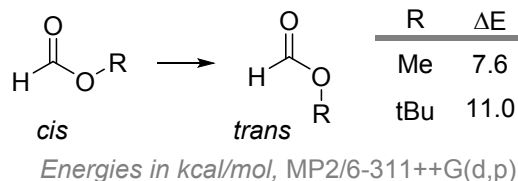
Figure 96. Conformational preference for bulky R-groups[239]

Esters where anomeric effect is weakened by imposing the E-conformation have lower stability and higher reactivity. This applies, for example, to aliphatic lactones constrained to the high-energy E-conformation within 4- to 7-membered rings. Huisgen and Ott reported that such lactones are more electrophilic and

hydrolyze faster than acyclic esters (Figure 97).[240] These observations agree with the inability of the anomeric $n_O \rightarrow \sigma^*_{C=O}$ donation to decrease the carbonyl acceptor ability in E-COOR as much as it does in Z-COOR.

The effects of ring size on the hydrolysis rates for the lactones constrained to E-conformation (having 4- to 7-membered rings) are interesting by themselves – the 6-membered lactone (δ-valerolactone) is hydrolyzed with NaOH in a 3:2 dioxane:water mixture ~40 times faster than the 5-membered lactone (γ-butyrolactone) and ~20 times faster than the 7-membered lactone (ε-caprolactone). These differences suggest additional structural effects on the stability and reactivity of lactones.

Hydrolysis rate, mol/(l·s)	1480	55000	2550	3530	116	0.22

Equilibrium ratio of Z-conformer, %	0	0	$3*10^{-5}$	3	~100	~100
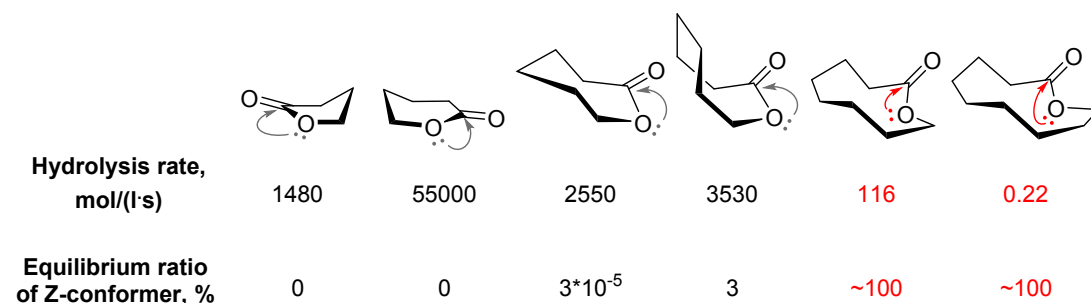
Figure 97. Comparison of experimental lactone hydrolysis rates with computed equilibrium ratios of Z- and E-conformations. Ratios of Z- and E-conformations are computed at the PBE0-D3BJ/aug-cc-pVTZ/CPCM(H2O) level of theory. Hydrolysis rates are taken from ref. [240].

Lactone strain can be evaluated from their ring opening reactions, such as the reaction with methanol or a "metathesis" reaction with methyl acetate (Figure 98).[235] Both reactions preserve the number of identical functional groups but transform a cyclic E-ester into an acyclic Z-ester. The ΔH value for these reactions for the 5-membered γ-lactone (~-9 kcal/mol) is similar to the E/Z-energy difference in methyl acetate. Interestingly, the 6-membered δ-lactone is 2-3 kcal/mol more strained.
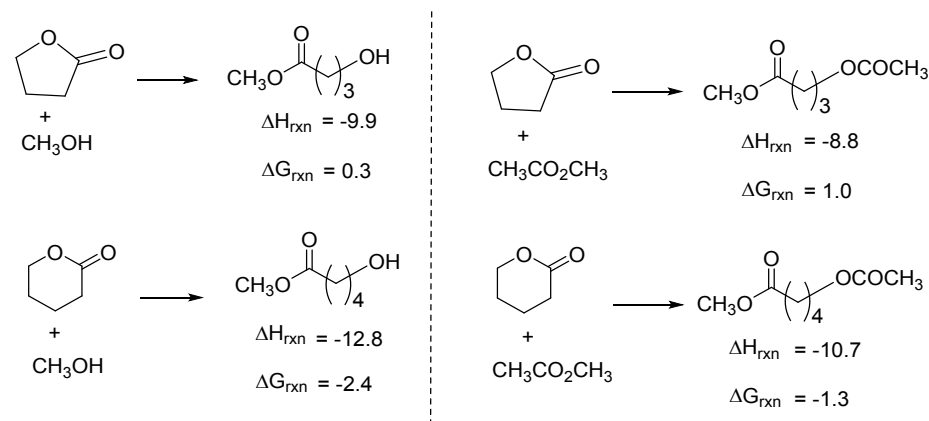
Figure 98. Estimates of lactones strain from thermodynamics of their ring opening at the B3LYP/6-31G(d) level of theory. (Left) methanolysis; (right) "metathesis" with methyl acetate; data in kcal/mol[235]

The practical importance of these stereoelectronic factors stems from their contribution to the high reactivity of lactones, glycolides and cyclic carbonates in polymerization reactions.[241-243] Lactone ring opening reactivates anomeric $n_O \rightarrow \sigma^*_{C-O}$ donation as the rings are converted into acyclic units capable of adopting the favorable Z-ester geometry. This release of stereoelectronic frustration is assisted by favorable entropic contribution for the ring opening (Figure 99). Aliphatic polyesters prepared by ring-opening polymerization (ROP) of these cyclic strained molecules found applications as biocompatible polymers for tissue engineering, controlled drug delivery and many other purposes.[244]
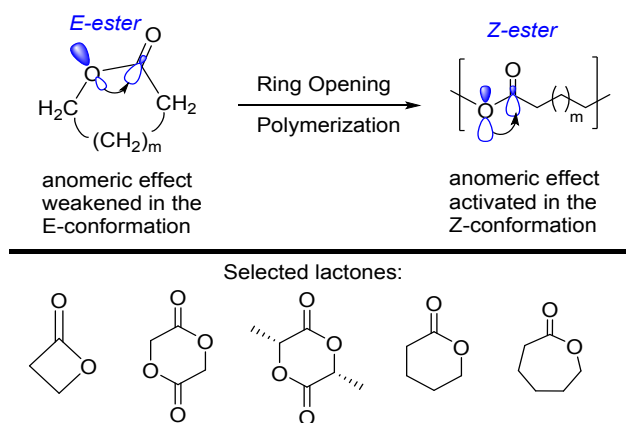
Figure 99. Role of anomeric hyperconjugation in ring opening polymerization of lactones

The energy difference between the E- and Z-esters has interesting indirect consequences in other reactions of this functional group. For example, it has a large effect on deprotonation of esters with the formation of respective enolates.[245] Computational analysis of Wang and Houk revealed that the ~9 kcal/mol difference between the neutral E- and Z-isomers of methyl acetate decreases to ~4 kcal/mol for the respective E- and Z-enolates. As a result, the calculated difference in the deprotonation energy for the E- and Z-conformers of methyl acetate ($\Delta\Delta G$) is ~5 kcal/mol.[246] Because of this difference, lactones are 10,000-times more acidic than acyclic esters (pK_a ~25 vs. pK_a ~30).

A number of factors contribute to this difference, but at least partially, this effect can be explained by the reduced importance of the anomeric $n_O \rightarrow \sigma^*_{C=O}$ stabilization which one can expect from lowered acceptor ability of the C-O bond in the enolate where the oxygen atom has significant negative charge (Figure 100). Electrostatic effects contribute as well but, as shown by Evanseck et al.,[247] they are unlikely to be the dominant factor as addition of solvation (either water or acetonitrile) only reduces $\Delta\Delta G$ by 1 kcal/mol.
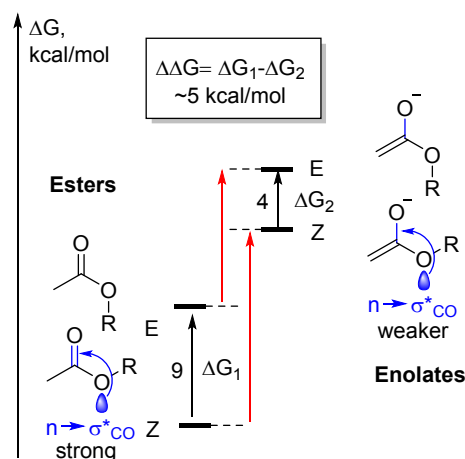
Figure 100. Comparison of $n_O \rightarrow \sigma^*_{C-O}$ stabilization in esters and their enolates vs. the difference in the C-H acidity of E- and Z-esters: The E-conformer is significantly more acidic than the Z-conformer.[247]

Interestingly, the difference in the free energy of deprotonation can be significantly greater for the diesters. For example, the penalty for deprotonation is reduced by 11.7 kcal/mol in going from dimethylmalonate (pKa=15.9) to Meldrum's acid (pKa=7.3, Figure 101, left).[248] As a result, Meldrum's acid is more acidic than dimedone (pKa 11.2), a remarkable example of an ester being _more_ acidic than its ketone analog! The detailed analysis by Byun et al.[249] revealed that the unusual acidity of Meldrum's acid is not simply the case of having the combined effect of _two_ esters confined to the unfavorable E-geometry. In addition, the NBO analysis identified one more component – a new anomeric effect not available to the acyclic analogue, methyl malonate (Figure 101, right). Careful analysis via a combination of NBO deletion energies and isodesmic equations suggested that the difference between E and Z conformations of two ester bonds contributes ~8.6 kcal/mol and the preferential anomeric stabilization of the enolate anion adds another 3.3 kcal/mol. The sum of these factors (11.9 kcal/mol), is consistent with the computed increase in the acidity of Meldrum's acid.
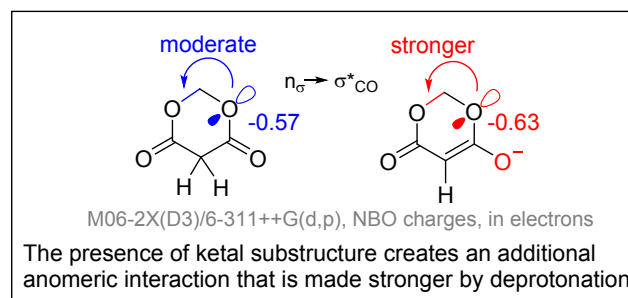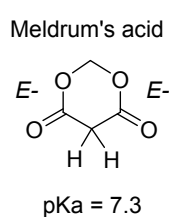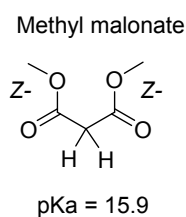
Figure 101. Left: Difference in the C-H acidity of E- and Z-esters: The Meldrum's acid (pK$_a$ 7.3, in DMSO at 25 °C) is significantly more acidic than its open-chain analog, dimethyl malonate (pK$_a$ 15.9, in DMSO at 25 °C). Right: New anomeric $n_O \rightarrow \sigma^*_{C-O}$ stabilization available only to the cyclic system.[249]

As shown in Figure 94, there is one more anomeric-like interaction in esters – donation from the carbonyl lone pair to the σ^*_{COR} orbitals to substituents at the carbonyl carbon (Figure 102). This interaction is quite large according to the NBO analysis.[250] Because it is not switchable by conformational changes, it can only be observed via its effect on reactivity where it facilitates the C-X bond scission in carboxylic acid derivatives, RC(O)X. Conceptually, this intramolecular delocalizing interaction can be converted into a chemical reaction in two ways. If X (Figure 102) is a good leaving group, the $n_O \rightarrow \sigma^*_{CX}$ donation can evolve into C-X bond scission leading to the formation of an acylium ion.[251] A weaker leaving group can be activated by coordination with a Lewis acid, rendering the anomeric $n_O \rightarrow \sigma^*_{CX}$ donation stronger and C-X scission more favorable.

AE amplified by creating a better acceptor

Lewis Acid (LA) assistance   or   X is a good leaving group
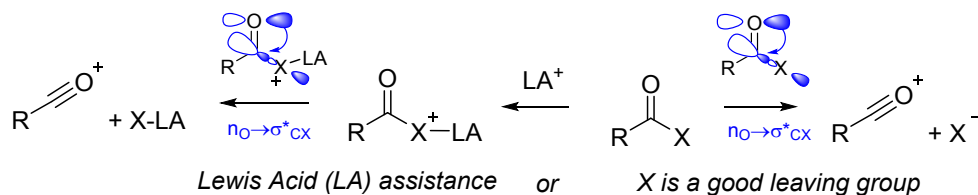
AE amplified by creating a better donor
X is a mediocre leaving group
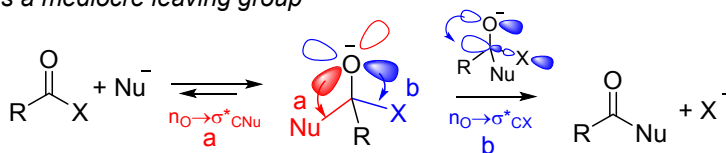
*Competition between going forward or backward depends
on the tug-of-war between two anomeric effects*

Figure 102. Amplification of anomeric effect assists in nucleophilic substitution in RC(O)X

Another way to make the $n_O \rightarrow \sigma^*_{CX}$ donation stronger and facilitate C-X bond heterolytic scission in carboxylic acid derivatives is to increase the donor ability of the oxygen lone pair. This increase can be achieved in reactions with anionic nucleophiles which proceed via the formation of tetrahedral intermediates with a negatively charged oxygen (the textbook addition/elimination mechanism). An interesting feature of negatively charged oxygen is that the presence of two p-type lone pairs with high donor ability can potentially activate two donor/acceptor interactions (i.e., this is the case of a "double anomeric effect"). For example, the interplay between $n_O \rightarrow \sigma^*_{CX}$ and $n_O \rightarrow \sigma^*_{CNu}$ interactions can

determine the balance between going forward or backward from the tetrahedral intermediate (Figure 102).

For an experienced organic chemist, introduction of anomeric interactions for the above "textbook" transformations may seem "unnecessary". However, the role of anomeric effect here is unambiguous - in fact, it is the anomeric hyperconjugation that decides the fate of the tetrahedral intermediate. The balance of the two anomeric interactions determines the preferred collapse direction for the latter. In order to illustrate that the chemistry of esters is impossible to fully understand without explicit consideration of anomeric effect, let us consider the mechanistic puzzle in Figure 103. This example is provided by the work of Deslongchamps and coworkers[252-254] who reported a startling difference in the extent of ^{18}O label incorporation into partially hydrolyzed lactones vs. acyclic esters. Whereas acyclic esters readily incorporate the ^{18}O label, unreacted lactones resist this process, even though the label is incorporated in their ring-opened product
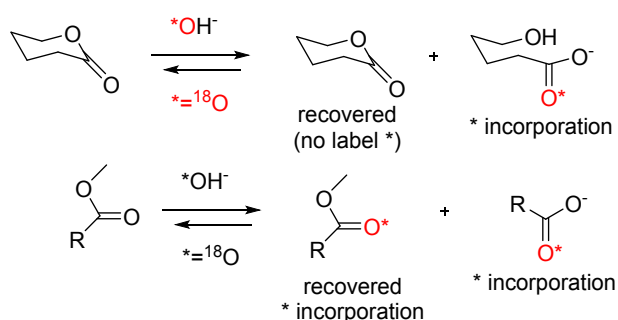
Figure 103. Dramatic difference in the partial incorporation of ^{18}O label in the recovered cyclic and acyclic esters in the process of their alkaline hydrolysis

For a particularly detailed analysis of these results, one can consult the earlier discussions.[255, 256] Although this discussion will not be fully reproduced here, we will highlight the key mechanistic points responsible for this behavior in Figure 104. For simplicity, we will show only the p-type lone pairs (one on each of the neutral oxygen atoms and two at the anionic oxygen) and will only present the major pathway starting with the axial attack of the labeled anionic nucleophile at the carbonyl moiety.
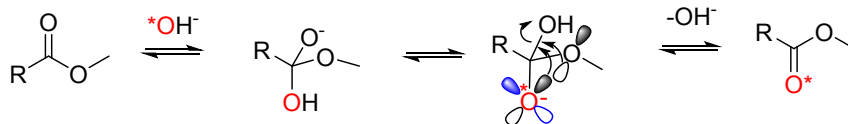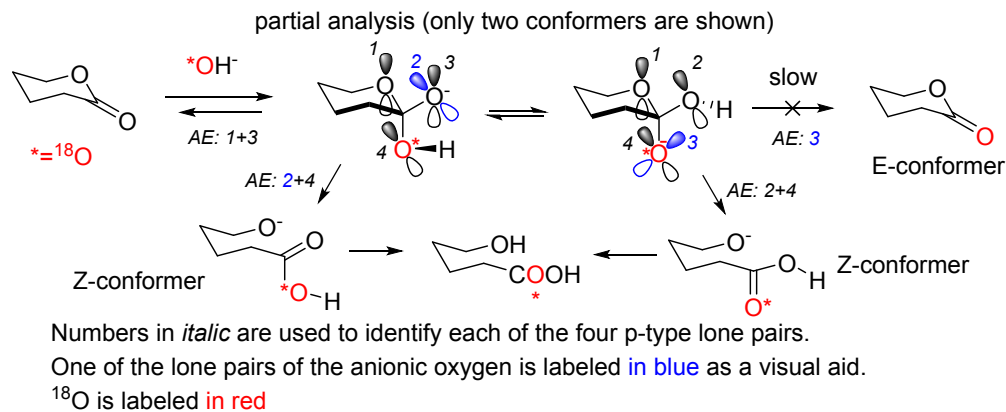
Figure 104. Dramatic difference in the incorporation of labeled oxygen in the recovered cyclic and acyclic esters in the process of their alkaline hydrolysis. "AE" stands for "Anomeric Effect", numbers next to "AE" indicate which lone pairs are involved in the anomeric effect(s) assisting each of the indicated C-O bond scissions

The initial nucleophilic attack creates an anionic hemi-orthoester intermediate which can exist in two prototropic forms with the alkoxide group axial or equatorial. Each favorable fragmentation of these two species is assisted by *two* anomeric $n_O \rightarrow \sigma^*_{CO}$ interactions, where the donor orbital is one of the four p-type lone pairs shown for the three oxygen atoms in Figure 104. Fragmentations assisted by a single anomeric interaction are less favored. Furthermore, only formation of the ring-opened products can give the favorable Z-conformer of the product, whereas the formation of lactones has to revert to an unstable E-conformer. In contrast, incorporation of ^{18}O label in an acyclic ester can involve a stereoelectronically favorable fragmentation of an intermediate anionic tetrahedral intermediate which is not only assisted by two anomeric interactions with the breaking C-O bond in the transition state but also leads directly to the favorable Z- ester geometry.

For the derivatives of formic acid, the analogous $n_O \rightarrow \sigma^*_{CH}$ activates the C(O)-H bond. This has useful implications – for example, the conversion of DMF into $C(O)NMe_2$ radicals in the presence of base and molecular oxygen is used to initiate radical transformations at room temperature.[111, 257-260]

Anhydrides:

Anhydrides are highly reactive in reactions with nucleophiles and are used often for acyl transfer, including biological systems and enzymatic reactions.[261] Although anhydrides have more than two oxygens, we will include them in the present sequence since each carbon has only two oxygen substituents.

The parent compound of this class, the formic anhydride, HC(O)-O-C(O)H is unusual in having a single preferred planar [sp,ap] (or "syn, anti"-) conformation that is stabilized by an intramolecular O…H bond.[262, 263] On the other hand, conformational analysis of acetic anhydride reveals it to be a flexible system with relatively low interconversion barriers with two preferred geometric arrangements of nearly equal energies corresponding to six symmetry-related conformations.[264] The syn,syn-conformation is analogous to the preferred conformation of esters and carboxylic acids but with slight deviations from planarity (~20 degrees). The second conformation is non-planar with one of the C-O-C-O dihedrals of ~130-140 degrees. In the first arrangement, the p-type pair of bridging oxygen donates to the π*-orbitals of both carbonyls (ester resonance) while the σ-type lone pair donates to σ* orbitals of each of the two carbonyls (anomeric effect). The 2nd arrangement is particularly interesting and reflects the tug of war between two carbonyl acceptors for the two lone pairs of the bridging oxygen. In this geometry, each of these lone pairs participates in both of the above delocalizing interactions (ester resonance with one carbonyl and anomeric effect with the other) (Figure 105). Presence of the two nearly isoenergetic conformations accounts for the relatively broad distribution of OCOC dihedral angles in the crystal structure of acyclic anhydrides in the Cambridge Structural Database. However, the anti,anti-conformation is higher in energy and is not represented in the known X-ray structures of acyclic anhydrides.
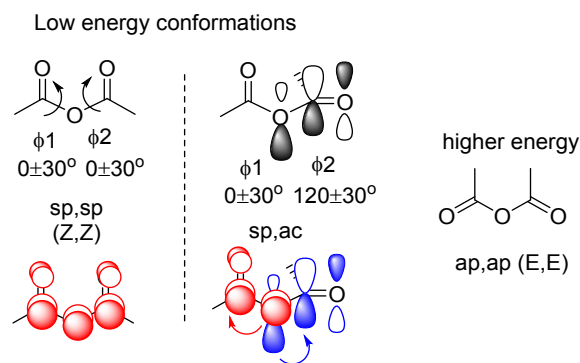
Figure 105. Conformational analysis of acetic anhydride.

The high energy anti,anti-conformation of an anhydride is analogous to the E-conformation of an ester, suggesting a similar role of anomeric effect in these functionalities. Taking this stereoelectronic analogy further, one would expect the difference between acyclic and cyclic anhydrides would be similar to the difference between acyclic esters and lactones (Figure 106). Constraining the anhydride moiety in a cyclic

structure imposes an unstable anti-geometry where the σ-type lone pair of the bridging oxygen is not able to fully participate in the hyperconjugative $n_O \rightarrow \sigma^*_{CO}$ interactions.
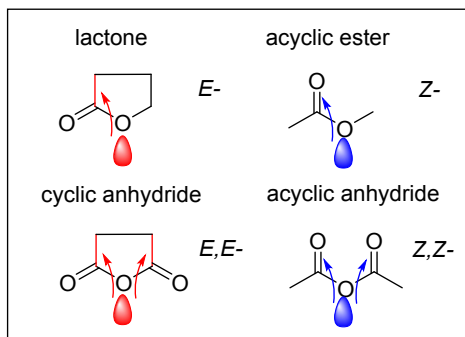
Figure 106. Difference between the antiperiplanar $n_O \rightarrow \sigma^*_{C-X}$ interactions in cyclic and acyclic esters is analogous to difference between cyclic and acyclic anhydrides

In other words, as cyclic anhydrides are constrained in a E-conformation where the $n_O \rightarrow \sigma^*_{CO}$ interaction is weakened, one could expect that, in analogy to lactones, cyclic anhydrides would be a) more strained, b) more electrophilic, and c) easier to enolize than acyclic anhydrides. However, analysis of available experimental data suggests that this analogy with the cyclic esters is imperfect as anhydrides hide several stereoelectronic surprises.

For example, in contrast to the expectation that cyclic anhydrides are strained relative to their acyclic counterparts, Eberson and Welinder[265] reported that, when several cyclic anhydrides were given a chance to equilibrate with acetic anhydride, the equilibrium favored the *cyclic* anhydrides. In particular, the equilibrium constants for the reversible reactions between cyclic anhydrides and acetic acid to form acetic anhydride and the corresponding carboxylic acid, were reported as 4.9×10^{-4} and 4.6×10^{-1} M for succinic and glutaric anhydrides, respectively. The equilibrium constants reflect the 1000-fold *greater* relative stability of the five-membered cyclic anhydride in comparison to acetic anhydride. Maleic and phthalic anhydrides are even more stable, indicating the presence of additional structural effects. Interestingly, the rate-determining step for the forward reaction appears to be the breakdown of the tetrahedral intermediate formed by the attack of an acetic acid molecule on the protonated cyclic anhydride. The relative stability of this intermediate illustrates the power of anomeric effect in stabilizing these oxygen-rich species.

Although these results seem to go against the expected strain accumulation in the cyclic anhydrides, the seeming controversy is resolved by computational analysis. In particular, DFT computations show that transformation of succinic anhydride to acetic anhydride is uphill by ~ 2 kcal/mol (Figure 107). Although the six-membered cycle of glutaric anhydrides is ~3-4 kcal/mol more strained, the isomerization enthalpy

is close to zero in water and only slightly (-5 kcal/mol) exothermic in the gas phase. Encouragingly, the strain differences (3.8 kcal/mol with solvation) correspond very well to the experimentally measured 1000-fold difference in stabilities. The reason for unfavorable equilibrium between cyclic and acyclic anhydrides has to originate in the entropic contribution to the Gibbs free energy that overshadow a greater strain of the cyclic structures.

K_{eq} = 2.6 x 10^{-8} M
ΔE = 1.1, -1.5 kcal/mol
ΔH = 2.0, -1.0 kcal/mol

K_{eq} = 1.8 x 10^{-6} M
ΔE = -0.7, -5.1 kcal/mol
ΔH = -0.6, -4.8 kcal/mol

PBE0-D3BJ/aug-cc-pVTZ
blue values - CPCM(H_2O);
grey values - vacuum
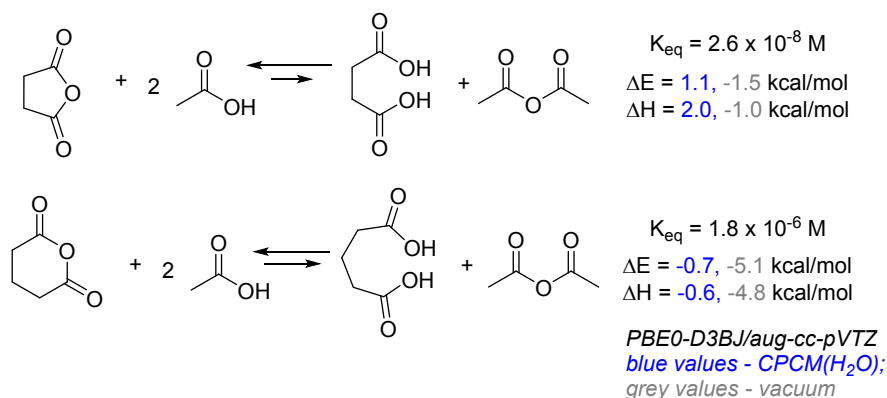
Figure 107. Comparison of stability of cyclic and acyclic anhydrides (only the energy and enthalpy contributions are shown while the overall K_{eq} value is also affected by the entropy change).

In order to understand the unusual nature of anhydrides, it is helpful to analyze their stereoelectronic portraits presented in Figure 108. They reveal several features that are different from the other O-functionalities. First, the classic $n_O \rightarrow \pi^*_{C=O}$ interaction in acetic anhydride is considerably weaker (31 kcal/mol) than the analogous interaction in methyl acetate (52 kcal/mol). This change is understandable since the anhydride's central oxygen atom has to satisfy two carbonyl acceptors - the donor does what it can but there is only so much electron density it can spare. On the other hand, the anomeric $n_O \rightarrow \sigma^*_{C-O}$ hyperconjugative donation *from* the carbonyl is greater in the anhydride than in the ester (44 vs 36 kcal/mol). The situation where the magnitude of π-conjugative interactions decrease while the σ-conjugative interaction grows stronger leads to a switch in the relative importance of conjugation and hyperconjugation. *In anhydrides, the anomeric donation <u>from</u> the carbonyl is the dominant stereoelectronic effect.* The fact that carbonyl oxygen mainly serves as a donor reveals an imbalance of conjugative effects that contribute to the much greater electrophilicity of anhydrides in comparison to esters.

$n_O(p) \rightarrow \pi^*_{C-O}$: **strong** $n_O(p) \rightarrow \sigma^*_{C-O}$: **strong** $n_O(sp^{1.6}) \rightarrow \sigma^*_{C-O}$: **moderate**

$n_O(p) \rightarrow \pi^*_{C-O}$
34.8 kcal/mol

$n_O(p) \rightarrow \sigma^*_{C-O}$
41.4 kcal/mol

$n_O(sp^{1.6}) \rightarrow \sigma^*_{C-O}$
7.2 kcal/mol

$n_O(p) \rightarrow \pi^*_{C-O}$: **strong** $n_O(p) \rightarrow \sigma^*_{C-O}$: **strong** $n_O(sp^{1.3}) \rightarrow \sigma^*_{C-O}$: **weak**

$n_O(p) \rightarrow \pi^*_{C-O}$
40.3 kcal/mol

$n_O(p) \rightarrow \sigma^*_{C-O}$
39.4 kcal/mol

$n_O(sp^{1.3}) \rightarrow \sigma^*_{C-O}$
1.4 kcal/mol

PBE0-D3BJ/aug-cc-pVTZ/CPCM(H$_2$O)
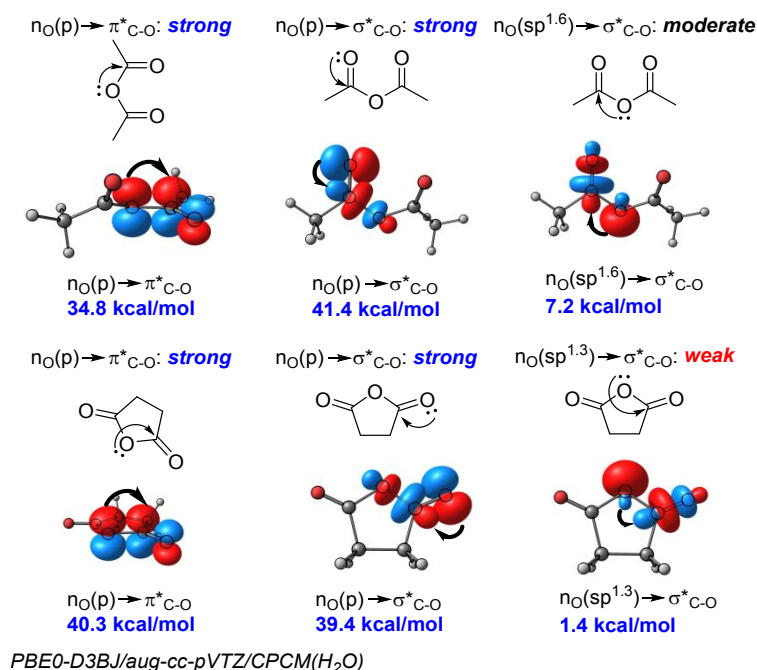
Figure 108. Stereoelectronic portraits of acetic and succinic anhydrides

Transitioning from an acyclic to cyclic anhydride has a dramatic effect on the balance of delocalizing effects. Again, NBO comparison of acetic and succinic anhydride in Figure 108 is very instructive. It shows that sigma donation from the bridge oxygen to the carbonyl's σ^*_{CO} is indeed weakened by ~5 kcal/mol (from 6.5 to 1.3 kcal/mol) in the five-membered cycle. This is expected for the change from a favorable antiperiplanar geometry to a less favorable synperiplanar arrangement between the donor and the acceptor. However, this effect is counterbalanced by a ~9 kcal/mol increase in π-conjugation, i.e., the donation from the p-type oxygen lone pair to the carbonyl's π^*_{CO} (from 30.9 to 39.9 kcal/mol). This balance agrees very well with the relatively low strain and small ΔH values for the interconversion of cyclic and acyclic anhydrides (Figure 107). The increase in $p_O \rightarrow \pi^*_{CO}$ interaction is consistent with the greater planarity of the cyclic anhydride imposed by the five-membered ring. In contrast, acetic anhydride is not completely planar, and, as a consequence, its π-conjugation is weakened (Figure 109).

enforced in

ap,ap   *should be unfavorable but is it?*

slightly non-planar

planar

Two effects:
$p_O \rightarrow \pi^*_{CO}$ interaction increases
$\sigma_O \rightarrow \sigma^*_{CO}$ interaction decreases
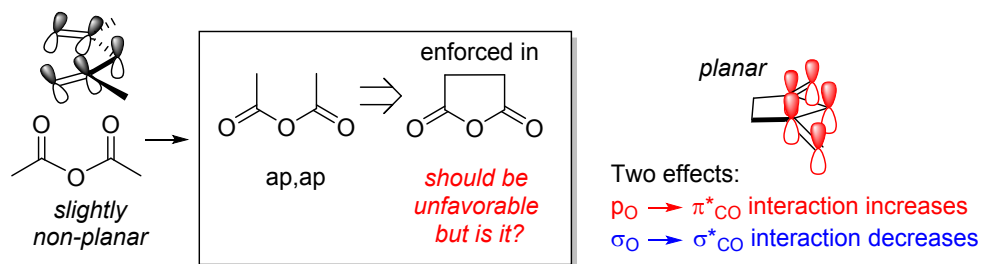
Figure 109. The interplay of two delocalizing effects accounts for similar stabilities of acetic and succinic anhydrides

Cyclic anhydrides are useful reagents for preparing heterocyclic compounds because they readily participate in cycloaddition reactions where they behave as "extended dipoles" upon conversion into an enol or an enolate. A particularly common example is enol derived from homophthalic anhydride where enolization is further assisted by conjugation with the benzene core. The list of partners in such reactions is broad and includes aldimines, ketimines, imidates, aromatic aldehydes and ketones, anhydrides, acyl chlorides, alkenes, and alkynes.[266] An interesting feature of enolization in cyclic anhydrides is that it drastically changes the network of anomeric interactions: from competition of two carbonyl acceptors for the lone pairs of the bridging oxygen to cumulative effect of two donors interacting with the carbonyl acceptor (one direct and another through the bridging bond, Figure 110).

competition   synergy   cycloadditions
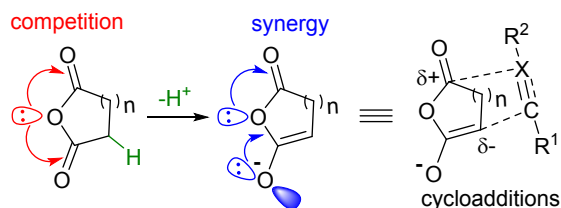
Figure 110. Enol or enolate formation from cyclic anhydrides changes competition of two acceptors for one donor to a situation where the remaining single carbonyl acceptor gets donation from two type lone pairs (direct and through-bond). The resulting polar species are highly reactive partners in cycloaddition reactions.[267]

An example of such process is provided by the Tamura cycloaddition.[268] This process takes advantage of C-H acidity of cyclic molecules where the C(O)-O moiety is constrained in the Z-conformation to generate the hidden dipole cycloaddition partner. Interestingly, this process generates an anomerically stabilized hemiacetal moiety and proceeds much faster when the reactant anhydride is transformed into an enolate by deprotonation (Figure 111). A useful feature of these anhydride cycloadditions is that the product is poised for CO_2 elimination, so the carboxyl moiety incorporated in the anhydride reactant can be considered as a traceless activating group.
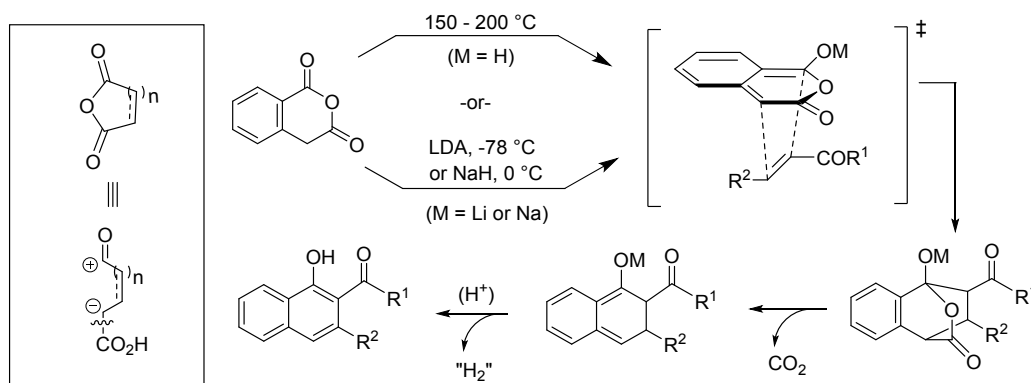
Figure 111. Enolization of a cyclic anhydride activates it for a Diels-Alder reaction with an α,β-unsaturated ketone

Peroxyanhydrides (Diacyl peroxides)

This functionality occupies an interesting stereoelectronic niche between esters and anhydrides. Because there is one -O- oxygen per each C=O acceptor in peroxyanhydrides (diacyl peroxides), their n$\rightarrow\pi^*$ interactions are stronger than such interactions in anhydrides where the single bridge oxygen has to interact with *two* acceptors. From this point of view, diacyl peroxides are stereoelectronically closer to esters as the latter also have one -O- oxygen per one C=O acceptor. Furthermore, (Figure 108), the anomeric $n_O\rightarrow\sigma^*_{CO}$ interactions in cyclic diacyl peroxides are considerably weaker in comparison to the analogous acyclic diacyl peroxides and, in contrast to cyclic anhydrides, this weakness is not compensated by an additional factor. As the result, cyclic diacyl peroxides are more strained and more reactive than acyclic diacyl peroxides (Figure 112). Diacyl peroxides are more electrophilic than esters because n$\rightarrow\pi^*$ interactions in diacyl peroxides are weaker than the analogous donations in esters (a manifestation of inverse α-effect[269] discussed later).
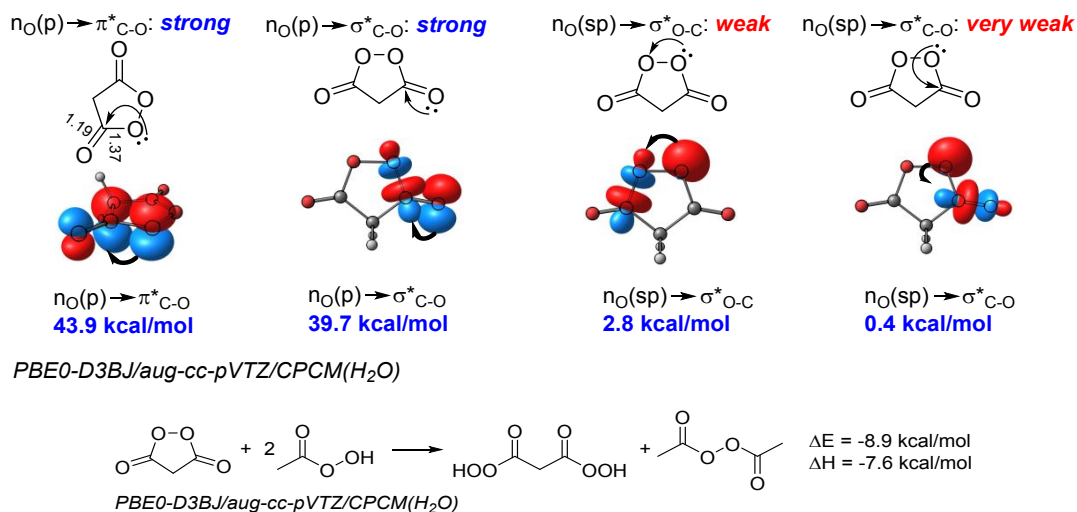
Figure 112. Top: the stereoelectronic portrait of a cyclic diacyl peroxides. Bottom: evaluation of strain in cyclic diacyl peroxides

The synthetic potential of cyclic diacyl peroxides, first prepared in the 1950s,[270-275] expanded greatly in the recent years with the discoveries of new synthetic transformations such as arene oxidation,[276-279] as well stereoselective dioxygenation[280-287] and oxyamination of alkenes.[288, 289] In addition, cyclic diacyl peroxides participate in oxidative C-O coupling with various CH-acids,[290-293] and enol ethers.[294]

Cyclic diacyl peroxides are more powerful oxidants than non-cyclic diacyl peroxides. For example, dibenzoyl peroxides do not oxidize silyl enol ethers, alkyl enol ethers and arenes while cyclic diacyl peroxides oxidize these functionalities readily.[276, 294] One has to mention, however, that not all of this reactivity originates directly from the higher strain and lower intrinsic penalty for breaking the O-O bond in such cyclic peroxides. For example, the greater reactivity of diacyl peroxides in the peroxide-mediated C-O bond formation with aromatics[276] stems from intramolecular assistance of the second radical center in aromatization with H-atom transfer (i.e., the rebound step).

The difference in reactivity of cyclic and acyclic diacyl peroxides have been demonstrated in the reaction with 1,3-dicarbonyl compounds.[292] Whereas the oxidative C-O coupling of ketoesters with malonoyl peroxide led to the desired product even in the absence of a catalyst, the oxidative C-O coupling with dibenzoyl peroxide only proceeded in the presence of a catalyst and in a lower yield (Figure 113). It is tempting to associate these differences in reactivity to more favorable antiperiplanar arrangement of the breaking O-O bond to the σ^*CO bond of the carbonyl. As the negative charge accumulates at the departing oxygen of the O-O bond in the TS, such anomeric interaction is expected to become stronger.
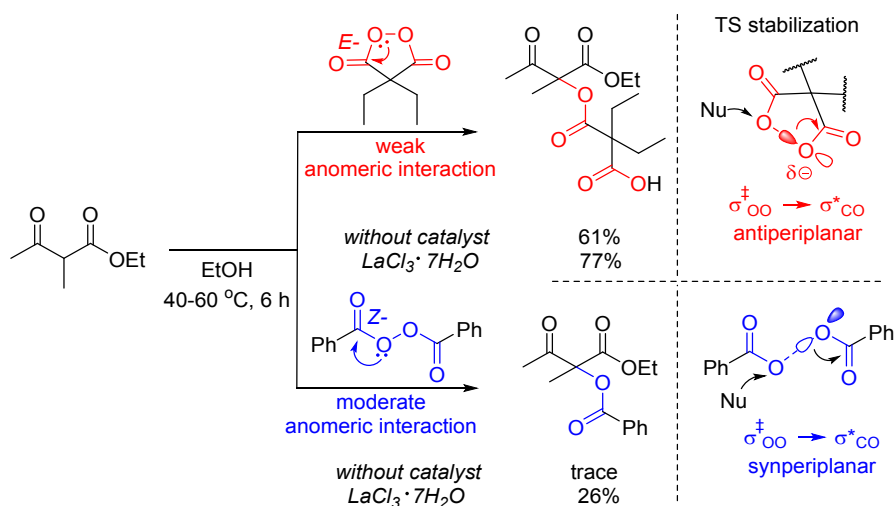
Figure 113. Comparison of cyclic and acyclic diacyl peroxides in oxidative C-O coupling reactions with ketoesters

Reaction of dibenzoyl peroxide with the methyl enol ether is so slow that only the products of acid-catalyzed hydrolysis are observed. In contrast, reactions of malonoyl peroxides with methyl and silyl enol ethers proceed readily. These processes are very interesting as they involve at least two other steps in the subsequent cascade transformation where anomeric assistance or lack thereof are important.[294] The diacyl peroxide reacts as an O-electrophile with the activated alkene but, unlike previous examples, the departing carboxylate group "rebounds" at the second alkene carbon in a formal oxidative [5+2] cycloaddition. The product of this reaction is a bis- lactone, the functional group where, as discussed earlier, the weakened anomeric stabilization facilitates ring opening. Indeed, subsequent work-up induces the expected lactone ring opening and restores the double bond. Out of two possible directions for the C-O scission, the C-OC(O) bond at the OCH_3-substituted carbon breaks selectively to form α-acyloxy enol ethers. The regioselectivity of this process originates from the anomeric assistance provided by the exocyclic OCH_3 group (Figure 114).
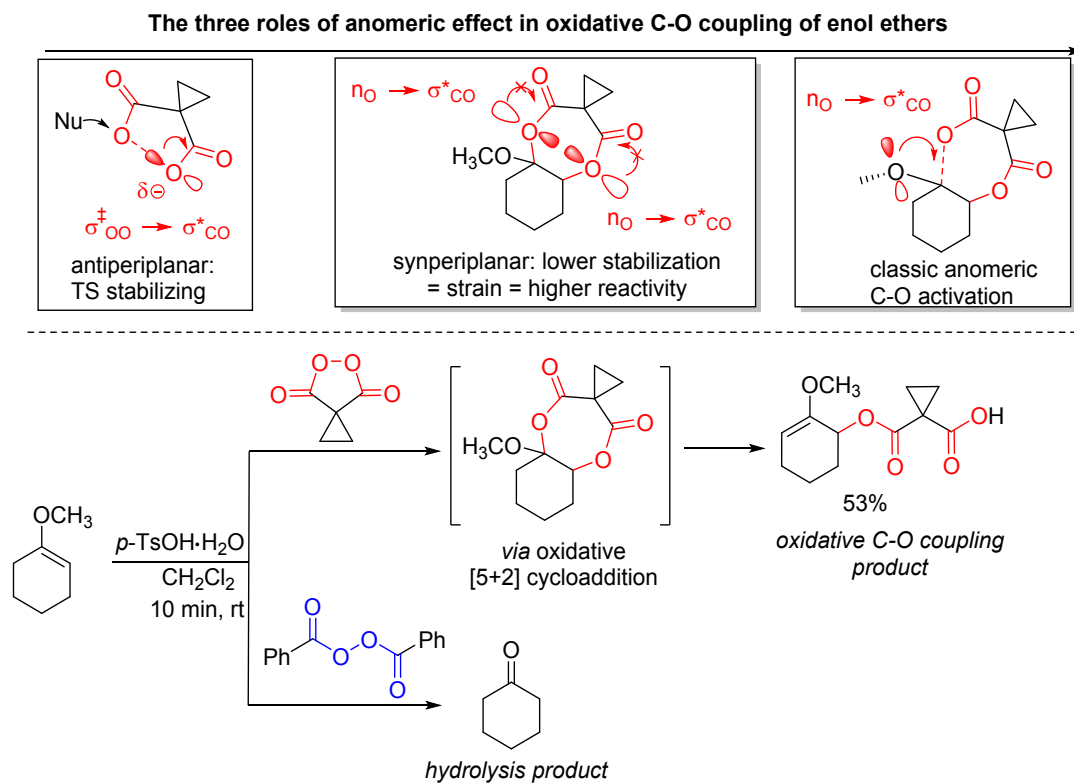
Figure 114. Difference in reactivity of cyclic and acyclic diacyl peroxides towards an enol ether.

Strained cyclic diacyl peroxides readily react with alcohols. For example, malonoyl peroxides are nearly quantitatively converted into the mixed ester/peracid in 15 minutes in methanol in the presence of one equivalent of potassium acetate. The peracid moiety is unstable and, upon isolation, partially converts into a carboxylic acid (Figure 115). The presence of a cyclopropane ring is not necessary and other malonoyl peroxides that contain four- and five-membered spiro rings also readily react with methanol in the presence of AcOK.[295]
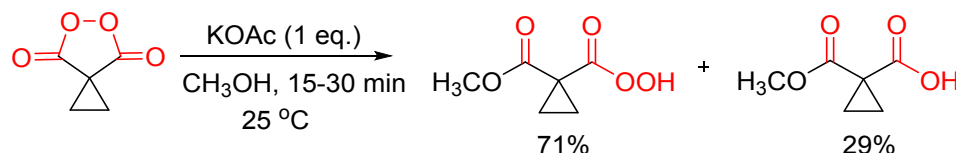
Figure 115. Solvolysis of cyclic diacyl peroxide is fast

Acyclic diacyl peroxides are more stable in the presence of alcohols. In fact, alcohols are often used as solvents in reactions of acyclic diacyl peroxides.[296, 297]

Carboxylic acids:

The conformational properties of carboxylic acids are similar to those discussed above for esters due to the shared stereoelectronic origin, i.e., the anomeric $n{\rightarrow}\sigma^*_{CO}$ interaction. The Z- ("syn") conformations of simple carboxylic acids and esters are 6-8 kcal/mol more stable than the E (anti).[245, 298] Even in formic acid, the E-rotamer is 3.9 kcal/mol higher in energy than the Z-rotamer.[299] The Z-preference decreases in polar solvents. Understanding these intrinsic preferences has been essential for correcting erroneous assumptions regarding the molecular structure of important molecules, e.g. the carbonic acid.[300]

Similar to esters, the stereoelectronic NBO portraits of the two conformers of acetic acid reveals three important interactions: $n_O(p){\rightarrow}\pi^*_{C=O}$, $n_O(p){\rightarrow}\sigma^*_{C-OH}$ and $n_O(sp^{1.5}){\rightarrow}\sigma^*_{C=O}$ (Figure 116). The balance is shifted slightly in comparison to esters, as the hydroxy oxygen in acids is a weaker donor in comparison the alkoxy oxygen in esters (52 vs. 55 kcal/mol) while the C-OH bond is a slightly better acceptor than the C-OR bond (35 vs. 34 kcal/mol). Still, in the absence of H-bonding with acidic or basic additives, carboxylic acids and esters are, as one would intuitively expect, similar.
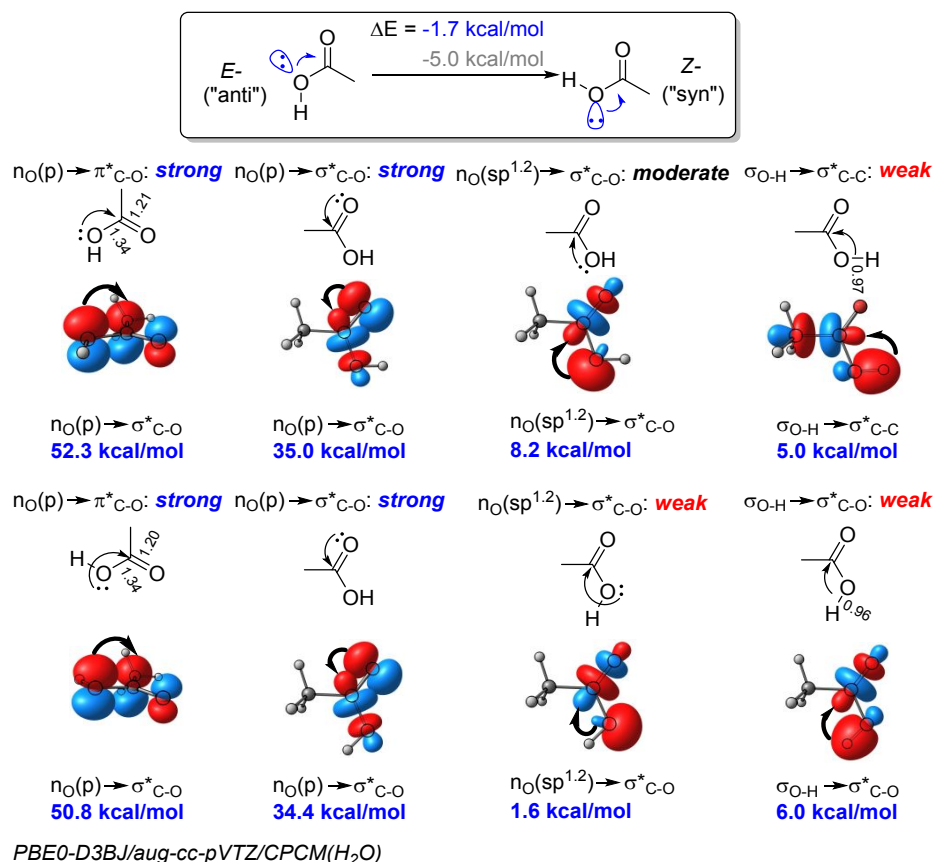
Figure 116. Stereoelectronic "portrait" and conformational preferences of acetic acid.

In agreement with this conformational preference, the distribution of carboxylic acid conformers in the Cambridge Structural Database favors the syn conformers (roughly 9:1).[301] The population of the anti-conformers is more heterogeneous because many of them are involved in H-bonds, especially of intra-molecular nature, that stabilize this relatively unfavorable conformation.

Carboxyl groups are numerous in proteins and there are microenvironments that preserve this functionality in its protonated form.[302] Since the conformational profiles of carboxylic acids embedded in proteins and small peptides are potentially useful for bio-molecular engineering, some of them have been studied in detail. For example, the carboxyl group of N-acetylaspartic acid amide exists in two conformations, both in DMSO and water.[303] For the syn-conformer, the carbonyl stretch vibration has a relatively low frequency of ~1720 cm^{-1} whereas for the anti-conformer the carbonyl stretch vibration has a higher frequency of ~1745 cm^{-1}. The difference in the frequencies is consistent with the greater CO bond weakening due to the $n_O \rightarrow \sigma^*_{C=O}$ interaction in the syn-conformer. The relative ratios of the two conformers in these polar solvents (~25% of the anti-conformer) is much higher than the <1% observed in gas-phase studies. This difference is likely to stem from the more favorable hydration of the anti-

conformer. Based on these findings, the anti-conformer was suggested to be more acidic then syn-conformer, another example of molecular conformation in control of chemical properties (*vide infra*). Intrinsic conformational preferences of carboxylic acids have supramolecular consequences. The natural Z-preference is essential for the formation of the textbook carboxylic dimers and use of carboxylic acids as elements of crystal engineering (Figure 117).[304, 305] Formation of the alternative patterns such as the chains (catemers) is possible when additional structural and electronic factors contribute to the intrinsic preferences.
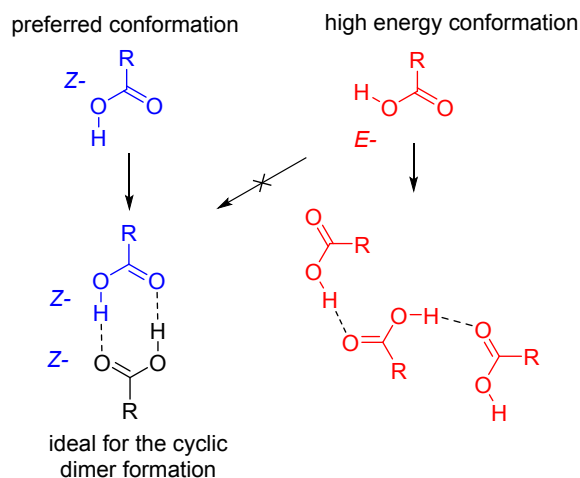
Figure 117. Supramolecular consequences of preferred conformations of carboxylic acids

The high proportion of E-carboxylic acids as compared to E-esters in the Cambridge Structural Database inspired Medvedev et al. to investigate this phenomenon.[306] Since almost every carboxylic acid in CSD acts as a donor of a hydrogen bond, the authors explored the role of H-bonding in this conformational preference. The retrieved distances between the C(O)OH oxygens and the H-bond-accepting atoms (limited to oxygens) show a much larger proportion of the lowest-distance component (red in Figure 118, recovered with Normal Mixture Modeling) in E-conformers (trans) than in Z-conformers (cis) (18% vs. 4%). This lowest-distance component expectedly corresponds to complexes with anionic species, suggesting that the nature of the hydrogen bond acceptor can significantly affect conformational preference of the carboxylic group.
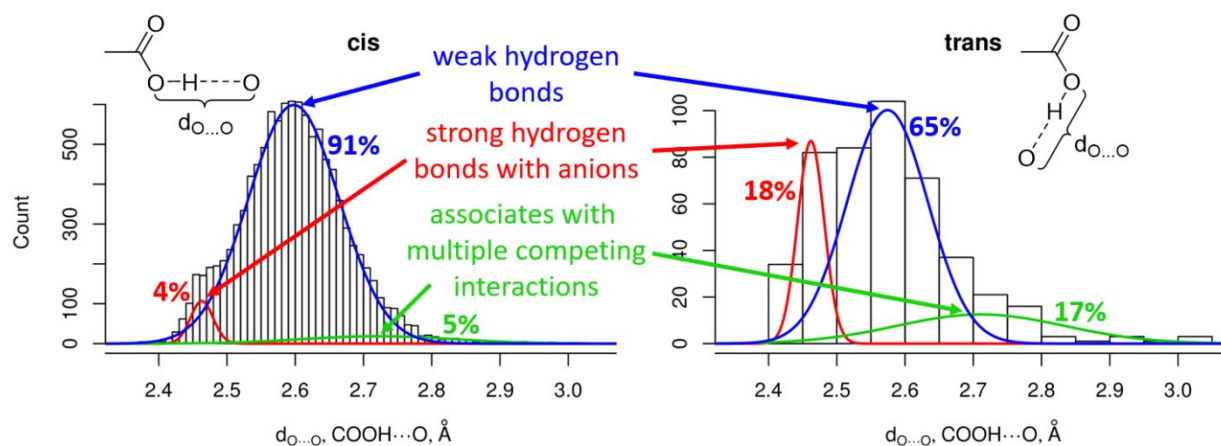
Figure 118. Distributions of distances between carboxylic OH oxygen and the hydrogen bond-accepting oxygen in Z- and E-carboxylic acids complexes according to CSD (data retrieved in 2016). Colored Gaussian distributions show components found by Normal Mixture Modeling, assigned to different H-bonding situations according to Emsley.[307] Estimated contributions of the components are given in bold.

In a nutshell, these observations can be explained by analyzing the two H-bonded complexes of acetic acid in Figure 119. Independent on the choice of the partner (an H-bond donor or an H-bond acceptor), the Z-preference decreases. This observation may seem confusing but only on a first glance. Unlike the Z-isomer where the σ-lone pair of hydroxyl oxygen is antiperiplanar to a strong $\sigma^*_{C=O}$ acceptor, the less stable E-isomer is stereoelectronically unbalanced – the σ-lone pair is interacting with a weaker σ^*_{C-C} acceptor whereas the $\sigma_{C=O}$ bond is aligned with another acceptor, i.e, the σ_{O-H} bond. Hence, the σ-lone pair and the O-H bond of the E-isomer are, respectively, a better donor and a better acceptor than they are in the Z-isomer. Due to this difference, the E-isomer is a better partner in both types of H-bonding interactions, either as a donor or as an acceptor. In other words, the fully developed *intramolecular* donor-acceptor (i.e., anomeric) orbital interactions in the Z-isomer leads to an increase in the HOMO-LUMO gap and, thus, the molecular hardness.[12, 308] This behavior satisfies the "maximum hardness principle" (MHP) of Pearson[47] but renders Z-isomer a poor partner in *intermolecular* donor-acceptor interactions.

PBE0-D3BJ/aug-cc-pVTZ/CPCM(H₂O), kcal/mol
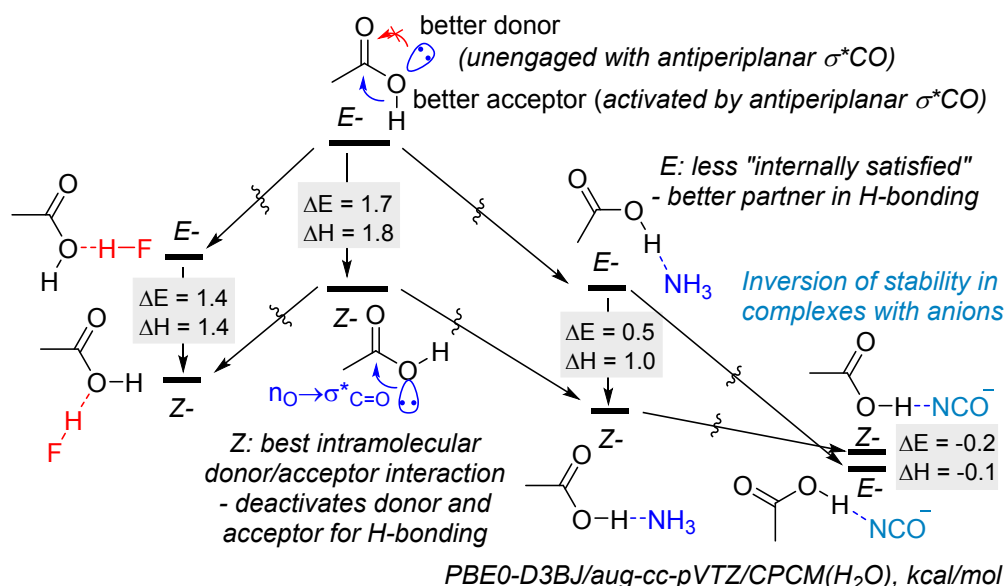
Figure 119. Influence of hydrogen bonding on the E/Z preference of acetic acid in water.

Because O-H deprotonation converts a σ_{O-H} bond into a p-type lone pair, anomeric effect is expected to contribute to the stabilization of conjugate bases of carboxylic acids. Although it is hard to separate the contributions of n→σ*C=O and n→π*C=O interactions as *both* of them are increased by deprotonation, the relative increase in these contributions can be estimated from the NBO delocalization energies. When the two contributions are evaluated as an increase in the interaction upon deprotonation, the relative importance of the increase in n→π* resonance vs. n→σ* hyperconjugation can be estimated as approximately 5:1 (Figure 120).

Energies in kcal/mol, NBO B3LYP(D3)/6-31++G(d,p) Int=UF
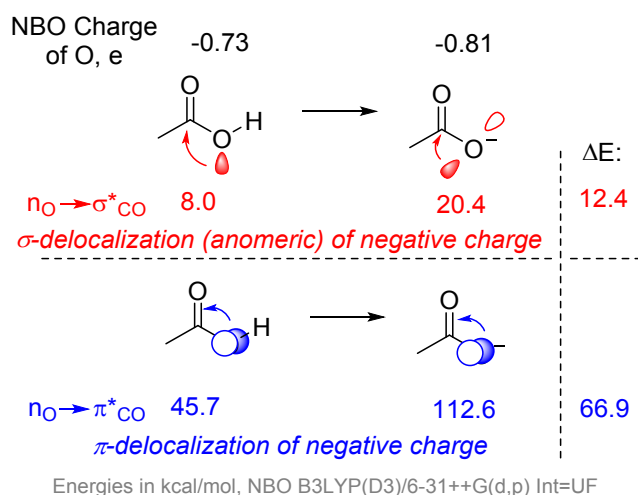
Figure 120. Comparison of σ- (anomeric) and π-delocalization of negative charge in carboxylates

Additional interesting features are associated with the stereochemistry of H-bonding and proton transfer to carboxylate anion. In a thought-provoking analysis, Gandour suggested that the "syn lone pair" of a carboxylate is >10^4 more basic than the "anti lone pair".[309] Although "syn and anti pairs" is not a preferred description in this review as we advocate using the p and sp^n-hybrid lone pairs of oxygen instead (or the two p-orbitals and sp^n-hybrid for anionic systems), here the alternative model with two ~sp^2 orbitals is instructive. This concept stems from the thermodynamic cycle shown in Figure 121. Based on the relative stability of the two conformers, the equilibrium constant, K, for the interconversion of syn and anti-conformers in acetic acid can be estimated as K = 10^{-4}. As both conformers provide the same conjugate base upon deprotonation, K_a' is 10^4-fold larger than K_a from Figure 121. From this reasoning, the "syn lone pair" in a carboxylate anion is more basic than the "anti lone pair" exactly by the energy difference between the syn- and anti-conformations of the carboxylic acid.
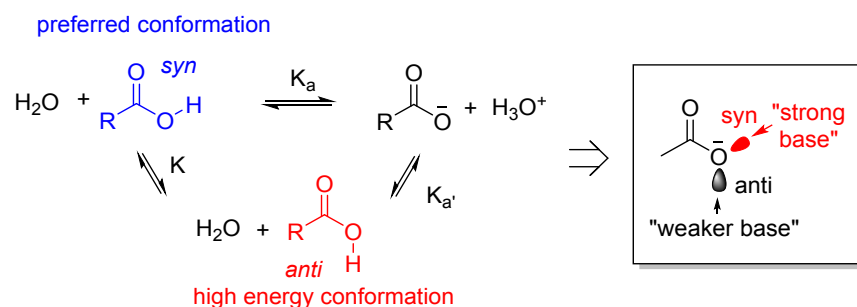
Figure 121. The concept of different basicity of "syn" and "anti" lone pair in carboxylates

This observation was suggested to be essential for understanding of the role of carboxylates as general bases in enzyme catalysis as it underscores the considerable differences between intramolecular "models" and intermolecular catalytic systems. Depending on the particular system and the extent of proton transfer in the transition states, the catalytic power of syn orientation was estimated to be 10-1000 times greater than that of anti. However, when applying this analysis, one should keep in mind that the kinetic penalty is not always imposed to the full possible extent as proton transfer is not always complete in the transition state.

Nevertheless, the intramolecular systems have a common geometric feature: the catalytically bridging proton is positioned on the opposite side from the C=O bond. If the proton is fully transferred, a less stable conformation of the carboxyl group is formed (Figure 122, top). In contrast, catalytically important carboxylate groups in enzymes are generally positioned so they are protonated from the syn-direction and utilize the "more basic syn lone pair" (see Figure 81).
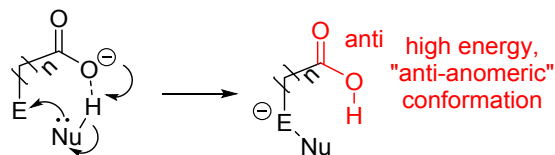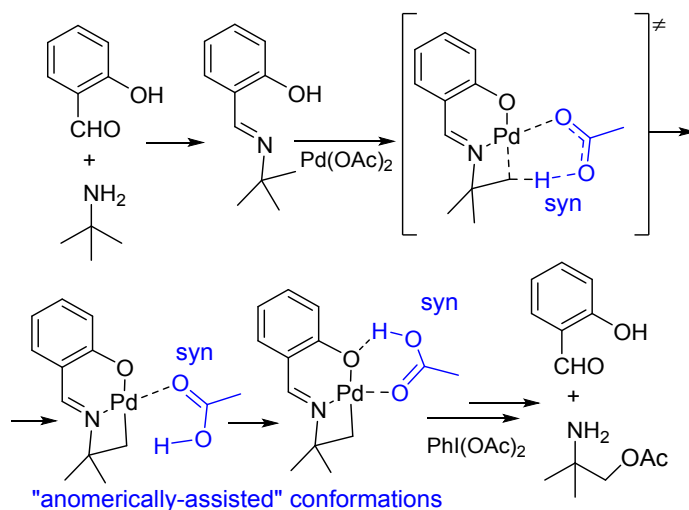
Figure 122. Top: the "wrong" way to use RCO_2^- moiety for catalysis is less favorable because intramolecular constraints impose the "anti lone pair" assistance. Bottom: the "right" way to use RCO_2^- for catalysis (metal..O coordination is compatible with the stereoelectronically favorable assistance by carboxylate). Note that the E/Z-preference can change, if an anionic center forms a Nu…H-O hydrogen bond in the product (Figure 119).

A better way to use carboxylate can be illustrated by an example from a challenging palladium-catalyzed oxidation of primary C–H bonds (Figure 122, bottom).[310] Hartwig et al. used this process to introduce an AcO-group at a β-position relative to a nitrogen. Among many interesting mechanistic features of this process, that traverses through a four-membered palladacyclic intermediate, is the versatile assistance by the acetate ligand. As the proton from the targeted C-H bond is transferred to the acetate, the latter is transformed to the favorable syn-isomer of acetic acid. Furthermore, when the proton coordination at the phenolic oxygen is needed for a following step, the Pd-coordinated AcOH can pivot to the oxygen and engage in a stabilizing H-bond without sacrificing this stereoelectronically favorable Z-arrangement. Understanding this stereoelectronic aspect of carboxylate assistance to proton transfer is important if one wants to use the full power of base catalysis. Molecular clefts developed by Rebek and coworkers on the basis of Kemp's triacid represent another way to orient a carboxylate group in a way that takes advantage

of the "syn lone pair".[311] An illustrative example is provided by enolization of the bicyclic ketone in Figure 123. Authors compared this process with systems that used the less basic lone pair and found about an order of magnitude in rate enhancement.[312]
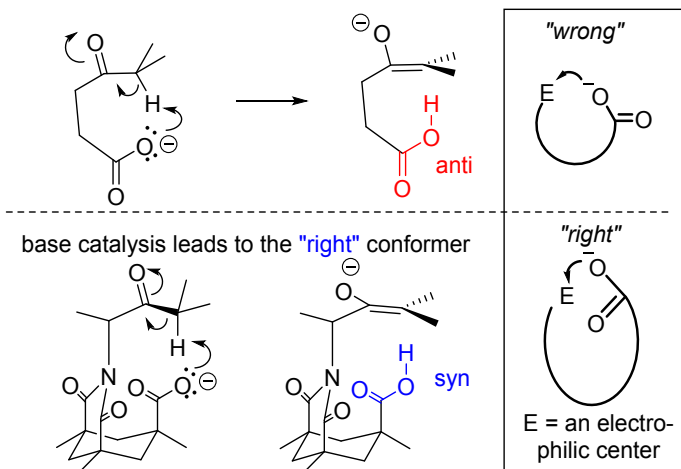
Figure 123. Top: stereoelectronically unfavorable use of intermolecular base catalysis with carboxylate. Bottom: Rebek's stereoelectronically favorable approach via a U-shape molecular scaffold

In order to get deeper insight into these issues, Zimmerman et al.[313] prepared model compounds containing an imidazole and a carboxylic acid as models for the His-Asp couple found in serine proteases and other enzymes. The carboxylate ability to increase the basicity of the imidazole via an H-bonding relay could potentially play a role in nucleophilic and general base catalysis by the imidazole. From the two systems with the relatively close $CO_2^-...H-N^+$ distances (2.5-2.6 Å), authors concluded that a syn carboxylate can raise the pK_a, of a proximate imidazolium ion by ca 0.4-0.6 pKa units over that of anti carboxylate. These model studies suggest that the syn-carboxylate provides only a small direct catalytic advantage in the hydrolytic reactions mediated by such an acid-base relay (Figure 124).

Proton relay assists nucleophilic attack

Asp-102

His-57

Ser-195

Z-isomer

Model compounds

E-isomer

Z-isomer
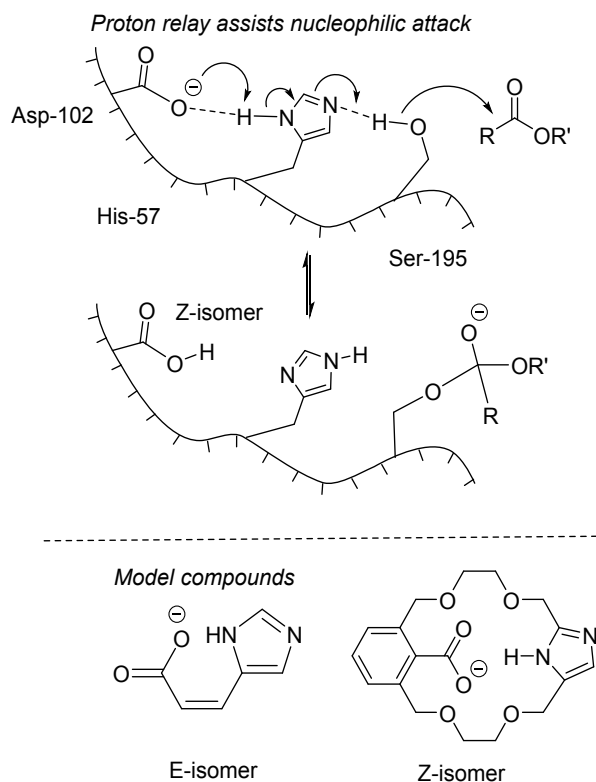
Figure 124. The hypothetical role of a remote carboxylate in general base catalysis by the imidazole

A similar stereoelectronic penalty was also evaluated for many classical chelating agents bearing carboxylate groups such as EDTA where, due to the constraint imposed by their molecular shapes, only the anti lone pairs of the carboxylates achieve contact with the metal ion in the complex. Structures in which the syn lone pairs are available for binding are promising chelating agents.[314] The affinity of these lipophilic structures to alkaline earth ions can be used for extraction of Ca^{2+} or Mg^{2+} from aqueous phases. The trans-relationship of the ligands surrounding the metal centers may be useful for design of metal catalysts with the catalytic behavior different from the more conventional chelates (Figure 125).

chelation with the anti lone pair

chelation with the syn lone pair
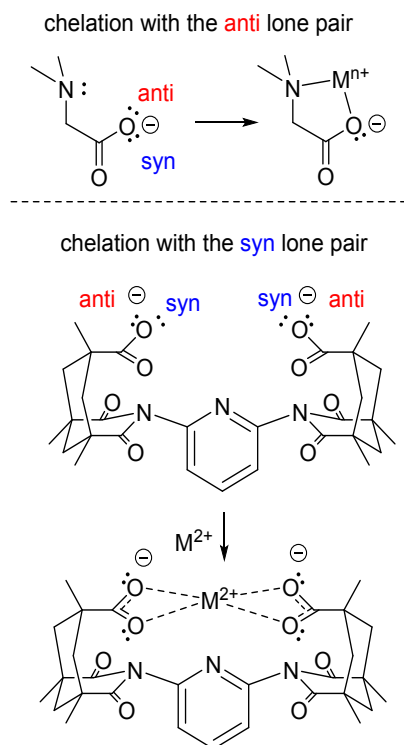
Figure 125. Stereoelectronic design of metal-chelating reagents

The importance of anomerically controlled carboxylic activations can be potentially expanded to the textbook alkene epoxidation reactions. In particular, one of the reasons why the nearly concerted butterfly mechanism suggested by Bartlett[315] operates efficiently is that the multi-bond reorganization agrees with the intrinsic Z-preferences of carboxylic acids. For example, the Z-conformation of the reactant peroxyacid is favorable – hence, the "butterfly" geometry can be adopted without a stereoelectronic penalty (Figure 126). One can also notice that the lowest energy TS leads to the favorable Z-isomer of the carboxylic acid by-product. However, the latter effect is likely to be of minor importance since the proton transfer is not started at the epoxidation TS and the initial O-H bond is largely unbroken.[316]
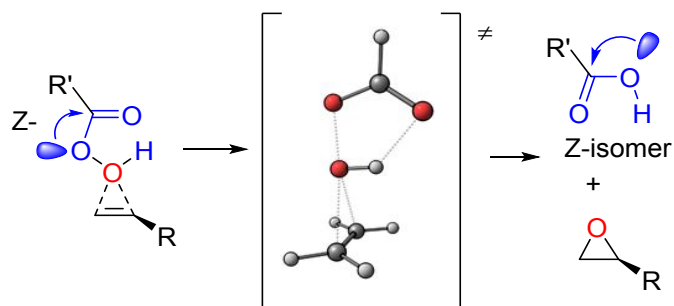
Figure 126. Conformational preferences of carboxylic acids contribute to epoxidation of alkenes with peroxyacids

Montzka et al.[317] noted that the degree of the "syn lone pair effect" depends on the extent of proton transfer in the transition state and showed computationally that the difference between syn- and trans-LPs significantly diminishes (and even reverses) when the proton is half-transferred. This result is consistent with the computational data of Houk and coworkers[318] who analyzed this situation in model systems by comparing carbonyl α-deprotonation and H-bond formation for the "syn and anti lone pairs" of formate anions. For the proton transfer the difference was found to be very small, consistent with incomplete H-transfer in the TS (Figure 127). Solvation effects and higher level theory are likely to be important in correctly describing the balance of conjugative and electrostatic effects in these polar systems. The analysis was also extended to the S_N2 reaction with methyl fluoride. Although the "pre-reaction complex" is slightly more stable for coordination with the "syn"-lone pair, the transition state energies may show the opposite trend.

HF/ 3-21G//3-21G	0.0	0.4
HF/ 6-31+G*//3-21G	0.0	1.6
HF/ 6-31G*//6-31G*	0.0	0.6
HF/ 6-31+G*//6-31G*	0.0	0.3
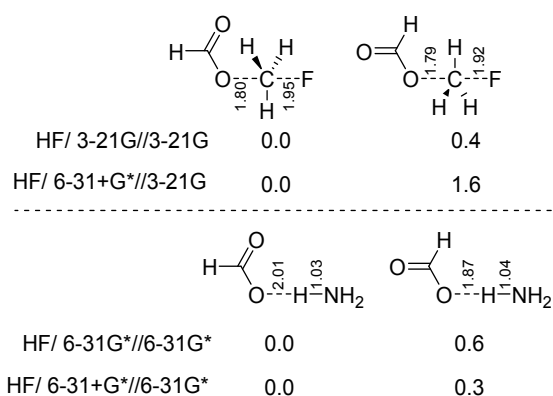
Energies are given in kcal/mol

Figure 127. Computational assessments of the nucleophilicity and H-bonding ability of carboxylate syn and anti lone pairs.

Furthermore, when hydrogen bonding is made stronger by using anionic H-bond acceptors, the Z-effect can be *reversed* (Figure 119).[306] The preference of E-carboxylic acid conformer is apparent in complexes of acids with carboxylates common in the protein environment. As an example, the insulin hexamer in its most common crystalline form consists of three protein dimers linked by three *trans*-COOH...OOC interactions of independent GluB13 residues (Figure 128), with the $O^{\varepsilon 2}...O^{\varepsilon 2}$ distances of 2.46 Å. Analysis of a 1.0 Å resolution structure obtained for a space-grown crystals of insulin T_6 hexamer[319] confirmed that this GluB13 $O^{\varepsilon 2}...O^{\varepsilon 2}$ hydrogen bond is the strongest in the T_6 complex and is absent in the other insulin forms suggesting that this interaction plays an important role in the T$\rightarrow$R insulin transition, studied for preparation of new insulin polymorphs.[320]
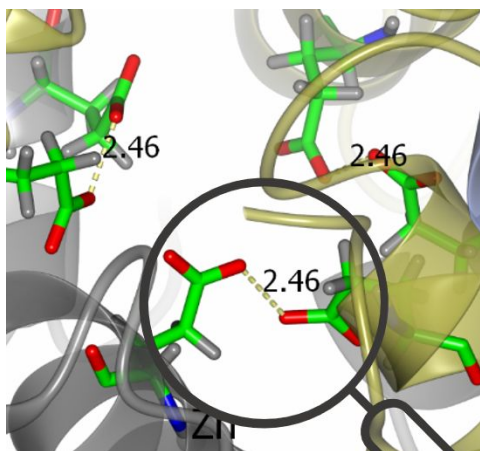
Figure 128. Trans-COOH…OOC contacts of GluB13 residues in the insulin T_6 hexamer assisted by SSE. $O^{\varepsilon 2}…O^{\varepsilon 2}$ distances are shown. Protein chains are colored by symmetry equivalence. Atomic coloring: red – oxygen, green – carbon, blue – nitrogen, grey – hydrogen.

The preference for the E-conformation in complexes of carboxylic acids with anionic species can be quite strong (e.g., >4 kcal/mol in the complexes of acetic acid with NCO^- in vacuum).[306] This preference can be also illustrated by the tug-of-war between the cis- and trans-carboxylic groups in competition for one proton. The proton goes to the trans-isomer (Figure 129), which is a better partner for intermolecular interactions due to its incomplete "internal satisfaction". This system has an interesting network of interconnected hyperconjugative interactions. First, not only is the "syn-lone pair" of the Z-carboxylate a better donor but the $n_O{\rightarrow}\sigma^*_{O-H}$ interaction is made stronger by the presence of another $\sigma^*_{C=O}$ acceptor which is antiperiplanar to the OH bond in the E-carboxylic acid. Furthermore, the O-H elongation elevates the σ_{O-H} energy similar to other cases of stronger hyperconjugative donation from the partially broken bonds (i.e. a stretched bond becomes a much better donor in a $\sigma_{O-H}{\rightarrow}\sigma^*_{C=O}$ interaction Figure 129).[321, 322] Since here a stereoelectronic (anomeric) effect is reversed by intermolecular bonding, Medvedev et al. have called it the "Supramolecular Stereoelectronic Effect" (SSE).[306] Later, a similar effect was found in in complexes of hemiketals.[323]
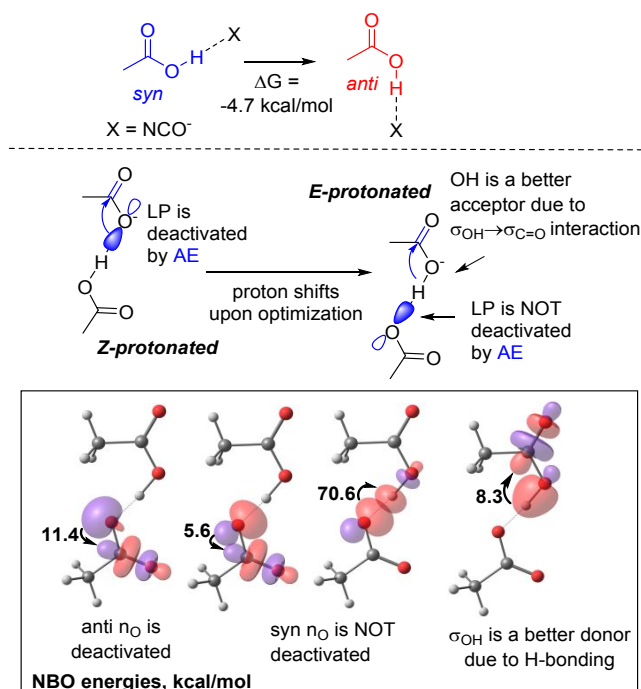
Figure 129. Top: The E-preference in a carboxylic acid complex with an anion. Bottom: The tug-of-war of two carboxylate anion isomers for a proton. The H-bond between a better donor lone pair and a better σ* acceptor is stronger.

Overall, this data suggests that more research is needed for fully understanding stereoelectronics of carboxylic acids. It would be interesting to revisit these interesting stereoelectronic hypotheses with the more advanced experimental and computational techniques that are currently available.

Connected networks of anomeric effects in carbonyl chemistry:

Considering the above examples, it is not surprising that the importance of anomeric effect extends throughout the carbonyl chemistry. In order to highlight how wide-spread its influence is, let us consider the typical path of reactions of a ketone and an ester with a nucleophile. Both proceed through the formation of a tetrahedral intermediate (TI) which can either be trapped by a proton transfer (e.g., in an addition reaction to a ketone) or via elimination of a leaving group X (e.g., in a substitution reaction at an ester).

The leaving group X departure is the additional direction that is only available to carboxylic acid derivatives because they have a "productive" extra anomeric interaction that leads to the C-X scission and formation of the nucleophilic substitution products.[324] The TIs with two oxygen atoms are formed via two types of reactions: addition of O-centered nucleophiles to ketones/aldehydes and addition of C-centered nucleophiles to esters.
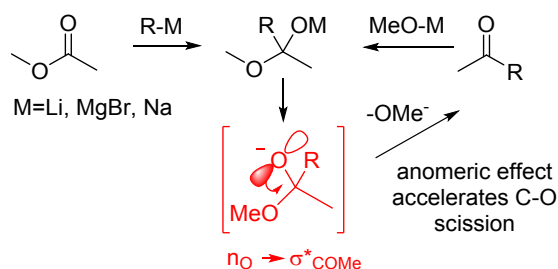
Figure 130. The possible role of enhanced anomeric effect on the stability and reactivity of an anionic tetrahedral intermediate

Note that the large accelerating role of anomeric interaction in the C-OMe scission shown above (Figure 130) has practical consequences. For reaction of ketones (or esters) with alkoxides, this interaction transforms the TI back to the starting materials while for the reaction of an ester with a carbanion analog (e.g., an RLi reactant), it transforms the TS quickly to the ketone. The latter effect is responsible for the textbook problem of why ketones can be hard to make from the ester reactions with carbanion equivalents. The kinetic anomeric effect is responsible for the fast collapse of the TI and the premature formation of the ketones before the initial reaction of nucleophile with the ester is complete. In order to prevent the premature ketone formation giving rise to the formation of tertiary alcohols, it is essential to stabilize such TIs by an "orthogonal factor", not associated with the anomeric effect. For example, the classic use of Weinreb amides stabilizes the TIs via chelation. Only when this additional stabilizing force is removed upon the aqueous work-up, the TI is transformed into a ketone.[325]

For good leaving groups, the anomeric donation can be so high that the TI is not even formed and the nucleophilic substitution proceeds via a concerted path where the nucleophilic attack and leaving group departure occur simultaneously.[326-329]

An interesting example of a TI that was isolated and where the role of negative hyperconjugation was analyzed in detail is provided recently by Vil' et al.[330] who described isolation and characterization of the Criegee intermediate of the Baeyer–Villiger (BV) rearrangement. The parent hydroxyl version of this TI was never captured and characterized because of its instability. The authors recognized that kinetic stability of the Criegee intermediate can be controlled using selective deactivation of the two stereoelectronic effects that promote the 1,2-alkyl shift in this oxygen-rich structure.[185] The focus of our subsequent discussion will be on the so-called "secondary stereoelectronic effect" (Figure 131) because it is related to the anomeric effect in an interesting way.
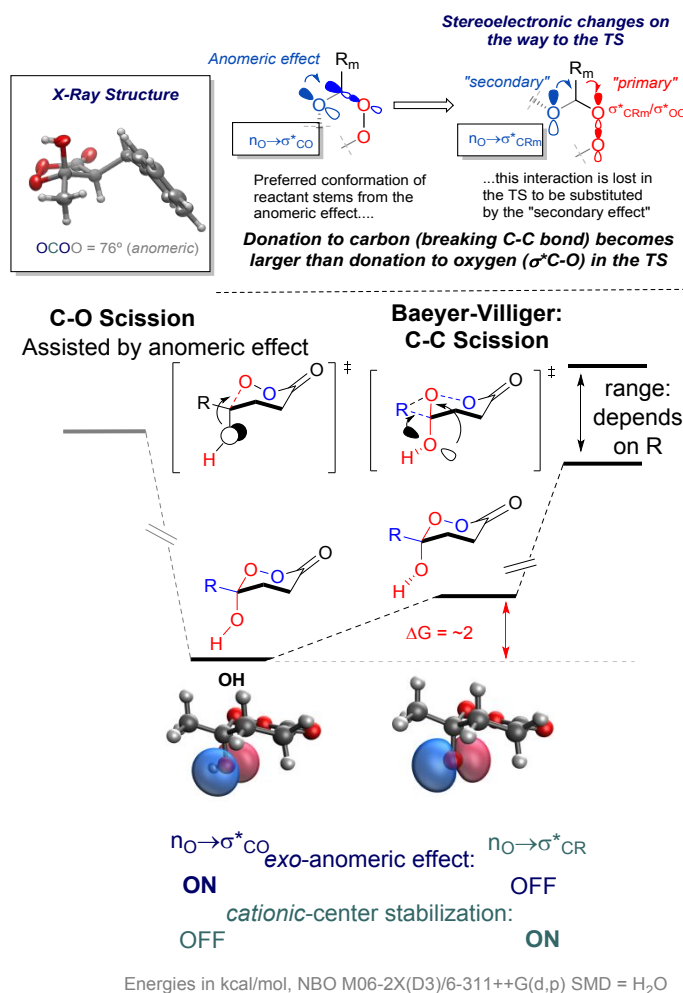
Figure 131. The interplay of anomeric effect with the two stereoelectronic effects in the Baeyer-Villiger (BV) rearrangement of a Criegee intermediate

A common feature of transition states is that they can impose quite significant electronic demand, larger than that in the ground state. In the BV TS, the migrating electron-deficient carbon becomes a better acceptor than oxygen. This change is the reason for the "secondary stereoelectronic effect in BV rearrangement" - the OH group adopts an appropriate conformation by aligning the lone pair with the breaking C-C bond at the migrating group (Figure 131).

The X-ray structure of a Criegee intermediate in Figure 131, illustrates that the lone pair of the OH group is aligned with the endocyclic C-O bond. This is the classic exo-anomeric effect. This structural preference agrees well with the computational analysis of the Criegee intermediate. However, this stabilizing interaction has to be lost in the TS of the 1,2-Me group shift that completes the BV process. The driving force for that change is that significant positive charge develops at the migrating group R, forcing the lone

pair of the adjacent oxygen to realign with the breaking C-R bond. This departure from the anomeric conformations and concomitant loss of anomeric stabilization are the necessary conditions for activating the BV secondary stereoelectronic effect. They serve as a hidden penalty for this industrially important family of reactions.[331]

The above discussion illustrates a few of the interesting stereoelectronic properties of peroxides and introduces this underutilized O-rich organic functionality. Let's look at its reactivity more closely in the next section through the prism of anomeric effect.

Peroxides: the anomeric effect is dead, long live the anomeric effect!

Although organic peroxides are barely mentioned in undergraduate textbooks and have a poor reputation due to their purported instability, this class of organic molecules recently started to become popular in pharmaceutical research (Figure 132).[332-340] Stable peroxides have gained acceptance as a source of new drugs, such as the Nobel Prize-winning antimalarial drug artemisinin.

Artemisinin
antimalarial
anthelmintic
anticancer

Arterolane
"Synriam"
antimalarial

Verruculogen: R = H;
Fumitremorgin A: R = prenyl

(+)-cardamom peroxide
antimalarial
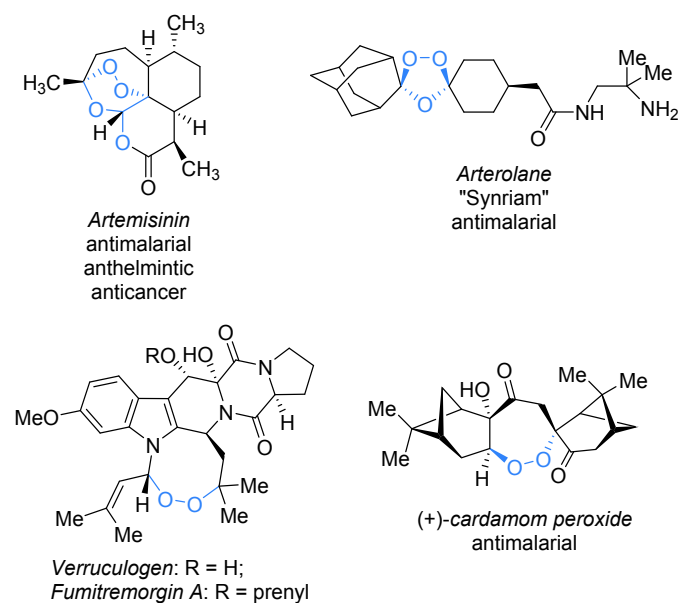
Figure 132. Examples of pharmaceutically important peroxides

Peroxides are very different stereoelectronically from other functional groups with two oxygen atoms (e.g., ketals, gem-diols, esters) because they lack strong anomeric interactions. In fact, anomeric effect is usually weak in dimethyl peroxides.[185] However, recent collaborations between the groups of Terent'ev (ZIOC RAS, Moscow) and Alabugin (FSU) revealed that peroxides hide a large number of dormant stereoelectronic features associated with anomeric effect. Activation of these features provides a key to the design of stabilized peroxides, whereas insights into the anomeric effect led to the discovery of novel peroxide reactivity.

The stereoelectronic differences between peroxides and acetals[185] are clearly manifested in the conformational preferences of these two O-containing functionalities. As mentioned earlier, $MeOCH_2OMe$ prefers the *gauche - gauche* (GG) conformation as a consequence of the general anomeric effect. NBO analysis provides a stereoelectronic rationale for this preference by identifying two strong $n_O \rightarrow \sigma^*_{C-O}$ interactions (with the NBO energies of 14.9 kcal each) maximized at the 60-degree COCO dihedral. On the other hand, the conformational preferences of peroxides are drastically different. In particular, the most stable rotamer of dimethyl peroxide corresponds to the COOC dihedral angle of ~150° with an essentially isoenergetic ensemble of conformations with dihedral angles from 110 to 180° (all within 1 kcal/mol at the MP2/6-311++g(d,p) level).[184, 185] Overall, these conformational profiles point to the dramatically different stereoelectronics of acetals and peroxides which, to a large extent, stem from the weakening of the anomeric effect in peroxides.[184, 185]
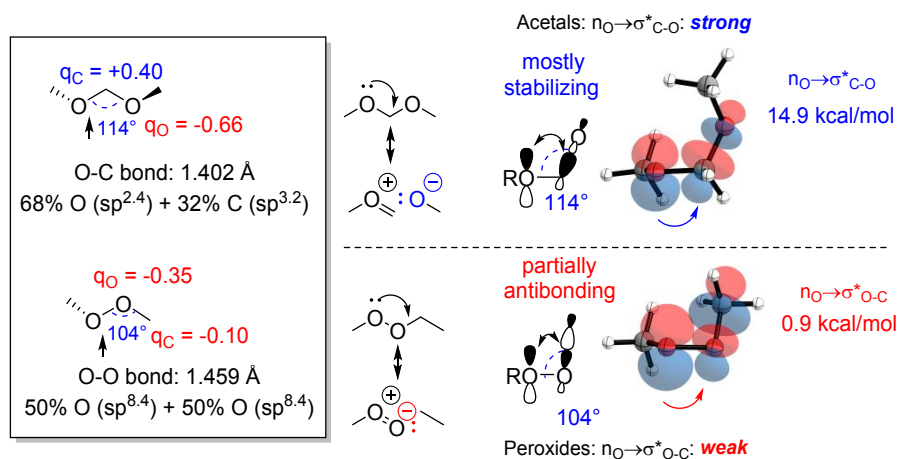
Figure 133. Difference in hybridization and polarization features of OCO vs OOC moieties leads to >16-fold difference between $n_O \rightarrow \sigma^*_{C-O}$ interactions in acetals and $n_O \rightarrow \sigma^*_{O-C}$ interactions in peroxides

The difference in the magnitude of anomeric interactions in peroxides and acetals is striking. At the same level of theory, the NBO energy for $n_O \rightarrow \sigma^*_{C-O}$ interactions in the acetal is 14.9 kcal/mol, whereas the energy of $n_O \rightarrow \sigma^*_{O-C}$ interactions in the peroxide is only ~0.9 kcal/mol (Figure 133). This difference is much larger than the usual difference in the acceptor ability of C-O and O-C bonds in ethers[3] (C-O bonds are ~40% stronger acceptors than O-C bonds in $\sigma_{C-H} \rightarrow \sigma^*_{X-Y}$ interactions (X,Y=O,C) as a consequence of σ^*_{CO} orbital polarization towards carbon). Not only is the stereoelectronic difference amplified for stronger donors (n_O (peroxides/acetals) vs. σ_{C-H} (ethers)), but the hyperconjugative anisotropy is greatly increased by an intricate combination of effects illustrated in Figure 133. When a ***p-orbital*** serves as a donor in an anomeric interaction, the notions of syn- and anti-periplanarity vanish. In this case, the n_p/σ^* overlap is

significant with **both** the back lobe of the σ*orbital and the antibonding region *between* the two atoms (e.g., O and C). In peroxides, the unusually small OOC angle brings the σ^*_{OC} node closer to the p-orbital. The destabilizing interaction with the out-of-phase hybrid at carbon largely offsets the in-phase stabilizing interaction of the p-donor with the oxygen part of the σ^*_{O-C} orbital (Figure 133).

The striking >16-fold decrease in the magnitude of $n_O \rightarrow \sigma^*_{O-C}$ interactions in peroxides in comparison to $n_O \rightarrow \sigma^*_{C-O}$ interactions in acetals reveals the loss of anomeric hyperconjugation as an additional source of thermodynamic instability of dialkyl peroxides.

A logical expansion of this stereoelectronic analysis leads to a paradoxical prediction that bis-peroxides can possess greater thermodynamic stability than monoperoxides as long a second peroxide moiety is separated from the first peroxide by a one-atom bridge. Stereoelectronically, such bis-peroxides can be viewed instead as bis-acetals enjoying strong anomeric $n_O \rightarrow \sigma^*_{C-O}$ interactions. The NBO dissection and group separation equations in Figure 134 agree in predicting increased stability of bis-peroxides.
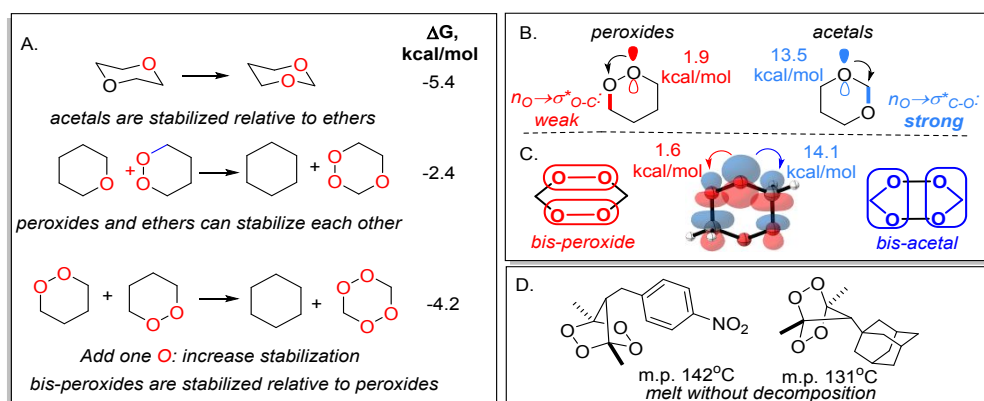
Figure 134. A) Group separation reactions show the stabilization from the introduction of $n_O \rightarrow \sigma^*_{CO}$ interactions in bis-peroxides and peroxyacetals. B-C) Relative weakness of hyperconjugative donation from oxygen lone pairs to vicinal σ*-acceptors in peroxides vs. acetals (B) can be compensated by stereoelectronic transformation of bis-peroxides to bis-acetals (C). D) Examples of unusually stable bis-peroxides which melt at temperatures exceeding 100°C without decomposition

Interestingly, there are reports of such bis-peroxides melting at temperatures exceeding 100°C without decomposition (Figure 134D). Stable bridged 1,2,4,5-tetraoxanes can be easily synthesized from 1,3-diketones and hydrogen peroxide.[341-345] The oxygen–oxygen bond dissociation energies, BDE(O−O) is significantly larger for the CF₃O−OCF₃ peroxide (~48 kcal/mol) than for Me₃CO−OCMe₃ (39 kcal/mol),[346] illustrating that anomeric effect stabilize peroxides against homolytic bond scission as well.

These unusual electronic features of bis-peroxides turned out to be more than just an esoteric observation. Instead, it is the key to unlocking new peroxide reactions. Below, we will illustrate how control of anomeric effects in peroxides led to the development of an ozone-free synthesis of ozonides. Traditionally, secondary ozonides (trioxolanes) are obtained via the reaction of alkenes with ozone or via ozonolysis of *O*-methyl oximes in the presence of ketones (Griesbaum coozonolysis). Potentially, the condensation of two carbonyl groups with H_2O_2 can open an alternative ozone-free route to ozonides (Figure 135). Unfortunately, this attractively simple route is usually not followed in practice because, instead of ozonides, such condensations provide the aforementioned anomerically-stabilized bis-peroxides.
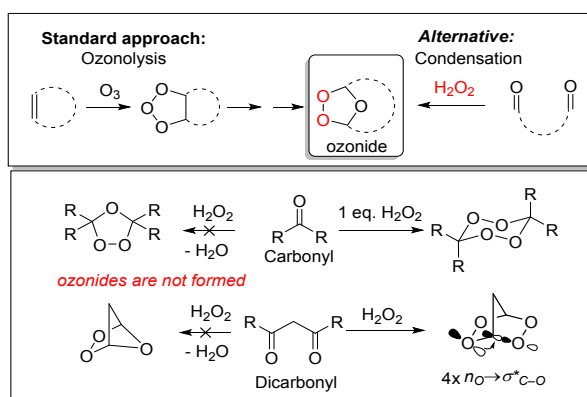
Figure 135. Top: The classic and the new approaches to ozonide synthesis. Bottom: Failure of the "ozone-free" approach for acyclic ketones and 1,3-diketones.

However, understanding the origin of this selectivity also provides a key to overriding the intrinsic preferences. In this context, the stereoelectronic solution for directing carbonyl condensations towards ozonides should include selective *deactivation* of the anomeric effect. If this source of bis-peroxide stabilization is weakened, ozonides should have a greater chance to win the thermodynamic tug-of-war in the process of condensation of ketones and H_2O_2.
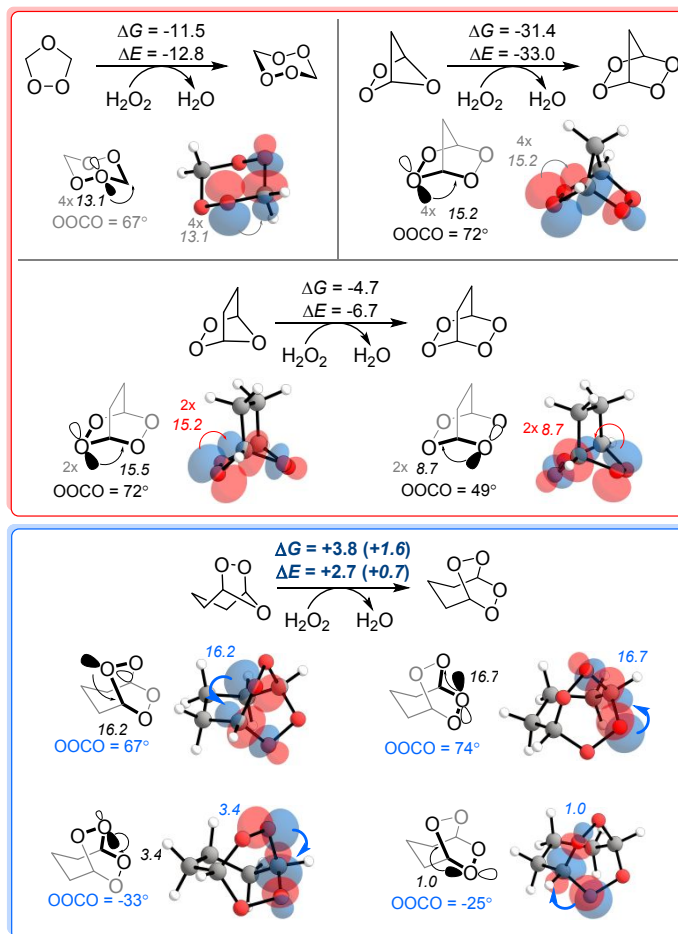
Figure 136. Deactivation of anomeric effects by structural constraints and Illustrative NBO plots for the key $n_O \rightarrow \sigma^*_{C-O}$ interactions. Calculations at the (SMD=MeCN)/B2PLYP-D2/6-311++G(d,p) level of theory. Relative energies of ozonides and bis-peroxides as a function of tether length.

The stereoelectronic model of the anomeric effect suggests that it can be weakened by changing geometries in a way that decreases the stabilizing orbital overlap. Gomes, Yaremenko, et al.[347] suggested that the thermodynamic preferences of bis-peroxides would diminish when the 1,2,4,5-tetraoxane moiety is twisted by incorporation into a bicyclic system. From the orbital point of view, the greater misalignment of lone pairs and σ^*_{CO} orbitals is the key to finding the right bridge size for disfavoring the bis-peroxide formation.

In order to understand the effect of the two additional bridge atoms, the key interactions in the two bicyclic families were quantified with NBO analysis. Indeed, the additional bridge in bicyclic structures perturbs anomeric $n_O \rightarrow \sigma^*_{C-O}$ interactions. In particular, the three-carbon bridge imposes a non-symmetric twist on the boat conformations of the tetraoxacyclohexane subunits. The geometric

constraints imposed by the [3.2.2] frame deactivate two of the four $n_O \rightarrow \sigma^*_{C-O}$ interactions in the bicyclic tetraoxane (from ~16 to 3 and 1 kcal/mol, respectively, Figure 136).

The thermodynamics of the ozonide formation from bis-carbonyl systems with a varying degree of separation between the two ketone groups illustrated the validity of NBO estimates (Figure 136). As stated above, the bis-peroxides are clearly more favorable in monocyclic systems, without the effect of additional bridge. A small, one-carbon, bridge accentuates this effect but the larger (two- and three-carbons) bridges have the opposite effect. In particular, the three-carbon bridge (i.e., using 1,5-diketones as the starting material) shifted the competition between the [3.2.1]/[3.2.2] products (i.e., ozonides/bis-peroxides) toward ozonides. In this system, the ozonide is 2-4 kcal/mol *more* stable than the bis-peroxide according to the DFT calculations.

Although less stabilized by anomeric interactions than bis-peroxides, ozonides have an intrinsic advantage of having only one weak O-O bond. The combined anomeric stabilization in bis-peroxides helps to overcome this intrinsic disadvantage. As illustrated by the above analysis, this is only possible when stabilizing negative hyperconjugation in bis-peroxides is activated to their *fullest* degree.

Encouraged by the large stereoelectronic differences between the seemingly similar bicyclic bis-peroxides, Yaremenko et al.[229, 348] have investigated the reactivity of 1,5-diketones and H_2O_2 in the presence of Brønsted or Lewis acids under homogeneous and heterogeneous conditions. Remarkably, these condensations result in the exclusive formation of bicyclic ozonides. The alternative bis-peroxide products were not observed. The synthetic value of this approach is that it can be extended to substrates which contain alkene and alkyne functionalities that would not survive the classic ozone-based approach to ozonides.
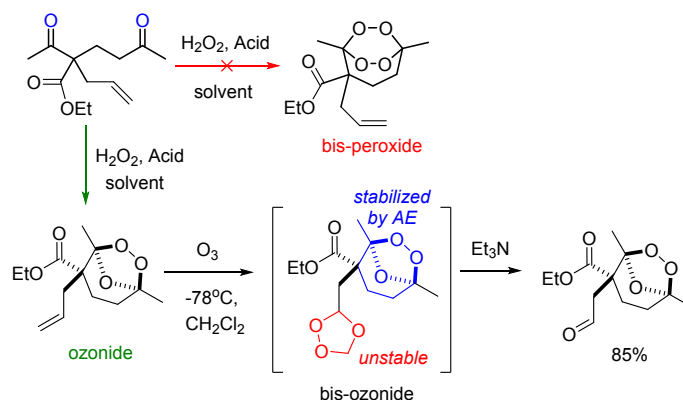
Figure 137. Ozone-free synthesis of an ozonide with a pendant alkene and its subsequent ozonolysis illustrates higher stability of bicyclic ozonides

In contrast to simple ozonides, bicyclic ozonides enjoy some anomeric stabilization. This difference is consistent with their greater stability relative to the monocyclic ozonides. In particular, the bicyclic ozonide remains intact in the presence of Et_3N while monocycic ozonides derived from the terminal alkene readily undergo fragmentation (Figure 137).

Recently, Yaremenko et al.[349] described an atom-economical process where H_2O_2 serves as a "lasso" for tying tri-functional acyclic reactants into stereochemically and structurally rich tricyclic structures (Figure 138). In particular, β,γ'-triketones can be converted into tricyclic mono- and bis-peroxides.
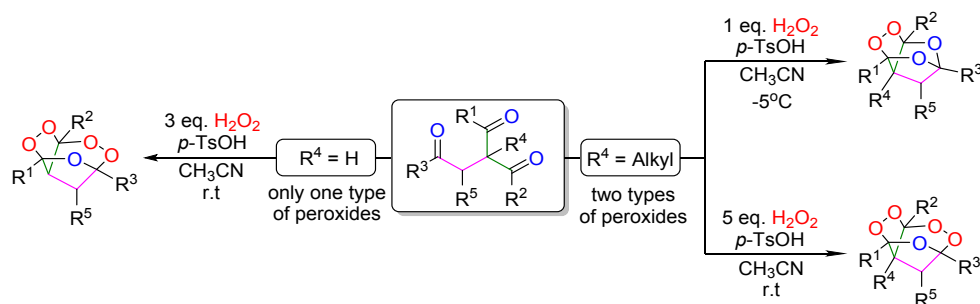
Figure 138. The assembly of tricyclic peroxides from β,γ'-triketones and H_2O_2

Computations reveal that stereoelectronic frustration of H_2O_2 is relieved in the tricyclic peroxide products, where strongly stabilizing anomeric $n_O \rightarrow \sigma^*_{C-O}$ interactions are activated. The calculated potential energy surfaces combine labile dynamically formed cationic species with deeply stabilized intermediate structures corresponding to the introduction of one, two, or three peroxide moieties. Comparison of kinetics and thermodynamics in these reactions reveals a paradoxical situation: formation of each neutral peroxide in the three-stage cascade condensation of β,γ'-triketones with H_2O_2 is more and more favorable thermodynamically but less and less favorable kinetically (Figure 139).
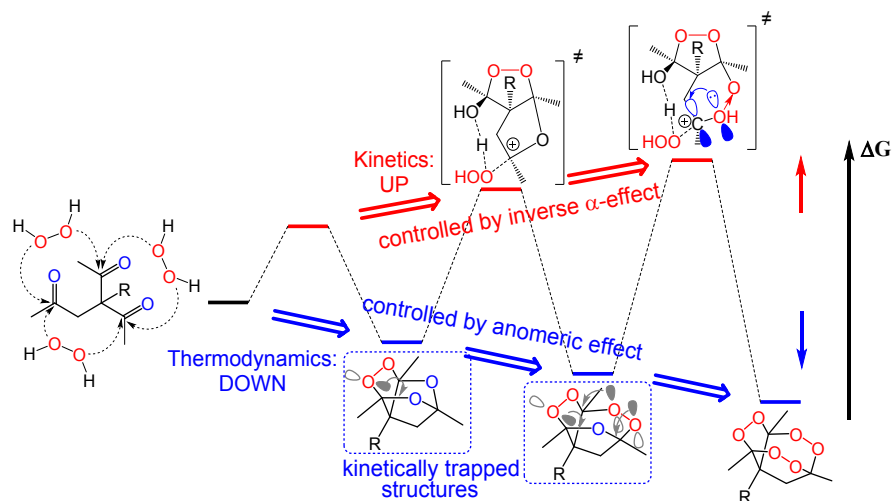
Figure 139. The simplified potential energy surface of the peroxide-forming condensation cascades. Each of the deep minima is connected by a dynamically interconverting sequence of higher energy intermediates and transition states of similar energies. Only the rate-limiting transition states are shown.

The paradoxical divergence of kinetic and thermodynamic parameters stems from the interplay of two stereoelectronic effects. The product peroxides are progressively more stabilized by the classic anomeric effect, which is dormant in H_2O_2 but resurrected in bis- and tris-peroxides. On the other hand, the transition states are destabilized by the inverse α-effect,[269] i.e., the weaker carbocation stabilization by a peroxide group in comparison to an ether group that maybe amplified by structural constraints in the bicyclic transition states (Figure 140).
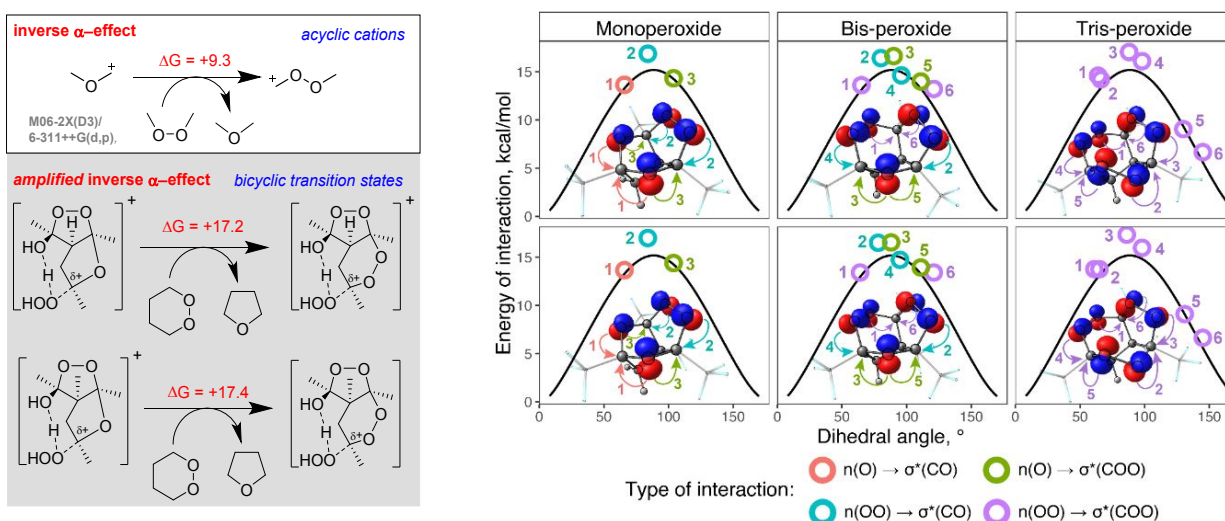
Figure 140. Impact of the anomeric effect and the inverse α-effect on the assembly of tricyclic peroxides.

However, with an increase in the distance between carbonyl groups, i.e., upon change from β,γ'-triketones to β,δ'-triketones, only tricyclic monoperoxides were obtained. Neither bis- or tris-peroxides were observed (Figure 141).[350, 351]

R = Me, Ar; R' = H, Alk

yield 39-90%
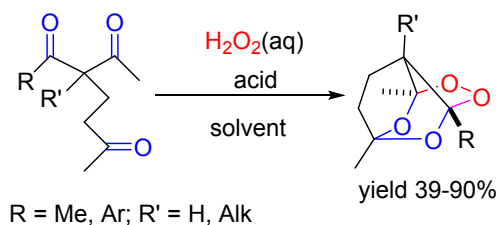
Figure 141. The assembly of tricyclic monoperoxides from β,δ'-triketones and H_2O_2

Although introduction of a longer "insulating" bridge on one side of a cyclic peroxyacetals removes part of the stabilizing interactions, NBO analysis shows that donation of electron density in each direction in the peroxyacetal moiety significantly stabilizes 1,2,4-trioxepanes, trioxocanes, and trioxononanes (Figure 142). In the case of the seven- and eight-membered cycles, the interactions are sufficient to promote the formation of the ring from the starting acyclic structure. However, in the nine-membered cycle, the relatively strong pair of anomeric interactions cannot fully compensate for the unfavorable strain of a medium-size ring formation.[352]
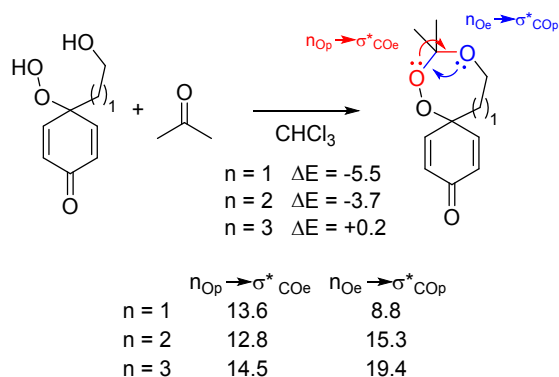
Figure 142. The stabilizing anomeric interactions in peroxyacetals can be utilized to promote the formation of target 1,2,4-trioxepanes and trioxocanes.

An interesting observation is the apparent violation of the inverse-α effect for n = 1 (Figure 142). According to the inverse-α effect, the peroxide oxygen should be a weaker donor than the ether oxygen. It is likely that the geometry distortions of the seven-membered cycle misalign the interacting donor/acceptor orbitals.

Functional Groups with Three Oxygens

Orthoesters and tetrahedral intermediates in addition to carboxylic acid derivatives

Ortho-esters display a complex network of multiple anomeric interactions, the strongest of which are illustrated in the stereoelectronic portrait of 1,1,1-trimethoxyethane in Figure 143. The lowest energy t,g,g conformation is a compromise of sterics and anomeric hyperconjugation. All interactions are slightly different (variations from 11 to 14 kcal/mol) but still relatively large, supporting the important role of negative hyperconjugation in stabilizing orthoesters.

$n_O(p) \rightarrow \sigma^*_{C-O}$: **strong** $n_O(p) \rightarrow \sigma^*_{C-O}$: **strong** $n_O(p) \rightarrow \sigma^*_{C-O}$: **strong** $n_O(p) \rightarrow \sigma^*_{C-O}$: **strong**

$n_O(p) \rightarrow \sigma^*_{C-O}$	$n_O(p) \rightarrow \sigma^*_{C-O}$	$n_O(p) \rightarrow \sigma^*_{C-O}$	$n_O(p) \rightarrow \sigma^*_{C-O}$
14.0 kcal/mol	**12.2 kcal/mol**	**12.1 kcal/mol**	**10.9 kcal/mol**

PBE0-D3BJ/aug-cc-pVTZ/CPCM(H₂O)
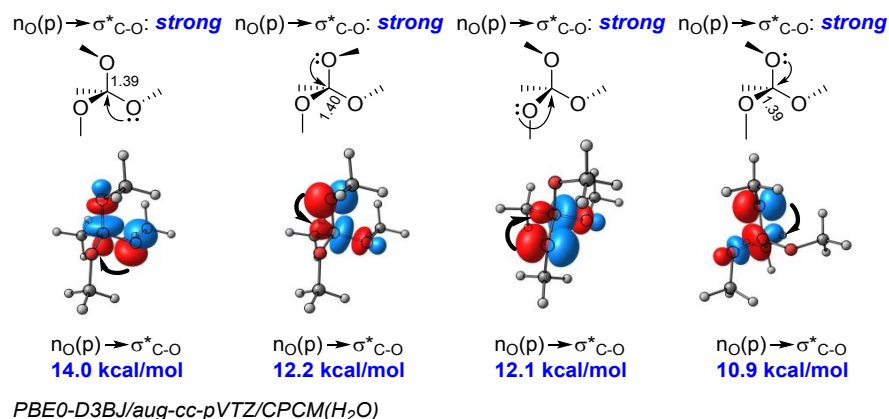
Figure 143. Stereoelectronic portrait of 1,1,1-trimethoxyethane. Only interactions with the p-type orbitals are shown

The interplay between sterics and the network of anomeric interactions in acyclic ortho-esters leads to rather complex conformational behavior. The combination of IR- and Raman analysis indicated that trimethyl orthoformate in solid phase exists in the C_3-symmetric conformation E, but in solution it exists as a mixture of the conformations F (C_s) and G (C_1) (Figure 144).[353] Aped and coworkers considered eight nondegenerate conformers of trimethyl orthoformate (structures A-H in Figure 144).[354] Computational study (HF/3-21G) found that the inner C-O bonds are shorter than the outer ones. Also, the central C-H bond elongates as the number of lone pairs aligned to it increases. For example, the C-H bond is the longest (1.090 Å) in the conformer E where three $n_O \rightarrow \sigma^*_{C-H}$ interactions operate together.

Relative energies, kcal/mol	A	B	C	D	E	F	G	H
R=H, HF/3-21G	4.8	Converged to G	Converged to G	9.2	3.2	1.8	0	-
R=H, PBE0-D3BJ/ aug-cc-pVTZ	8.2	3.2	4.0*	4.3*	0.6	0.4	0	3.7
R=Me, PBE0-D3BJ/ aug-cc-pVTZ	5.6	1.7	5.6*	7.9*	3.1	0.7	0	6.6
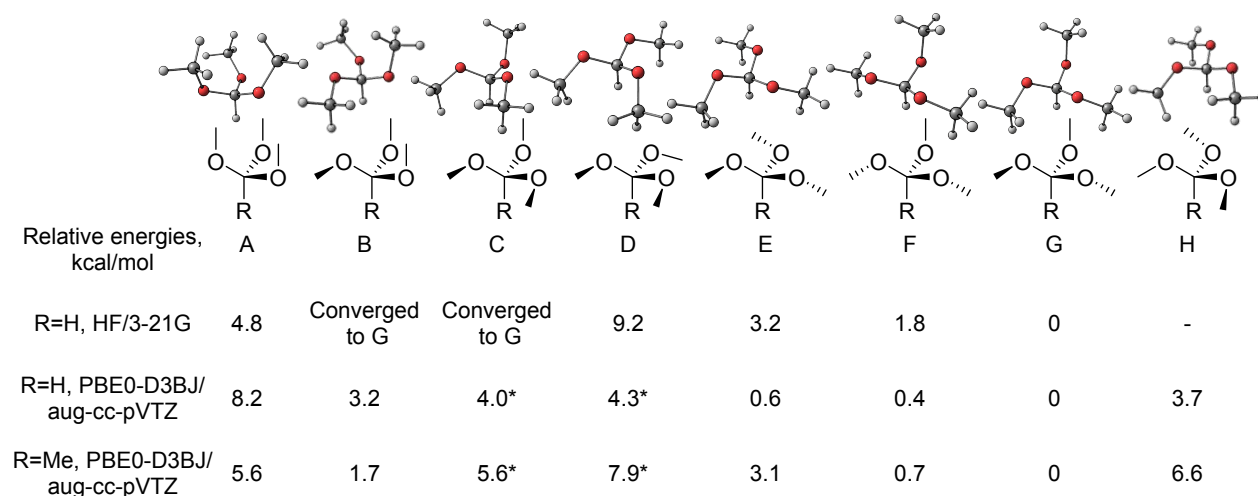
Figure 144. Eight independent and nondegenerate conformers of trimethyl orthoformate and trimethyl orthoacetate.[354] Relative energies of saddle points are denoted with asterisks.

Note that the conformation E with the "triply anomerically activated" C-H bond is relatively high in energy. In agreement with that, the radical chemistry of ortho-esters seems to be quite unexplored. One can extrapolate from the computational data for methane triol that the C-H bond in ortho-formates may be more activated than the α-C-H bonds in ethers and acetals.[355] It is clear, however, that the activation due to the additional OR groups is not additive. Resonance stabilization energies (RSEs) by one, two, and three gem-hydroxy groups were evaluated as 8.6, 8.8, and 10.3 kcal/mol, respectively (Figure 145). These values indicate that the deviation from additivity for the 2nd and 3rd OH groups in radical stabilization are substantial (-8.4 and -15.3 kcal/mol).
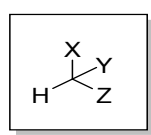
X, Y, Z:	C-H BDE	RSE	DARSE
H, H, H	102.0	0	-
OH, H, H	93.2	8.6	-
OH, OH, H,	93.0	8.8	-8.4
OH, OH, OH	91.3	10.3	-15.3

Figure 145. The effects of one, two, and three geminal OH groups on the C-H BDEs (RSE=Radical Stabilization Energy, DARSE – Deviation from Additivity in RSE, B2PLYP /6-311+G(3df,2p), kcal/mol)[355]

Figure 146 compares changes in BDE, hydride affinity, and proton affinity associated with the presence of one, two, and three methoxy groups at a carbon atom. Since DFT methods are often not very accurate for these properties[356], while experimental values are usually unavailable, we provide both to demonstrate the trends even as we show the accurate (experimental) values. The trend in BDEs is similar to that for the hydroxy-substituted systems in Figure 145 – there is a large drop in the BDE for the first OMe substituent but a smaller change for the 2nd and 3rd OMe groups. This trend suggests that radical stabilization in the di- and tri-OR-substituted radical products is similar to the anomeric stabilization in the reactants. As the anomeric $n_O \rightarrow \sigma^*_{CO}$ stabilization has to be sacrificed to use the lone pair of oxygen for the 2c,3e bond in the product, the cost of reactant stabilization partially compensates for the gain in product stabilization. In contrast, cation stabilization increases continuously with the greater number of oxygen substituents at the cationic center. This trend illustrates that the role of oxygen donor ability is amplified in the product where cation stabilization due to conjugation with the cationic carbon center is greater than anomeric stabilization in the product.

Interestingly, the trend in *proton* affinities illustrates that *carbanions* are also progressively stabilized by the additional geminal OR group. In the latter case, the network of anomeric n/σ^*CO interactions is generally preserved in the product, so the dominant factor explaining the increased stability of the oxygen-containing anions is likely to have a different origin such as a combination of CH bond rehybridization/polarization. Because, according to Bent's rule, carbon directs more p-character into

hybrid orbitals in the C-O bonds,[77] s-character in the C-H-forming hybrid increases with additional geminal OR groups.

BDE, kcal/mol	sp^3 CH$_3$–H	$sp^{2.9}$ CH$_2$(OMe)–H	$sp^{2.8}$ CH(OMe)$_2$–H	$sp^{2.7}$ C(OMe)$_3$–H
R–H → R• + H•	101.7 105.0 ±0.1	92.0 96.1	92.1 92.9	91.4
R–H → R⁺ + H⁻	318.7 313.8	242.4	209.7	192.5
R–H → R⁻ + H⁺	417.5 415.2 ±0.7	412.5 407	407.7	399.8

PBE0-D3BJ/aug-cc-pVTZ
Experimental

Figure 146. The effects of one, two, and three geminal methoxy-groups on the C-H BDEs, hydride affinities of O-substituted carbocations, and proton affinities of O-substituted carbanions. The available experimental data is shown in red; BDEs are from [217]; methyl cation hydride affinity is from [357]; CH$_4$ acidity is from [358]; and Me$_2$O acidity is from [359].

Considering the relatively strong stabilizing anomeric interactions in Figure 143, one may wonder why are ortho-esters less common than the other O-containing functionalities and why do they have the reputation of relatively unstable functionalities. Formation of a parent ortho-acetate and its hemi-ester precursor in the reaction of methanol with acetic acid and methyl acetate illustrate that the origin of ortho-ester instability is mostly entropic (Figure 147).
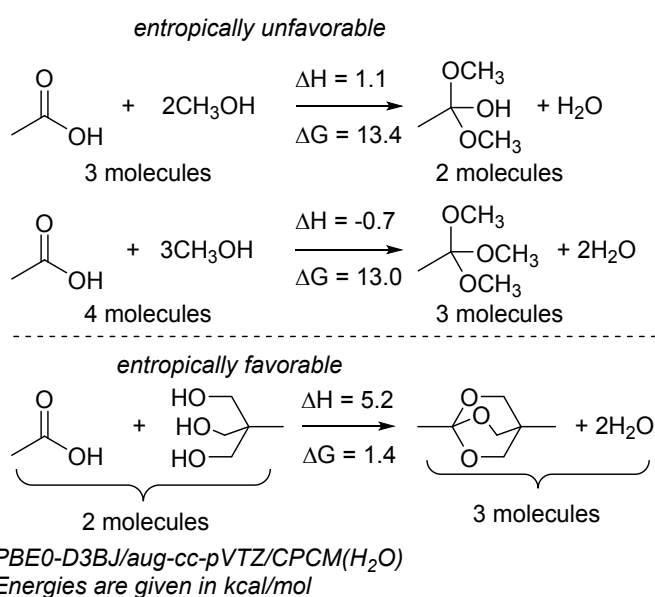
Figure 147. Thermodynamics of acyclic and bicyclic ortho-acetate formation from acetic acid and methyl acetate in reactions with methanol and a branched triol (2-(hydroxymethyl)-2-methylpropane-1,3-diol).

Importantly, the ΔH values for the reactions with MeOH in Figure 147 are close to zero, indicating that the combination of steric and electronic factors present in a carboxylic acid and an ortho-ester provide similar stabilization to these two functionalities. Furthermore, if one accepts that the carboxylic acid to be less sterically hindered, the nearly identical ΔH values suggest that *electronically* ortho-esters are stabilized *more* than carboxylic acids. The real reason why the equilibrium with acids or esters disfavors ortho-esters is not enthalpic. As the formation of acyclic ortho-esters decreases number of molecules in solution, the Gibbs free energy for their formation is raised by the entropic penalty, rendering the overall process thermodynamically uphill. Shifting this unfavorable equilibrium by removing water allows to prepare the high energy ortho-esters. Interestingly, ortho-ester forming reactions with methyl acetate are ~ 5 kcal/mol more endergonic than similar reactions with acetic acid.

On the other hand, the formation of cyclic orthoesters is free of the entropic penalty and thermodynamics of their formation is more favorable. For a bicyclic orthoester, the entropy of formation is sufficiently favorable to mostly offset a slight increase in the ΔH. The latter may come from the penalty for distortions in these constrained and rigid bicyclic structures from the optimal geometries.

Ortho-esters are especially reactive under conditions that lead to the formation of electron-deficient species. This reactivity stems from the stabilization derived by the carbonium ion from the lone pairs of the two heteroatoms (X = a leaving group, Y and Z = O or N, Figure 148). Often, substitutions at such tri-substituted carbons proceed via dissociative, S_N1-like processes.[360] The key stereoelectronic feature of such processes is the increased efficiency of the departing C-X bond cleavage when the lone pairs of the remaining heteroatoms Y and Z reach antiperiplanarity to the leaving group X. For the case of two endocyclic donors (e.g., two oxygen atoms of 1,3-dioxane core), their cooperativity is assured if the exocyclic leaving group is axial. Facile ionization of such compounds yields cations that are sufficiently stable to be studied by X-ray crystallography.
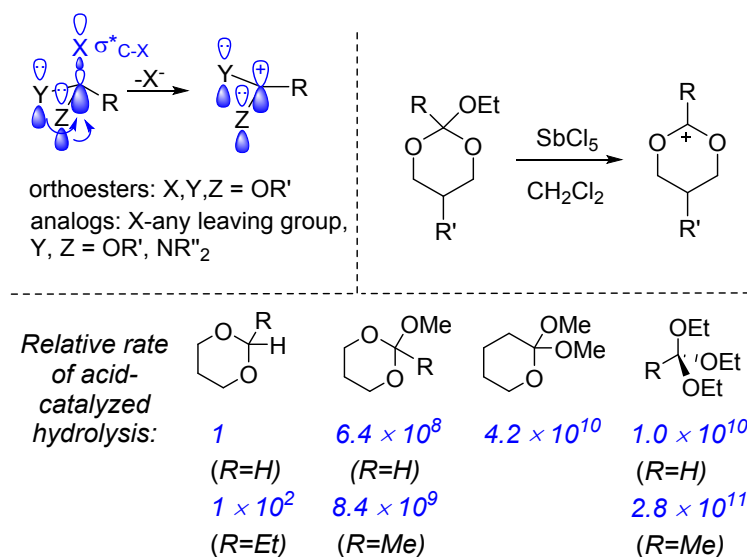
Figure 148. Top: Cooperative anomeric assistance to ionization of orthoesters and related compounds. Bottom: relative rates of hydrosylsis for selected acetals and ortho-esters

Hydrolysis of cyclic ortho-esters reveals additional stereoelectronic features that stem from cooperativity of individual anomeric interactions. A particularly detailed set of experimental results was provided by Deslongchamps and Dory.[361] Ortho-esters are hydrolyzed much faster than acetals. If one takes 1,3-dioxane and triethyl ortho-acetate, the two extremes in Figure 148, the difference in the rates of hydrolysis exceeds 10^{11}. Interestingly, the accelerating effects are greater when the OR groups are not confined in a cycle where the optimal orientation of the p-type lone pair and the leaving group is more difficult. Many subtle aspects of these processes have been thoroughly analyzed[255, 362] and will not be discussed here.

The acid-catalyzed exchange of orthoesters with a wide range of alcohols proceeds readily under mild conditions. A variety of tested acid catalysts gave rise to nearly identical product distributions (Figure 149). Under the influence of 1% of TFA in benzene, this metathesis reaction proceeded cleanly to a statistical product distribution within only one hour. These equilibration times establish orthoester exchange as a relatively fast dynamic covalent reaction.[363]
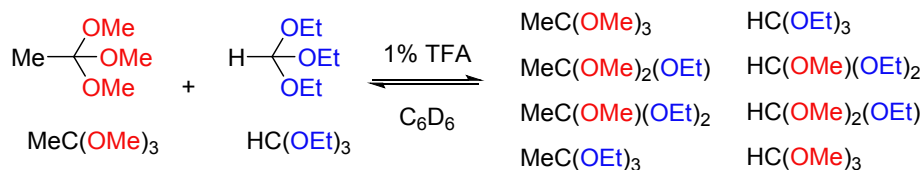
Figure 149. Mild exchange of alcohol groups in ortho-esters

The ability of ortho-esters to engage in reversible covalent reactions property accounts for their utility in dynamic covalent chemistry. In particular, the tripodal architecture of orthoesters suggests unique applications for the construction of dynamic polymers, porous materials and host–guest architectures (Figure 150).[364]
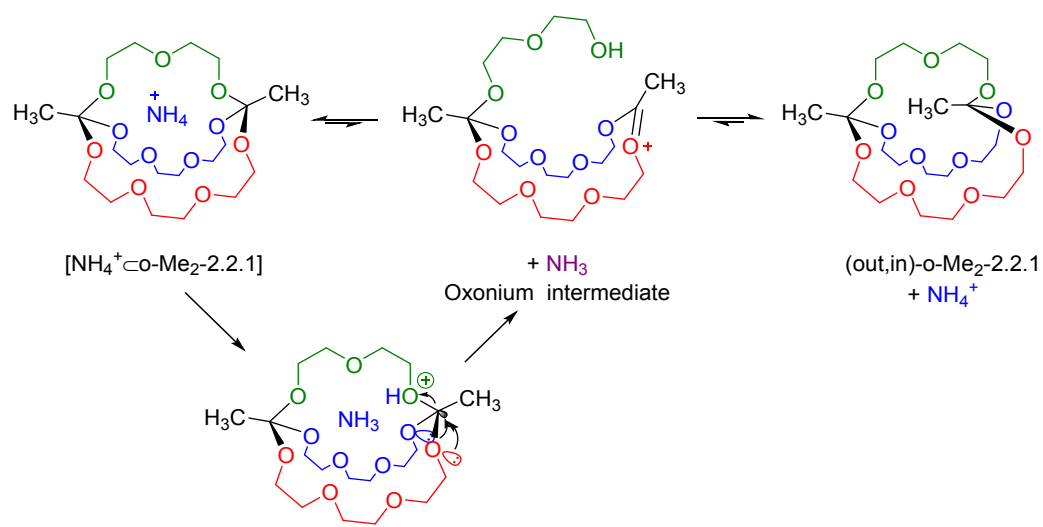
Figure 150. Inherently dynamic and adaptive host-guest system bearing orthoester moiety

von Delius and co-workers reported the preparation of a small organic cage through reversible covalent reactions starting from ortho-esters. Interestingly, these structures can be formed without the templating effect of a metal cation. X-ray crystallographic data found the "in,in"-conformation stabilized by the two sets of intramolecular, four-center hydrogen bonds. In these unusual contacts, each of the electron-deficient ortho-ester C-H bonds interacts with the oxygens of the three ether bridges (Figure 151).[365] Comparison of average R–C–O–M torsion angles of orthoformate and orthoacetate cryptands in their Li- and Na-complexes reveals interesting differences which clearly have a stereoelectronic origin. The average torsion angles in the orthoformate cryptands are significantly smaller (~150-170 degrees) than in the orthoacetate cryptands (narrow distribution around 180 degrees). As the result of this preference, orthoacetate cages are effectively larger and more rigid than orthoformate cages which explains the observed cation selectivity. The origin of this difference awaits theoretical analysis.

DEG= Diethylene glycol
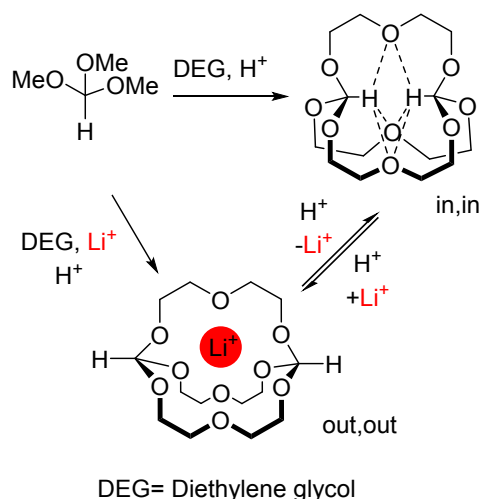
Figure 151. Synthesis of Li⁺-templated out,out-cryptand and self-templated in,in-cryptand orthoformate cryptands and their interconversion by dynamic bridgehead inversion.

Conversion of a carboxylic acid to an orthoester provides protection toward nucleophiles and strong bases. Interestingly, bicyclic orthoesters have greater stability, possibly due to geometric constraints on the anomeric assistance in the transition states for their reactions.[366]

The bicyclic OBO protecting group (4-methyl-2,6,7-trioxa-bicyclo[2.2.2]octan-1-yl) was developed by Corey.[367] It is formed by the action of (3-methyloxetan-3-yl)methanol on activated carboxylic acids in the presence of Lewis acids. The group is base stable and can be cleaved in two steps under mild conditions – first into an ester under mildly acidic hydrolysis and then disassembled completely in an aqueous carbonate. The addition of gem-dimethyl substitution to the oxetane precursor of [2.2.2]-bicyclic OBO orthoester significantly accelerates the orthoester formation and increases its resistance to hydrolysis. NMR kinetics show the DMOBO protecting group is formed 85 times faster than the OBO group, and is 36 times more stable toward aqueous hydrolysis.[366] The faster cyclization may be attributed to the gem-dimethyl effect but the stereoelectronic reasons for the slow hydrolysis are so far unknown. The situation here is likely to be interesting due to the unusual boat conformation imposed by the bicyclic [2.2.2] structure and due to the cooperativity of the six $n_O{\rightarrow}\sigma^*_{C\text{-}O}$ interactions in these systems, where each lone pair is aligned with the two endocyclic C-O bonds (Figure 152). When one of the oxygens is protonated under acidic conditions, two of the six $n_O{\rightarrow}\sigma^*_{C\text{-}O}$ anomeric interactions are amplified to facilitate the first ring opening. The intermediate cyclic dioxacarbenium ion can be trapped with water to generate another anomerically activated hemi-orthoester intermediate that can undergo the second ring opening. The mono-ester of tris(hydroxymethyl)ethane is relatively stable under the acidic conditions but can be hydrolyzed further into the fully deprotected carboxylic acid in base.
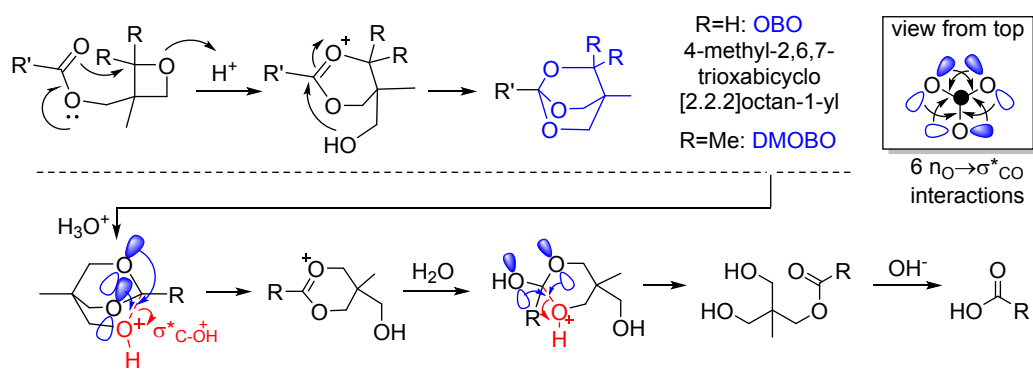
Figure 152. OBO and DMBO orthoester formation and hydrolysis involve multiple anomeric interactions

Anionic or cationic analogues of ortho-esters are also formed transiently as tetrahedral intermediates (TIs) in the process of carboxylic acid derivatives reacting with O-centered nucleophiles (Figure 153). These species feature in a complex network of coexisting stereoelectronic interactions. Untangling this network would be a long exercise that we will not pursue here. Furthermore, the anomeric network in the Tis is difficult to study experimentally because TIs are transient and rarely isolated. However, it is clear that all three interactions contribute to the negative charge delocalization and stabilize this transient structure.
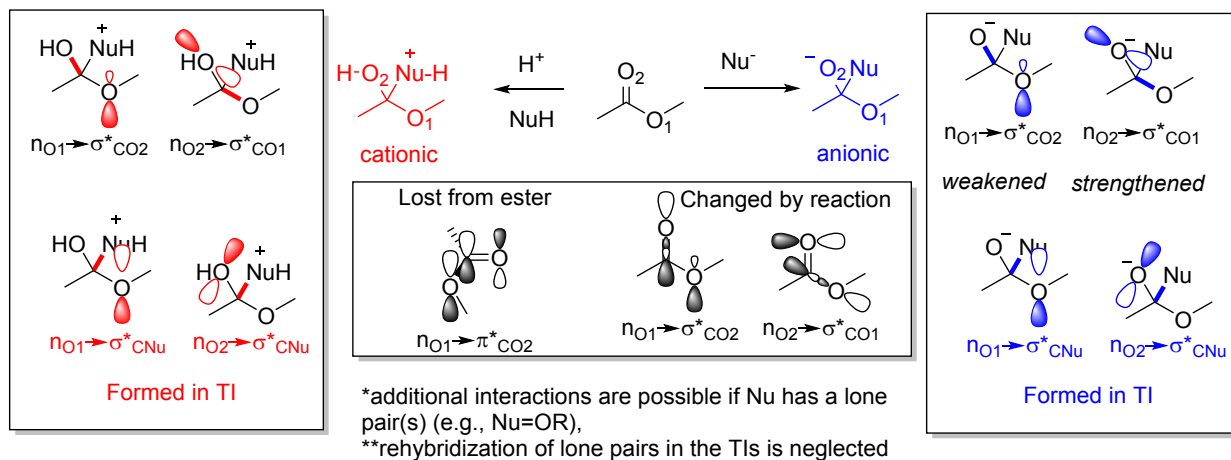
Figure 153. Selected anomeric effects that are important in a typical nucleophilic substitution reaction in a carboxylic ester derivative

For example, let's consider just one part of the network—hyperconjugative donation from the carbonyl oxygen and how it evolves along the reaction path for reaction of an anionic nucleophile (Nu) with a generic carboxylic acid derivative. In the starting material, the effect is manifested as a strong $n_O \rightarrow \sigma^*_{C-LG}$ interaction (where LG is a leaving group) while in the product it is present as a $n_O \rightarrow \sigma^*_{C-Nu}$ interaction (where Nu is the nucleophile, Figure 154). The interesting part is the intermediate stage in this process. The anionic tetrahedral intermediate (TI) is stabilized by *both* of the above interactions, $n_O \rightarrow \sigma^*_{C-LG}$ *and a*

$n_O{\rightarrow}\sigma^*_{C\text{-}Nu}$. Such "double anomeric effect" is a crucial component in making nucleophilic substitution at the carboxylic acid derivatives a fast process.

The evolution of anomeric effects at the carbonyl oxygen

the overall effect may be complex
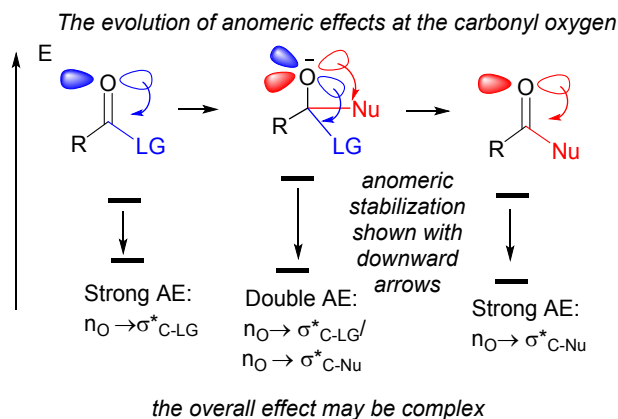
Figure 154. The evolution of anomeric effects in an anionic nucleophilic substitution reaction at a carboxylic ester derivative. Note that two anomeric interactions combine in a synergistic way to stabilize the tetrahedral intermediate

The pronounced acidity increase in the methanol<methanediol<methanetriol sequence (~ 9 kcal/mol for each new gem-OH group) can be attributed to the increased stabilization of conjugate base by $n_O{\rightarrow}\sigma^*_{CO}$ interactions where the donor oxygen is anionic (Figure 155).

PBE0-D3BJ/aug-cc-pVTZ/CPCM(H_2O), kcal/mol
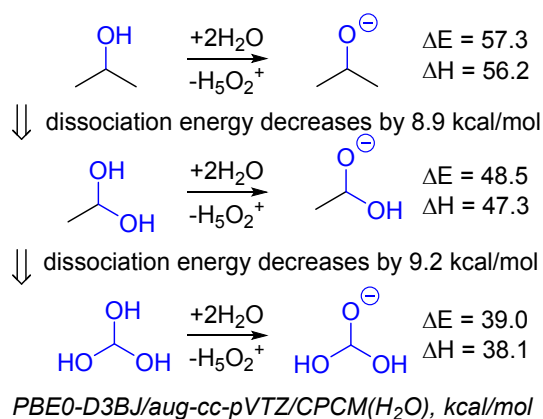
Figure 155. The calculated difference in the OH acidities of alcohols, gem-diols, and gem-triols using the $ROH + 2H_2O \rightarrow RO^- + H_5O_2^+$ reaction

Some of the deprotonated ortho-ester analogs are quite stable as illustrated by structure of Tetrodotoxin, a neurotoxin found in many pufferfish species considered a delicacy in many countries around the world, especially Japan. The toxicity of the TTX originates in its binding to the sodium channels and blocking the ions from passing the cellular membrane.[368]

Tetrodotoxin is a marvel of molecular architecture - an incredible zwitter-ionic dioxaadamantane structure, densely functionalized with heteroatoms (11 heterotoms for 11 carbons).[369] The charges are separated in two halves of the molecule – the oxygen-rich part is negatively charged while the nitrogen-rich structure is positively charged. Interestingly, the opposite charges are stabilized in a conceptually similar way via cooperative donor-acceptor interactions with participation of heteroatom lone pairs: the negative charge in the oxygen-rich part is stabilized by two sigma acceptors ($n_O{\rightarrow}\sigma^*_{CO}$ interactions) while the positive charge in the nitrogen-rich part is stabilized by three p-donors ($n_N{\rightarrow}p_{C+}$ interactions). The high stabilization is negative charge is illustrated by the fact that Tetrodotoxin is only weakly basic, despite having an anionic center. Tetrodotoxin is clearly a highly stabilized version of tetrahedral intermediate for an alkoxide addition to an ester. The equilibrium is shifted from the ester to the hemilactal for two reasons: a) the compromised anomeric stabilization of the cyclic esters (discussed above) and b) the preorganized cyclic nature of this molecule that greatly alleviates the entropic penalty that would be significant for an intermolecular nucleophilic addition (Figure 156).
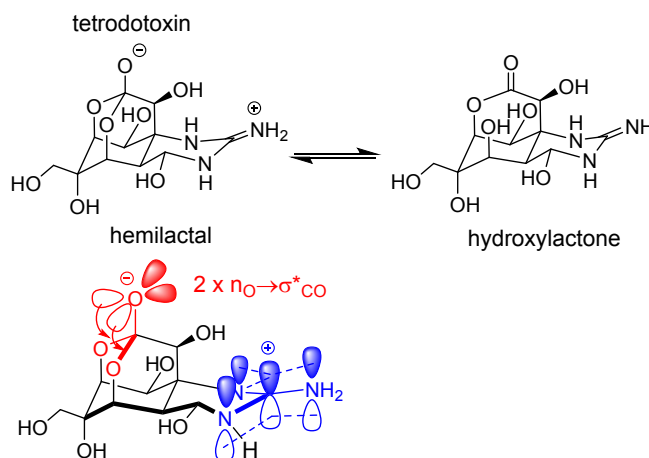
Figure 156. Synergy between $n_O{\rightarrow}\sigma^*_{CO}$ and $n_N{\rightarrow}p_{C+}$ interactions in stabilizing the negatively and positively charged centers of tetrodotoxin

In intermolecular ester hydrolysis, the tetrahedral intermediate is ~ 11 kcal/mol less stable than the ester.[370] Therefore, it is generally a transient intermediate present in low concentrations. However, this situation can change as illustrated by hydrolysis of the ester group in neurotransmitter acetylcholine (ACh) by enzyme acetylcholinesterase (AChE), a process of great importance for deactivation of firing neurons in many organisms. ACh is a neurotransmitter whose action at the synaptic cleft is terminated by the hydrolyzing action of AChE. This process is essential for preventing constant stimulation of the post-synaptic membrane and an excessive firing of neurons. Interfering with this process is associated with the mechanism of action of nerve gases and related chemical warfare.

AChE is noted for its very high catalytic activity. The k_{cat} values of $\sim 10^4$ s^{-1} exceed the rate constant for non-enzymatic hydrolysis of ACh by 13-14 orders of magnitude, which corresponds to 18-19 kcal/ mol of transition state stabilization. It was shown that formation and stabilization of the tetrahedral intermediate is an essential step of the two-step hydrolysis mechanism. Tormos et al. provided strong evidence that the tetrahedral intermediate is the accumulating reactant state.[370] In particular, the markedly normal isotope effect on k_{cat} is consistent with hybridization change from sp^3 toward sp^2, i.e. the tetrahedral intermediate collapse to form the products of hydrolysis. A remarkable conclusion is that the tetrahedral intermediate in the AChE-catalyzed hydrolysis of Ach is stabilized by at least 11 kcal/mol or more[371] and that the stabilization of the tetrahedral intermediate is a large fraction of the catalytic transition state stabilization.

So how is the TI stabilized? As we discussed above, the double anomeric $n_O \rightarrow \sigma^*_{CO}$ interactions in the conjugate base render the OH group quite acidic. Alternatively, one can say that these intramolecular interactions intrinsically stabilize the anionic form (i.e., the conjugate base) of the tetrahedral intermediate which is the species formed inside the enzyme cavity after intermolecular attack of the adjacent serine OH group at the acetyl moiety of AChe. Furthermore, the strategically placed H-bonding N-H groups engage the TI in three H-bonds: two with the newly formed anionic center and one with the O-atom from the nucleophilic serine moiety (note that this oxygen also gets a significant share of the negative charge through the same $n_O \rightarrow \sigma^*_{CO}$ interaction) (Figure 157). Such very strong H-bonded networks, which has evolved for stabilizing transition states structurally close to the tetrahedral intermediates, are common in enzyme catalysis and often referred to in biochemistry as the "oxyanion holes".[372]
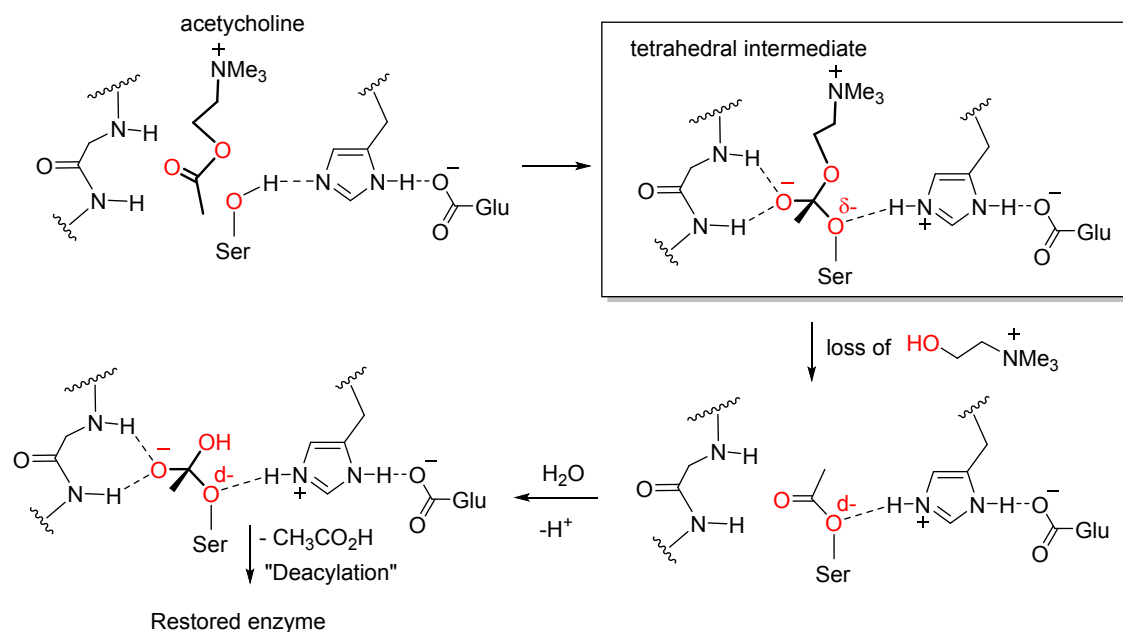
Figure 157. The key steps in enzyme-catalyzed hydrolysis of acetylcholine involve the formation of anionic tetrahedral intermediates.

In the second step, i.e., "deacylation", an external nucleophile (usually water) attacks the acylated serine moiety with the formation of another TI that proceeds to form acetic acid and restored enzyme active site.

Furthermore, the importance of TI in the mechanism of the ACh hydrolysis is connected to the inhibition of AChE by the organophosphorus nerve agents such as sarin.[373] Sarin reacts with AChE via attack at the active site serine with the formation of an initial neutral adduct at phosphorus, resembling the tetrahedral intermediate of the ACh hydrolysis. Although the initial adduct is unreactive toward spontaneous hydrolysis (Nu: = H_2O), it can be dephosphorylated by reactive oxime nucleophiles, such as 2-pyridinealdoxime methiodide (2-PAM) (Nu: = ArCH=NOH) or related compounds.[374-379] Unfortunately, the initial neutral adduct may convert into a monoanionic adduct via a dealkylation reaction ("aging"). The aged adduct is remarkably unreactive and resists reactivation.

Why is aged AChE so difficult to reactivate? The secret behind the unreactivity of aged AChE toward methylation with 2-methoxy-1-methylpyridinium reagents again lies in the fact that the aged adduct is a close structural analog of the TI and the TS that connects the TI to deacylated ACh. In this case, stabilization of the TI is counterproductive since it interferes with "rescuing" and reactivating the enzyme. Interestingly, stabilization of the anionic phosphorus-analog of the TI in aged AChE is derived, to a significant extent, from the anomeric effect of phosphorus which involves two lone pairs of each of the monosubstituted oxygen atoms of the phosphoryl moiety with a suitably oriented σ^*_{P-O} orbital (Figure

158). Manifestations of anomeric effect in chemistry of phosphorus have many other interesting biological implications.[380]
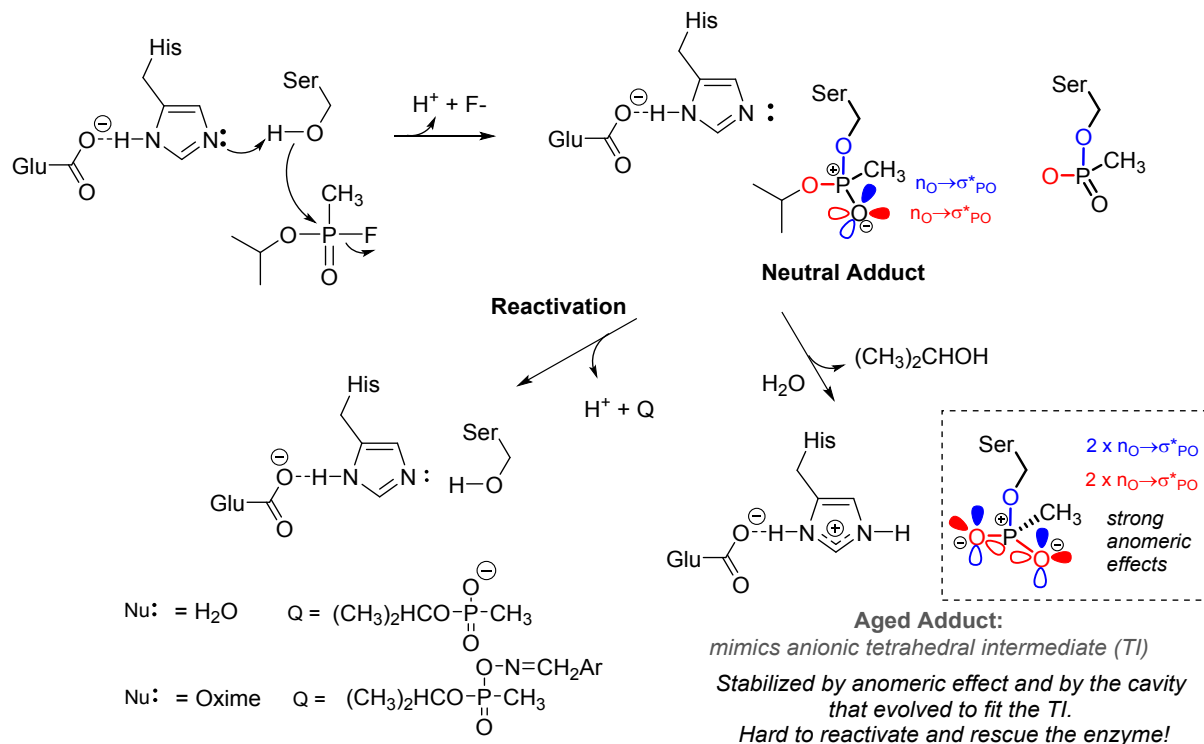
Figure 158. Inhibition of AChE by the organophosphorus nerve agent sarin. Both the initially formed and especially the aged adduct mimic the tetrahedral intermediate for the AChe deacylation.

The catalytic pathways of serine, cysteine, and threonine proteases all involve formation and stabilization of a tetrahedral intermediate shown below. This stabilization is an important element in overcoming the kinetic stability of the peptides in enzyme catalysis. Fortunately for the protein-based life forms, the non-catalyzed hydrolysis of a peptide bond is extremely slow. To break such inert bonds, the active site residues of serine, cysteine, and threonine proteases have an active site nucleophile and a basic residue ready to orchestrate the nucleophilic attack at the targeted peptide unit along with a supplementary network of H-bonds that can stabilize the intermediate TI and its connected transition states (Figure 159). Understanding the nature of TI stabilization is essential for the design of TS-mimicking inhibitors of such enzymes as illustrated by the search of drugs targeting the main protease of SARS-CoV-2.[381, 382]
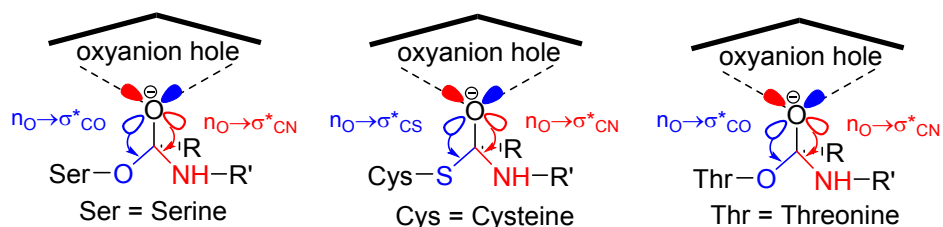
Figure 159. Anomeric stabilization in tetrahedral intermediates that can mimic the transition states for the hydrolysis of peptide bonds by serine, cysteine, and threonine proteases

This amplification of anomeric effects is one of the factors that needs to be considered for understanding the role of "oxyanionic holes" in enzyme catalysis. The preferred H-bonding in oxyanion holes is very different from the common H-bonding with small molecules found in the Cambridge Structural Database.[383, 384] As reactant stabilization is counterproductive and has to be compensated by an even greater stabilization of the TS, the enzyme active sites do not have optimal H-bonding for the reactant molecules but rather evolved to minimize the barrier for the reaction.

To avoid the unproductive reactant stabilization, enzymes arrange their hydrogen bonds so that H-bond donors coordinate at the carbonyl π-bond instead of the oxygen lone pair. Goodman and coworkers coined a term "grand jete"[383, 384] to distinguish such twisted H-bonded complexes from the more common flat H-bonded structures with carbonyls (Figure 160). A flat structure is reminiscent of Leonardo da Vinci's Vetruvian Man whereas the twisted one is similar to the long jump ("grand jeté") in ballet where the dancer extends his/her arms in a perpendicular position to his/her legs.

At the "grand jeté" geometry, stabilization of the reactant is relatively small whereas stabilization of the TS is noticeably increased because the anionic oxygen in the TS and the product is a better partner for an H-bond. An interesting connection of this H-bonding pattern with the anomeric effect becomes obvious is one considers the product of the nucleophilic addition to the carbonyl. The anomeric $n_O \rightarrow \sigma^*_{C\text{-}Nu}$ interaction between the newly formed C-Nu bond and the p-lone pair at anionic oxygen weakens the C-Nu bond and can promote its fragmentation. In order to avoid the unproductive C-Nu bond cleavage and move the reaction forward, it would be helpful to make the anomeric $n_O \rightarrow \sigma^*_{C\text{-}Nu}$ interaction weaker. However, the anomeric interaction is stabilizing and removing it would make the barrier for the C-Nu bond formation higher as well. A way to address these conflicting requirements is to involve a 2nd interaction that can provide an alternative compensating stabilization source to the TS while making the anomeric donation weaker. The "grand jeté" H-bond is such interaction. It engages the exact lone pair that participates in the $n_O \rightarrow \sigma^*_{C\text{-}Nu}$ interaction and hence makes the anomeric effect weaker (moderates it)

while compensating for the loss of stabilization. This H-bonding describes the tug-of-war between intermolecular ($n_O \rightarrow \sigma^*_{H-X}$) and intramolecular ($n_O \rightarrow \sigma^*_{C-Nu}$) delocalization of the anionic lone pair of oxygen.
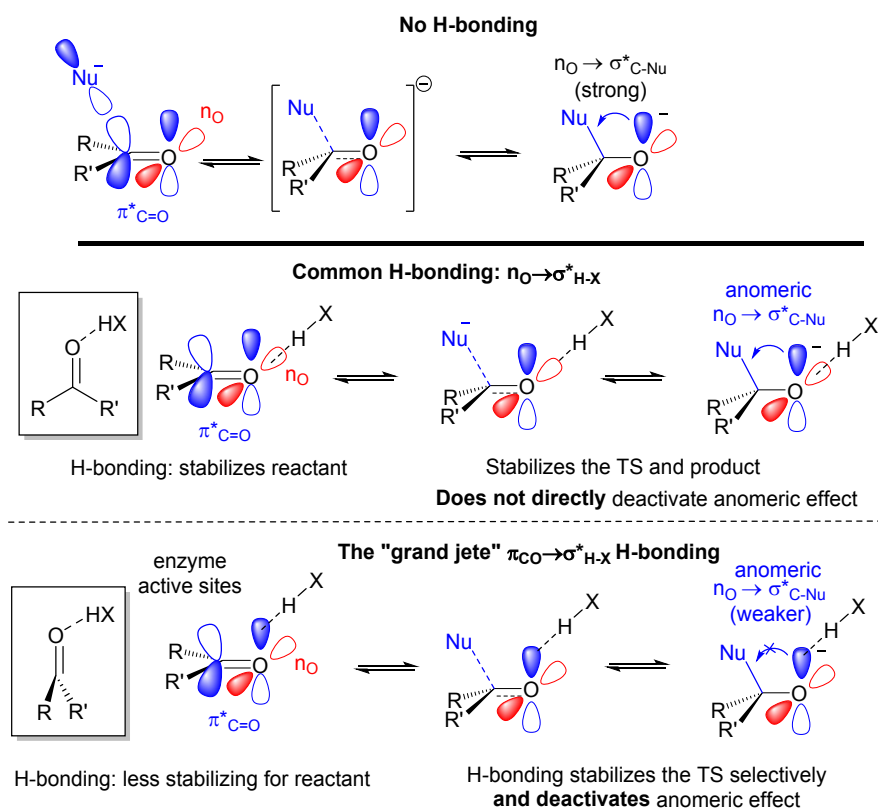
Figure 160. The role of anomeric effect in unusual H-bonding preferences in oxyanion holes

The above example illustrates how additional design opportunities can arise from the combination of the several factors. In the following section, we will expand this discussion to additional systems where multiple stereoelectronic effects have to coexist in the same molecule. Here, our focus will change from the individual functional groups to the logical connections *between* the groups.

"When anomeric effects collide": cooperative and anticooperative patterns

Figure 161 describes a number of possible ways for several donors and/or several acceptors to interact with each other. Sometimes, these interactions are cooperative and reenforce each other; sometimes they "collide".[385] It is not our goal to provide an exhaustive list of many possible manifestations of such patterns but we hope that the selection provided below will be instructive.
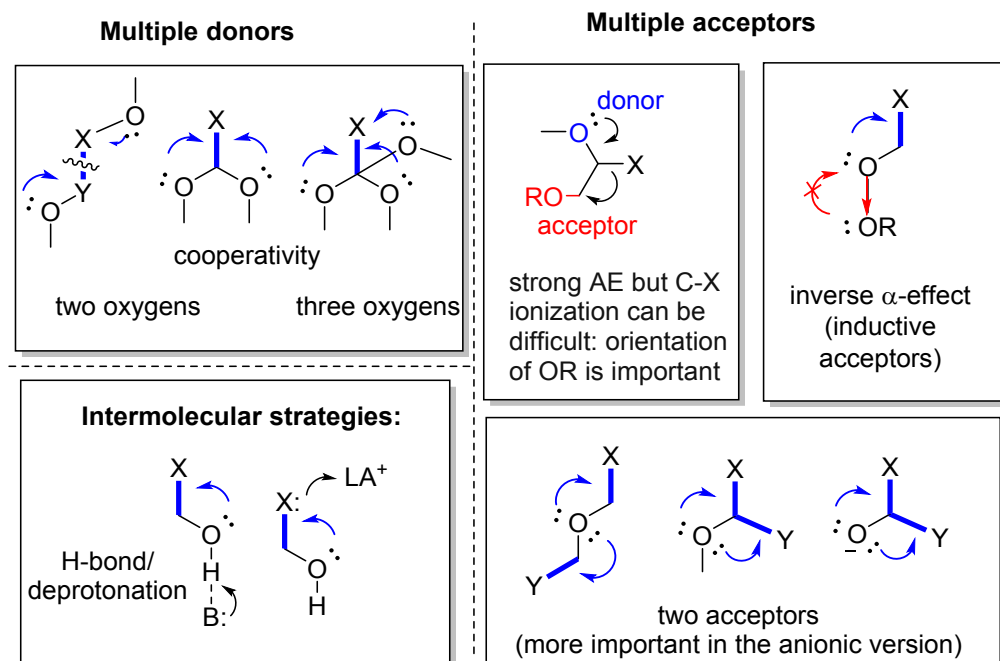
Figure 161. Selected orbital patterns for the interplay of several anomeric interactions or interplay of anomeric interactions with other effects

From our previous discussions, it is already clear that anomeric interactions often come in pairs (e.g., the endo- and exo-anomeric effects) when both heteroatoms X and Y in an X-CH$_2$-Y moiety have a lone pair that can interact with an appropriate σ* C-Y (or C-X) acceptor. So, the "two donors/two acceptors" situation is typical. In the next sections, we discuss more unusual situations – a) a variation of the two donor/two acceptor system when both donor orbitals are the same atom (i.e., the double anomeric effect in oxyanionic systems), and b) the case of two donors donating to one acceptor. Such systems are interesting because the joint effect of multiple interactions can unlock unusual reactivity. In this part, we will keep the discussion simple by limiting ourselves to groups of no more than three participating orbitals.

How to keep anomeric effect under control: interplay with other stereoelectronic interactions

The idea that anomeric effect weakening can be used to stop chemical reactions is useful when selectivity is important. Below, we will illustrate how it applies to chemistry of carbohydrates.

Cooperativity/competition among acceptors (armed/disarmed carbohydrates): Cleavage of the C-X bond at the anomeric position proceeds via evolution of the anomeric $n_O \rightarrow \sigma$*C-X interaction that culminates in the formation of oxocarbenium ion. Although such carbocations are strongly stabilized and relatively easily to form, one has to *differentiate* the reactivity of two saccharides when designing a

selective cross-coupling glycosylation reaction. The competition and cooperativity between stereoelectronic effects can be used to fine-tune the reactivity of anomeric systems.

Substituents adjacent to the anomeric carbon can affect the conformational equilibrium. For example, the axial hydroxyl group at C(2) in D-mannopyranose increases the contribution of the axial conformer ("α-anomer") at the equilibrium in comparison to that in D-glucopyranose (69 vs. 36%, respectively).

An elegant approach to control reactivity in glycosides and related compounds for selective cross-couplings in oligosaccharide synthesis is based on "arming" or "disarming" of the anomeric reactants by structural modifications in the vicinity of the cationic center.[386, 387] For example, the presence of a β-OR substituent disfavors oxocarbenium formation. The destabilization imposed on the cationic intermediate by an ester (R=COR) is much larger than the destabilization imposed by an ether (R=alkyl, benzyl) (Figure 162). Disfavored oxacarbenium formation by the stronger acceptor, i.e. the ester group, "disarms" the sugar.

Figure 162. Glycosides can be disarmed by adding a competing stereoelectronic effect to destabilize the cationic intermediate. The stronger OBz-acceptor deactivates the anomeric position to a larger extent.

Fraser-Reid and co-workers applied this concept in the one-pot di- and trisaccharide synthesis outlined in Figure 163. The armed OBn-substrate is considerably more reactive and can be chemoselectively activated in the presence of the OBz-sugar. Hence, the reaction of an armed glycoside with a disarmed glycoside (deprotected at one of the hydroxyls) can lead exclusively to the desired heterocoupling of the two glycosides with no need for an intermediate purification and deprotection steps. The high selectivity of activation is based on balancing the anomeric effect by an electronic effect of opposite direction. Presence of a more electron deficient benzoyl substituent "disarms" the anomeric position by making the formation of electrophilic oxacarbenum ion more difficult. This is an example of the "stereoelectronic chameleonism"[34] of oxygen (donor at the α-position and acceptor at the β-position relative to the developing cationic center).
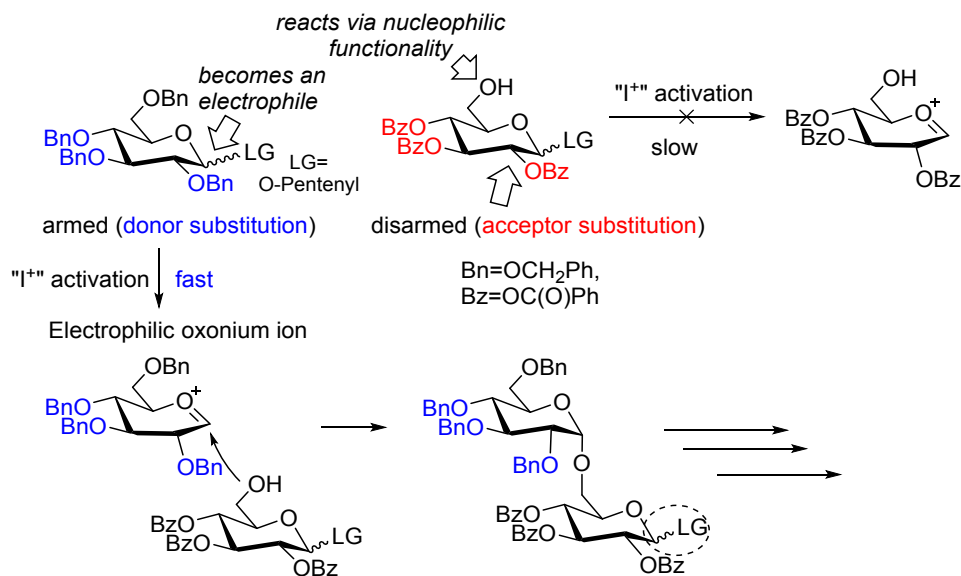
Figure 163. Application of armed/disarmed substrates for selective one-pot synthesis of di- and trisaccharides.

The stereoelectronic interplay of anomeric activation at an α-position with an effect of a β-acceptor is illustrated by effects of fluorinated substituents on hydrolytic stability of Thromboxane A2 (TxA2) analogs. TxA2 is a strained acetal produced enzymatically from arachidonic acid in response to tissue injury. Because the study of TxA2 has been limited by its high instability ($t_{1/2}$ = 32 s, pH = 7.4), the much higher stability of the difluoro analogue ($t_{1/2}$ > 30 days, pH = 7.4) was very interesting.[388] Recently, Aggarwal and coworkers evaluated the stereoelectronic aspects of this stabilization by comparing stability of the α-F vs. β-F isomers of the monofluoro analog of TxA2.[389] The difference between hydrolyitic stability of the two isomers is dramatic: the α-F isomer, having a better σ-donor (C–H vs. C–F bond) aligned with the incipient oxocarbenium ion, has the $t_{1/2}$ of ~ 15 h, whereas the β-F isomer has the $t_{1/2}$ of >30 days (both at pH = 7.4). This stereoelectronic penalty was estimated to be ca. 5 kcal/mol from DFT calculations for the two oxarbenium ions formed from a model substrate (Figure 164).
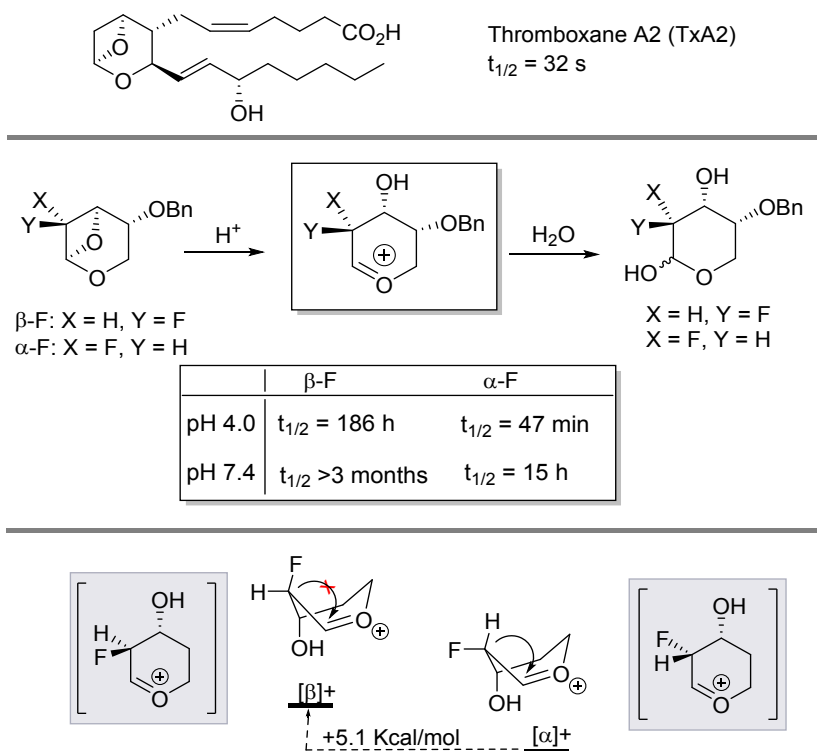
Figure 164. Hydrolysis of model compounds related to Thromboxane A2 (TxA2) reveals remote stereoelectronic effects that can counter-balance the effect of anomeric activation

The cationic reactions of orthoesters are initiated quickly and under relatively mild conditions.[390] For example, *myo*-inositol 1,3,5-orthoformates are converted in dioxacarbenium ions within minutes in a 10:1 TFA:water mixture at room temperature. It is interesting that out of the three geminal C-O bonds of the orthoformate moiety, the C-O bond scission involves the most electron deficient of the three orthoformate axial oxygens, i.e. the oxygen of the C-O bond with the *two* antiperiplanar vicinal C-OH bonds at the adjacent axial positions (Figure 165).
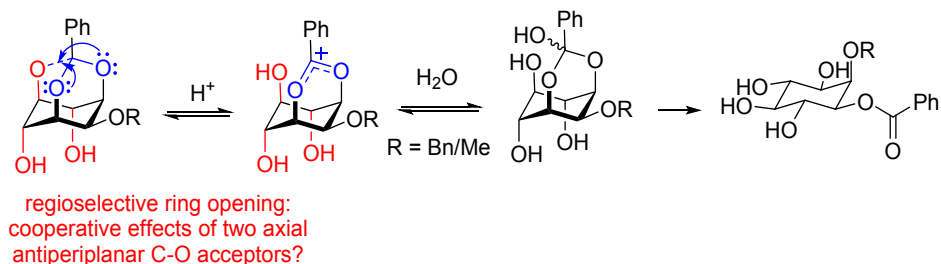
Figure 165. Regioselective formation of cationic intermediates from orthoesters can originate from cooperative stereoelectronic interactions.

Making anomeric effect stronger by using cooperativity:

Cooperative effects of two donor oxygens:

Oxygens are at the opposite ends of the breaking bond. The bis-anionic oxy-Cope[391, 392] rearrangement of bis-alkynes produced by the reaction of acetylides with ethane-1,2-dione (benzyl) occurs below room temperature (Figure 166).[393] Computational studies confirm a significant barrier decrease for the rearrangement where the central C-C bond is weakened by the four radical stabilizing groups (Ph and O⁻). Interestingly, the two deprotonations decrease the barrier considerably more (15-16 kcal/mol) than the two Ph groups (~12 kcal/mol barrier lowering). As a result, the calculated Cope rearrangement barrier falls from >30 to ~5 kcal/mol. The rearrangement is completed by an electrocyclic ring closure of the bis-allenic Cope-product or its intramolecular aldol condensation (not shown). The processes are fast and proceed below room temperature even though the Li-alkoxides are involved. The central C-C bond is weakened so much that the Cope rearrangements becomes a dissociative process [394-396] where the central C-C bond scission is greatly advanced at the early reaction stage before the new C-C bond forms. Indeed, the fragmentation products were observed in the presence of bulky TIPS substituents at the alkyne termini.
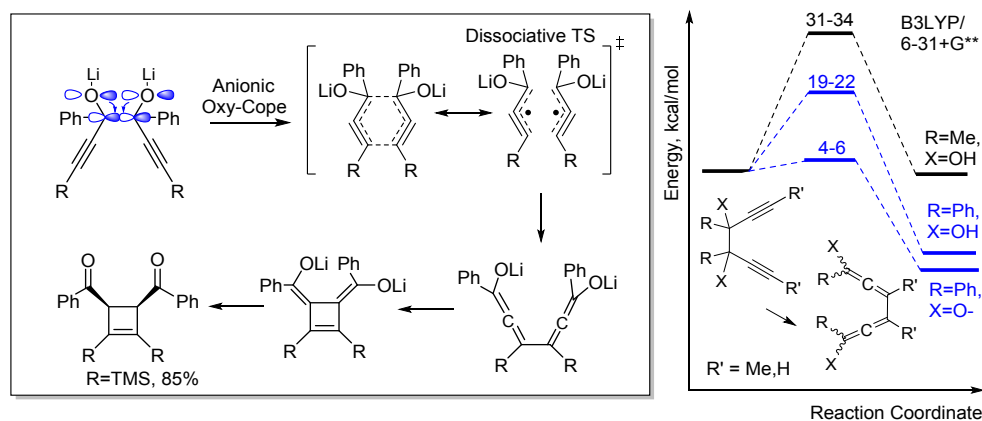
Figure 166. Increased donor ability of anionic oxygen dramatically accelerates the oxy-Cope rearrangement of bis-alkynes.

Two oxygens connected to the same carbon atom at the breaking bond: Antiperiplanar Lone Pair Hypothesis (ALPH) theory.

The power of stereoelectronic effects can be amplified when more than one donor can interact with a single acceptor. A well-studied set of such anomeric systems involves orthoesters and other structures related to tetrahedral intermediates of nucleophilic reactions of carbonyls. For such systems, Deslongchamps introduced the "antiperiplanar lone pair" (ALP) model based on cooperativity of multiple

anomeric $n_O \rightarrow \sigma^*_{C-X}$ interactions.[28, 362] Herein, we will limit ourselves to only a relatively short discussion of this widely discussed concept[397, 398] using a simplified model (vide infra). For clarity, we will concentrate on the best donor (p-type lone pair) on oxygen instead of considering the two "rabbit ears" hybrid lone pairs in the original model. A corollary of this choice is that the notion of syn- and anti-periplanarity is not applicable anymore – as such notions only apply to σ-bonds and hybrid lone pairs. Because in p-type lone pairs the "syn"- and the "anti"-lobes are identical, one only needs to consider whether the acceptor orbital and the p-lone pair are aligned (parallel) or misaligned (not parallel) if the p-lone pairs of oxygen are considered as the first stereoelectronic approximation.

This model is illustrated below using the chair geometry of tetrahydropyran. In short, heterolysis of an anomeric C-X bond (or another reaction where this bond is cleaved with the development of a positive charge at the anomeric carbon) in this system was suggested to be accelerated when the endo-anomeric effect and the exo-anomeric effect can work together to weaken the axial C-X bond. Such double assistance for breaking the endocyclic C-O bond is only possible if there are two exocyclic substituents with the right conformation to place their lone pairs antiperiplanar to the endocyclic C-O bond (Figure 167).
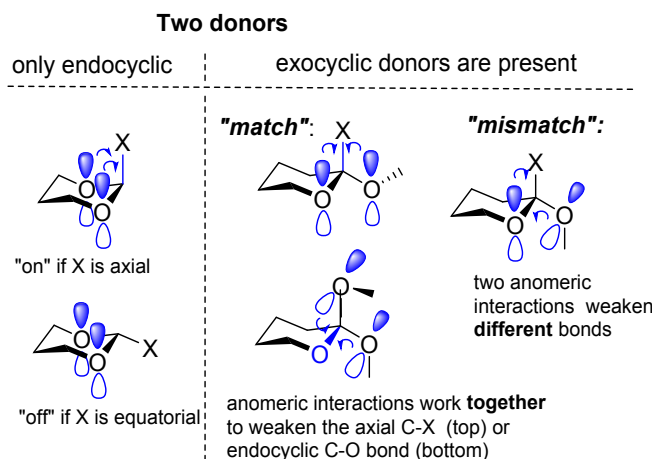
Figure 167. Several stereoelectronic scenarios can lead to cooperation, mismatch, or deactivation of the anomeric donations of two donors.

A more accurate treatment of such systems involves the interconversion of reactive and unreactive conformers as well as the evolution of stereoelectronic effects along the reaction pathways.[399] The critical examination of ALP theory by Perrin also suggested that the role of conformational equilibria of reactive species, the involvement of syn-periplanar lone pairs and different stability of products can be essential.[398] Nevertheless, the cooperative stereoelectronic effects, regulated by the relative orientation of the p-type lone pairs of the two oxygens in cyclic acetals, can be dramatic. For example, Deslongchamps and Li found

that, of the two epimeric cyclic acetals in Figure 168 left, only one is oxidized by ozone.[400] The reaction is only observed when lone pairs from *both* oxygen atoms can assist in the axial C-H bond oxidation. For the other bicyclic epimer, only the exocyclic oxygen can align its p-type lone pair with the C-H bond. A more detailed analysis of such effects is available in the classic book of Deslongchamps[362] and a more recent review.[401]
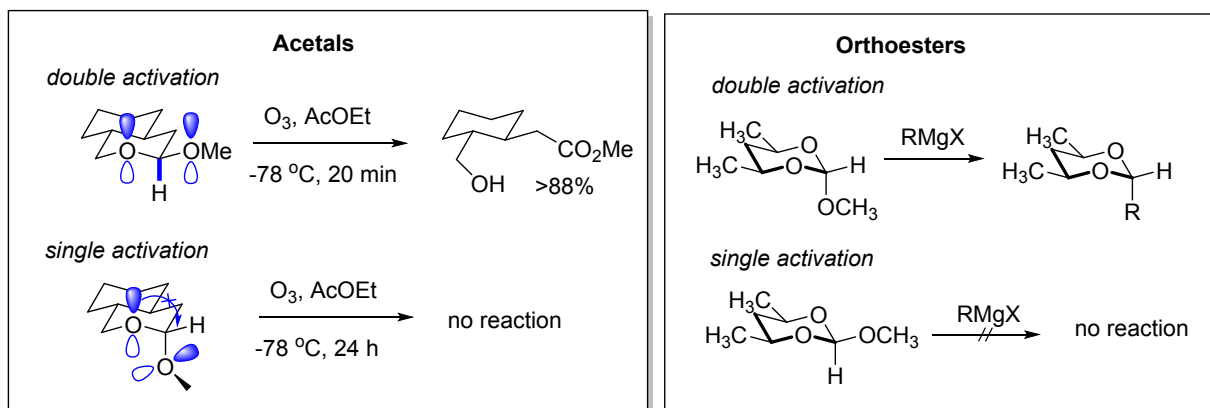
Figure 168. Double activation by using cooperativity of donors at the anomeric position in acetals (left) and orthoesters (right).

Analogously, orthoesters in the conformationally constrained 1,3-dioxane systems show a striking preference for cleavage of an axial exocyclic C-O bond compared to an equatorial C-O bond (Figure 168 right).[402, 403]

Only the axial 2-methoxy- 1,3-dioxane reacts with Grignard reagents whereas the equatorial isomer was unreactive. These difference in reactivity and the observed retention of configuration were suggested to stem from assistance by the lone-pair orbitals on the ring oxygens to both the C-O bond scission and C-R bond formation.

The accelerating effect of anionic oxygens on C-C and C-H bond activation applies to a variety of other processes. For example, in the benzilic acid (and benzilic ester) rearrangement—recently used for the synthesis of (-)-taiwaniaquinone H[404] and preuisolactone A[405] —the lone pairs on the oxygen atoms in the tetrahedral intermediate donate electron density into the antibonding σ^*_{CC} orbital. This donation weakens the C-C bond and allows the group to shift to the adjacent carbonyl. Similar anomeric interactions assist in the Cannizzaro reaction by converting the C-H into a formal hydride source to reduce a second molecule of aldehyde.[406] In each of these processes, the interaction with the oxygen lone pairs stabilizes the positive charge being formed.
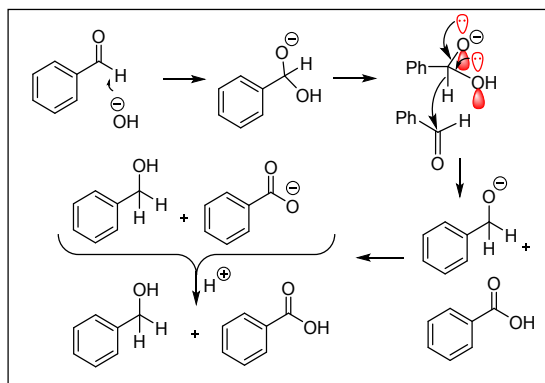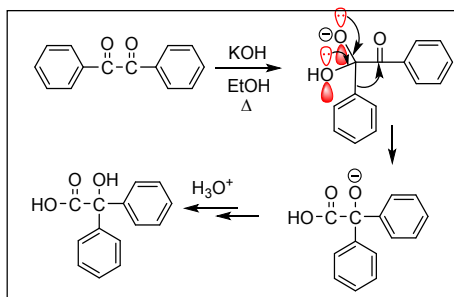
Figure 169. Anomeric assistance leads to hydride transfer in the Cannizzaro reaction (left) and the formal phenyl anion shift in benzilic acid rearrangement (right).

Double anomeric effects: donation of anionic oxygen to two σ-acceptors:

The effect of spectator groups in phosphate hydrolysis indicate that the p-type lone pairs at a negatively charged oxygen can interact with the suitably positioned σ-acceptors, potentially creating the possibility of two mutually orthogonal anomeric interactions (Figure 170). The two effects can explain several interesting features of phosphate chemistry, e.g., why and how the non-leaving groups at the P atom can strongly affect hydrolysis of phosphate triesters. Both experimental and computational data suggest that an increase in the electron-withdrawing ability of the "spectator" groups can accelerate the reaction by many orders of magnitude. For example, change from Me to CH_2CF_3 decreases experimental free energy of activation by ~ 5 kcal/mol.[407]

R	Exp.	Calc.
CH_3	24.8	26.2
CH_2CF_3	29.6	30.0
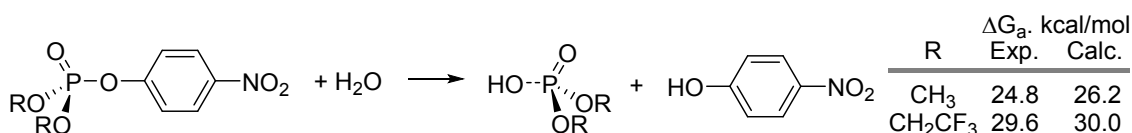
Phosphorane or related substitution TS:

equatorial groups in black
apical groups in blue

with apical σ*-orbitals

anomeric effect assists in C-Nu bond formation and C-LG bond scission

⇓
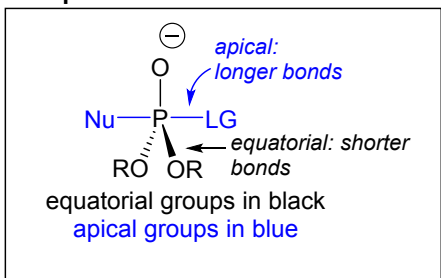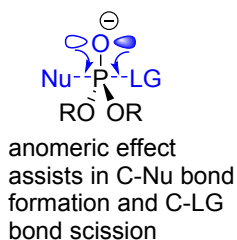
Effect of leaving groups

with equatorial σ*-orbitals

"orthogonal" anomeric effect stabilizes the hypervalent intermediate and the TS by donation to $σ*_{P-OR}$ orbitals

⇓
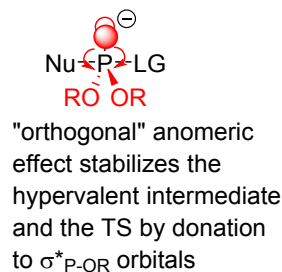
Effect of non-leaving groups

Figure 170. Top: Comparison of the rates of spontaneous hydrolysis of 4-nitrophenyl dialkyl triesters with the alkyl groups of different acceptor ability. Bottom: Cooperation of two anomeric effects in hydrolysis of phosphate triesters.

The interplay between the two anomeric effects has other consequences in chemistry of pentacoordinated phosphorus. For example, acidity of apical and equatorial OH bonds is known to be different and to correlate with the lengths of the apical (longer) and equatorial (shorter) C–OP bonds.[408] The differences between the two types of OH groups are remarkably large (the pK_a values of 13.5 ± 1.5 and 8.6 ± 1.9, respectively) in hydroxyphosphoranes (Figure 171). This structural effect leads to almost a 10,000-fold difference in the acidity of the same substituents at the same atom!

Why would the bond length affect acidity so strongly? The modulation of the anomeric effect readily explains this difference. The lone pair of the conjugate base is a strong donor in the $n_O \rightarrow \sigma^*_{PO}$ interactions, the key stabilizing force for the anion. These hyperconjugative interactions are stronger for the equatorial OR groups where the donor lone pair and the acceptor σ^* orbitals are brought closer as a result of the shorter P-O distances. As the P-O distance between the donor and the acceptor decrease for the apical substituent, the stabilizing effect of anomeric interaction greatly decreases as well. As a consequence, the formation of an apical anion is less favorable (Figure 171).
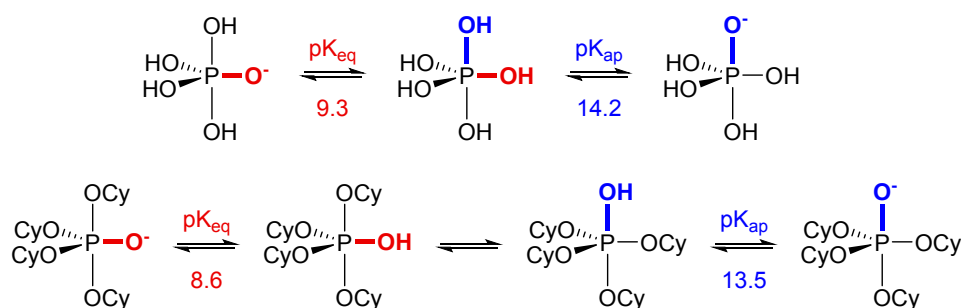
Figure 171. Two estimates for pK_a's of apical and equatorial OH groups in hydroxyphosphoranes.[409]

Three heteroatoms connected to the same carbon: controlling the directionality of anomeric interactions.

Our discussion of oxyanion holes within proteases (Figure 158) focused on the formation of the tetrahedral intermediate, where the directionality of H-bonds simultaneously provides optimal TS stabilization and weaken unproductive anomeric $n_O \rightarrow \sigma^*_{C-Nu}$ interactions that would push the reaction backwards. Enzymes have evolved to promote a difficult reaction by highly stabilizing the TI. This stabilization is illustrated by the tight-binding of sarin, a TI mimic, which shuts down enzymatic activity.

In aspartic proteases, proteolysis is catalyzed by a water molecule, held in place by a pair of aspartic acid residues (Figure 172). TS stabilization of the oxyanion hole is replaced by a concerted proton transfer, as well as substrate-assistance via $n \rightarrow \pi^*$ interactions.[410, 411] As the intermediate is now a *geminal* diol, not an oxyanion, the breakdown of the TI to the products is more complex than the "double anomeric effect" (Figure 154), where two lone pairs are available to facilitate C-N cleavage. In fact, the relative donor and acceptor abilities within the *gem*-diol intermediate favors anomeric $n_N \rightarrow \sigma^*_{C-O}$ interactions that *strengthen* the C-N bond. How, then, does the reaction proceed from the tetrahedral intermediate to the cleaved peptide product?

Gold and coworkers analyzed the evolution of these interactions in a model of the HIV-1 protease active site and suggested that the answer, again, involves fine-tuning of anomeric interactions—both the magnitude and the directionality.[411] During nucleophilic attack to form the *gem*-diol intermediate, the loss of amidic resonance is partially compensated by anomeric $n_N \rightarrow \sigma^*_{C-O}$ interactions. Again, this interaction strengthens the scissile bond and the anomeric $n_O \rightarrow \sigma^*_{C-N}$ interactions required for C-N cleavage are much weaker (~7.5 and ~6 kcal/mol). However, proton transfer to the *N*-terminal amine reverses the direction of donor/acceptor interactions while greatly enhancing their magnitudes. As the result, anomeric $n_O \rightarrow \sigma^*_{C-N}$ interactions of ~26 and ~20 kcal/mol dwarf the <1 kcal/mol anomeric $n_N \rightarrow \sigma^*_{C-O}$ interaction. The stereoelectronics of the *N*-protonated *gem*-diol are now set for proton abstraction from the carbonyl to push the reaction to completion.

Figure 172. Proton transfer enhances anomeric interactions that favor the forward reaction in aspartic proteases.

Making anomeric effect weaker with intramolecular α-effect

The above examples illustrated how making the anomeric effect stronger can open new reaction venues. However, sometimes one needs to go in the opposite direction and partially deactivate anomeric effect, so a different reaction path would become possible (Figure 173). An important example is provided in systems where two oxygens are *connected to each other*. Paradoxically, this situation leads to weakening of anomeric effect despite the expectations based on the so called α-effect, a classic (but controversial) concept introduced to describe increased reactivity of nucleophiles connected to an atom with a lone pair.

Figure 173. Two ways for the two oxygen atoms to interact with a single σ-acceptor

α-Effect: α-Effect was suggested by Edwards and Pearson[412] based on kinetics of nucleophilic reactions by Jencks and Carriuolo.[413] Subsequently, α-effect was defined as "a positive deviation from Brönsted-type nucleophilicity plots in comparison with a reference nucleophile of the same basicity".[414, 415] Later, it was found that such deviations ($k_{\alpha\text{-Nu}}/k_{\text{normal-Nu}}$) vary significantly in magnitude for different reactions and sometimes disappear. The controversies and differences of opinion regarding the magnitude and origin of α-effect are further propagated by the interplay of kinetic and thermodynamic factors as well as the effects of solvation (Figure 174).[416] Below, we will show that an essential part of this complexity is in the relation between α-effect and anomeric effect.

Figure 174. A simplified definition of α-effect that neglects the possible difference in basicity for the two nucleophiles: X and Y-X anions.

Anomeric effect has to be sacrificed for the α-effect to operate: α-Effect requires two lone pairs on two adjacent atoms to be aligned to produce a higher energy antibonding combination with a greater donor ability.[417, 418] However, such mixing and concomitant "reactant destabilization" are often irrelevant for the ground state of flexible molecules because the more stable geometries are different. For example, both

hydrogen peroxide and hydrazine prefer a stereoelectronically favored *gauche* arrangement where their donor lone pairs are aligned with the acceptor σ^*_{X-H} (X=O or N) orbitals.

Because the orbital alignment that switches on the α-effect has to disrupt the favorable ground state arrangement, it includes an intrinsic penalty that can mask stereoelectronic TS stabilization. For example, Mayr and coworkers found that acceleration in reactions with benzhydrylium ions and quinone methides due to the change of H to NH_2 ($NH_3 \rightarrow N_2H_4$) is significant (~100-fold) but not as large as acceleration by a Me group ($NH_3 \rightarrow CH_3NH_2$: >200-fold). Acceleration by an OH group in hydroxylamines (~factor of 10) is also significantly smaller than the effect of a methyl group.[419] A more relevant stereoelectronic model of the α-effect should include the evolution of anomeric interactions in this system along the reaction path.[420]

It is illustrated below for the simplest case with one lone pair on each atom X and Y (Figure 175). In the starting materials, the best donors (lone pairs of X and Y) align antiperiplanar to the best acceptors ($\sigma^*_{Y-R'}$ and σ^*_{X-R} –orbitals, respectively, Figure 175). In the TS for making a bond between X and an electrophile (E^+), strong anomeric donation ($n_Y \rightarrow \sigma^{\ddagger *}_{X-E}$) develops from the high energy lone pair to the low energy antibonding orbital associated with the incipient bond. This interaction can provide selective stabilization to the TS, serving as a source of kinetic α-effect. In the product, the lone pair of Y has the choice to align itself with either the X-E or X-R bonds. If the X-Y reactant was neutral, X is positively charged at this stage and both of these σ^*-orbitals are strong acceptors. Depending on the acceptor ability of the X-E bond, the thermodynamic α-effect may contribute to the stability of the products.
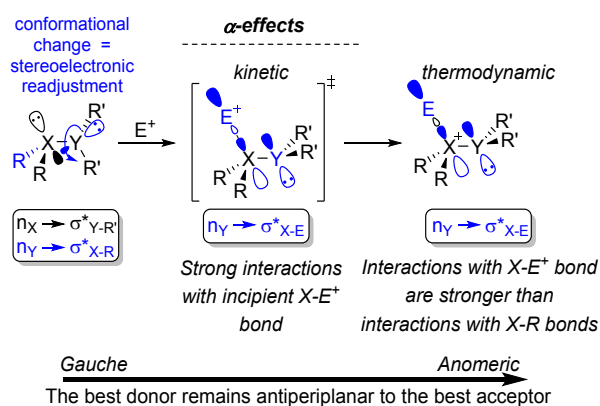
Figure 175. The normal α-effect results when a weakly stabilizing stereoelectronic interaction in the reactant is transformed to a stronger anomeric effect during the reaction. Kinetic effects correlate with TS stabilization, while thermodynamic effects correlate with product stabilization.

Proper modeling of α-effect is impossible if the stereoelectronic complexity of peroxides is unrecognized. A key example is provided by the re-evaluation of the gas-phase S_N2 barriers[421] at saturated carbon by Ren and Yamataka[422, 423] who found that TS energy for the gas-phase S_N2 reaction of CH_3Cl for HOO^- depends on the orientation of the α-OH group in the nucleophile (Figure 176). When the lone pairs of the two oxygen atoms are aligned properly, HOO^- becomes more reactive than HO^-. In the lower energy TS, the lone pairs of the two heteroatoms are aligned as expected from the classic MO model for the α-effect. An alternative TS where the incipient $O\cdots C$ bond is misaligned with the p-type lone pair at the α-oxygen is 2.1 kcal/mol less stable.
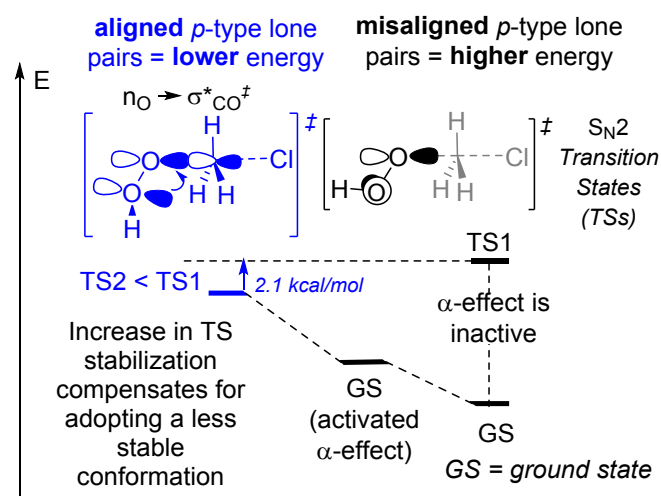
Figure 176. In a situation where the more stable ground state conformer does not have α-effect activated, the increased TS stabilization is needed for α-effect to overcome the unproductive reactant stabilization and become kinetically important. Note that such TS stabilization can be considered a kinetic anomeric effect mediated by a $n_O\rightarrow\sigma^*_{CO}{}^\ddagger$ interaction with the incipient C-O‡ bond. The two transition states for the reaction of $HOO^- + CH_3Cl$ are shown for illustration. Orbital assistance by the properly aligned lone pair stabilizes the lower energy TS2 (2.1 kcal/mol difference at G2(+) level).[330]

Inverse α-effect: moderating anomeric assistance in peroxide reactions. Considering the controversial nature of α-effect, Juaristi et al.[269] decided to use the anomeric effect as an internal stereoelectronic probe for the existence of intramolecular α-effect. The goal was to answer the fundamental question at the heart of α-effect, i.e., whether the lone pairs of two directly connected heteroatoms can combine into a *more* powerful donor than each of the lone pairs taken *separately* (Figure 177).

intramolecular inverse α-effect

$n_{(YX)} \rightarrow \sigma^*_{CZ} < n_X \rightarrow \sigma^*_{CZ}$

anomeric interactions as an intramolecular
probe for the **α–effect**
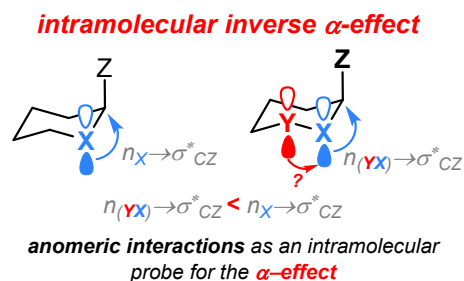
Figure 177. The scope of substrates for evaluating intramolecular α-effect by modulation of the anomeric effect

One can evaluate interaction between two functional groups by using a "separation" reaction which compares a molecule with the two groups adjacent with related molecules that have the two groups separated. According to this analysis, the axial C-F group is strongly stabilized by the anomeric effect in the axial 2-fluoro-tetrahydropyran (ΔE = −6.1 kcal/mol). Contrary to expectation in terms of the α-effect (i.e., the increased donor ability of peroxides), the axial C-F group is significantly less stabilized by the two endocyclic oxygen atoms in 3-fluoro-1,2-dioxane (2.8 kcal/mol, Figure 178). Interestingly, the 3.3 kcal/mol decrease in the anomeric stabilization evaluated through these isodesmic equations agrees well with the 3.6 kcal/mol decrease in the NBO energies for the $n_{(O)} \rightarrow \sigma^*_{(C-F)ax}$ interactions in peroxides.
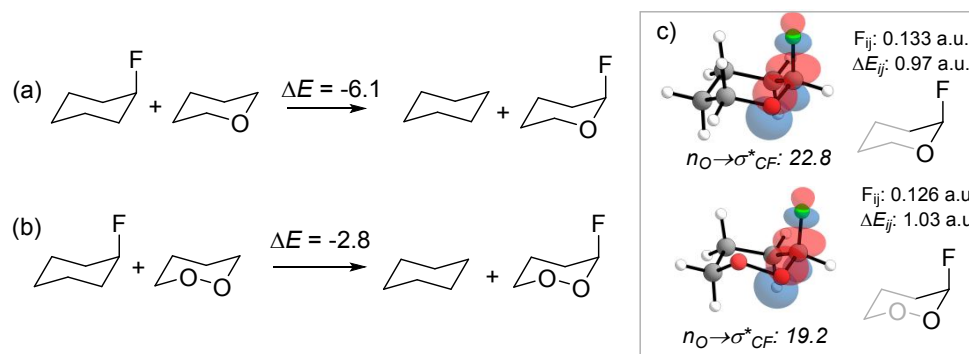
Figure 178. The "separation" reactions for evaluating anomeric effect in an ether (a) and a respective peroxide (b). Comparison of NBO $n_O \rightarrow \sigma^*_{C-F}$ interactions (c). (MP2/6-311+G(d,p) calculations, energies are in kcal/mol)

This theoretical evidence indicates that the donor ability of the peroxide segments is smaller than the donor ability of the ether segments in the gas phase, against expectations in terms of the α-effect. Because the anomeric stabilization in peroxides is weaker than in ethers, the intramolecular α-effect is *negative, or inverse*![269]

Contrary to the expectations based on the simple orbital mixing model, the lone pairs in a pair of neutral directly connected heteroatoms are not raised in energy to become stronger donors. Instead, the $n_{(X-}$

$_{Y)}{\rightarrow}\sigma^*_{C\text{-}F}$ interactions (X,Y=O,N) in the "α-systems" (both acyclic and constrained within a heterocyclohexane frame) are weaker than $n_X{\rightarrow}\sigma^*_{C\text{-}F}$ interactions in "normal" anomeric systems.

Even in the electron deficient reactive species (radicals, cations, and stretched C-F bonds), the α-effect is not activated and anomeric stabilization in peroxides remains low. Both carbocations and radicals are more stabilized by an α-ether than from an α-peroxide moiety. This finding sheds light at the mechanistic complexity associated with the interaction of carbonyl compounds with hydroperoxides and H_2O_2 in acidic media, as such reactions involve α-cationic peroxy intermediates (vide infra).

The theoretical discovery of "inverse" α-effect starts to play an important role in guiding the development of synthesis and new synthetic applications of organic peroxides. We will illustrate this below using the two new peroxide transformations reported by the group of A. Terent'ev.

Applications of inverse α-effect:

Stable peroxy-Criegee intermediates ("CIs"): As discussed earlier, the Criegee Intermediates are difficult to characterize due to their instability towards the BV rearrangement. However, stable hydroperoxy version of this species were isolated and characterized by Vil' et al.[330, 331] The paradoxical situation where a hydroperoxide is more stable than its hydroxyl counterpart illustrates the value of stereoelectronic analysis in anomeric systems.

Geometries along the calculated reaction path for the BV of a peroxy CI reveal the same competition between the exo-anomeric effect and the BV's "secondary stereoelectronic effect" as discussed earlier. In this competition, the ground state anomeric stabilization has to be sacrificed in order to provide TS stabilization to the C-C bond breaking (Figure 179). As one stereoelectronically active lone pair at neutral oxygen is not enough to satisfy the two strong acceptors at the vicinal carbon, the *exo*cyclic OOH has to rotate in the same way as it happens for the OH analogue. In both cases, the *exo*-anomeric effect in reactant is turned off in favor of cationic center stabilization in the TS.

2nd-order interactions calculated with NBO6
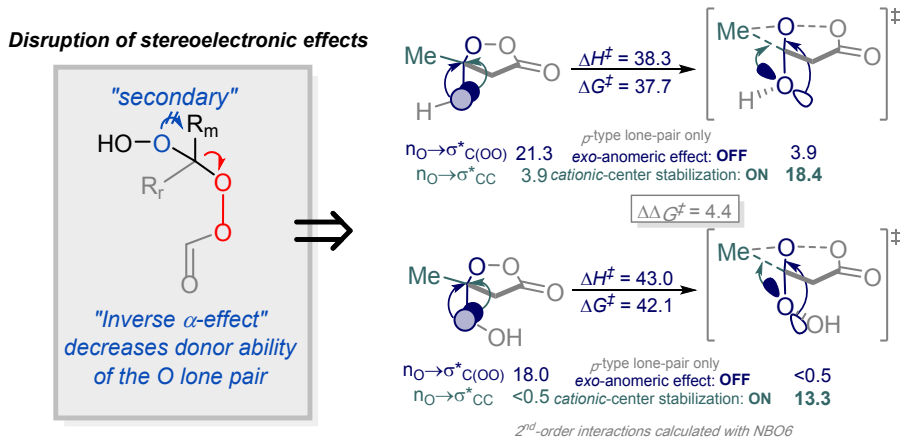
Figure 179. "Inverse" α-effect can protect Criegee intermediate from the 1,2-alkyl shift

However, an important consequence of the inverse α-effect is that the negative hyperconugative stabilization by donation from the oxygen lone pair is *decreased* for both the reactant and the TS in comparison to the classic OH-variant of the Criegee Intermediate. Because the loss of TS stabilization is more pronounced, the barrier for the 1,2-shift is increased by ~4 kcal/mol. The NBO analysis confirms that the donor ability of the OOH lone pairs is significantly lower than it is for the OH (the 3 and 5 kcal/mol differences in the reactant and TS, respectively).

The utility of the inverse α-effect was also illustrated by preparation of an acyclic bis-peroxide shown in Figure 180. This species was sufficiently stable to be isolated but underwent a fast BV rearrangement once converted into the "normal" OH derivative by an *in situ* reaction with PPh$_3$.
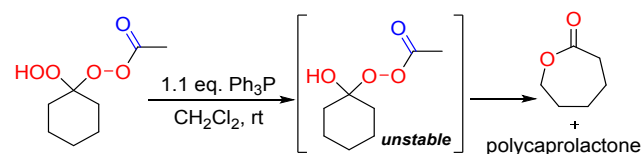
Figure 180. Rearrangement of a non-cyclic Criegee Intermediate triggered by PPh$_3$

Three-component condensations of peroxides: Amplification of inverse α-effect in keto-substituted peroxycarbenium ions increases their destabilization relative to a simple oxacarbenium ions increases to >13 kcal/mol (nearly 50% increase relative to the simple peroxycarbenium ion). This difference could be attributed to the inductive effect of the carbonyl moiety and to the unfavorable interaction of the π-acceptors (the cationic center and the carbonyl group) that have to compete for the donor p-orbitals of the peroxide bridge.
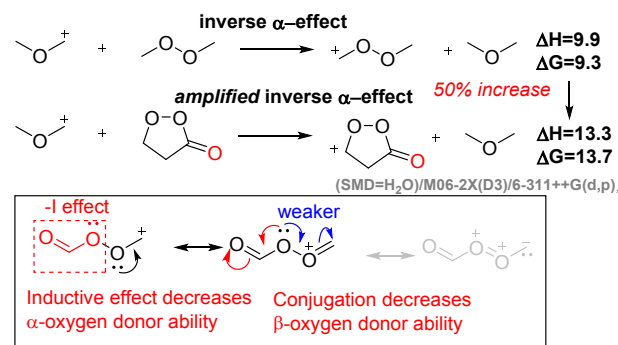
Figure 181. Amplification of inverse α-effect in the cyclic keto-substituted peroxycarbenium ion.

Below we illustrate how this electronic effect was useful for discovering a new three-component reaction where the stereoelectronic control over reactivity of peroxycarbenium cations open easy synthetic approach to β-alkoxy-β-peroxylactones, a new type of organic peroxides.

Computational analysis[424] suggests that alcohol involvement as a third component in the carbonyl/peroxide reactions remained invisible due to the absence of sufficiently deep kinetic traps needed to prevent the escape of mixed alcohol/peroxide products to the more stable bis-peroxides.
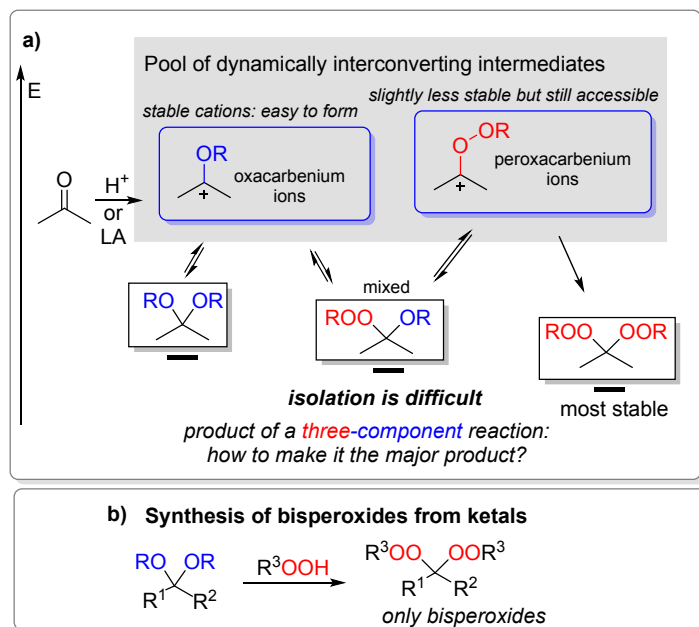
Figure 182. a) Stages in ketal and ketone peroxidation, b) Transformation of ketals into bisperoxides

Interrupting a thermodynamically driven peroxidation cascade was achieved by destabilizing a reactive intermediate (along with the associated TS) on the path that would transform the higher energy β-alkoxy-β-peroxylactones into the thermodynamically favorable bisperoxides. The practical consequence of the stereoelectronically-imposed instability of a cyclic peroxycarbenium intermediate is the first three-component cyclization/condensation of β-ketoesters, H_2O_2, and alcohols that provides β-alkoxy-β-peroxylactones in 15-80% yields (Figure 183).[424]
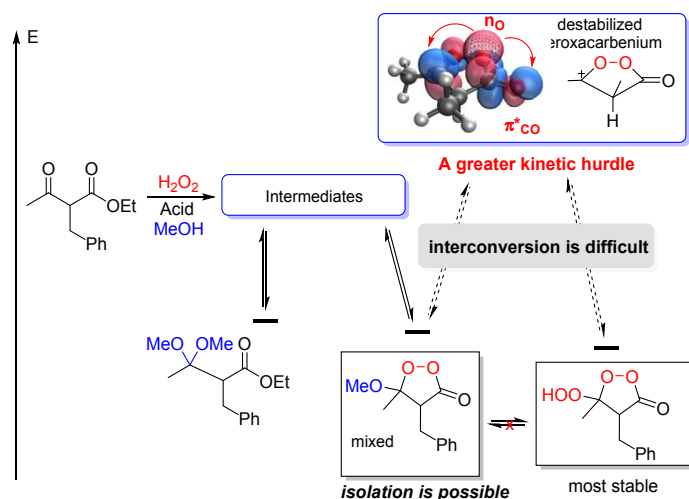
Figure 183. An additional kinetic hurdle is created by further destabilizing the key peroxacarbenium ion, i.e., amplifying the inverse α-effect.

The condensation of β-hydroxy hydroperoxide with orthocarbonates is stopped on the mono-peroxo stage. The subsequent condensation of the 2nd mole of the initial β-hydroxy hydroperoxide with the product failed. One can attribute this lack of reactivity due to the inverse α-effect that would disfavor the departure of an OMe group from a peroxy-substituted carbon (Figure 184).[425]
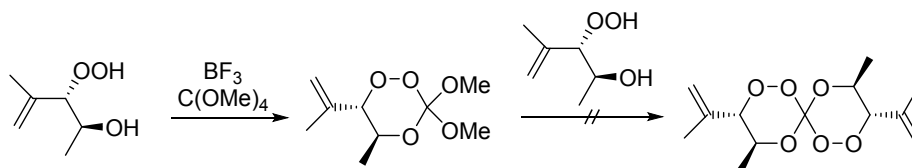
Figure 184. The role of the inverse α-effect in the synthesis of perorthocarbonate.

Separating donor and acceptor in the anomeric system with a relay orbital

"Quasi-homo-anomeric effect":

The pyranosyl C1 radicals, derived from all-equatorially substituted (glucosyl-type) precursors, transform into a boat-like conformation instead of retaining the sterically more favored chair conformation. In contrast, no conformational change is observed in 2-mannopyranosyl-type systems, where the β-C-O bond is already in the axial position (Figure 185).
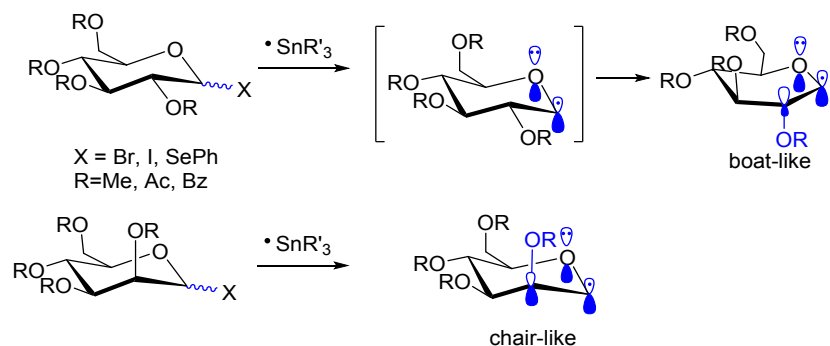
Figure 185. The radical-mediated homoanomeric effect can lead to distortion of pyranosyl C1 radicals to a boat-like conformation

Giese and coworkers[35] explained these conformational effects by a "quasi‑homo‑anomeric" orbital interaction of the lone pair of the ring oxygen atom with the σ^* MO of the β–C-O bond, in which the singly occupied p orbital at C‑1 acts as a mediator for the 1,3‑donor-acceptor n_O/σ^*_{CO} interaction. This interaction is different from the usual homoanomeric effects that correspond to direct through-space interactions of a lone pair with a σ-acceptor.[426]

Vinylogous anomeric effect (VAE)

An extension of the classic anomeric effect, the vinylogous anomeric effect (VAE)[427] stems from the delocalization of electrons between the n and σ^* orbitals through an intervening π orbital. As the classic anomeric effect, this interaction is able to influence the conformational preference to counteract steric effects (Figure 186).[427-435] Due to the increased separation of the endo and exocyclic heteroatoms, the contribution of dipole interactions and other electrostatic effects is greatly decreased and the role of hyperconjugation can be more obvious, albeit "diluted" by the relay orbital.
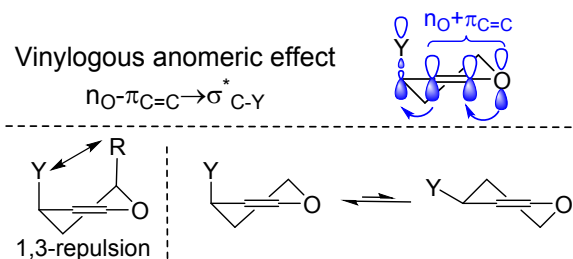
Figure 186. Vinylogous anomeric effect (VAE) vs. 1,3-repulsiont.[420]

VAE is not strong and can efficiently affect the ${}^4H_{5}/{}^5H_4$ conformational equilibrium in glycals only in the absence of significant quasi 1,3-diaxial interactions. For example, the ${}^5H_4$ conformation of acetylated D-allal and D-gulal has no 1,3-diaxial interactions as the 3-OAc group is *trans* to the 5-CH$_2$OAc substituent.

In this situation, the VAE is the only factor controlling the $^4H_5/^5H_4$ conformational equilibrium (Figure 187) and, hence, the 3-OAc group is in the pseudo axial orientation in both of these compounds. In contrast, the 3-OAc and 5-CH$_2$OAc groups are *cis* in D-galactal and D-glucal. The competition between the 1,3-diaxial interactions and the VAE leads to an equilibrium between the $^4H_5$ and $^5H_4$ ring forms.[433]
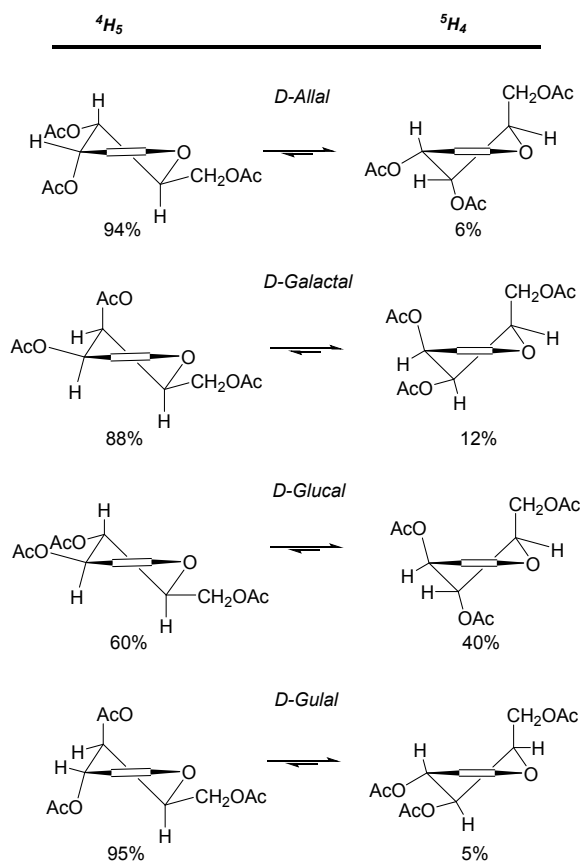
Figure 187. VAE in selected glycals

VAE can be used to control reactivity. For example, it can promote the Ferrier Rearrangement (also called Ferrer I reaction), i.e., the transformation of glycals into 2,3-unsaturated glycosyl derivatives that proceeds as nucleophilic substitution with allylic rearrangement. This process is greatly facilitated when the leaving group adopts the pseudo-axial position where it is aligned with the endocyclic oxygen lone pair via the relay π-system (Figure 188).[436]

Vinylogous anomeric effect is ON:

ROH

IDCP
promotor

65%

Vinylogous anomeric effect is OFF:

ROH

IDCP
promotor

26%   +   44%
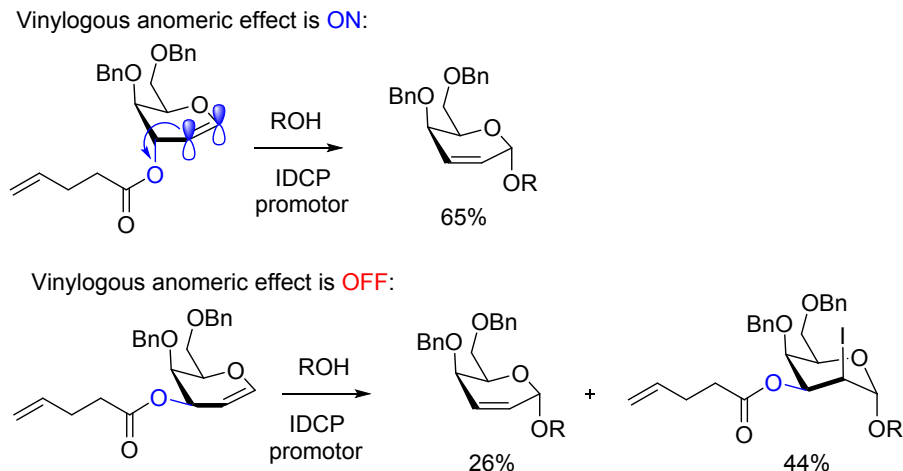
Figure 188. Vinylogous anomeric effect on the iodonium-catalyzed Ferrier rearrangement (IDCP=iodonium dicollidinium perchlorate).

The double bond in the vinylogous anomeric systems is not just a relay that mediates electronic interaction between the donor and the acceptor. Its own properties can be changed by variations in the acceptor character of the allylic OR group as well. Such variations change alkene nucleophilicity and found application in the design of "armed" and "disarmed" partners for coupling reactions (Figure 189). For example, formation of halonium ions at the double bond of glycals is disfavored for esters relative to ethers.[387]

"armed"   "disarmed"

"I+"

weaker σ-acceptor   strong σ-acceptor
next to halonium ion   next to halonium ion
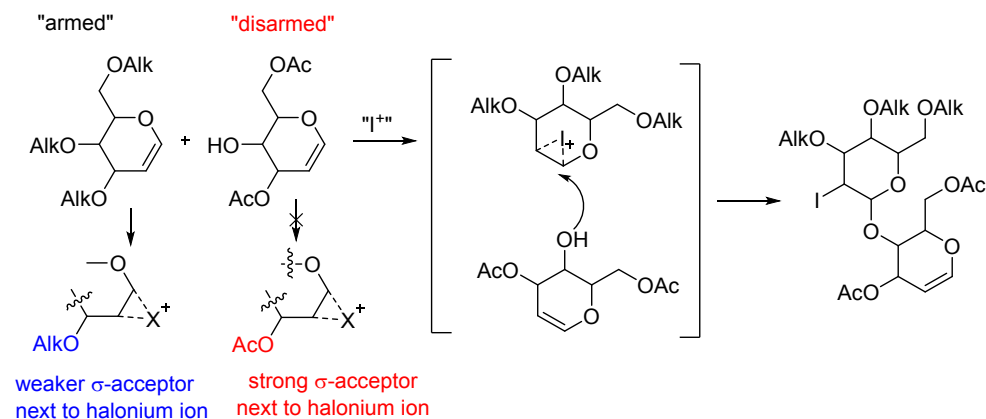
Figure 189. Vinylogous "arming" and "disarming" of glycals.

Zolfigol et al. have recently introduced "vinylogous anomeric-based oxidations" based on the use of the vinylogous anomeric effect for the removal of hydride, a step needed to complete the final oxidation/aromatization in their synthesis of a wide range of substituted pyrazoles and pyridines.[399, 437-447]

Of course, the well-known accelerating effect of ortho- and para alkoxy groups on benzylic reactivity can also be considered as an "arylogous" version of vinylogous AE. The large negative Hammett σ^+(para) parameter for p-OMe group (-0.78) allows benzylic halide solvolysis and subsequent Friedel–Crafts alkylations of activated aromatics to proceed *in the absence* of Lewis acids.[448] For example, Mayr and coworkers has shown that no Lewis Acid catalysis is needed for electrophilic aromatic substitutions in 1M solutions of arenes with 4-methoxybenzyl halides as long as the arenes are more nucleophilic than the solvent (Figure 190).

> 90%
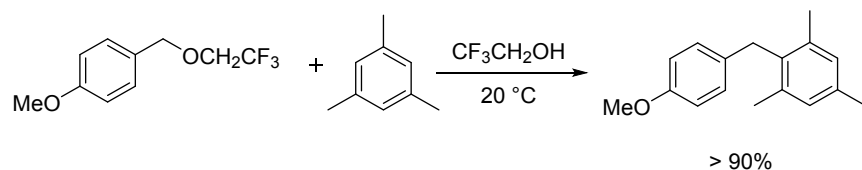
Figure 190. "Acid-free" Friedel–Crafts alkylation with a 4-methoxybenzyl halide

How to keep anomeric effect under control: the influence of hydrogen bonding

Finally, it is worth summarizing the supramolecular strategies to controlling the anomeric effect. We have discussed a few of such examples earlier. For example, intermolecular H-bonding with OH-group can be used to control C-H activation of alcohols, and complexes of carboxylic acids with H-bond acceptors are more likely to prefer E-configuration than free carboxylic acids (the "Supramolecular Stereoelectronic Effect", SSE).[306, 323]

Selected H-bond-induced variations in the donor ability of oxygen lone pairs are illustrated in Figure 191. Notably, changes in AEs are closely related to electron density in the OH-group and vary significantly. In particular, when the OH-group interacts with an H-bond donor, the $n_O \rightarrow \sigma^*_{C-X}$ donations from the hydroxyl lone pair are weakened while the intramolecular donation to the σ^*_{C-O} from the other oxygen atom (in acetals, hemiacetals, esters, and carboxylic acids) is strengthened (Figure 191). On the other hand, when the OH-group interacts with an H-bond acceptor (i.e., an electron donor), the oxygen atom gains electron density, so the hydroxyl becomes a better donor and a weaker acceptor.
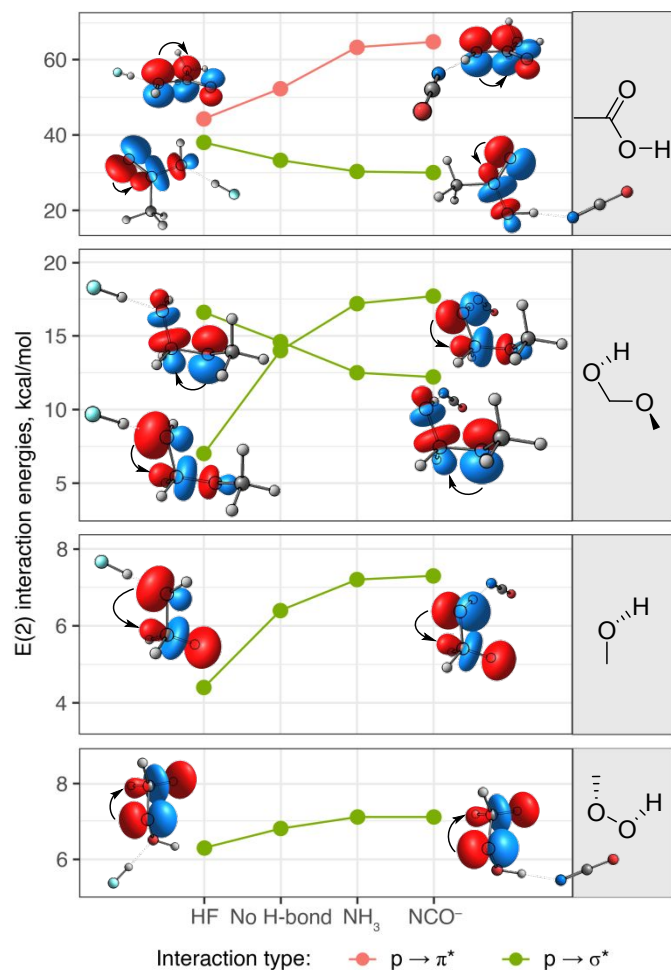
Figure 191. Influence of hydrogen bonding on stereoelectronic effects in molecules containing OH-group. Quantum chemical calculations are performed at PBE0-D3BJ/aug-cc-pVTZ/CPCM(H$_2$O) level of theory.

For example, the n$_O$→σ*$_{C-H}$ interactions in MeOH is about 40% weaker when the hydroxyl group is bonded with HF(an H-bond donor) but ~15% stronger in the complex with the NCO$^-$ anion (an H-bond acceptor), Figure 191. Note also, that in the complexes of MeOH, MeOOH and hemiacetal with the hydrogen bond donor (HF), the oxygen lone pair involved in the H-bond rehybridizes to become an ~sp^3 orbital. This example shows the how C-H activation in alcohols can be assisted by H-bond acceptors and prevented by H-bond donors. In peroxides, the H-bonded oxygen is separated from the alkyl group by another oxygen atom, so these effects are weaker.

Another interesting feature of H-bonding is that it generally favors geometries that are not fully stabilized by the internal donor-acceptor interactions, i.e., the E-conformation of carboxylic acids or equatorial conformation of cyclic acetals. The classic anomeric interaction patterns lead to internal charge

delocalization and render such stable molecules less willing participants in *external*, i.e, intermolecular, interactions such as H-bonding.

Executive summary of organic chemistry of O-containing functional groups.

Oxygen is a peculiar element. The presence of two lone pairs at the neutral divalent oxygen makes chains made from the repeating O-O units unstable, so, unlike carbon, oxygen is not a good building block for itself – the chances of oxygen-based life forms are slim. But in a combination with carbon, oxygen becomes an essential element of organic architecture. Not only does it impart polarity and increases hydrophilicity, but the presence of the lone pairs also gives oxygen the stereoelectronic power to direct chemical reactions. This power is especially clearly manifested when an electron-deficient intermediate or transition state are formed in the direct proximity. From this point of view, the role of oxygen in chemical reactions is similar to a conductor directing a musical performance. In this review, we have used a variety of oxygen-orchestrated reactions to highlight the value of a simple idea – a lone pair aligned with an acceptor is a powerful force assisting in C-X, C-C, C-H bond activations at the β-carbon. To paraphrase J.K. Rowling, "help will always be given in anomeric systems, to those who ask for it".

However, presence of the two lone pairs is not the only stereoelectronically important feature of oxygen functionalities. Oxygen is an element with a "split" personality, often behaving as a chemical chameleon. On one hand, it is a powerful acceptor (as one would expect from a highly electronegative element) but, paradoxically, it can also be a powerful donor. This paradox is where oxygen draws its chemical versatility from. Molecules with two or more appropriately positioned oxygens possess the right properties for synergistic donor/acceptor interactions that can stabilize molecules without excessive charge separation. Examples discussed in this review illustrate that α-hydrogen in OR-systems can serve as the source of hydride whereas organic textbooks reiterate often that OH and β-hydrogens have a protic character as illustrated by facile deprotonation of alcohols and their E2 elimination reactions, respectively.

Oxygen as stereoelectronic chameleon:
effect on the adjacent hydrogens

protic (electronegativity of oxygen polarizes the bond)

hydridic (density
provided by
vicinal p-donor)

protic (density lost to the
vicinal hyperconjugative
σ*CO acceptor)
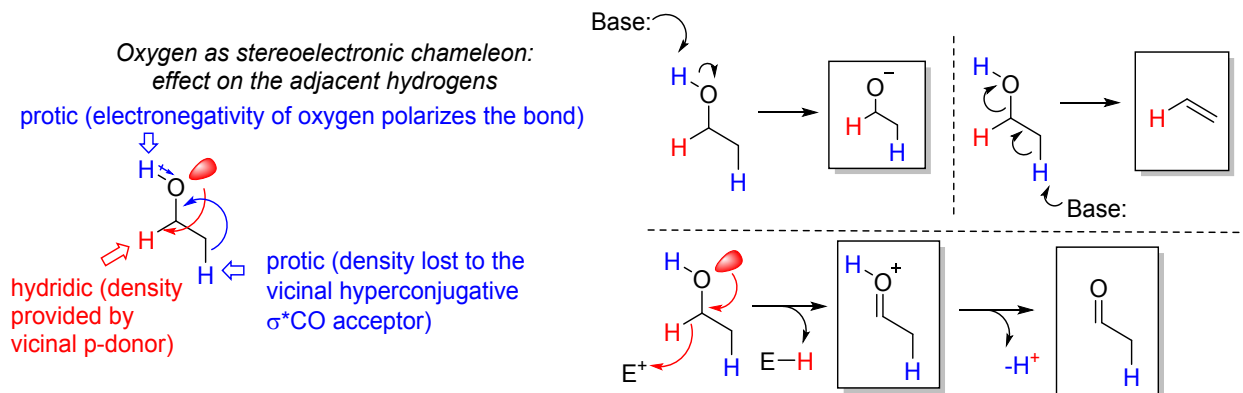
Figure 192. Oxygen acting as a stereoelectronic chameleon with both hydridic and protic reactions of the adjacent hydrogens

Although in classic anomeric systems, e.g., in the O-C-O unit in acetals, each of the oxygen groups is both a donor and an acceptor in a stable balanced arrangement, amplification of only one in the pair of such donor acceptor interactions upsets this balance and leads to a chemical transformation, i.e. the oxacarbenium ion formation. Remote or intermolecular versions of such donor/acceptor interactions can lead to other chemical reactions. For example, it is this donor-acceptor complementarity that enables the C-O bond formation in a 6-exo-tet cyclization shown in Figure 193. Here, one of the two oxygens is clearly a donor whereas the other one becomes, by virtue of protonation, an acceptor.

pair of
$n \rightarrow \sigma^*_{CO}$
interactions

balance is lost:
a single strong
$n \rightarrow \sigma^*_{CO}$ interaction

chemical
transformation

σ-acceptor

$n_O \rightarrow \sigma^*_{CO}$
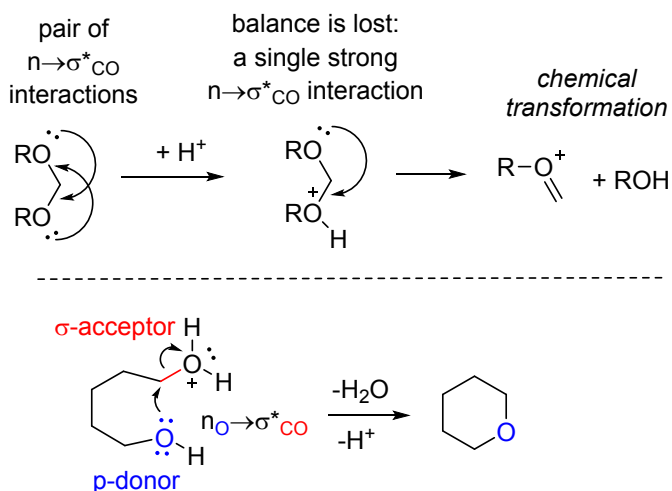
p-donor

Figure 193. The ability of oxygen functionalities to act as either a donor or an acceptor can serve as the driving force for a chemical bond formation. Top: a vicinal interaction leading to an elimination. Bottom: remote interaction leading to a cyclization

Like individual players in a team sport several factors combine to account for the overall conformational trends. However, it is the hyperconjugative contribution that is a star player in a team and it is the orbital

description that has the highest predictive power. When the electronic demand is high (bonds are breaking and molecules are distorted from their equilibrium geometries), the role of orbital interactions increases even when distribution of charges does not change significantly. From that point of view, stereoelectronic effects play a unique predictive power in guiding reaction design and reactivity studies. In this review, we have analyzed the role of negative hyperconjugation with the participation of oxygen lone pairs in structure, stability, and reactivity of the key organic O-containing functional groups.

Because most of reactivity trends discussed in this review are based on negative hyperconjugation, is helpful to discuss the range of hyperconjugative energies in O-functionalities. A summary of delocalizing interactions in Table 1 illustrates the remarkable range of NBO interaction energy values for the lone pair interaction with a vicinal σ-acceptor even in the ground state stable geometries. Several factors are responsible for this broad distribution. The difference between 2-3 kcal/mol for the σ^*_{O-C} in peroxides to 13-15 kcal/mol for the σ^*_{C-O} in acetals illustrates the directionality of stereoelectronic interactions (a C-O bond is a good acceptor at the carbon end but a poor acceptor at the oxygen end). The differences between donation to the σ^*_{C-O} in acetals and esters (14-15 vs. 30-40 kcal/mol) and donation to the σ^*_{C-H} in ethers and ketones (7-9 vs. 23-26 kcal/mol) illustrates the often underappreciate importance of hybridization effects on the anomeric delocalization.

Table 1. Summary of NBO negative hyperconjugation energies and lone pair hybridizations in O-containing functional groups. Upper energy bounds are given for conformers with fully activated interaction.

Types of molecules	Hybridization and energy of LP1	Hybridization and energy of LP2
Ethers	p. 6.6 – 9.0 to C-H, up to 7.7 to C-C	$sp^{1.3}$. 2.7 – 3.4 to C-H, up to 4.8 to C-C
Alcohols	p. 6.4 – 8.6 to C-H	sp. 2.7 – 2.9 to C-H
Peroxides	p. 1.9 – 2.8 to O-C. 6.5 – 6.9 to C-H.	$sp^{0.7}$. 1.0 – 1.2 to O-C. 1.4 – 1.5 to C-H.
Acetals	p. 13.6 – 15.2 to C-O	$sp^{1.0}$(OH), $sp^{1.3}$(OMe). 0.4 – 4.0 to C-O
Aldehydes and ketones	p. 23.2 – 25.5 to C-H. 19.6 – 22.9 to C-C.	$sp^{0.7}$. 0.6 to C-H. 1.5 – 2.4 to C-C
Esters (from C=O to C-OR)	p. 32.3 – 37.8	$sp^{0.6}$ (HCO), $sp^{0.7}$ (MeCO). 0.7-1.7
Esters (from C-OR to C=O)	p. 48.4 – 57.4	$sp^{1.2}$ (OH), $sp^{1.5}$ (OMe). 7.3 – 8.7

The anomeric effects can help to explain some of the peculiar features of oxygen functionalities. As the first example, let's look at the drastic difference in the apparent energy content of the C=C and C=O bonds.

The relative weakness of π-bond between two carbon atoms in comparison to an σ-bond is the basis of the textbook explanation to why alkenes and alkynes are more reactive than alkanes. One can quantify the excessive energy (i.e., destabilization) of alkenes vs. alkanes using the equation in Figure 194. Although this simple equation is not perfectly balanced in terms of hybridization, it is suitable for evaluating the overall energy content of an alkene relative to propane and ethane, the two strain-free alkane reference points. The results are revealing – ethene is ~23 kcal/mol destabilized relative to the alkanes![449] However, when a similar analysis is applied to formaldehyde, the destabilization is negligible while ketones are *more stable* relative to the saturated reference points (-8 kcal/mol for acetone). Furthermore, esters are stabilized even more (-31 kcal/mol). These differences are especially significant if one considers that the ketone and ester equations probably *under*estimate the stability of these carbonyl compounds as "reactants" (i.e., 2,2-dimethyl propane) is a branched alkane that is stabilized relative to linear alkanes by protobranching.[450]
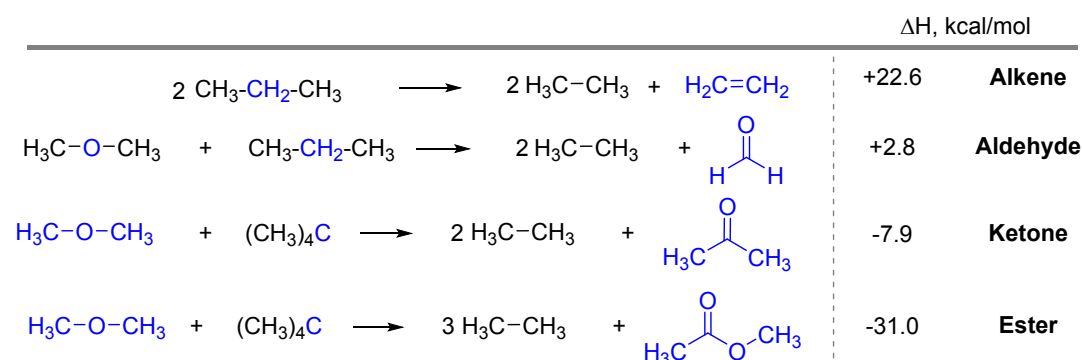
Figure 194. Energy content of C=C and C=O bonds: carbonyl compounds are much more stable than one would expect for unsaturated molecules (enthalpies calculated using the gas phase enthalpies of formation taken from the Active Thermochemical Tables)[31]

These equations illustrate why alkenes and alkynes are high energy functionalities but carbonyls are not, despite all three being π-functionalities! Thinking about lone pair delocalization can also explain why CO_2 is such a stable molecule and why sequestering it from the environment chemically is a difficult task.[451, 452]

The increasing stabilization of carbonyls compared to their alkene counterparts can be attributed, at least partially, to anomeric effects. There is little doubt that very strong $n_O \rightarrow \sigma^*_{C-H}$ and $n_O \rightarrow \sigma^*_{C-C}$ interactions in aldehydes and ketones (Figure 4) contribute to the almost 30 kcal/mol energy difference between the anomerically stabilized aldehydes and the unfavorable alkenes. Ketones and esters are even more favored than aldehydes due to their increased number of donor-acceptor interactions. Both ketones and esters also benefit from positive hyperconjugation (i.e. the $\sigma_{C-H} \rightarrow \pi^*_{C=O}$ interactions). Esters are even

further stabilized by the $n_O \rightarrow \pi^*_{C=O}$ ester resonance, adding up to the combination of four strong donor-acceptor interactions ($\sigma_{C-H} \rightarrow \pi^*_{C=O}$, $n_O \rightarrow \pi^*_{C=O}$, $n_O \rightarrow \sigma^*_{C-C}$, and $n_O \rightarrow \sigma^*_{C-O}$).

Increased thermodynamic stabilization of carbonyl compounds contributes to many textbook features of this functional group. For example, it explains why enolization of ketones is so uphill and why aldol additions are not as favorable as one would expect from a reaction where a π-bond is traded to form a σ-bond.

However, in addition to the general features, each of the textbook O-functionalities has its own personality colored by the nature of their own, specific patterns of the lone-pair-delocalizing interactions. Below we will summarize the individual take-home messages for the functional groups discussed in this review.

In *ethers and alcohols*, the anomeric effect is mostly dormant, even though its presence is manifested in structural and spectroscopic features of the α-C-H bonds (i.e., the Perlin effect). Activation of the anomeric donation occurs once an α-C-H or an α-C-C bond starts to react, especially with an electron deficient partner such as an electrophilic radical or a carbenium ion. Such kinetic effects have found a number of applications for selective C-H and C-C activation and their utility is likely to expand further in the future. An interesting feature of anomeric activation is that it is sensitive to supramolecular control, i.e. H-bonding. For ethers, the O…H-X interactions can provide protection from radical reactions. For alcohols, the H-bonding interactions are more versatile, serving as either an activating or a protecting effect, depending whether the alcohols OH serves as a H-bond donor (O-H…Y) or a H-bond acceptor (O…H-Y).

In *aldehydes and ketones*, the magnitude of the anomeric effect is significantly stronger than in alcohols and ethers due to the shorter C=O bond and the greater electronegativity of sp²-carbons. This large anomeric effect in aldehydes leads to anomalously low C(O)-H BDEs, rendering aldehydes a convenient source of acyl radicals. It also plays the key role in oxidative transformations of aldehydes into carboxylic acid derivatives. When $n_O \rightarrow \sigma^*_{C-H}$ interaction is weakened by C=O…H-X hydrogen bonding, the anomeric activation is partially deactivated and the oxidation can be avoided. Alternatively, n-π* photochemical excitation can transform oxygen from a 2-electron donor to a 1-electron acceptor (the stereoelectronic "umpolung" of the anomeric effect). The convenient alignment of this acceptor with the σ-bonds at the carbonyl atom leads to important photochemical transformations of ketones (Norrish Type 1 fragmentation, ring expansion etc).

The importance of anomeric effect increases even further when the second oxygen atoms is introduced. In such systems, a pair of moderately strong anomeric $n_O \rightarrow \sigma^*_{C-O}$ interactions are present even in the ground state. Activation of such effects contributes to the thermodynamic stability of *esters, acetals and*

related compounds. For example, it explains why disproportionation of two aldehydes into an ester is favorable in the classic Canizzaro reaction. Paradoxically, the anomeric effect can also serve as a source of some kinetic protection as the anomeric reactant stabilization often has to be sacrificed for the lone pairs of oxygen atoms to become engage in a different process (e.g., assist in α-C-H or C-C activation). In such systems, the role of anomeric effect in reactivity can often be described as a "tug-of-war" between ground state stabilization (e.g., $n_O \rightarrow \sigma^*_{C-O}$) vs transition state stabilization (e.g., $n_O \rightarrow \sigma^*_{C-Y}$, where C-Y is the breaking bond).

The role of oxygen lone pair delocalization becomes even more complex in *esters*, where the lone pairs of both oxygen atoms participate in a network of three important donor-acceptor interactions. In particular, both lone pairs of the alkoxy group can engage in interactions with the acceptor orbitals of the carbonyl group. The stronger of the two interactions, known as ester resonance, involves donation of the p-type lone pair on oxygen to the π^* of the carbonyl which results in the perceived weakening of the C=O bond when compared to alkenes (Figure 194). The stereoelectronic importance of the ester resonance is also apparent in the large (10-15 kcal/mol) rotational barrier around the ester C-O bond. The secondary interaction, where the carbonyl acts as a σ-acceptor, results from the σ-type lone pair of oxygen and contributes to the syn-preference in the conformational equilibria of esters and other similar functional groups. This effect is responsible for greater reactivity of lactones – when these cyclic esters are constrained to the higher-energy E-isomer, they are more electrophilic than their acyclic ester equivalents. The syn- vs. anti- (i.e., Z- vs. E-) preference also renders lactones 10,000-times more acidic than similar acyclic esters.

An additional stereoelectronic effect in esters results from the carbonyl oxygen acting as a *donor* in a $n_O \rightarrow \sigma^*_{C-OR}$ interaction. While similar to the analogous interaction in acetals, the magnitude of this effect in esters is larger due to the short C=O distance bringing the donor and acceptor orbitals closer together. This interaction is the second strongest of the three delocalizing interactions in esters and helps compensate for the charge separation resulting from the $n_O \rightarrow \pi^*_{C=O}$ ester resonance by transferring electron density away from the carbonyl. Additionally, this interaction plays an important role in facilitating C-X bond scission in carboxylic acid derivatives.

On the other hand, the catalytic effects based on difference in basicity of "syn" and "anti" lone pairs of *carboxylates* are not supported by the presently available computational evidence. Although this effect may operate for late transition states where the proton transfer to carboxylate is well-developed, further studies for a broader scope of systems and at higher levels of theory are needed to understand the possible relevance of this interesting concept to practical control of reactivity.

A flurry of reports within the last five years disclosed that anomeric interactions are highly impactful in *peroxide chemistry*. There, they offer a new element of control with the potential of dramatically expanding the value of this underutilized oxygen-rich functional group for synthetic and medicinal applications. Simple peroxides are "stereoelectronically frustrated" because their anomeric interactions are very weak - even weaker than in ethers. Once anomeric effects are activated (e.g., by introduction of a β-heteroatom), the thermodynamic stability of peroxide significantly increases. Under thermodynamic control, fine-tuning of anomeric interactions allows selective construction of different types cyclic peroxides including ozone-free synthesis of bicyclic ozonides and other oxygen-rich polycyclic systems.

In parallel, the *inverse α-effect*, i.e., the attenuation of anomeric effect, influences kinetic control in the peroxide-forming cationic pathways. This effect explains the relative instability of peroxycarbenium ions in comparison with oxycarbenium ions. As these species often serve as the key intermediates of peroxide transformations, understanding the interplay of reactivity with structural and electronic features of peroxycarbenium ions opens broad opportunities for the better control of synthetic peroxide chemistry. Such phenomenon has found a number of applications in selective organic peroxide synthesis. Blocking the anomeric effects ($n_O \rightarrow \sigma^*_{C-Rm}$ and $\sigma^*_{C-Rm} \rightarrow \sigma^*_{O-O}$) in Criegee intermediate provides sufficient stabilization of this transient species and interrupts the Baeyer-Villiger rearrangement.[185]

The paradoxical greater stability of bis-peroxides in comparison with mono-peroxides results from activation of strong anomeric $n_O \rightarrow \sigma^*_{C-O}$ interactions of one or more of the peroxide oxygen atoms with the C-O bond of the other peroxide moiety. Such stability opens access to molecules that seemed beyond our reach until recently, including unusually stable macrocyclic and/or heteroatom-containing organic peroxides.

The emerging new trends in organic peroxide chemistry illustrate that further investigations of stereoelectronic effects can expand the predictive power of theoretical concepts in this field. This expansion would speed up the development of efficient synthetic methods leading to new bioactive compounds derived from this underutilized O-functionality.

Conclusion

If a shorter and more general summary is desired, one can state that for organic functionalities with one O atom and no other heteroatoms, the anomeric delocalization is nearly always activating, e.g., serving as an important Transition State (TS) stabilization force for H-atom and hydride transfer reactions. For other O-functionalities, anomeric interactions come in pairs (e.g., endo- and exo AE in cyclic acetals) or as a network of interconnected delocalizing effects. In such systems, the overall role of anomeric effect

can be either stabilizing or destabilizing, depending on whether such effects are greater in the reactants or in the TS. Very often, reaction selectivity can be described as a competition of "colliding" anomeric effects.   Anomeric interactions can get stronger or fade away along the reaction path, combine to cause remarkable accelerations or compete, nearly canceling each other. Amplification of anomeric effects in anionic oxygen compounds leads to particularly large effects, even in the absence of vicinal C-X bonds with electronegative elements X. Amplified by "stereoelectronic promiscuity" of negatively charged oxygen, such effects can lead to cascade fragmentations or an unexpected facilitating role of "bystander" substituents.

When needed, anomeric delocalization can be controlled. For example, H-bonding to oxygen can moderate its donor ability, while deprotonation of OH groups can dramatically activate negative hyperconjugation. Amplification of anomeric effects at anionic oxygen compounds is assisted by "stereoelectronic promiscuity" of negatively charged oxygen leading to cascade C-C fragmentations or unexpected roles of "bystander" substituents.

It is also important to say that, although our focus is on orbital interactions, one should not underestimate the importance of electrostatic, steric, dispersive interactions. They are also essential parts of the overall molecular puzzle. In particular, charges certainly matter. However, their influence generally comes, especially in neutral systems, from a combination of several components. In contrast, the predictive power of stereoelectronic analysis can often be traced down to a single dominant effect.

We hope that this review will be useful to a broad chemical audience - from theoretical physical chemists to industrial practitioners - because it can serve as the conceptual bridge between fundamental stereoelectronic interactions and the practical reactivity trends in omnipresent O-containing compounds. The stereoelectronic give-and-take of oxygen lone pairs and C-O orbitals with the neighboring functionalities can induce new reactivity features, define physical properties, and even serve as the main reason for certain oxygen-containing compounds to exist at the practical timescales.

References

1.   Juaristi, E.; Cuevas, G., Recent Studies of the Anomeric Effect. *Tetrahedron* **1992,** *48* (24), 5019-5087.

2.   Edward, J. T., Stability of Glycosides to Acid Hydrolysis. *Chemistry and Industry* **1955,** *3*, 1102-1104.

3.   Deslongchamps, P., Intramolecular Strategies and Stereoelectronic Effects - Glycosides Hydrolysis Revisited. *Pure and Applied Chemistry* **1993,** *65* (6), 1161-1178.

4.   Franck, R. W., A revision of the value for the anomeric effect. *Tetrahedron* **1983,** *39* (20), 3251-3252.

5.   Reed, A. E.; Schleyer, P. v. R., The anomeric effect with central atoms other than carbon. 2. Strong interactions between nonbonded substituents in mono- and polyfluorinated first- and second-row amines, FnAHmNH2. *Inorganic Chemistry* **1988,** *27* (22), 3969-3987.

6.   David, S.; Eisenstein, O.; Hehre, W. J.; Salem, L.; Hoffmann, R., Superjacent orbital control. Interpretation of the anomeric effect. *Journal of the American Chemical Society* **1973,** *95* (11), 3806-3807.

7.   Altona, C.; Knobler, C.; Romers, C., The conformation of non-aromatic ring compounds. VII. Crystal structure of trans-2,5-dichloro-1,4-dioxane at 125degreesC. *Acta Crystallographica* **1963,** *16* (12), 1217-1225.

8.   Romers, C.; Altona, C.; Buys, H. R.; Havinga, E., Geometry and Conformational Properties of Some Five- and Six-Membered Heterocyclic Compounds Containing Oxygen or Sulfur. In *Topics in Stereochemistry*, 1969; pp 39-97.

9.   Petillo, P. A.; Lerner, L. E., Origin and Quantitative Modeling of Anomeric Effect. In *The Anomeric Effect and Associated Stereoelectronic Effects*, American Chemical Society: 1993; Vol. 539, pp 156-175.

10.   Alabugin, I. V., Stereoelectronic Interactions in Cyclohexane, 1,3-Dioxane,

1,3-Oxathiane, and 1,3-Dithiane: W-Effect, σC-X T σ*C-H

Interactions, Anomeric EffectsWhat Is Really Important? *J Org Chem* **2000,** *65*, 3910-3919.

11.   Freitas, M. P., The anomeric effect on the basis of natural bond orbital analysis. *Org Biomol Chem* **2013,** *11* (17), 2885-90.

12.   Nori-Shargh, D.; Mousavi, S. N.; Tale, R.; Yahyaei, H., Hyperconjugative interactions are the main responsible for the anomeric effect: a direct relationship between the hyperconjugative anomeric effect, global hardness and zero-point energy. *Struct Chem* **2016,** *27* (6), 1753-1768.

13.   Salzner, U.; Schleyer, P. v. R., Ab Initio Examination of Anomeric Effects in Tetrahydropyrans, 1,3-Dioxanes, and Glucose. *The Journal of Organic Chemistry* **1994,** *59* (8), 2138-2155.

14.   Glendening, E. D.; Landis, C. R.; Weinhold, F., Natural bond orbital methods. *Wiley Interdisciplinary Reviews: Computational Molecular Science* **2012,** *2* (1), 1-42.

15.   Wiberg, K. B.; Bailey, W. F.; Lambert, K. M.; Stempel, Z. D., The Anomeric Effect: It's Complicated. *The Journal of Organic Chemistry* **2018,** *83* (9), 5242-5255.

16.   Wang, C.; Ying, F.; Wu, W.; Mo, Y., How solvent influences the anomeric effect: roles of hyperconjugative versus steric interactions on the conformational preference. *J Org Chem* **2014,** *79* (4), 1571-81.

17.   Wang, C.; Chen, Z.; Wu, W.; Mo, Y., How the Generalized Anomeric Effect Influences the Conformational Preference. *Chemistry – A European Journal* **2013,** *19* (4), 1436-1444.

18.   Ferro-Costas, D.; Mosquera, R. A., Excluding hyperconjugation from the Z conformational preference and investigating its origin: formic acid and beyond. *Physical Chemistry Chemical Physics* **2015,** *17* (40), 26946-26954.

19.   Ferro-Costas, D.; Vila, A.; Mosquera, R. A., Anomeric Effect in Halogenated Methanols: A Quantum Theory of Atoms in Molecules Study. *The Journal of Physical Chemistry A* **2013,** *117* (7), 1641-1650.

20.   Ferro-Costas, D.; Mosquera, R. A., Complementarity of QTAIM and ELF Partitions: Deeper Understanding of the Anomeric Effect. *Journal of Chemical Theory and Computation* **2013,** *9* (11), 4816-4824.

21.   Ferro-Costas, D.; Otero, N.; Graña, A. M.; Mosquera, R. A., A QTAIM-based energy partitioning for understanding the physical origin of conformational preferences: Application to the Z effect in O=C-X-R and related units. *Journal of Computational Chemistry* **2012,** *33* (32), 2533-2543.

22.   Vila, A.; Estévez, L.; Mosquera, R. A., Influence of the Solvent on the Charge Distribution of Anomeric Compounds. *The Journal of Physical Chemistry A* **2011,** *115* (10), 1964-1970.

23.   Vila, A.; Mosquera, R. A., QTAIM explanation of the anomeric effect in the O–C–O unit II: 2-Methoxyoxane and 2,2-dimethoxypropane. *Chemical Physics Letters* **2007,** *443* (1), 22-28.

24.   Vila, A.; Mosquera, R. A., Atoms in molecules interpretation of the anomeric effect in the O--C--O unit. *J Comput Chem* **2007,** *28* (9), 1516-1530.

25.   Alabugin, I. V.; Kuhn, L.; Krivoshchapov, N. V.; Abdo, M.; Mehaffy, P.; Yarie, M.; Zolfigol, M. A.; Medvedev, M. G., Anomeric Effect: Lessons from Complexity in a Classic Stereoelectronic Phenomenon. *Chemical Society Reviews* **2020, Submitted**.

26.   Filloux, C. M., The Problem of Origins and Origins of the Problem: Influence of Language on Studies Concerning the Anomeric Effect. *Angewandte Chemie International Edition* **2015,** *54* (31), 8880-8894.

27.   Reed, A.; Curtiss, L.; Weinhold, F., Intermolecular Interactions from a Natural Bond Orbital, Donor-Acceptor Viewpoint. *Chem Rev* **1988,** *88*, 899-926.

28.   Kirby, A. J., *The Anomeric Effect and Related Stereoelectronic Effects at Oxygen*. Springer, Berlin, Heidelberg: 1983.

29.   Thatcher, G. R. J., *The Anomeric Effect and Associated Stereoelectronic Effects*. American Chemical Society: 1993.

30.   Fortes, A. D.; Wood, I. G.; Knight, K. S., The crystal structure of perdeuterated methanol monoammoniate (CD3OD.ND3) determined from neutron powder diffraction data at 4.2 and 180 K. *Journal of Applied Crystallography* **2009,** *42* (6), 1054-1061.

31.   Ruscic, B.; Bross, D. H., Active Thermochemical Tables (ATcT) values based on ver. 1.122p of the Thermochemical Network. ATcT.anl.gov, 2020.

32.   Agapito, F.; Cabral, B. J. C.; Simões, J. A. M., Carbon–hydrogen bond dissociation enthalpies in ethers: a theoretical study. *Journal of Molecular Structure: THEOCHEM* **2005,** *719* (1), 109-114.

33.   Menon, A. S.; Wood, G. P. F.; Moran, D.; Radom, L., Bond dissociation energies and radical stabilization energies: An assessment of contemporary theoretical procedures. *The Journal of Physical Chemistry A* **2007,** *111* (51), 13638-13644.

34.   Vatsadze, S. Z.; Loginova, Y. D.; Gomes, G. D.; Alabugin, I. V., Stereoelectronic Chameleons: The Donor-Acceptor Dichotomy of Functional Groups. *Chem-Eur J* **2017,** *23* (14), 3225-3245.

35.   Korth, H. G.; Sustmann, R.; Giese, B.; Ruckert, B.; Groninger, K. S., Electron-Spin-Resonance Spectroscopic Investigation of Carbohydrate Radicals .6. Conformational Effects in 2-Deoxyglucopyranos-1-Yl Radicals. *Chemische Berichte* **1990,** *123* (9), 1891-1898.

36.   Agapito, F.; Cabral, B.; Simões, J., Carbon-hydrogen bond dissociation enthalpies in ethers: A theoretical study. *J. Mol. Struct. Theochem.* **2005,** *719*, 109-114.

37.   Chen, M. S.; White, M. C., Combined Effects on Selectivity in Fe-Catalyzed Methylene Oxidation. *Science* **2010,** *327* (5965), 566-571.

38.   Yoshimitsu, T.; Arano, Y.; Nagaoka, H., Radical alpha-C-H hydroxyalkylation of ethers and acetal. *The Journal of Organic Chemistry* **2005,** *70* (6), 2342-2345.

39.   Malatesta, V.; Ingold, K. U., Kinetic Applications of Electron-Paramagnetic Resonance Spectroscopy .36. Stereoelectronic Effects in Hydrogen-Atom Abstraction from Ethers. *Journal of the American Chemical Society* **1981,** *103* (3), 609-614.

40.   Shtarev, A. B.; Tian, F.; Dolbier, W. R.; Smart, B. E., Absolute rates of intermolecular carbon-hydrogen abstraction reactions by fluorinated radicals. *Journal of the American Chemical Society* **1999,** *121* (32), 7335-7341.

41.   Vil, V. A.; Grishin, S. S.; Baberkina, E. P.; Kostyagina, V. A.; Kovalenko, A. E.; Terent'ev, A. O., Radical addition of tetrahydrofuran to imines assisted by tert-butyl hydroperoxide. *Tetrahedron Lett.* **2020,** *61* (30).

42.   Cheng, K.; Huang, L.; Zhang, Y., CuBr-Mediated Oxyalkylation of Vinylarenes under Aerobic Conditions via Cleavage of sp3 C–H Bonds α to Oxygen. *Org Lett* **2009,** *11* (13), 2908-2911.

43.   Dian, L.; Zhao, H.; Zhang-Negrerie, D.; Du, Y., Cobalt-Catalyzed Twofold Direct C(sp2)–C(sp3) Bond Coupling: Regioselective C-3 Alkylation of Coumarins with (Cyclo)alkyl Ethers. *Adv Synth Catal* **2016,** *358* (15), 2422-2426.

44.   Li, Z.; Wei, Q.; Song, L.; Han, W.; Wu, X.; Zhao, Y.; Xia, F.; Liu, S., Highly Regioselective Radical Transformation of N-Sulfonyl-1,2,3-triazoles in Air. *Org Lett* **2019,** *21* (16), 6413-6417.

45.   Huang, C.-Y.; Li, J.; Liu, W.; Li, C.-J., Diacetyl as a "traceless" visible light photosensitizer in metal-free cross-dehydrogenative coupling reactions. *Chemical Science* **2019,** *10* (19), 5018-5024.

46.   Sun, H.; Zhang, Y.; Guo, F.; Zha, Z.; Wang, Z., Regioselective Oxyalkylation of Vinylarenes Catalyzed by Diatomite-Supported Manganese Oxide Nanoparticles. *The Journal of Organic Chemistry* **2012,** *77* (7), 3563-3569.

47.   Doan, S. H.; Nguyen, V. H. H.; Nguyen, T. H.; Pham, P. H.; Nguyen, N. N.; Phan, A. N. Q.; Tu, T. N.; Phan, N. T. S., Cross-dehydrogenative coupling of coumarins with Csp3–H bonds using an iron–organic framework as a productive heterogeneous catalyst. *Rsc Adv* **2018,** *8* (20), 10736-10745.

48.   Quattrini, M. C.; Fujii, S.; Yamada, K.; Fukuyama, T.; Ravelli, D.; Fagnoni, M.; Ryu, I., Versatile cross-dehydrogenative coupling of heteroaromatics and hydrogen donors via decatungstate photocatalysis. *Chem Commun* **2017,** *53* (15), 2335-2338.

49.   Li, Q.; Hu, W. P.; Hu, R. J.; Lu, H. J.; Li, G. G., Cobalt-Catalyzed Cross-Dehydrogenative Coupling Reaction between Unactivated C(sp(2))-H and C(sp(3))-H Bonds. *Org Lett* **2017,** *19* (17), 4676-4679.

50.   Shields, B. J.; Doyle, A. G., Direct C(sp(3))-H Cross Coupling Enabled by Catalytic Generation of Chlorine Radicals. *Journal of the American Chemical Society* **2016,** *138* (39), 12719-12722.

51.   Abe, H.; Terauchi, M.; Matsuda, A.; Shuto, S., A Study on the Conformation–Anomeric Effect–Stereoselectivity Relationship in Anomeric Radical Reactions, Using Conformationally Restricted Glucose Derivatives as Substrates. *The Journal of Organic Chemistry* **2003,** *68* (19), 7439-7447.

52.   Tamura, S.; Abe, H.; Matsuda, A.; Shuto, S., Control of α/β Stereoselectivity in Lewis Acid Promoted C-Glycosidations Using a Controlling Anomeric Effect Based on the Conformational Restriction Strategy. *Angewandte Chemie International Edition* **2003,** *42* (9), 1021-1023.

53.   Sagadevan, A.; Hwang, K. C.; Su, M. D., Singlet oxygen-mediated selective C-H bond hydroperoxidation of ethereal hydrocarbons. *Nat Commun* **2017,** *8*, 1812.

54.   Asensio, G.; Castellano, G.; Mello, R.; Nunez, M. E. G., Oxyfunctionalization of aliphatic esters by methyl(trifluoromethyl)dioxirane. *The Journal of Organic Chemistry* **1996,** *61* (16), 5564-5566.

55.   Gonzalez-Nunez, M. E.; Castellano, G.; Andreu, C.; Royo, J.; Baguena, M.; Mello, R.; Asensio, G., Influence of remote substituents on the equatorial/axial selectivity in the monooxygenation of methylene C-H bonds of substituted cyclohexanes. *Journal of the American Chemical Society* **2001,** *123* (31), 7487-7491.

56.   Yun, S. Y.; Zheng, J.-C.; Lee, D., Stereoelectronic Effect for the Selectivity in C−H Insertion of Alkylidene Carbenes and Its Application to the Synthesis of Platensimycin. *Journal of the American Chemical Society* **2009,** *131* (24), 8413-8415.

57.   Adams, J.; Poupart, M. A.; Grenier, L.; Schaller, C.; Ouimet, N.; Frenette, R., Rhodium Acetate Catalyzes the Addition of Carbenoids Alpha-Oxygens to Ether Oxygens. *Tetrahedron Lett* **1989,** *30* (14), 1749-1752.

58.   Davies, H. M. L.; Beckwith, R. E. J.; Antoulinakis, E. G.; Jin, Q. H., New strategic reactions for organic synthesis: Catalytic asymmetric C-H activation alpha to oxygen as a surrogate to the aldol reaction. *The Journal of Organic Chemistry* **2003,** *68* (16), 6126-6132.

59.   Liang, C. G.; Robert-Pedlard, F.; Fruit, C.; Muller, P.; Dodd, R. H.; Dauban, P., Efficient diastereoselective intermolecular rhodium-catalyzed C-H amination. *Angew Chem Int Edit* **2006,** *45* (28), 4641-4644.

60.   Newhouse, T.; Baran, P. S., If C-H Bonds Could Talk: Selective C-H Bond Oxidation. *Angew Chem Int Edit* **2011,** *50* (15), 3362-3374.

61.   Peng, B.; Maulide, N., The Redox-Neutral Approach to C-H Functionalization. *Chem-Eur J* **2013,** *19* (40), 13274-13287.

62.   Haibach, M. C.; Seidel, D., C similar to H Bond Functionalization through Intramolecular Hydride Transfer**. *Angew Chem Int Edit* **2014,** *53* (20), 5010-5036.

63.   Yoshimatsu, M.; Hatae, N.; Shimizu, H.; Kataoka, T., 1,7-Acetal Carbon Rearrangement Via 1,5-Hydride Transfer in an Oxocanyl Carbenium Ion - Conversion of O-(5-Hexenyl)-Se,O-Heteroacetals or O,O-Acetals into 7-Oxohexanols or 7-Oxohexyl Chlorides. *Chem Lett* **1993,** (9), 1491-1494.

64.   Smith, W. B., Hydrogen as a migrating group in some pinacol -rearrangements: a DFT study. *J Phys Org Chem* **1999,** *12* (10), 741-746.

65.   Li, J.; Preinfalk, A.; Maulide, N., Enantioselective Redox-Neutral Coupling of Aldehydes and Alkenes by an Iron-Catalyzed "Catch-Release" Tethering Approach. *Journal of the American Chemical Society* **2019,** *141* (1), 143-147.

66.   Gilmore, K.; Mohamed, R. K.; Alabugin, I. V., The Baldwin rules: revised and extended. *Wires Comput Mol Sci* **2016,** *6* (5), 487-514.

67.   Wang, B.; Gandamana, D. A.; Gagosz, F.; Chiba, S., Diastereoselective Intramolecular Hydride Transfer under Bronsted Acid Catalysis. *Org Lett* **2019,** *21* (7), 2298-2301.

68.   Vadola, P. A.; Sames, D., C-H bond functionalization via hydride transfer: direct coupling of unactivated alkynes and sp(3) C-H bonds catalyzed by platinum tetraiodide. *Journal of the American Chemical Society* **2009,** *131* (45), 16525-16528.

69.   Jurberg, I. D.; Odabachian, Y.; Gagosz, F., Hydroalkylation of Alkynyl Ethers via a Gold(I)-Catalyzed 1,5-Hydride Shift/Cyclization Sequence. *Journal of the American Chemical Society* **2010,** *132* (10), 3543-3552.

70.   Somsak, L., Carbanionic reactivity of the anomeric center in carbohydrates. *Chem Rev* **2001,** *101* (1), 81-135.

71.   Florio, S.; Perna, F. M.; Salomone, A.; Vitale, P., 1.14 Oxygen-Stabilized Carbanions. In *Comprehensive Organic Synthesis II (Second Edition)*, Knochel, P., Ed. Elsevier: Amsterdam, 2014; pp 471-515.

72.   Zhu, F.; Walczak, M. A., Stereochemistry of transition metal complexes controlled by the metallo-anomeric effect. *Journal of the American Chemical Society* **2020**.

73.   Bordwell, F. G.; Liu, W. Z., Effects of sulfenyl, sulfinyl and sulfonyl groups on acidities and homolytic bond dissociation energies of adjacent C-H and N-H bonds. *J Phys Org Chem* **1998,** *11* (6), 397-406.

74.   Cohen, T.; Matz, J. R., A General Preparative Method for Alpha-Lithioethers and Its Application to a Concise, Practical Synthesis of Brevicomin. *Journal of the American Chemical Society* **1980,** *102* (22), 6900-6902.

75.   Cohen, T.; Lin, M. T., 2-Flask Preparation of Alpha-Lithio Cyclic Ethers from Gamma-Lactones and Delta-Lactones - Reductive Lithiation as a Route, Via Radical Intermediates, to Axial 2-Lithiotetrahydropyrans and Their Equilibration to the Equatorial Isomers. *Journal of the American Chemical Society* **1984,** *106* (4), 1130-1131.

76.   Rychnovsky, S. D.; Mickus, D. E., Preparation of 2-Lithiotetrahydropyrans - Kinetic and Thermodynamic Generation of Alkyllithium Reagents. *Tetrahedron Lett.* **1989,** *30* (23), 3011-3014.

77.   Alabugin, I. V.; Bresch, S.; Gomes, G. D., Orbital hybridization: a key electronic factor in control of structure and reactivity. *J Phys Org Chem* **2015,** *28* (2), 147-162.

78.   Hoang, K. M.; Lees, N. R.; Herzon, S. B., Programmable Synthesis of 2-Deoxyglycosides. *Journal of the American Chemical Society* **2019,** *141* (20), 8098-8103.

79.   Alabugin, I. V.; Manoharan, M., Effect of double-hyperconjugation on the apparent donor ability of sigma-bonds: Insights from the relative stability of delta-substituted cyclohexyl cations. *The Journal of Organic Chemistry* **2004,** *69* (26), 9011-9024.

80.   Alabugin, I. V.; Zeidan, T. A., Stereoelectronic effects and general trends in hyperconjugative acceptor ability of sigma bonds. *Journal of the American Chemical Society* **2002,** *124* (12), 3175-3185.

81.   Haines, B. E.; Sarpong, R.; Musaev, D. G., Generality and Strength of Transition Metal β-Effects. *Journal of the American Chemical Society* **2018,** *140* (33), 10612-10618.

82.   Ye, J.; Bhatt, R. K.; Falck, J. R., Stereospecific palladium/copper cocatalyzed cross-coupling of .alpha.-alkoxy- and .alpha.-aminostannanes with acyl chlorides. *Journal of the American Chemical Society* **1994,** *116* (1), 1-5.

83.   Luescher, M. U.; Geoghegan, K.; Nichols, P. L.; Bode, J. W., SnAP Reagents for a Cross-Coupling Approach to the One-Step Synthesis of Saturated N-Heterocycles. *Aldrichim Acta* **2015,** *48* (2), 43-48.

84.   Luescher, M. U.; Bode, J. W., SnAP-eX Reagents for the Synthesis of Exocyclic 3-Amino- and 3-Alkoxypyrrolidines and Piperidines from Aldehydes. *Org Lett* **2016,** *18* (11), 2652-2655.

85.   Luescher, M. U.; Bode, J. W., Catalytic Synthesis of N-Unprotected Piperazines, Morpholines, and Thiomorpholines from Aldehydes and SnAP Reagents. *Angewandte Chemie International Edition* **2015,** *127* (37), 11034-11038.

86.   Li, H.; He, A.; Falck, J. R.; Liebeskind, L. S., Stereocontrolled Synthesis of α-Amino-α'-alkoxy Ketones by a Copper-Catalyzed Cross-Coupling of Peptidic Thiol Esters and α-Alkoxyalkylstannanes. *Org Lett* **2011,** *13* (14), 3682-3685.

87.   Zhu, F.; Zhang, S.-q.; Chen, Z.; Rui, J.; Hong, X.; Walczak, M. A., Catalytic and Photochemical Strategies to Stabilized Radicals Based on Anomeric Nucleophiles. *Journal of the American Chemical Society* **2020,** *142* (25), 11102-11113.

88.   Molander, G. A.; Wisniewski, S. R., Stereospecific Cross-Coupling of Secondary Organotrifluoroborates: Potassium 1-(Benzyloxy)alkyltrifluoroborates. *Journal of the American Chemical Society* **2012,** *134* (40), 16856-16868.

89.   Wender, P. A.; Hilinski, M. K.; Mayweg, A. V. W., Late-Stage Intermolecular CH Activation for Lead Diversification: A Highly Chemoselective Oxyfunctionalization of the C-9 Position of Potent Bryostatin Analogues. *Org Lett* **2005,** *7* (1), 79-82.

90.   Dantignana, V.; Milan, M.; Cussó, O.; Company, A.; Bietti, M.; Costas, M., Chemoselective Aliphatic C–H Bond Oxidation Enabled by Polarity Reversal. *ACS Central Science* **2017,** *3* (12), 1350-1358.

91.   Alabugin, I. V.; Bresch, S.; Manoharan, M., Hybridization Trends for Main Group Elements and Expanding the Bent's Rule Beyond Carbon: More than Electronegativity. *The Journal of Physical Chemistry A* **2014,** *118* (20), 3663-3677.

92.   Zhang, L.; Cradlebaugh, J.; Litwinienko, G.; Smart, B. E.; Ingold, K. U.; Dolbier, J. W. R., Absolute rate constants for some hydrogen atom abstraction reactions by a primary fluoroalkyl radical in water. *Organic & Biomolecular Chemistry* **2004,** *2* (5), 689.

93.   Morris, M.; Chan, B.; Radom, L., Effect of Protonation State and Interposed Connector Groups on Bond Dissociation Enthalpies of Alcohols and Related Systems. *The Journal of Physical Chemistry A* **2014,** *118* (15), 2810-2819.

94.   Gawlita, E.; Lantz, M.; Paneth, P.; Bell, A. F.; Tonge, P. J.; Anderson, V. E., H-Bonding in Alcohols Is Reflected in the Cα–H Bond Strength: Variation of C–D Vibrational Frequency and Fractionation Factor. *Journal of the American Chemical Society* **2000,** *122* (47), 11660-11669.

95.   Maiti, N. C.; Zhu, Y.; Carmichael, I.; Serianni, A. S.; Anderson, V. E., 1JCH correlates with alcohol hydrogen bond strength. *J Org Chem* **2006,** *71* (7), 2878-80.

96.   Wessig, P.; Muehling, O., Spin-Center Shift (SCS) – A Versatile Concept in Biological and Synthetic Chemistry. *Eur J Org Chem* **2007,** *2007* (14), 2219-2232.

97.   Jeffrey, J. L.; Terrett, J. A.; Macmillan, D. W. C., O-H hydrogen bonding promotes H-atom transfer from C-H bonds for C-alkylation of alcohols. *Science* **2015,** *349* (6255), 1532-1536.

98.   Jin, J.; Macmillan, D. W. C., Alcohols as alkylating agents in heteroarene C–H functionalization. *Nature* **2015,** *525* (7567), 87-90.

99.   Deslongchamps, P.; Rowan, D. D.; Pothier, N., The acid-catalyzed oxido-reduction of spiroketals. Evidence for stereoelectronic control in hydride transfer to cyclic oxenium ions. *Can J Chem* **1981,** *59* (18), 2787-2802.

100.   De Graauw, C. F.; Peters, J. A.; Vanbekkum, H.; Huskens, J., Meerwein-Ponndorf-Verley Reductions and Oppenauer Oxidations - an Integrated Approach. *Synthesis* **1994,** (10), 1007-1017.

101.   Hayon, E.; Ibata, T.; Lichtin, N. N.; Simic, M., Electron and hydrogen atom attachment to aromatic carbonyl compounds in aqueous solution. Absorption spectra and dissociation constants of ketyl radicals. *The Journal of Physical Chemistry* **1972,** *76* (15), 2072-2078.

102.   Barroso, M.; Arnaut, L. G.; Formosinho, S. J., Tunnelling corrections in hydrogen abstractions by excited-state ketones. *J Phys Org Chem* **2010,** *23* (7), 702-710.

103.   Wishart, D. S.; Tzur, D.; Knox, C.; Eisner, R.; Guo, A. C.; Young, N.; Cheng, D.; Jewell, K.; Arndt, D.; Sawhney, S.; Fung, C.; Nikolai, L.; Lewis, M.; Coutouly, M. A.; Forsythe, I.; Tang, P.; Shrivastava, S.; Jeroncic, K.; Stothard, P.; Amegbey, G.; Block, D.; Hau, D. D.; Wagner, J.; Miniaci, J.; Clements, M.; Gebremedhin, M.; Guo, N.; Zhang, Y.; Duggan, G. E.; Macinnis, G. D.; Weljie, A. M.; Dowlatabadi, R.; Bamforth, F.; Clive, D.; Greiner, R.; Li, L.; Marrie, T.; Sykes, B. D.; Vogel, H. J.; Querengesser, L., HMDB: the Human Metabolome Database. *Nucleic Acids Res* **2007,** *35* (Database issue), D521-6.

104.   So, S.; Kirk, B. B.; Wille, U.; Trevitt, A. J.; Blanksby, S. J.; da Silva, G., Reactions of a distonic peroxyl radical anion influenced by SOMO-HOMO conversion: an example of anion-directed channel switching. *Physical Chemistry Chemical Physics* **2020,** *22* (4), 2130-2141.

105.   Evans, D. A.; Golob, A. M., [3,3] Sigmatropic rearrangements of 1,5-diene alkoxides. Powerful accelerating effects of the alkoxide substituent. *Journal of the American Chemical Society* **1975,** *97* (16), 4765-4766.

106.   Koreeda, M.; Luengo, J. I., The anionic oxy-claisen rearrangement of enolates of .alpha.-allyloxy ketones. A remarkable rate accelerating effect exhibited by the nature of the counterion. *Journal of the American Chemical Society* **1985,** *107* (19), 5572-5573.

107.   Jansma, M. J.; Hoye, T. R., Oxyanionic Sigmatropic Rearrangements Relevant to Cyclooctadienone Formation in Penostatins I and F. *Org Lett* **2012,** *14* (18), 4738-4741.

108.   Chogii, I.; Das, P.; Fell, J. S.; Scott, K. A.; Crawford, M. N.; Houk, K. N.; Njardarson, J. T., New Class of Anion-Accelerated Amino-Cope Rearrangements as Gateway to Diverse Chiral Structures. *Journal of the American Chemical Society* **2017,** *139* (37), 13141-13146.

109.   Bunnage, M. E.; Nicolaou, K. C., The Oxide Anion Accelerated Retro-Diels-Alder Reaction. *Chem-Eur J* **1997,** *3* (2), 187-192.

110.   Baumann, H.; Chen, P., Density Functional Study of the Oxy-Cope Rearrangement. *Helvetica Chimica Acta* **2001,** *84* (1), 124-140.

111.   Evoniuk, C. J.; Gomes, G. d. P.; Hill, S. P.; Fujita, S.; Hanson, K.; Alabugin, I. V., Coupling N–H Deprotonation, C–H Activation, and Oxidation: Metal-Free C(sp3)–H Aminations with Unprotected Anilines. *Journal of the American Chemical Society* **2017,** *139* (45), 16210-16221.

112.   Mondal, S.; Gold, B.; Mohamed, R. K.; Alabugin, I. V., Design of Leaving Groups in Radical C☐C Fragmentations: Through-Bond 2c-3e Interactions in Self-Terminating Radical Cascades. *Chem-Eur J* **2014,** *20* (28), 8664-8669.

113.   Mohamed, R. K.; Mondal, S.; Gold, B.; Evoniuk, C. J.; Banerjee, T.; Hanson, K.; Alabugin, I. V., Alkenes as Alkyne Equivalents in Radical Cascades Terminated by Fragmentations: Overcoming Stereoelectronic Restrictions on Ring Expansions for the Preparation of Expanded Polyaromatics. *Journal of the American Chemical Society* **2015,** *137* (19), 6335-6349.

114.   Evoniuk, C. J.; Gomes, G. d. P.; Ly, M.; White, F. D.; Alabugin, I. V., Coupling Radical Homoallylic Expansions with C–C Fragmentations for the Synthesis of Heteroaromatics: Quinolines from Reactions of o-Alkenylarylisonitriles with Aryl, Alkyl, and Perfluoroalkyl Radicals. *The Journal of Organic Chemistry* **2017,** *82* (8), 4265-4278.

115.   Lübbesmeyer, M.; Mackay, E. G.; Raycroft, M. A. R.; Elfert, J.; Pratt, D. A.; Studer, A., Base-Promoted C–C Bond Activation Enables Radical Allylation with Homoallylic Alcohols. *Journal of the American Chemical Society* **2020,** *142* (5), 2609-2616.

116.   Dewanji, A.; Mück-Lichtenfeld, C.; Studer, A., Radical Hydrodeiodination of Aryl, Alkenyl, Alkynyl, and Alkyl Iodides with an Alcoholate as Organic Chain Reductant through Electron Catalysis. *Angewandte Chemie International Edition* **2016,** *55* (23), 6749-6752.

117.   Eschenmoser, A.; Frey, A., Über die Spaltung des Mesylesters von 2-Methyl-2-oxymethyl-cyclopentanon mit Basen. *Helvetica Chimica Acta* **1952,** *35* (5), 1660-1666.

118.   Grob, C. A.; Baumann, W., Die 1,4-Eliminierung unter Fragmentierung. *Helvetica Chimica Acta* **1955,** *38* (3), 594-610.

119.   Wharton, P. S.; Hiegel, G. A., Fragmentation of 1,10-Decalindiol Monotosylates1. *The Journal of Organic Chemistry* **1965,** *30* (9), 3254-3257.

120.   Caine, D., Wharton Fragmentations of Cyclic 1,3-Diol Derivatives - a Review. *Organic Preparations and Procedures International* **1988,** *20* (1-2), 1-&.

121.   Holton, R. A., Synthesis of the Taxane Ring-System. *Journal of the American Chemical Society* **1984,** *106* (19), 5731-5732.

122.   Eschenmoser, A.; Felix, D.; Ohloff, G., Eine neuartige Fragmentierung cyclischer α, ß-ungesättigter Carbonylsysteme; Synthese von Exalton und rac-Muscon aus Cyclododecanon Vorläufige Mitteilung. *Helvetica Chimica Acta* **1967,** *50* (2), 708-713.

123.   Tanabe, M.; Crowe, D. F.; Dehn, R. L., A novel fragmentation reaction of α,β-epoxyketones the synthesis of acetylenic ketones. *Tetrahedron Lett* **1967,** *8* (40), 3943-3946.

124.   Hoang, T. T.; Dudley, G. B.; Williams, L. J., 6.19 Fragmentation Reactions. In *Comprehensive Organic Synthesis II (Second Edition)*, Knochel, P., Ed. Elsevier: Amsterdam, 2014; pp 842-860.

125.   Kamijo, S.; Dudley, G. B., A tandem carbanion addition/carbon-carbon bond cleavage yields alkynyl ketones. *Journal of the American Chemical Society* **2005,** *127* (14), 5028-5029.

126.   Yang, J. Y.; Hoang, T. T.; Dudley, G. B., Alkynogenic fragmentation. *Org Chem Front* **2019,** *6* (15), 2560-2569.

127.   Kolakowski, R. V.; Manpadi, M.; Zhang, Y.; Emge, T. J.; Williams, L. J., Allene Synthesis via C-C Fragmentation: Method and Mechanistic Insight. *Journal of the American Chemical Society* **2009,** *131* (36), 12910-+.

128.   Saget, T.; Cramer, N., Heteroatom-Nucleophile-Induced C-C Fragmentations: Synthesis of Allenes and Entry to Domino Reactions. *Angewandte Chemie International Edition* **2010,** *49* (47), 8962-8965.

129.   Laconsay, C. J.; Tsui, K. Y.; Tantillo, D. J., Tipping the balance: theoretical interrogation of divergent extended heterolytic fragmentations. *Chemical Science* **2020,** *11* (8), 2231-2242.

130.   Esselman, B. J.; Hill, N. J., Proper Resonance Depiction of Acylium Cation: A High-Level and Student Computational Investigation. *Journal of Chemical Education* **2015,** *92* (4), 660-663.

131.   Blanksby, S. J.; Ellison, G. B., Bond Dissociation Energies of Organic Molecules. *Accounts of Chemical Research* **2003,** *36* (4), 255-263.

132.   Chatgilialoglu, C.; Crich, D.; Komatsu, M.; Ryu, I., Chemistry of acyl radicals. *Chem Rev* **1999,** *99* (8), 1991-2069.

133.   Chatgilialoglu, C.; Lunazzi, L.; Macciantelli, D.; Placucci, G., Absolute rate constants for hydrogen abstraction from aldehydes and conformational studies of the corresponding aromatic acyl radicals. *Journal of the American Chemical Society* **1984,** *106* (18), 5252-5256.

134.   Berman, J. D.; Stanley, J. H.; Sherman, W. V.; Cohen, S. G., Sensitization and Catalysis of Light-Induced Decarbonylation of Aldehydes. *Journal of the American Chemical Society* **1963,** *85* (24), 4010-4013.

135.   Banerjee, A.; Lei, Z.; Ngai, M. Y., Acyl Radical Chemistry via Visible-Light Photoredox Catalysis. *Synthesis* **2019,** *51* (2), 303-333.

136.   Zhang, X. H.; MacMillan, D. W. C., Direct Aldehyde C-H Arylation and Alkylation via the Combination of Nickel, Hydrogen Atom Transfer, and Photoredox Catalysis. *Journal of the American Chemical Society* **2017,** *139* (33), 11353-11356.

137.   Lumb, J. P., Stopping Aerobic Oxidation in Its Tracks: Chemoselective Synthesis of Benzaldehydes from Methylarenes. *Angewandte Chemie International Edition* **2017,** *56* (32), 9276-9277.

138.   Gaster, E.; Kozuch, S.; Pappo, D., Selective Aerobic Oxidation of Methylarenes to Benzaldehydes Catalyzed by N-Hydroxyphthalimide and Cobalt(II) Acetate in Hexafluoropropan-2-ol. *Angewandte Chemie International Edition* **2017,** *56* (21), 5912-5915.

139.   Dirksen, A.; Dirksen, S.; Hackeng, T. M.; Dawson, P. E., Nucleophilic catalysis of hydrazone formation and transimination: Implications for dynamic covalent chemistry. *Journal of the American Chemical Society* **2006,** *128* (49), 15602-15603.

140.   Kool, E. T.; Park, D. H.; Crisalli, P., Fast Hydrazone Reactants: Electronic and Acid/Base Effects Strongly Influence Rate at Biological pH. *Journal of the American Chemical Society* **2013,** *135* (47), 17663-17666.

141.   Ulrich, S., Growing Prospects of Dynamic Covalent Chemistry in Delivery Applications. *Accounts of Chemical Research* **2019,** *52* (2), 510-519.

142.   Ji, Q.; Lirag, R. C.; Miljanic, O. S., Kinetically controlled phenomena in dynamic combinatorial libraries. *Chemical Society Reviews* **2014,** *43* (6), 1873-1884.

143.   Hutin, M.; Cramer, C. J.; Gagliardi, L.; Shahi, A. R. M.; Bernardinelli, G.; Cerny, R.; Nitschke, J. R., Self-sorting chiral subcomponent rearrangement during crystallization. *Journal of the American Chemical Society* **2007,** *129* (28), 8774-8780.

144.   Cantrill, S. J.; Chichak, K. S.; Peters, A. J.; Stoddart, J. F., Nanoscale borromean rings. *Accounts of Chemical Research* **2005,** *38* (1), 1-9.

145.   Lin, I.; Day, A. R., A Study of the Mixed Tischtschenko Reaction. *Journal of the American Chemical Society* **1952,** *74* (20), 5133-5135.

146.   Evans, D. A.; Hoveyda, A. H., Samarium-Catalyzed Intramolecular Tishchenko Reduction of Beta-Hydroxy Ketones - a Stereoselective Approach to the Synthesis of Differentiated Anti 1,3-Diol Monoesters. *Journal of the American Chemical Society* **1990,** *112* (17), 6447-6449.

147.   Mascarenhas, C. M.; Miller, S. P.; White, P. S.; Morken, J. P., First catalytic asymmetric aldol-Tishchenko reaction - Insight into the catalyst structure and reaction mechanism. *Angewandte Chemie International Edition* **2001,** *40* (3), 601-603.

148.   Asano, T.; Kotani, S.; Nakajima, M., Stereoselective Synthesis of 2-Fluoro-1,3-Diols via Lithium Binaphtholate-Catalyzed Aldol-Tishchenko Reaction. *Org Lett* **2019,** *21* (11), 4192-4196.

149.   Horiuchi, Y.; Gnanadesikan, V.; Ohshima, T.; Masu, H.; Katagiri, K.; Sei, Y.; Yamaguchi, K.; Shibasakita, M., Dynamic structural change of the self-assembled lanthanum complex induced by lithium triflate for direct catalytic asymmetric aldol-tishchenko reaction. *Chem-Eur J* **2005,** *11* (18), 5195-5204.

150.   Mlynarski, J.; Rakiel, B.; Stodulski, M.; Suszczynska, A.; Frelek, J., Chiral ytterbium complex-catalyzed direct asymmetric aldol-Tishchenko reaction: Synthesis of anti-1,3-diols. *Chem-Eur J* **2006,** *12* (31), 8158-8167.

151.   Ichibakase, T.; Nakajima, M., Direct Enantioselective Aldol-Tishchenko Reaction Catalyzed by Chiral Lithium Diphenylbinaphtholate. *Org Lett* **2011,** *13* (7), 1579-1581.

152.   Rohr, K.; Herre, R.; Mahrwald, R., Toward Asymmetric Aldol-Tishchenko Reactions with Enolizable Aldehydes: Access to Defined Configured Stereotriads, Tetrads, and Stereopentads. *The Journal of Organic Chemistry* **2009,** *74* (10), 3744-3749.

153.   Abu-Hasanayn, F.; Streitwieser, A., Kinetics and isotope effects of the Aldol-Tishchenko reaction between lithium enolates and aldehydes. *The Journal of Organic Chemistry* **1998,** *63* (9), 2954-2960.

154.   Chen, Z. W.; Aota, Y.; Nguyen, H. M. H.; Dong, V. M., Dynamic Kinetic Resolution of Aldehydes by Hydroacylation. *Angewandte Chemie International Edition* **2019,** *58* (14), 4705-4709.

155.   Murphy, S. K.; Dong, V. M., Enantioselective hydroacylation of olefins with rhodium catalysts. *Chem Commun* **2014,** *50* (89), 13645-13649.

156.   Willis, M. C., Transition Metal Catalyzed Alkene and Alkyne Hydroacylation. *Chem Rev* **2010,** *110* (2), 725-748.

157.   Garralda, M. A., Aldehyde C-H activation with late transition metal organometallic compounds. Formation and reactivity of acyl hydrido complexes. *Dalton Transaction* **2009,** (19), 3635-3645.

158.   Fairlie, D. P.; Bosnich, B., Homogeneous catalysis. Conversion of 4-pentenals to cyclopentanones by efficient rhodium-catalyzed hydroacylation. *Organometallics* **1988,** *7* (4), 936-945.

159.   Fairlie, D. P.; Bosnich, B., Homogeneous catalysis. Mechanism of catalytic hydroacylation: the conversion of 4-pentenals to cyclopentanones. *Organometallics* **1988,** *7* (4), 946-954.

160.   Zimmerman, H. E.; Alabugin, I. V., Excited state energy distribution and redistribution and chemical reactivity; Mechanistic and exploratory organic photochemistry. *Journal of the American Chemical Society* **2000,** *122* (5), 952-953.

161.   Morton, D. R.; Lee-Ruff, E.; Southam, R. M.; Turro, N. J., Molecular photochemistry. XXVII. Photochemical ring expansion of cyclobutanone, substituted cyclobutanones, and related cyclic ketones. *Journal of the American Chemical Society* **1970,** *92* (14), 4349-4357.

162.   dos Passos Gomes, G.; Wimmer, A.; Smith, J. M.; König, B.; Alabugin, I. V., CO2 or SO2: Should It Stay, or Should It Go? *The Journal of Organic Chemistry* **2019,** *84* (10), 6232-6243.

163.   Harris, T.; Gomes, G. d. P.; Clark, R. J.; Alabugin, I. V., Domino Fragmentations in Traceless Directing Groups of Radical Cascades: Evidence for the Formation of Alkoxy Radicals via C–O Scission. *The Journal of Organic Chemistry* **2016,** *81* (14), 6007-6017.

164.   Murakami, M.; Ishida, N., β-Scission of Alkoxy Radicals in Synthetic Transformations. *Chem Lett* **2017,** *46* (12), 1692-1700.

165.   Gao, P.; Wu, H.; Yang, J.-C.; Guo, L. N., Iron-Catalyzed Decarboxylative Olefination of Unstrained Carbon–Carbon Bonds Relying on Alkoxyl Radical Induced Cascade. *Org Lett* **2019,** *21* (17), 7104-7108.

166.   Walling, C.; Padwa, A., Positive Halogen Compounds. VI. Effects of Structure and Medium on the β-Scission of Alkoxy Radicals. *Journal of the American Chemical Society* **1963,** *85* (11), 1593-1597.

167.   Deng, Y.; Nguyen, M. D.; Zou, Y.; Houk, K. N.; Smith, A. B., Generation of Dithianyl and Dioxolanyl Radicals Using Photoredox Catalysis: Application in the Total Synthesis of the Danshenspiroketallactones via Radical Relay Chemistry. *Org Lett* **2019,** *21* (6), 1708-1712.

168.   Zlotorzynska, M.; Sammis, G. M., Photoinduced Electron-Transfer-Promoted Redox Fragmentation of N-Alkoxyphthalimides. *Org Lett* **2011,** *13* (23), 6264-6267.

169.   Rueda-Becerril, M.; Leung, J. C. T.; Dunbar, C. R.; Sammis, G. M., Alkoxy Radical Cyclizations onto Silyl Enol Ethers Relative to Alkene Cyclization, Hydrogen Atom Transfer, and Fragmentation Reactions. *The Journal of Organic Chemistry* **2011,** *76* (19), 7720-7729.

170.	Zhu, H.; Leung, J. C. T.; Sammis, G. M., Strategies to Control Alkoxy Radical-Initiated Relay Cyclizations for the Synthesis of Oxygenated Tetrahydrofuran Motifs. *The Journal of Organic Chemistry* **2015,** *80* (2), 965-979.

171.	Hernández-Guerra, D.; Kennedy, A. R.; León, E. I.; Martín, Á.; Pérez-Martín, I.; Rodríguez, M. S.; Suárez, E., Synthetic Approaches to Phosphasugars (2-oxo-1,2-oxaphosphacyclanes) Using the Anomeric Alkoxyl Radical β-Fragmentation Reaction as the Key Step. *The Journal of Organic Chemistry* **2020,** *85* (7), 4861-4880.

172.	Ishida, N.; Sawano, S.; Murakami, M., Stereospecific ring expansion from orthocyclophanes with central chirality to metacyclophanes with planar chirality. *Nat Commun* **2014,** *5* (1), 3111.

173.	Zhao, P.; Incarvito, C. D.; Hartwig, J. F., Direct Observation of β-Aryl Eliminations from Rh(I) Alkoxides. *Journal of the American Chemical Society* **2006,** *128* (10), 3124-3125.

174.	Gomes, G. D.; Loginova, Y.; Vatsadze, S. Z.; Alabugin, I. V., Isonitriles as Stereoelectronic Chameleons: The Donor-Acceptor Dichotomy in Radical Additions. *Journal of the American Chemical Society* **2018,** *140* (43), 14272-14288.

175.	Peterson, P. W.; Shevchenko, N.; Breiner, B.; Manoharan, M.; Lufti, F.; Delaune, J.; Kingsley, M.; Kovnir, K.; Alabugin, I. V., Orbital Crossings Activated through Electron Injection: Opening Communication between Orthogonal Orbitals in Anionic C1-C5 Cyclizations of Enediynes. *Journal of the American Chemical Society* **2016,** *138* (48), 15617-15628.

176.	Streitwieser, A., *Solvolytic Displacement Reactions*. McGraw-Hill: New York, 1964; p 214.

177.	Ballinger, P.; De La Mare, P. B. D.; Kohnstam, G.; Prestt, B. M., The reaction of chlorodimethyl ether with ethanol and with ethoxide ions. *Journal of the Chemical Society* **1955**, 3641 - 3647.

178.	Dussault, P.; Sahli, A., 2-Methoxyprop-2-Yl Hydroperoxide - a Convenient Reagent for the Synthesis of Hydroperoxides and Peracids. *The Journal of Organic Chemistry* **1992,** *57* (3), 1009-1012.

179.	Kyasa, S.; Meier, R. N.; Pardini, R. A.; Truttmann, T. K.; Kuwata, K. T.; Dussault, P. H., Synthesis of Ethers via Reaction of Carbanions and Monoperoxyacetals. *The Journal of Organic Chemistry* **2015,** *80* (24), 12100-12114.

180.	Terent'ev, A. O.; Kutkin, A. V.; Starikova, Z. A.; Antipin, M. Y.; Ogibin, Y. N.; Nikishin, G. I., New preparation of 1,2,4,5-tetraoxanes. *Synthesis* **2004,** (14), 2356-2366.

181.	Terent'ev, A. O.; Borisov, D. A.; Yaremenko, I. A., General methods for the preparation of 1,2,4,5-tetraoxanes - key structures for the development of peroxidic antimalarial agents. *Chem. Heterocycl. Comp.* **2012,** *48* (1), 55-58.

182.	Terent'ev, A. O.; Platonov, M. M.; Sonneveld, E. J.; Peschar, R.; Chernyshev, V. V.; Starikova, Z. A.; Nikishin, G. I., New preparation of 1,2,4,5,7,8-hexaoxonanes. *The Journal of Organic Chemistry* **2007,** *72* (19), 7237-7243.

183.	Radulov, P. S.; Belyakova, Y. Y.; Demina, A. A.; Nikishin, G. I.; Yaremenko, I. A.; Terent'ev, A. O., Selective synthesis of cyclic triperoxides from 1,1-dihydroperoxydi(cycloalkyl)peroxides and acetals using SnCl4. *Russ. Chem. Bull* **2019,** *68* (6), 1289-1292.

184.   Schalley, C. A.; Harvey, J. N.; Schröder, D.; Schwarz, H., Ether Oxides: A New Class of Stable Ylides? A Theoretical Study of Methanol Oxide and Dimethyl Ether Oxide. *The Journal of Physical Chemistry A* **1998,** *102* (6), 1021-1035.

185.   Gomes, G. D.; Vil', V. A.; Terent'ev, A. O.; Alabugin, I. V., Stereoelectronic source of the anomalous stability of bis-peroxides. *Chemical Science* **2015,** *6* (12), 6783-6791.

186.   Ferrier, R. J., Unsaturated carbohydrates. Part 21. A carbocyclic ring closure of a hex-5-enopyranoside derivative. *Journal of the Chemical Society, Perkin Transactions 1* **1979,** (0), 1455-1458.

187.   Petasis, N. A.; Lu, S.-P., Stereocontrolled synthesis of substituted tetrahydropyrans from 1,3-dioxan-4-ones. *Tetrahedron Lett* **1996,** *37* (2), 141-144.

188.   Smith, A. B.; Fox, R. J.; Razler, T. M., Evolution of the Petasis–Ferrier Union/Rearrangement Tactic: Construction of Architecturally Complex Natural Products Possessing the Ubiquitous cis-2,6-Substituted Tetrahydropyran Structural Element. *Accounts of Chemical Research* **2008,** *41* (5), 675-687.

189.   Smith, A. B.; Bosanac, T.; Basu, K., Evolution of the Total Synthesis of (−)-Okilactomycin Exploiting a Tandem Oxy-Cope Rearrangement/Oxidation, a Petasis–Ferrier Union/Rearrangement, and Ring-Closing Metathesis. *Journal of the American Chemical Society* **2009,** *131* (6), 2348-2358.

190.   Bae, H. J.; Jeong, W.; Lee, J. H.; Rhee, Y. H., Gold(I)-Catalyzed Access to Tetrahydropyran-4-ones from 4-(Alkoxyalkyl)oxy-1-butynes: Formal Catalytic Petasis–Ferrier Rearrangement. *Chemistry - A European Journal* **2011,** *17* (5), 1433-1436.

191.   Liu, L.; Zhang, L., Access to electron-rich arene-fused hexahydroquinolizinones through a gold-catalysis-initiated cascade process. *Angewandte Chemie International Edition* **2012,** *51* (29), 7301-7304.

192.   Sze, E. M. L.; Rao, W.; Koh, M. J.; Chan, P. W. H., Gold-Catalyzed Tandem Intramolecular Heterocyclization/Petasis–Ferrier Rearrangement of 2-(Prop-2-ynyloxy)benzaldehydes as an Expedient Route to Benzo[b]oxepin-3(2 H)-ones. *Chem-Eur J* **2011,** *17* (5), 1437-1441.

193.   Gade, A. B.; Patil, N. T., Gold(I)-Catalyzed Hydroaminaloxylation and Petasis–Ferrier Rearrangement Cascade of Aminaloalkynes. *Org Lett* **2016,** *18* (8), 1844-1847.

194.   Aaseng, J. E.; Iqbal, N.; Sperger, C. A.; Fiksdahl, A., 3-Fluorotetrahydropyran-4-one derivatives from homopropargyl acetal. *Journal of Fluorine Chemistry* **2014,** *161* (1), 142-148.

195.   Pati, K.; Alabugin, I. V., Synthesis of Substituted Biaryls through Gold-Catalyzed Petasis–Ferrier Rearrangement of Propargyl Ethers. *Eur J Org Chem* **2014,** *2014* (19), 3986-3990.

196.   Alabugin, I.; Gonzalez-Rodriguez, E.; Kawade, R.; Stepanov, A.; Vasilevsky, S., Alkynes as Synthetic Equivalents of Ketones and Aldehydes: A Hidden Entry into Carbonyl Chemistry. *Molecules* **2019,** *24* (6), 1036-1073.

197.   Crich, D., Mechanism of a Chemical Glycosylation Reaction. *Accounts of Chemical Research* **2010,** *43* (8), 1144-1153.

198.   Klemm, D.; Heublein, B.; Fink, H. P.; Bohn, A., Cellulose: Fascinating biopolymer and sustainable raw material. *Angewandte Chemie International Edition* **2005,** *44* (22), 3358-3393.

199.   Cumpstey, I., On a so-called "kinetic anomeric effect" in chemical glycosylation. *Organic & Biomolecular Chemistry* **2012,** *10* (13), 2503-2508.

200.   Capon, B., Mechanism in carbohydrate chemistry. *Chem Rev* **1969,** *69* (4), 407-498.

201.   Hall, A. N.; Hollingshead, S.; Rydon, H. N., 845. The acid and alkaline hydrolysis of some substituted phenyl α-D-glucosides. *Journal of the Chemical Society* **1961,** (0), 4290-4295.

202.   Nigudkar, S. S.; Demchenko, A. V., Stereocontrolled 1,2-cis glycosylation as the driving force of progress in synthetic carbohydrate chemistry. *Chemical Science* **2015,** *6* (5), 2687-2704.

203.   Premathilake, H. D.; Demchenko, A. V., Superarmed and Superdisarmed Building Blocks in Expeditious Oligosaccharide Synthesis. *Reactivity Tuning in Oligosaccharide Assembly* **2011,** *301*, 189-221.

204.   Bohe, L.; Crich, D., A propos of glycosyl cations and the mechanism of chemical glycosylation; the current state of the art. *Carbohydrate Research* **2015,** *403*, 48-59.

205.   Adero, P. O.; Amarasekara, H.; Wen, P.; Bohé, L.; Crich, D., The Experimental Evidence in Support of Glycosylation Mechanisms at the SN1–SN2 Interface. *Chem Rev* **2018,** *118* (17), 8242-8284.

206.   Lee, S. S.; Greig, I. R.; Vocadlo, D. J.; McCarter, J. D.; Patrick, B. O.; Withers, S. G., Structural, Mechanistic, and Computational Analysis of the Effects of Anomeric Fluorines on Anomeric Fluoride Departure in 5-Fluoroxylosyl Fluorides. *Journal of the American Chemical Society* **2011,** *133* (40), 15826-15829.

207.   Schindler, B.; Barnes, L.; Renois, G.; Gray, C.; Chambert, S.; Fort, S.; Flitsch, S.; Loison, C.; Allouche, A. R.; Compagnon, I., Anomeric memory of the glycosidic bond upon fragmentation and its consequences for carbohydrate sequencing. *Nat Commun* **2017,** *8*.

208.   Pellegrinelli, R. P.; Yue, L.; Carrascosa, E.; Warnke, S.; Ben Faleh, A.; Rizzo, T. R., How General Is Anomeric Retention during Collision-Induced Dissociation of Glycans? *Journal of the American Chemical Society* **2020,** *142* (13), 5948-5951.

209.   Greis, K.; Mucha, E.; Lettow, M.; Thomas, D. A.; Kirschbaum, C.; Moon, S.; Pardo-Vargas, A.; von Helden, G.; Meijer, G.; Gilmore, K.; Seeberger, P. H.; Pagel, K., The Impact of Leaving Group Anomericity on the Structure of Glycosyl Cations of Protected Galactosides. *Chemphyschem* **2020**.

210.   Hosoya, T.; Takano, T.; Kosma, P.; Rosenau, T., Theoretical Foundation for the Presence of Oxacarbenium Ions in Chemical Glycoside Synthesis. *The Journal of Organic Chemistry* **2014,** *79* (17), 7889-7894.

211.   Chandrasekhar, S.; Kirby, A. J.; Martin, R. J., Stereoelectronic Effects at Oxygen - the Hydrolysis of 2-Aryloxy-Trans-1-Oxadecalins. *Journal of the Chemical Society, Perkin Transactions 2* **1983,** (11), 1619-1626.

212.   Kirby, A. J.; Martin, R. J., Stereoelectronic Control of the Hydrolysis of a Conformationally Locked Acetal. *Journal of the Chemical Society-Perkin Transactions 2* **1983,** (11), 1627-1632.

213.   Briggs, A. J.; Evans, C. M.; Glenn, R.; Kirby, A. J., Stereoelectronic effects at oxygen. A very large effect on the hydrolysis of a conformationally locked acetal: implications for β-glycosidase mechanisms. *Journal of the Chemical Society, Perkin Transactions 2* **1983,** (9), 1637-1640.

214.   Chatterjee, S.; Moon, S.; Hentschel, F.; Gilmore, K.; Seeberger, P. H., An Empirical Understanding of the Glycosylation Reaction. *Journal of the American Chemical Society* **2018,** *140* (38), 11942-11953.

215.   McCarter, J. D.; Withers, S. G., Mechanisms of enzymatic glycoside hydrolysis. *Curr. Opin. Struct. Biol.* **1994,** *4* (6), 885-92.

216.   Sinnott, M. L., Catalytic mechanism of enzymic glycosyl transfer. *Chem Rev* **1990,** *90* (7), 1171-1202.

217.   Luo, Y. R., *Handbook of Bond Dissociation Energies in Organic Compounds*. CRC Press: 2002.

218.   Tumanov, V., Calculation of the C-H bond dissociation energies in linear and cyclic acetals and thioacetals from kinetic data. *Petroleum Chemistry* **2005,** *45*, 350-363.

219.   Bergman, R. G., Reactive 1,4-dehydroaromatics. *Accounts of Chemical Research* **1973,** *6* (1), 25-31.

220.   Langley, D. R.; Golik, J.; Krishman, B.; Doyle, T. W.; Beveridge, D. L., The DNA-esperamicin A1 complex. A model based on solvated molecular dynamics simulations. *Journal of the American Chemical Society* **1994,** *116* (1), 15-29.

221.   Baroudi, A.; Mauldin, J.; Alabugin, I. V., Conformationally Gated Fragmentations and Rearrangements Promoted by Interception of the Bergman Cyclization through Intramolecular H-Abstraction: A Possible Mechanism of Auto-Resistance to Natural Enediyne Antibiotics? *Journal of the American Chemical Society* **2010,** *132* (3), 967-979.

222.   Zeidan, T. A.; Manoharan, M.; Alabugin, I. V., Ortho Effect in the Bergman Cyclization: Interception of p-Benzyne Intermediate by Intramolecular Hydrogen Abstraction. *The Journal of Organic Chemistry* **2006,** *71* (3), 954-961.

223.   Baroudi, A.; Alicea, J.; Flack, P.; Kirincich, J.; Alabugin, I. V., Radical O→C transposition: a metal-free process for conversion of phenols into benzoates and benzamides. *J. Org. Chem.* **2011,** *76* (6), 1521-37.

224.   Hayday, K.; Mckelvey, R. D., Photochemistry of Carbohydrate Model Compounds .2. Anomeric Effect in Photochemical Hydrogen Abstraction Reactions of Tetrahydropyranyl Ethers. *The Journal of Organic Chemistry* **1976,** *41* (12), 2222-2223.

225.   Beckwith, A. L. J.; Easton, C. J., Stereoelectronic effects in hydrogen atom abstraction from substituted 1,3-dioxanes. *Journal of the American Chemical Society* **1981,** *103* (3), 615-619.

226.   Nielsen, M. K.; Shields, B. J.; Liu, J.; Williams, M. J.; Zacuto, M. J.; Doyle, A. G., Mild, Redox-Neutral Formylation of Aryl Chlorides through the Photocatalytic Generation of Chlorine Radicals. *Angew. Chem.* **2017,** *56* (25), 7191-7194.

227.   Boultadakis-Arapinis, M.; Lemoine, P.; Turcaud, S.; Micouin, L.; Lecourt, T., Rh(II) Carbene-Promoted Activation of the Anomeric C–H Bond of Carbohydrates: A Stereospecific Entry toward α- and β-Ketopyranosides. *Journal of the American Chemical Society* **2010,** *132* (44), 15477-15479.

228.   Seitz, G.; Imming, P., Oxocarbons and Pseudooxocarbons. *Chem Rev* **1992,** *92* (6), 1227-1260.

229.   Yaremenko, I. A.; Gomes, G. D.; Radulov, P. S.; Belyakova, Y. Y.; Vilikotskiy, A. E.; Vil', V. A.; Korlyukov, A. A.; Nikishin, G. I.; Alabugin, I. V.; Terent'ev, A. O., Ozone-Free Synthesis of Ozonides: Assembling Bicyclic Structures from 1,5-Diketones and Hydrogen Peroxide. *The Journal of Organic Chemistry* **2018,** *83* (8), 4402-4426.

230.   Harvey, J. N.; Himo, F.; Maseras, F.; Perrin, L., Scope and Challenge of Computational Methods for Studying Mechanism and Reactivity in Homogeneous Catalysis. *ACS Catalysis* **2019,** *9* (8), 6803-6813.

231.   Drahoňovský, D.; Lehn, J.-M., Hemiacetals in Dynamic Covalent Chemistry: Formation, Exchange, Selection, and Modulation Processes. *The Journal of Organic Chemistry* **2009,** *74* (21), 8428-8432.

232.   Cacciapaglia, R.; Di Stefano, S.; Mandolini, L., Metathesis Reaction of Formaldehyde Acetals: An Easy Entry into the Dynamic Covalent Chemistry of Cyclophane Formation. *Journal of the American Chemical Society* **2005,** *127* (39), 13666-13671.

233.   Schaerfer, C.; Schulz-Gasch, T.; Ehrlich, H. C.; Guba, W.; Rarey, M.; Stahl, M., Torsion Angle Preferences in Druglike Chemical Space: A Comprehensive Guide. *J Med Chem* **2013,** *56* (5), 2016-2028.

234.   Blom, C. E.; Günthard, H. H., Rotational isomerism in methyl formate and methyl acetate; a low-temperature matrix infrared study using thermal molecular beams. *Chemical Physics Letters* **1981,** *84* (2), 267-271.

235.   Houk, K. N.; Jabbari, A.; Hall, H. K.; Alemán, C., Why δ-Valerolactone Polymerizes and γ-Butyrolactone Does Not. *The Journal of Organic Chemistry* **2008,** *73* (7), 2674-2678.

236.   Wiberg, K. B.; Wong, M. W., Solvent effects. 4. Effect of solvent on the E/Z energy difference for methyl formate and methyl acetate. *Journal of the American Chemical Society* **1993,** *115* (3), 1078-1084.

237.   de Kowalewski, D. G.; Kowalewski, V. J.; Contreras, R. H.; Diez, E.; Esteban, A. L., Conformational effects on C-13 NMR parameters in alkyl formates. *Magn Reson Chem* **1998,** *36* (5), 336-342.

238.   Michinori, O.; Hiroshi, N., Conformations of the Ester Group. *Bulletin of the Chemical Society of Japan* **1970,** *43* (8), 2558-2566.

239.   Zhao, Y.; Mouhib, H.; Li, G.; Kleiner, I.; Stahl, W., Conformational analysis of tert-butyl acetate using a combination of microwave spectroscopy and quantum chemical calculations. *Journal of Molecular Spectroscopy* **2016,** *322*, 38-42.

240.   Huisgen, R.; Ott, H., Die konfiguration der carbonestergruppe und die sondereigenschaften der lactone. *Tetrahedron* **1959,** *6* (3), 253-267.

241.   Alemán, C.; Betran, O.; Casanovas, J.; Houk, K. N.; Hall, H. K., Thermodynamic Control of the Polymerizability of Five-, Six-, and Seven-Membered Lactones. *The Journal of Organic Chemistry* **2009,** *74* (16), 6237-6244.

242.   Fortman, D. J.; Brutman, J. P.; Hillmyer, M. A.; Dichtel, W. R., Structural effects on the reprocessability and stress relaxation of crosslinked polyhydroxyurethanes. *Journal of Applied Polymer Science* **2017,** *134* (45), 44984.

243.   Nifant'ev, I.; Ivchenko, P., DFT Modeling of Organocatalytic Ring-Opening Polymerization of Cyclic Esters: A Crucial Role of Proton Exchange and Hydrogen Bonding. *Polymers* **2019,** *11* (12).

244.   Hillmyer, M. A.; Tolman, W. B., Aliphatic Polyester Block Polymers: Renewable, Degradable, and Sustainable. *Accounts of Chemical Research* **2014,** *47* (8), 2390-2396.

245.   Wang, X.; Houk, K. N., Theoretical elucidation of the origin of the anomalously high acidity of Meldrum's acid. *Journal of the American Chemical Society* **1988,** *110* (6), 1870-1872.

246.   Wiberg, K. B.; Laidig, K. E., Acidity of (Z)- and (E)-methyl acetates: relationship to Meldrum's acid. *Journal of the American Chemical Society* **1988,** *110* (6), 1872-1874.

247.   Evanseck, J. D.; Houk, K. N.; Briggs, J. M.; Jorgensen, W. L., Quantification of Solvent Effects on the Acidities of Z and E Esters from Fluid Simulations. *Journal of the American Chemical Society* **1994,** *116* (23), 10630-10638.

248.   Nakamura, S.; Hirao, H.; Ohwada, T., Rationale for the Acidity of Meldrum's Acid. Consistent Relation of C–H Acidities to the Properties of Localized Reactive Orbital. *The Journal of Organic Chemistry* **2004,** *69* (13), 4309-4316.

249.   Byun, K.; Mo, Y.; Gao, J., New Insight on the Origin of the Unusual Acidity of Meldrum's Acid from ab Initio and Combined QM/MM Simulation Study. *Journal of the American Chemical Society* **2001,** *123* (17), 3974-3979.

250.   Alabugin, I. V., *Stereoelectronic Effects: A Bridge Between Structure and Reactivity*. Wiley: 2016; p 392.

251.   Bender, M. L.; Chen, M. C., Acylium Ion Formation in the Reactions of Carboxylic Acid Derivatives. III. The Hydrolysis of 4-Substituted-2,6-dimethylbenzoyl Chlorides. *Journal of the American Chemical Society* **1963,** *85* (1), 30-36.

252.   Deslongchamps, P.; Cheriyan, U. O.; Guida, A.; Taillefer, R. J., New Evidence of Stereoelectronic Control from Basic Hydrolysis of Esters, Lactones, Amides and Lactams - Carbonyl Oxygen-Exchange - Reversible Ring-Opening of Lactams and Lactones. *Nouv J Chim* **1977,** *1* (3), 235-241.

253.   Deslongchamps, P.; Gerval, P.; Cheriyan, U. O.; Guida, A.; Taillefer, R. J., O-18 Carbonyl-Oxygen Exchange in Basic Hydrolysis of Tertiary Amides - New Evidence for Stereoelectronic Control. *Nouv J Chim* **1978,** *2* (6), 631-636.

254.   Deslongchamps, P.; Barlet, R.; Taillefer, R. J., Hydrolysis and Carbonyl-Oxygen Exchange in Tertiary Amides - Estimation of the Free-Energy Changes for Breakdown and Conformational-Changes of Tetrahedral Intermediates. *Can J Chem* **1980,** *58* (20), 2167-2172.

255.   Yadav, V. K., *Steric and Stereoelectronic Effects in Organic Chemistry*. Springer, Singapore: 2016.

256.   Perrin, C. L.; Arrhenius, G. M. L., A critical test of the theory of stereoelectronic control. *Journal of the American Chemical Society* **1982,** *104* (10), 2839-2842.

257.   Zhu, X.-Q.; Li, X.-T.; Han, S.-H.; Mei, L.-R., Conversion and Origin of Normal and Abnormal Temperature Dependences of Kinetic Isotope Effect in Hydride Transfer Reactions. *The Journal of Organic Chemistry* **2012,** *77* (10), 4774-4783.

258.   Chen, Y.-y.; Zhang, N.-n.; Ye, L.-m.; Chen, J.-h.; Sun, X.; Zhang, X.-j.; Yan, M., KOt-Bu/DMF promoted intramolecular cyclization of 1,1'-biphenyl aldehydes and ketones: an efficient synthesis of phenanthrenes. *Rsc Adv* **2015,** *5* (59), 48046-48049.

259.   Wang, H.; Wang, Z.; Huang, H.; Tan, J.; Xu, K., KOtBu-Promoted Oxidation of (Hetero)benzylic Csp3–H to Ketones with Molecular Oxygen. *Org Lett* **2016,** *18* (21), 5680-5683.

260.   Elliott, Q.; dos Passos Gomes, G.; Evoniuk, C. J.; Alabugin, I. V., Testing the limits of radical-anionic CH-amination: a 10-million-fold decrease in basicity opens a new path to hydroxyisoindolines via a mixed C–N/C–O–forming cascade. *Chemical Science* **2020,** *11* (25), 6539-6555.

261.   Wagner, G. R.; Bhatt, D. P.; O'Connell, T. M.; Thompson, J. W.; Dubois, L. G.; Backos, D. S.; Yang, H.; Mitchell, G. A.; Ilkayeva, O. R.; Stevens, R. D.; Grimsrud, P. A.; Hirschey, M. D., A Class of Reactive Acyl-CoA Species Reveals the Non-enzymatic Origins of Protein Acylation. *Cell Metabolism* **2017,** *25* (4), 823-837.e8.

262.   Lundell, J.; Rasanen, M.; Raaska, T.; Nieminen, J.; Murto, J., Matrix isolation infrared and ab initio studies on conformers of formic acid anhydride. *The Journal of Physical Chemistry* **1993,** *97* (18), 4577-4581.

263.   Wu, G.; Shlykov, S.; Van Alseny, F. S.; Geise, H. J.; Sluyts, E.; Van der Veken, B. J., Formic Anhydride in the Gas Phase, Studied by Electron Diffraction and Microwave and Infrared Spectroscopy, Supplemented with Ab-Initio Calculations of Geometries and Force Fields. *The Journal of Physical Chemistry* **1995,** *99* (21), 8589-8598.

264.   Wu, G.; Van Alsenoy, C.; Geise, H. J.; Sluyts, E.; Van der Veken, B. J.; Shishkov, I. F.; Khristenko, Acetic Anhydride in the Gas Phase, Studied by Electron Diffraction and Infrared Spectroscopy, Supplemented With ab Initio Calculations of Geometries and Force Fields. *The Journal of Physical Chemistry A* **2000,** *104* (7), 1576-1587.

265.   Eberson, L.; Welinder, H., Cyclic anhydrides. III. Equilibrium constants for the acid-anhydride equilibrium in aqueous solutions of certain vicinal diacids. *Journal of the American Chemical Society* **1971,** *93* (22), 5821-5826.

266.   Gonzalez-Lopez, M.; Shaw, J. T., Cyclic Anhydrides in Formal Cycloadditions and Multicomponent Reactions. *Chem Rev* **2009,** *109* (1), 164-189.

267.   Kaneti, J.; Bakalova, S. M.; Pojarlieff, I. G., Schiff Base Addition to Cyclic Dicarboxylic Anhydrides: An Unusual Concerted Reaction. An MO and DFT Theoretical Study. *The Journal of Organic Chemistry* **2003,** *68* (17), 6824-6827.

268.   Tamura, Y.; Wada, A.; Sasho, M.; Fukunaga, K.; Maeda, H.; Kita, Y., A new general regiocontrolled synthesis of anthracyclinones using cycloaddition of homophthalic anhydrides to 2-chloro-6-oxo-5,6,7,8-tetrahydro-1,4-naphthoquinone 1,2-ethanediyl acetal. *The Journal of Organic Chemistry* **1982,** *47* (22), 4376-4378.

269.   Juaristi, E.; Gomes, G. D.; Terent'ev, A. O.; Notario, R.; Alabugin, I. V., Stereoelectronic Interactions as a Probe for the Existence of the Intramolecular alpha-Effect. *Journal of the American Chemical Society* **2017,** *139* (31), 10799-10813.

270.   Greene, F. D., Cyclic Diacyl Peroxides. I. Monomeric Phthaloyl Peroxide1. *Journal of the American Chemical Society* **1956,** *78* (10), 2246-2250.

271.   Greene, F. D., Cyclic Diacyl Peroxides. II. Reaction of Phthaloyl Peroxide with cis- and trans-Stilbene. *Journal of the American Chemical Society* **1956,** *78* (10), 2250-2254.

272.   Greene, F. D.; Rees, W. W., Cyclic Diacyl Peroxides. III.1 The Reaction of Phthaloyl Peroxide with Olefins. *Journal of the American Chemical Society* **1958,** *80* (13), 3432-3437.

273.   Adam, W.; Cadiz, C.; Mazenod, F., Vacuum Flash Pyrolysis (Vfp) of Malonyl Peroxides - Decarboxylation Versus Decarbonylation of the Intermediary Alpha-Lactones. *Tetrahedron Lett* **1981,** *22* (13), 1203-1206.

274.   Adam, W.; Rucktaeschel, R., Cyclic peroxides. XVII. Solvolysis of dibutylmalonoyl peroxide. *The Journal of Organic Chemistry* **1972,** *37* (25), 4128-4133.

275.   Adam, W.; Rucktaschel, R., Cyclic Peroxide Series .71. Photolysis and Thermolysis of Di-Normal-Butylmalonyl Peroxide - Evidence for Alpha-Lactone Intermediates. *The Journal of Organic Chemistry* **1978,** *43* (20), 3886-3890.

276.   Yuan, C. X.; Liang, Y.; Hernandez, T.; Berriochoa, A.; Houk, K. N.; Siegel, D., Metal-free oxidation of aromatic carbon-hydrogen bonds through a reverse-rebound mechanism. *Nature* **2013,** *499* (7457), 192-196.

277.   Eliasen, A. M.; Thedford, R. P.; Claussen, K. R.; Yuan, C. X.; Siegel, D., A Protocol To Generate Phthaloyl Peroxide in Flow for the Hydroxylation of Arenes. *Org Lett* **2014,** *16* (14), 3628-3631.

278.   Dragan, A.; Kubczyk, T. M.; Rowley, J. H.; Sproules, S.; Tomkinson, N. C. O., Arene Oxidation with Malonoyl Peroxides. *Org Lett* **2015,** *17* (11), 2618-2621.

279.   Pilevar, A.; Hosseini, A.; Sekutor, M.; Hausmann, H.; Becker, J.; Turke, K.; Schreiner, P. R., Tuning the Reactivity of Peroxo Anhydrides for Aromatic C-H Bond Oxidation. *The Journal of Organic Chemistry* **2018,** *83* (17), 10070-10079.

280.   Griffith, J. C.; Jones, K. M.; Picon, S.; Rawling, M. J.; Kariuki, B. M.; Campbell, M.; Tomkinson, N. C. O., Alkene Syn Dihydroxylation with Malonoyi Peroxides. *Journal of the American Chemical Society* **2010,** *132* (41), 14409-14411.

281.   Jones, K. M.; Tomkinson, N. C. O., Metal-Free Dihydroxylation of Alkenes using Cyclobutane Malonoyl Peroxide. *The Journal of Organic Chemistry* **2012,** *77* (2), 921-928.

282.   Picon, S.; Rawling, M.; Campbell, M.; Tomkinson, N. C. O., Alkene Dihydroxylation with Malonoyl Peroxides: Catalysis Using Fluorinated Alcohols. *Org Lett* **2012,** *14* (24), 6250-6253.

283.   Rawling, M. J.; Rowley, J. H.; Campbell, M.; Kennedy, A. R.; Parkinson, J. A.; Tomkinson, N. C. O., Mechanistic insights into the malonoyl peroxide syn-dihydroxylation of alkenes. *Chemical Science* **2014,** *5* (5), 1777-1785.

284.   Rawling, M. J.; Tomkinson, N. C. O., Metal-free syn-dioxygenation of alkenes. *Organic & Biomolecular Chemistry* **2013,** *11* (9), 1434-1440.

285.   Yuan, C. X.; Axelrod, A.; Varela, M.; Danysh, L.; Siegel, D., Synthesis and reaction of phthaloyl peroxide derivatives, potential organocatalysts for the stereospecific dihydroxylation of alkenes. *Tetrahedron Lett* **2011,** *52* (20), 2540-2542.

286.   Alamillo-Ferrer, C.; Davidson, S. C.; Rawling, M. J.; Theodoulou, N. H.; Campbell, M.; Humphreys, P. G.; Kennedy, A. R.; Tomkinson, N. C. O., Alkene anti-Dihydroxylation with Malonoyl Peroxides. *Org Lett* **2015,** *17* (20), 5132-5135.

287.   Schwarz, M.; Reiser, O., Metal or No Metal: That Is the Question! *Angewandte Chemie International Edition* **2011,** *50* (45), 10495-10497.

288.   Alamillo-Ferrer, C.; Karaboumiotis-Sotti, M.; Kennedy, A. R.; Campbell, M.; Tomkinson, N. C. O., Alkene Dioxygenation with Malonoyl Peroxides: Synthesis of gamma-Lactones, Isobenzofuranones, and Tetrahydrofurans. *Org Lett* **2016,** *18* (13), 3102-3105.

289.   Alamillo-Ferrer, C.; Curle, J. M.; Davidson, S. C.; Lucas, S. C. C.; Atkinson, S. J.; Campbell, M.; Kennedy, A. R.; Tomkinson, N. C. O., Alkene Oxyamination Using Malonoyl Peroxides: Preparation of Pyrrolidines and Isoxazolidines. *The Journal of Organic Chemistry* **2018,** *83* (12), 6728-6740.

290.   Bityukov, O. V.; Vil, V. A.; Merkulova, V. M.; Nikishin, G. I.; Terent'ev, A. O., Silica gel mediated oxidative C-O coupling of beta-dicarbonyl compounds with malonyl peroxides in solvent-free conditions. *Pure and Applied Chemistry* **2018,** *90* (1), 7-20.

291.   Terent'ev, A. O.; Vil, V. A.; Gorlov, E. S.; Rusina, O. N.; Korlyukov, A. A.; Nikishin, G. I.; Adam, W., Selective Oxidative Coupling of 3H-Pyrazol-3-ones, Isoxazol-5(2H)-ones, Pyrazolidine-3,5-diones, and Barbituric Acids with Malonyl Peroxides: An Effective C-O Functionalization. *Chemistryselect* **2017,** *2* (11), 3334-3341.

292.   Terent'ev, A. O.; Vil', V. A.; Gorlov, E. S.; Nikishin, G. I.; Pivnitsky, K. K.; Adam, W., Lanthanide-Catalyzed Oxyfunctionalization of 1,3-Diketones, Acetoacetic Esters, And Malonates by Oxidative C-O Coupling with Malonyl Peroxides. *The Journal of Organic Chemistry* **2016,** *81* (3), 810-823.

293.   Terent'ev, A. O.; Vil', V. A.; Nikishin, G. I.; Adam, W., Lanthanide-Catalyzed Oxidative C-O Coupling of 1,3-Dicarbonyl Compounds with Diacyl Peroxides. *Synlett* **2015,** *26* (6), 802-806.

294.   Vil, V. A.; Gorlov, E. S.; Bityukov, O. V.; Barsegyan, Y. A.; Romanova, Y. E.; Merkulova, V. M.; Terent'ev, A. O., C-O coupling of Malonyl Peroxides with Enol Ethers via [5+2] Cycloaddition: Non-Rubottom Oxidation. *Adv Synth Catal* **2019,** *361* (13), 3173-3181.

295.   Lapitskaya, M. A.; Vil, V. A.; Daeva, E. D.; Terent'ev, A. O.; Pivnitsky, K. K., Alcoholysis of malonyl peroxides to give peracids. *Mendeleev Commun* **2016,** *26* (1), 14-15.

296.   Guo, Y. H.; Xiang, Y. F.; Wei, L.; Wan, J. P., Thermoinduced Free-Radical C-H Acyloxylation of Tertiary Enaminones: Catalyst-Free Synthesis of Acyloxyl Chromones and Enaminones. *Org Lett* **2018,** *20* (13), 3971-3974.

297.   Nikishin, G. I.; Moryasheva, S. I.; Starostin, E. K., Generation of Omega-Carbomethoxyalkyl Radicals and Syntheses Based on Them. *Russ Chem B+* **1975,** *24* (11), 2387-2391.

298.   Wiberg, K. B.; Laidig, K. E., Barriers to rotation adjacent to double bonds. 3. The carbon-oxygen barrier in formic acid, methyl formate, acetic acid, and methyl acetate. The origin of ester and amide resonance. *Journal of the American Chemical Society* **1987,** *109* (20), 5935-5943.

299.   Bjarnov, E.; Hocking, W. H., Structure of Other Rotamer of Formic-Acid, Cis-Hcooh. *Z Naturforsch A* **1978,** *33* (5), 610-618.

300.   Reisenauer, H. P.; Wagner, J. P.; Schreiner, P. R., Gas-Phase Preparation of Carbonic Acid and Its Monomethyl Ester. *Angewandte Chemie International Edition* **2014,** *53* (44), 11766-11771.

301.   D'Ascenzo, L.; Auffinger, P., A comprehensive classification and nomenclature of carboxyl-carboxyl(ate) supramolecular motifs and related catemers: implications for biomolecular systems. *Acta Crystallogr B* **2015,** *71*, 164-175.

302.   Hanz, S. Z.; Shu, N. S.; Qian, J. N.; Christman, N.; Kranz, P.; An, M.; Grewer, C.; Qiang, W., Protonation-Driven Membrane Insertion of a pH-Low Insertion Peptide. *Angew Chem Int Edit* **2016,** *55* (40), 12376-12381.

303.   Sofronov, O. O.; Giubertoni, G.; Pérez de Alba Ortíz, A.; Ensing, B.; Bakker, H. J., Peptide Side-COOH Groups Have Two Distinct Conformations under Biorelevant Conditions. *The Journal of Physical Chemistry Letters* **2020,** *11* (9), 3466-3472.

304.   Desiraju, G. R., Crystal Engineering: From Molecule to Crystal. *Journal of the American Chemical Society* **2013,** *135* (27), 9952-9967.

305.   Merz, K.; Vasylyeva, V., Development and boundaries in the field of supramolecular synthons. *CrystEngComm* **2010,** *12* (12), 3989-4002.

306.   Medvedev, M. G.; Bushmarinov, I. S.; Lyssenko, K. A., Z-effect reversal in carboxylic acid associates. *Chem Commun* **2016,** *52* (39), 6593-6596.

307.   Emsley, J., Very strong hydrogen bonding. *Chemical Society Reviews* **1980,** *9* (1), 91-124.

308.   Hati, S.; Datta, D., Anomeric effect and hardness. *J. Org. Chem.* **1992,** *57* (22), 6056-6057.

309.   Gandour, R. D., On the importance of orientation in general base catalysis by carboxylate. *Bioorganic Chemistry* **1981,** *10* (2), 169-176.

310.   Su, B.; Bunescu, A.; Qiu, Y.; Zuend, S. J.; Ernst, M.; Hartwig, J. F., Palladium-Catalyzed Oxidation of β-C(sp3)–H Bonds of Primary Alkylamines through a Rare Four-Membered Palladacycle Intermediate. *Journal of the American Chemical Society* **2020,** *142* (17), 7912-7919.

311.   Rebek, J., New molecular shapes for recognition and catalysis. *Journal of inclusion phenomena and molecular recognition in chemistry* **1989,** *7* (1), 7-17.

312.   Tadayoni, B. M.; Parris, K.; Rebek, J., Intramolecular catalysis of enolization: a probe for stereoelectronic effects at carboxyl oxygen. *Journal of the American Chemical Society* **1989,** *111* (12), 4503-4505.

313.   Zimmerman, S. C.; Korthals, J. S.; Cramer, K. D., Syn and Anti-Oriented Imidazole Carboxylates as Models for the Histidine-Aspartate Couple in Serine Proteases and Other Enzymes. *Tetrahedron* **1991,** *47* (14-15), 2649-2660.

314.   Marshall, L.; Parris, K.; Rebek, J.; Luis, S. V.; Burguete, M. I., A new class of chelating agents. *Journal of the American Chemical Society* **1988,** *110* (15), 5192-5193.

315.   Bartlett, P. D., Recent Work on the Mechanisms of Peroxide Reactions. *Rec. Chem. Prog.* **1950,** *11*.

316.   Singleton, D. A.; Merrigan, S. R.; Liu, J.; Houk, K. N., Experimental geometry of the epoxidation transition state. *Journal of the American Chemical Society* **1997,** *119* (14), 3385-3386.

317.   Montzka, T. A.; Swaminathan, S.; Firestone, R. A., Reversal of Syn-Anti Preference for Carboxylic Acids along the Reaction Coordinate for Proton Transfer. Implications for Intramolecular Catalysis. *The Journal of Physical Chemistry* **1994,** *98* (50), 13171-13176.

318.   Li, Y.; Houk, K. N., Theoretical Assessments of the Basicity and Nucleophilicity of Carboxylate Syn and Anti-Lone Pairs. *Journal of the American Chemical Society* **1989,** *111* (12), 4505-4507.

319.   Smith, G. D.; Pangborn, W. A.; Blessing, R. H., The structure of T6 human insulin at 1.0 A resolution. *Acta Crystallographica Section D* **2003,** *59*, 474-482.

320.   Fili, S.; Valmas, A.; Norrman, M.; Schluckebier, G.; Beckers, D.; Degen, T.; Wright, J.; Fitch, A.; Gozzo, F.; Giannopoulou, A. E.; Karavassili, F.; Margiolaki, I., Human insulin polymorphism upon ligand binding and pH variation: the case of 4-ethylresorcinol. *IUCrJ* **2015,** *2* (5), 534-544.

321.   Gold, B.; Dudley, G. B.; Alabugin, I. V., Moderating Strain without Sacrificing Reactivity: Design of Fast and Tunable Noncatalyzed Alkyne–Azide Cycloadditions via Stereoelectronically Controlled Transition State Stabilization. *Journal of the American Chemical Society* **2013,** *135* (4), 1558-1569.

322.   Gold, B.; Shevchenko, N. E.; Bonus, N.; Dudley, G. B.; Alabugin, I. V., Selective Transition State Stabilization via Hyperconjugative and Conjugative Assistance: Stereoelectronic Concept for Copper-Free Click Chemistry. *The Journal of Organic Chemistry* **2012,** *77* (1), 75-89.

323.   Panova, M. V.; Medvedev, M. G.; Bushmarinov, I. S.; Ananyev, I. V.; Lyssenko, K. A., Supramolecular stereoelectronic effect in hemiketals. *Mendeleev Commun* **2017,** *27* (6), 595-598.

324.   Lehn, J.-M.; Wipff, G., Stereoelectronic Properties of Tetrahedral Species Derived from Carbonyl Groups. Ab initio study of aminodihydroxymethane, CH(OH)2NH2, a model tetrahedral intermediate in amide hydrolysis. *Helvetica Chimica Acta* **1978,** *61* (4), 1274-1286.

325.   Qu, B.; Collum, D. B., Mechanism of Acylation of Lithium Phenylacetylide with a Weinreb Amide. *The Journal of Organic Chemistry* **2006,** *71* (18), 7117-7119.

326.   Andrés, G. O.; Pierini, A. B.; de Rossi, R. H., Kinetic and Theoretical Studies on the Mechanism of Intramolecular Catalysis in Phenyl Ester Hydrolysis. *The Journal of Organic Chemistry* **2006,** *71* (20), 7650-7656.

327.	Ba-Saif, S. A.; Maude, A. B.; Williams, A., Kinetics and equilibria of reactions between acetic anhydride and substituted phenolate ions in aqueous and chlorobenzene solutions. *Journal of the Chemical Society, Perkin Transactions 2* **1994,** (12), 2395.

328.	Stefanidis, D.; Cho, S.; Dhe-Paganon, S.; Jencks, W. P., Structure-reactivity correlations for reactions of substituted phenolate anions with acetate and formate esters. *Journal of the American Chemical Society* **1993,** *115* (5), 1650-1656.

329.	Ba-Saif, S.; Luthra, A. K.; Williams, A., Concertedness in acyl group transfer in solution: a single transition state in acetyl group transfer between phenolate ion nucleophiles. *Journal of the American Chemical Society* **1987,** *109* (21), 6362-6368.

330.	Vil, V. A.; Gomes, G. D.; Bityukov, O. V.; Lyssenko, K. A.; Nikishin, G. I.; Alabugin, I. V.; Terent'ev, A. O., Interrupted Baeyer-Villiger Rearrangement: Building A Stereoelectronic Trap for the Criegee Intermediate. *Angew Chem Int Edit* **2018,** *57* (13), 3372-3376.

331.	Vil, V. A.; Barsegyan, Y. A.; Kuhn, L.; Ekimova, M. V.; Semenov, E. A.; Korlyukov, A. A.; Terent'ev, A. O.; Alabugin, I. V., Synthesis of unstrained Criegee intermediates: inverse α-effect and other protective stereoelectronic forces can stop Baeyer–Villiger rearrangement of γ-hydroperoxy-γ-peroxylactones. *Chem. Sci.* **2020,** *11* (20), 5313-5322.

332.	Coghi, P.; Yaremenko, I. A.; Prommana, P.; Radulov, P. S.; Syroeshkin, M. A.; Wu, Y. J.; Gao, J. Y.; Gordillo, F. M.; Mok, S.; Wong, V. K. W.; Uthaipibull, C.; Terent'ev, A. O., Novel Peroxides as Promising Anticancer Agents with Unexpected Depressed Antimalarial Activity. *Chemmedchem* **2018,** *13* (9), 902-908.

333.	Feng, Y.; Holte, D.; Zoller, J.; Umemiya, S.; Simke, L. R.; Baran, P. S., Total Synthesis of Verruculogen and Fumitremorgin A Enabled by Ligand-Controlled C-H Borylation. *Journal of the American Chemical Society* **2015,** *137* (32), 10160-10163.

334.	Hu, X. R.; Maimone, T. J., Four-Step Synthesis of the Antimalarial Cardamom Peroxide via an Oxygen Stitching Strategy. *Journal of the American Chemical Society* **2014,** *136* (14), 5287-5290.

335.	Ingram, K.; Yaremenko, I. A.; Krylov, I. B.; Hofer, L.; Terent'ev, A. O.; Keiser, J., Identification of Antischistosomal Leads by Evaluating Bridged 1,2,4,5-Tetraoxanes, Alphaperoxides, and Tricyclic Monoperoxides. *J. Med. Chem.* **2012,** *55* (20), 8700-8711.

336.	Yaremenko, I. A.; Coghi, P.; Prommana, P.; Qiu, C. L.; Radulov, P. S.; Qu, Y. Q.; Belyakova, Y. Y.; Zanforlin, E.; Kokorekin, V. A.; Wu, Y. Y. J.; Fleury, F.; Uthaipibull, C.; Wong, V. K. W.; Terent'ev, A. O., Synthetic Peroxides Promote Apoptosis of Cancer Cells by Inhibiting P-Glycoprotein ABCB5. *Chemmedchem* **2020,** *15* (13), 1118-1127.

337.	Yaremenko, I. A.; Syroeshkin, M. A.; Levitsky, D. O.; Fleury, F.; Terent'ev, A. O., Cyclic peroxides as promising anticancer agents: in vitro cytotoxicity study of synthetic ozonides and tetraoxanes on human prostate cancer cell lines. *Med. Chem. Res.* **2017,** *26* (1), 170-179.

338.	Keiser, J.; Utzinger, J., Food-borne trematodiasis: current chemotherapy and advances with artemisinins and synthetic trioxolanes. *Trends Parasitology* **2007,** *23* (11), 555-562.

339.   Muraleedharan, K. M.; Avery, M. A., Progress in the development of peroxide-based anti-parasitic agents. *Drug Discovery Today* **2009,** *14* (15-16), 793-803.

340.   Vil', V. A.; Yaremenko, I. A.; Ilovaisky, A. I.; Terent'ev, A. O., Synthetic Strategies for Peroxide Ring Construction in Artemisinin. *Molecules* **2017,** *22* (1).

341.   Terent'ev, A. O.; Borisov, D. A.; Chernyshev, V. V.; Nikishin, G. I., Facile and Selective Procedure for the Synthesis of Bridged 1,2,4,5-Tetraoxanes; Strong Acids As Cosolvents and Catalysts for Addition of Hydrogen Peroxide to beta-Diketones. *The Journal of Organic Chemistry* **2009,** *74* (9), 3335-3340.

342.   Terent'ev, A. O.; Yaremenko, I. A.; Glinushkin, A. P.; Nikishin, G. I., Synthesis of peroxides from beta,delta-triketones under heterogeneous conditions. *Russ. J. Org. Chem.* **2015,** *51* (12), 1681-1687.

343.   Terent'ev, A. O.; Yaremenko, I. A.; Vil', V. A.; Moiseev, I. K.; Kon'kov, S. A.; Dembitsky, V. M.; Levitsky, D. O.; Nikishin, G. I., Phosphomolybdic and phosphotungstic acids as efficient catalysts for the synthesis of bridged 1,2,4,5-tetraoxanes from beta-diketones and hydrogen peroxide. *Org. Biomol. Chem.* **2013,** *11* (16), 2613-2623.

344.   Vil', V. A.; Yaremenko, I. A.; Fomenkov, D. I.; Levitsky, D. O.; Fleury, F.; Terent'ev, A. O., Ion exchange resin-catalyzed synthesis of bridged tetraoxanes possessing in vitro cytotoxicity against HeLa cancer cells. *Chem. Heterocycl. Comp.* **2020**, 722-726.

345.   Yaremenko, I. A.; Terent'ev, A. O.; Vil', V. A.; Novikov, R. A.; Chernyshev, V. V.; Tafeenko, V. A.; Levitsky, D. O.; Fleury, F.; Nikishin, G. I., Approach for the Preparation of Various Classes of Peroxides Based on the Reaction of Triketones with H2O2: First Examples of Ozonide Rearrangements. *Chem. Eur. J.* **2014,** *20* (32), 10160-10169.

346.   Reints, W.; Pratt, D. A.; Korth, H.-G.; Mulder, P., O−O Bond Dissociation Enthalpy in Di(trifluoromethyl) Peroxide (CF3OOCF3) as Determined by Very Low Pressure Pyrolysis. Density Functional Theory Computations on O−O and O−H Bonds in (Fluorinated) Derivatives. *The Journal of Physical Chemistry A* **2000,** *104* (46), 10713-10720.

347.   Gomes, G. D.; Yaremenko, I. A.; Radulov, P. S.; Novikov, R. A.; Chernyshev, V. V.; Korlyukov, A. A.; Nikishin, G. I.; Alabugin, I. V.; Terent'ev, A. O., Stereoelectronic Control in the Ozone-Free Synthesis of Ozonides. *Angew Chem Int Edit* **2017,** *56* (18), 4955-4959.

348.   Yaremenko, I. A.; Radulov, P. S.; Belyakova, Y. Y.; Demina, A. A.; Fomenkov, D. I.; Barsukov, D. V.; Subbotina, I. R.; Fleury, F.; Terent'ev, A. O., Catalyst Development for the Synthesis of Ozonides and Tetraoxanes Under Heterogeneous Conditions: Disclosure of an Unprecedented Class of Fungicides for Agricultural Application. *Chem. Eur. J.* **2020,** *26* (21), 4734-4751.

349.   Yaremenko, I. A.; Radulov, P. S.; Medvedev, M. G.; Krivoshchapov, N. V.; Belyakova, Y. Y.; Korlyukov, A. A.; Ilovaisky, A. I.; Terent'ev, A. O.; Alabugin, I. V., How to Build Rigid Oxygen-Rich Tricyclic Heterocycles from Triketones and Hydrogen Peroxide: Control of Dynamic Covalent Chemistry with Inverse α-Effect. *Journal of the American Chemical Society* **2020**.

350.   Terent'ev, A. O.; Yaremenko, I. A.; Chernyshev, V. V.; Dembitsky, V. M.; Nikishin, G. I., Selective Synthesis of Cyclic Peroxides from Triketones and H2O2. *The Journal of Organic Chemistry* **2012,** *77* (4), 1833-1842.

351.   Terent'ev, A. O.; Yaremenko, I. A.; Vil', V. A.; Dembitsky, V. M.; Nikishin, G. I., Boron Trifluoride as an Efficient Catalyst for the Selective Synthesis of Tricyclic Monoperoxides from beta,delta-Triketones and H2O2. *Synthesis* **2013,** *45* (2), 246-250.

352.   Eske, A.; Ecker, S.; Fendinger, C.; Goldfuss, B.; Jonen, M.; Lefarth, J.; Neudörfl, J.-M.; Spilles, M.; Griesbeck, A. G., Inside Cover: Spirofused and Annulated 1,2,4-Trioxepane-, 1,2,4-Trioxocane-, and 1,2,4-Trioxonane-Cyclohexadienones: Cyclic Peroxides with Unusual Ring Conformation Dynamics (Angew. Chem. Int. Ed. 42/2018). *Angewandte Chemie International Edition* **2018,** *57* (42), 13694-13694.

353.   Lee, H.; Wilmshurst, J. K., The structures and vibrational spectra of trimethoxymethane and tetramethoxymethane. *Spectrochimica Acta Part A: Molecular Spectroscopy* **1967,** *23* (2), 347-363.

354.   Aped, P.; Fuchs, B.; Goldberg, I.; Senderowitz, H.; Tartakovsky, E.; Weinman, S., Probing the Anomeric Effect in Orthoesters. Structure, Conformation, and Dynamic Behavior of a Unique Orthooxalate: 2,5,7,10,11,14-Hexaoxa[4.4.4]propellane. *Journal of the American Chemical Society* **1992,** *114*, 5585 - 5590.

355.   Menon, A. S.; Henry, D. J.; Bally, T.; Radom, L., Effect of substituents on the stabilities of multiply-substituted carbon-centered radicals. *Organic & Biomolecular Chemistry* **2011,** *9* (10), 3636-3657.

356.   Wheeler, S. E.; Houk, K. N.; Schleyer, P. v. R.; Allen, W. D., A Hierarchy of Homodesmotic Reactions for Thermochemistry. *Journal of the American Chemical Society* **2009,** *131* (7), 2547-2560.

357.   Aue, D. H., Carbocations. *WIREs Computational Molecular Science* **2011,** *1* (4), 487-508.

358.   Ervin, K. M.; DeTuri, V. F., Anchoring the Gas-Phase Acidity Scale. *The Journal of Physical Chemistry A* **2002,** *106* (42), 9947-9956.

359.   DePuy, C. H.; Bierbaum, V. M.; Damrauer, R., Relative gas-phase acidities of the alkanes. *Journal of the American Chemical Society* **1984,** *106* (14), 4051-4053.

360.   Pindur, U.; Müller, J.; Flo, C.; Witzel, H., Ortho esters and dialkoxycarbenium ions: reactivity, stability, structure, and new synthetic applications. **1987,** *16* (0), 75-87.

361.   Deslongchamps, P.; Dory, Y. L.; Li, S. G., The relative rate of hydrolysis of a series of acyclic and six-membered cyclic acetals, ketals, orthoesters, and orthocarbonates. *Tetrahedron* **2000,** *56* (22), 3533-3537.

362.   Deslongchamps, P., *Stereoelectronic effects in organic chemistry*. Pergamon Press: Oxford Oxfordshire, 1983.

363.   Brachvogel, R.-C.; Von Delius, M., Orthoester exchange: a tripodal tool for dynamic covalent and systems chemistry. *Chemical Science* **2015,** *6* (2), 1399-1403.

364.   Wang, X.; Shyshov, O.; Hanževački, M.; Jäger, C. M.; von Delius, M., Ammonium Complexes of Orthoester Cryptands Are Inherently Dynamic and Adaptive. *Journal of the American Chemical Society* **2019,** *141* (22), 8868-8876.

365.   Löw, H.; Mena-Osteritz, E.; von Delius, M., Self-templated synthesis of an orthoformate in,in-cryptand and its bridgehead inversion by dynamic covalent exchange. *Chem Commun* **2019,** *55* (76), 11434-11437.

366.   Giner, J.-L., DMOBO: An Improvement on the OBO Orthoester Protecting Group. *Org Lett* **2005,** *7* (3), 499-501.

367.   Corey, E. J.; Raju, N., A new general synthetic route to bridged carboxylic ortho esters. *Tetrahedron Lett* **1983,** *24* (50), 5571-5574.

368.   Makarova, M.; Rycek, L.; Hajicek, J.; Baidilov, D.; Hudlicky, T., Tetrodotoxin: History, Biology, and Synthesis. *Angewandte Chemie International Edition* **2019,** *58* (51), 18338-18387.

369.   Woodward, R. B.; Gougoutas, J. Z., The Structure of Tetrodotoxin. *Journal of the American Chemical Society* **1964,** *86* (22), 5030-5030.

370.   Tormos, J. R.; Wiley, K. L.; Wang, Y.; Fournier, D.; Masson, P.; Nachon, F.; Quinn, D. M., Accumulation of Tetrahedral Intermediates in Cholinesterase Catalysis: A Secondary Isotope Effect Study. *Journal of the American Chemical Society* **2010,** *132* (50), 17751-17759.

371.   Nemukhin, A. V.; Grigorenko, B. L.; Morozov, D. I.; Kochetov, M. S.; Lushchekina, S. V.; Varfolomeev, S. D., On quantum mechanical – molecular mechanical (QM/MM) approaches to model hydrolysis of acetylcholine by acetylcholinesterase. *Chemico-Biological Interactions* **2013,** *203* (1), 51-56.

372.   Powers, J. C.; Asgian, J. L.; Ekici, Ö. D.; James, K. E., Irreversible Inhibitors of Serine, Cysteine, and Threonine Proteases. *Chem Rev* **2002,** *102* (12), 4639-4750.

373.   Quinn, D. M.; Topczewski, J.; Yasapala, N.; Lodge, A., Why is Aged Acetylcholinesterase So Difficult to Reactivate? *Molecules* **2017,** *22* (9), 1464.

374.   Cochran, R.; Kalisiak, J.; Kucukkilinc, T.; Radic, Z.; Garcia, E.; Zhang, L. M.; Ho, K. Y.; Amitai, G.; Kovarik, Z.; Fokin, V. V.; Sharpless, K. B.; Taylor, P., Oxime-assisted Acetylcholinesterase Catalytic Scavengers of Organophosphates That Resist Aging. *J Biol Chem* **2011,** *286* (34), 29718-29724.

375.   Sit, R. K.; Radic, Z.; Gerardi, V.; Zhang, L. M.; Garcia, E.; Katalinic, M.; Amitai, G.; Kovarik, Z.; Fokin, V. V.; Sharpless, K. B.; Taylor, P., New Structural Scaffolds for Centrally Acting Oxime Reactivators of Phosphylated Cholinesterases. *J Biol Chem* **2011,** *286* (22), 19422-19430.

376.   Sit, R. K.; Fokin, V. V.; Amitai, G.; Sharpless, K. B.; Taylor, P.; Radic, Z., Imidazole Aldoximes Effective in Assisting Butyrylcholinesterase Catalysis of Organophosphate Detoxification. *J Med Chem* **2014,** *57* (4), 1378-1389.

377.   Sit, R. K.; Kovarik, Z.; Hrvat, N. M.; Zunec, S.; Green, C.; Fokin, V. V.; Sharpless, K. B.; Radic, Z.; Taylor, P., Pharmacology, Pharmacokinetics, and Tissue Disposition of Zwitterionic Hydroxyiminoacetamido Alkylamines as Reactivating Antidotes for Organophosphate Exposure. *J Pharmacol Exp Ther* **2018,** *367* (2), 363-372.

378.   Kovarik, Z.; Kalisiak, J.; Hrvat, N. M.; Katalinic, M.; Zorbaz, T.; Zunec, S.; Green, C.; Radic, Z.; Fokin, V. V.; Sharpless, K. B.; Taylor, P., Reversal of Tabun Toxicity Enabled by a Triazole-Annulated Oxime Library-Reactivators of Acetylcholinesterase. *Chem-Eur J* **2019,** *25* (16), 4100-4114.

379.   Kovarik, Z.; Hrvat, N. M.; Kalisiak, J.; Katalinic, M.; Sit, R. K.; Zorbaz, T.; Radic, Z.; Fokin, V. V.; Sharpless, K. B.; Taylor, P., Counteracting tabun inhibition by reactivation by pyridinium aldoximes that interact with active center gorge mutants of acetylcholinesterase. *Toxicol Appl Pharm* **2019,** *372*, 40-46.

380.   Ruben, E. A.; Plumley, J. A.; Chapman, M. S.; Evanseck, J. D., Anomeric Effect in "High Energy" Phosphate Bonds. Selective Destabilization of the Scissile Bond and Modulation of the Exothermicity of Hydrolysis. *Journal of the American Chemical Society* **2008,** *130* (11), 3349-3358.

381.   Zhang, L.; Lin, D.; Sun, X.; Curth, U.; Drosten, C.; Sauerhering, L.; Becker, S.; Rox, K.; Hilgenfeld, R., Crystal structure of SARS-CoV-2 main protease provides a basis for design of improved α-ketoamide inhibitors. *Science* **2020**, eabb3405.

382.   Jin, Z.; Du, X.; Xu, Y.; Deng, Y.; Liu, M.; Zhao, Y.; Zhang, B.; Li, X.; Zhang, L.; Peng, C.; Duan, Y.; Yu, J.; Wang, L.; Yang, K.; Liu, F.; Jiang, R.; Yang, X.; You, T.; Liu, X.; Yang, X.; Bai, F.; Liu, H.; Liu, X.; Guddat, L. W.; Xu, W.; Xiao, G.; Qin, C.; Shi, Z.; Jiang, H.; Rao, Z.; Yang, H., Structure of Mpro from SARS-CoV-2 and discovery of its inhibitors. *Nature* **2020,** *582* (7811), 289-293.

383.   Simón, L.; Goodman, J. M., Enzyme Catalysis by Hydrogen Bonds: The Balance between Transition State Binding and Substrate Binding in Oxyanion Holes. *The Journal of Organic Chemistry* **2010,** *75* (6), 1831-1840.

384.   Simón, L.; Goodman, J. M., Hydrogen-bond stabilization in oxyanion holes: grand jeté to three dimensions. *Org. Biomol. Chem.* **2012,** *10* (9), 1905.

385.   Cramer, C. J.; Kelterer, A.-M.; French, A. D., When anomeric effects collide. *Journal of Computational Chemistry* **2001,** *22* (11), 1194-1204.

386.   Fraser-Reid, B.; Wu, Z.; Udodong, U. E.; Ottosson, H., Armed/disarmed effects in glycosyl donors: rationalization and sidetracking. *The Journal of Organic Chemistry* **1990,** *55* (25), 6068-6070.

387.   Friesen, R. W.; Danishefsky, S. J., On the controlled oxidative coupling of glycals: a new strategy for the rapid assembly of oligosaccharides. *Journal of the American Chemical Society* **1989,** *111* (17), 6656-6660.

388.   Fried, J.; Hallinan, E. A.; Szwedo, M. J., Synthesis and properties of 7,7-difluoro derivatives of the 2,6-dioxa[3.1.1]bicycloheptane ring system present in thromboxane A2. *Journal of the American Chemical Society* **1984,** *106* (13), 3871-3872.

389.   Jing, C.; Mallah, S.; Kriemen, E.; Bennett, S. H.; Fasano, V.; Lennox, A. J. J.; Hers, I.; Aggarwal, V. K., Synthesis, Stability, and Biological Studies of Fluorinated Analogues of Thromboxane A2. *ACS Central Science* **2020,** *6* (6), 995-1000.

390.   Godage, H. Y.; Riley, A. M.; Woodman, T. J.; Thomas, M. P.; Mahon, M. F.; Potter, B. V. L., Regioselective Opening of myo-Inositol Orthoesters: Mechanism and Synthetic Utility. *The Journal of Organic Chemistry* **2013,** *78* (6), 2275-2288.

391.   Carpenter, B. K., A simple model for predicting the effect of substituents on the rates of thermal pericyclic reactions. *Tetrahedron* **1978,** *34* (13), 1877-1884.

392.   Evans, D. A.; Baillargeon, D. J.; Nelson, J. V., A general approach to the synthesis of 1,6-dicarbonyl substrates. New applications of base-accelerated oxy-Cope rearrangements. *Journal of the American Chemical Society* **1978,** *100* (7), 2242-2244.

393.   Pal, R.; Clark, R. J.; Manoharan, M.; Alabugin, I. V., Fast Oxy-Cope Rearrangements of Bis-alkynes: Competition with Central C–C Bond Fragmentation and Incorporation in Tunable Cascades Diverging from a Common Bis-allenic Intermediate. *The Journal of Organic Chemistry* **2010,** *75* (24), 8689-8692.

394.   Black, K. A.; Wilsey, S.; Houk, K. N., Alkynes, Allenes, and Alkenes in [3,3]-Sigmatropy: Functional Diversity and Kinetic Monotony. A Theoretical Analysis. *Journal of the American Chemical Society* **1998,** *120* (23), 5622-5627.

395.   Yoo, H. Y.; Houk, K. N.; Lee, J. K.; Scialdone, M. A.; Meyers, A. I., New Paradigm for Anionic Heteroatom Cope Rearrangements. *Journal of the American Chemical Society* **1998,** *120* (1), 205-206.

396.   Black, K. A.; Wilsey, S.; Houk, K. N., Dissociative and Associative Mechanisms of Cope Rearrangements of Fluorinated 1,5-Hexadienes and 2,2'-Bis-methylenecyclopentanes. *Journal of the American Chemical Society* **2003,** *125* (22), 6715-6724.

397.   Perrin, C. L., Is There Stereoelectronic Control in Formation and Cleavage of Tetrahedral Intermediates? *Accounts of Chemical Research* **2002,** *35* (1), 28-34.

398.   Sinnott, M. L., The Principle of Least Nuclear Motion and the Theory of Stereoelectronic Control. In *Advances in Physical Organic Chemistry*, Bethell, D., Ed. Academic Press: 1988; Vol. 24, pp 113-204.

399.   Safaiee, M.; Ebrahimghasri, B.; Zolfigol, M. A.; Baghery, S.; Khoshnood, A.; Alonso, D. A., Synthesis and application of chitosan supported vanadium oxo in the synthesis of 1,4-dihydropyridines and 2,4,6-triarylpyridines via anomeric based oxidation. *New J Chem* **2018,** *42* (15), 12539-12548.

400.   Li, S.; Deslongchamps, P., Experimental evidence for a synperiplanar stereoelectronic effect in the ozonolysis of a tricyclic acetal. *Tetrahedron Lett* **1993,** *34* (48), 7759-7762.

401.   Chandrasekhar, S., Some recent developments in stereoelectronic theory. Reevaluations of ALPH and the reverse anomeric effect. *Arkivoc* **2005**, 37-66.

402.   Eliel, E. L.; Nader, F. W., Conformational analysis. XX. Stereochemistry of reaction of Grignard reagents with ortho esters. Synthesis of 1,3-dioxanes with axial substituents at C-2. *Journal of the American Chemical Society* **1970,** *92* (3), 584-590.

403.   Eliel, E. L.; Nader, F. W., Conformational analysis. XXI. Reduction with metal hydrides. XX. Stereochemistry of reduction of ortho esters with lithium aluminum hydride and mixed hydrides. *Journal of the American Chemical Society* **1970,** *92* (10), 3045-3050.

404.   Jana, C. K.; Scopelliti, R.; Gademann, K., A Synthetic Entry into the Taiwaniaquinoids Based on a Biogenetic Hypothesis: Total Synthesis of (−)-Taiwaniaquinone H. *Chemistry – A European Journal* **2010,** *16* (26), 7692-7695.

405.   Novak, A. J. E.; Grigglestone, C. E.; Trauner, D., A Biomimetic Synthesis Elucidates the Origin of Preuisolactone A. *Journal of the American Chemical Society* **2019,** *141* (39), 15515-15518.

406.   Kiafar, M.; Zolfigol, M. A.; Yarie, M.; Taherpour, A., The first computational study for the oxidative aromatization of pyrazolines and 1,4-dihydropyridines using 1,2,4-triazolinediones: an anomeric-based oxidation. *Rsc Adv* **2016,** *6* (104), 102280-102291.

407.   Mora, J. R.; Kirby, A. J.; Nome, F., Theoretical Study of the Importance of the Spectator Groups on the Hydrolysis of Phosphate Triesters. *The Journal of Organic Chemistry* **2012,** *77* (16), 7061-7070.

408.   Kirby, A. J., Crystallographic approaches to transition state structures. *Adv Phys Org Chem* **1994,** *29*, 87-183.

409.   Davies, J. E.; Doltsinis, N. L.; Kirby, A. J.; Roussev, C. D.; Sprik, M., Estimating pKa Values for Pentaoxyphosphoranes. *Journal of the American Chemical Society* **2002,** *124* (23), 6594-6599.

410.   Windsor, I. W.; Gold, B.; Raines, R. T., An n→π* Interaction in the Bound Substrate of Aspartic Proteases Replicates the Oxyanion Hole. *ACS Catalysis* **2019,** *9* (2), 1464-1471.

411.   Feliciano, M. A. M.; Gold, B., Unique, yet Typical Oxyanion Holes in Aspartic Proteases. *ACS Catalysis* **2020**, 14201-14209.

412.   Edwards, J. O.; Pearson, R. G., The Factors Determining Nucleophilic Reactivities. *Journal of the American Chemical Society* **1962,** *84* (1), 16-24.

413.   Jencks, W. P.; Carriuolo, J., Reactivity of Nucleophilic Reagents toward Esters. *Journal of the American Chemical Society* **1960,** *82* (7), 1778-1786.

414.   Gold, V., Glossary of Terms Used in Physical Organic-Chemistry. *Pure and Applied Chemistry* **1979,** *51* (8), 1725-1801.

415.   Hoz, S.; Buncel, E., The Alpha-Effect - a Critical-Examination of the Phenomenon and Its Origin. *Israel J Chem* **1985,** *26* (4), 313-319.

416.   Buncel, E.; Um, I. H., The alpha-effect and its modulation by solvent. *Tetrahedron* **2004,** *60* (36), 7801-7825.

417.   Hoz, S.; Speizman, D., Nucleophilic Attacks on Activated 9-Methylenefluorenes - Application of the Ritchie Equation to Low-Lying Lumo Substrates. *J Org Chem* **1983,** *48* (17), 2904-2910.

418.   Buncel, E.; Hoz, S., Can ground-state destabilization of an α-nucleophile induce an α-effect? *Tetrahedron Lett* **1983,** *24* (44), 4777-4780.

419.   Nigst, T. A.; Antipova, A.; Mayr, H., Nucleophilic Reactivities of Hydrazines and Amines: The Futile Search for the α-Effect in Hydrazine Reactivities. *The Journal of Organic Chemistry* **2012,** *77* (18), 8142-8155.

420.   Alabugin, I. V.; Dos Passos Gomes, G.; Abdo, M. A., Hyperconjugation. *WIREs Computational Molecular Science* **2019,** *9* (2), e1389.

421.   Evanseck, J. D.; Blake, J. F.; Jorgensen, W. L., Ab initio study of the SN2 reactions of hydroxide and hydroperoxide with chloromethane. *Journal of the American Chemical Society* **1987,** *109* (8), 2349-2353.

422.   Ren, Y.; Yamataka, H., The α-Effect in Gas-Phase SN2 Reactions Revisited. *Org Lett* **2006,** *8* (1), 119-121.

423.   Ren, Y.; Yamataka, H., The α-Effect in Gas-Phase SN2 Reactions: Existence and the Origin of the Effect. *The Journal of Organic Chemistry* **2007,** *72* (15), 5660-5667.

424.   Vil, V. A.; Barsegyan, Y. A.; Barsukov, D. V.; Korlyukov, A. A.; Alabugin, I. V.; Terent'ev, A. O., Peroxycarbenium Ions as the "Gatekeepers" in Reaction Design: Assistance from Inverse Alpha-Effect in Three-Component beta-Alkoxy-beta-peroxylactones Synthesis. *Chem-Eur J* **2019,** *25* (63), 14460-14468.

425.   Griesbeck, A. G.; Brautigam, M.; Kleczka, M.; Raabe, A., Synthetic Approaches to Mono- and Bicyclic Perortho-Esters with a Central 1,2,4-Trioxane Ring as the Privileged Lead Structure in Antimalarial and Antitumor-Active Peroxides and Clarification of the Peroxide Relevance. *Molecules* **2017,** *22* (1).

426.   Alabugin, I. V.; Manoharan, M.; Zeidan, T. A., Homoanomeric effects in six-membered heterocycles. *Journal of the American Chemical Society* **2003,** *125* (46), 14014-14031.

427.   Ferrier, R. J.; Sankey, G. H., Unsaturated carbohydrates. Part VII. The preference shown by allylic ester groupings on pyranoid rings for the quasi-axial orientation. *Journal of the Chemical Society C: Organic* **1966,** (0), 2345-2349.

428.   Curran, D. P.; Suh, Y. G., Selective Mono-Claisen Rearrangement of Carbohydrate Glycals - a Chemical Consequence of the Vinylogous Anomeric Effect. *Carbohydrate Research* **1987,** *171*, 161-191.

429.   Denmark, S. E.; Dappen, M. S.; Sear, N. L.; Jacobs, R. T., The Vinylogous Anomeric Effect in 3-Alkyl-2-Chlorocyclohexanone Oximes and Oxime Ethers. *Journal of the American Chemical Society* **1990,** *112* (9), 3466-3474.

430.   Jakel, C.; Dotz, K. H., Organotransition metal modified sugars Part 22. Direct metalation of glycals: short and efficient routes to diversely protected stannylated glycals. *J Organomet Chem* **2001,** *624* (1-2), 172-185.

431.   Drew, M. D.; Wall, M. C.; Kim, J. T., Stereoselective propargylation of glycals with allenyltributyltin(IV) via a Ferrier type reaction. *Tetrahedron Lett* **2012,** *53* (23), 2833-2836.

432.   Nowacki, A.; Walczak, D.; Liberek, B., Fully acetylated 1,5-anhydro-2-deoxypent-1-enitols and 1,5-anhydro-2,6-dideoxyhex-1-enitols in DFT level theory conformational studies. *Carbohydrate Research* **2012,** *352*, 177-185.

433.   Nowacki, A.; Liberek, B., Comparative conformational studies of 3,4,6-tri-O-acetyl-1,5-anhydro-2-deoxyhex-1-enitols at the DFT level. *Carbohydrate Research* **2018,** *462*, 13-27.

434.   Asgari, M.; Nori-Shargh, D., Exploring the impacts of the vinylogous anomeric effect on the synchronous early and late transition states of the hydrogen molecule elimination reactions of cis-3,6-dihalocyclohexa-1,4-dienes. *Struct Chem* **2017,** *28* (6), 1803-1814.

435.   Nowacki, A.; Liberek, B., Acetylated methyl 1,2-dideoxyhex-1-enopyranuronates in density functional theory conformational studies. *Carbohydrate Research* **2013,** *371*, 1-7.

436. Gomez, A. M.; Lobo, F.; Uriel, C.; Lopez, J. C., Recent Developments in the Ferrier Rearrangement. *Eur J Org Chem* **2013,** *2013* (32), 7221-7262.

437. Yarie, M., Catalytic anomeric based oxidation. *Iran J Catal* **2017,** *7* (1), 85-88.

438. Karimi, F.; Zolfigol, M. A.; Yarie, M., A novel and reusable ionically tagged nanomagnetic catalyst: Application for the preparation of 2-amino-6-(2-oxo-2H-chromen-3-yl)-4-arylnicotinonitriles via vinylogous anomeric based oxidation. *Mol Catal* **2019,** *463*, 20-29.

439. Noura, S.; Ghorbani, M.; Zolfigol, M. A.; Narimani, M.; Yarie, M.; Oftadeh, M., Biological based (nano) gelatoric ionic liquids (NGILs): Application as catalysts in the synthesis of a substituted pyrazole via vinylogous anomeric based oxidation. *J Mol Liq* **2018,** *271*, 778-785.

440. Zolfigol, M. A.; Khazaei, A.; Karimitabar, F.; Hamidi, M.; Maleki, F.; Aghabarari, B.; Sefat, F.; Mozafari, M., Synthesis of Indolo[3,2-b] carbazoles via an Anomeric-Based Oxidation Process: A Combined Experimental and Computational Strategy. *J Heterocyclic Chem* **2018,** *55* (4), 1061-1068.

441. Babaee, S.; Zolfigol, M. A.; Zarei, M.; Zamanian, J., 1,10-Phenanthroline-Based Molten Salt as a Bifunctional Sulfonic Acid Catalyst: Application to the Synthesis of N-Heterocycle Compounds via Anomeric Based Oxidation. *Chemistryselect* **2018,** *3* (31), 8947-8954.

442. Baghery, S.; Zolfigol, M. A.; Maleki, F., [TEATNM] and [TEATCM] as novel catalysts for the synthesis of pyridine-3,5-dicarbonitriles via anomeric-based oxidation. *New J Chem* **2017,** *41* (17), 9276-9290.

443. Zolfigol, M. A.; Safaiee, M.; Ebrahimghasri, B.; Baghery, S.; Alaie, S.; Kiafar, M.; Taherpour, A.; Bayat, Y.; Asgari, A., Application of novel nanostructured dinitropyrazine molten salt catalyst for the synthesis of sulfanylpyridines via anomeric based oxidation. *J Iran Chem Soc* **2017,** *14* (9), 1839-1852.

444. Torabi, M.; Yarie, M.; Zolfigol, M. A., Synthesis of a novel and reusable biological urea based acidic nanomagnetic catalyst: Application for the synthesis of 2-amino-3-cyano pyridines via cooperative vinylogous anomeric based oxidation. *Appl Organomet Chem* **2019,** *33* (6).

445. Jalili, F.; Zarei, M.; Zolfigol, M. A.; Rostamnia, S.; Moosavi-Zare, A. R., SBA-15/PrN(CH2PO3H2)(2) as a novel and efficient mesoporous solid acid catalyst with phosphorous acid tags and its application on the synthesis of new pyrimido[4,5-b]Aquinolones and pyrido[2,3-d]pyrimidines via anomeric based oxidation. *Micropor Mesopor Mat* **2020,** *294*.

446. Ghasemi, P.; Yarie, M.; Zolfigol, M. A.; Taherpour, A. A.; Torabi, M., Ionically Tagged Magnetic Nanoparticles with Urea Linkers: Application for Preparation of 2-Aryl-quinoline-4-carboxylic Acids via an Anomeric-Based Oxidation Mechanism. *Acs Omega* **2020,** *5* (7), 3207-3217.

447. Kalhor, S.; Yarie, M.; Rezaeivala, M.; Zolfigol, M. A., Novel magnetic nanoparticles with morpholine tags as multirole catalyst for synthesis of hexahydroquinolines and 2-amino-4,6-diphenylnicotinonitriles through vinylogous anomeric-based oxidation. *Res Chem Intermediat* **2019,** *45* (6), 3453-3480.

448. Hofmann, M.; Hampel, N.; Kanzian, T.; Mayr, H., Electrophilic Alkylations in Neutral Aqueous or Alcoholic Solutions. *Angewandte Chemie International Edition* **2004,** *43* (40), 5402-5405.

449.   Alabugin, I. V.; Gonzalez-Rodriguez, E., Alkyne Origami: Folding Oligoalkynes into Polyaromatics. *Accounts of Chemical Research* **2018,** *51* (5), 1206-1219.

450.   Wodrich, M. D.; Wannere, C. S.; Mo, Y.; Jarowski, P. D.; Houk, K. N.; Schleyer, P. v. R., The Concept of Protobranching and Its Many Paradigm Shifting Implications for Energy Evaluations. *Chemistry – A European Journal* **2007,** *13* (27), 7731-7744.

451.   Alabugin, I.; Mohamed, R. K., A CO2 Cloak for the Cyanide Dagger. *Science* **2014,** *344* (6179), 45.

452.   Murphy, L. J.; Robertson, K. N.; Harroun, S. G.; Brosseau, C. L.; Werner-Zwanziger, U.; Moilanen, J.; Tuononen, H. M.; Clyburne, J. A. C., A Simple Complex on the Verge of Breakdown: Isolation of the Elusive Cyanoformate Ion. *Science* **2014,** *344* (6179), 75.